DEVELOPMENT OF DNA APTAMERS AGAINST SELECTED CELIAC DISEASE EPITOPES IN GLUTENIN

A thesis submitted in partial fulfilment of the
Requirements for the degree of

DOCTOR OF PHILOSOPHY

By

JON JYOTI KALITA

REGISTRATION No. 156106013

Department of Biosciences and Bioengineering,
Indian Institute of Technology Guwahati,
Guwahati-781039, Assam, India

April 2023

Development of DNA aptamers against selected Celiac disease epitopes in Glutenin

A thesis submitted in partial fulfilment of the
Requirements for the degree of

Doctor of Philosophy
by

Jon Jyoti Kalta

Registration No. 156106013

Under the supervision of

Prof. Utpal Bora
Department of Biosciences & Bioengineering,
IIT Guwahati

Department of Biosciences and Bioengineering,
Indian Institute of Technology Guwahati,
Guwahati-781039, Assam, India

April 2023

INDIAN INSTITUTE OF TECHNOLOGY GUWAHATI
Department of Biosciences and Bioengineering
Guwahati-781039

DECLARATION

This is to declare that the content embodied in this thesis entitled "**Development of DNA aptamers against selected Celiac disease epitopes in Glutenin**" is the result of an investigation carried out by me under the supervision of **Prof. Utpal Bora** and is submitted to the Department of Biosciences and Bioengineering, Indian Institute of Technology Guwahati, Kamrup 781039, Assam, India for the award of the degree of *Doctor of Philosophy in Biosciences and Bioengineering*. This work has not been submitted elsewhere for any degree or diploma of any institute or university to the best of my knowledge and belief.

In keeping with the general practice of reporting scientific observations, due acknowledgments have been made wherever the work described is based on the findings of other investigators and copyright permissions have been taken from respective publishers.

Jon Jyoti Kalita.

April 2023

Jon Jyoti Kalita
(Registration no. 156106013)

INDIAN INSTITUTE OF TECHNOLOGY GUWAHATI
Department of Biosciences and Bioengineering
Guwahati-781039

CERTIFICATE

This is to certify that the content embodied in this thesis entitled "**Development of DNA aptamers against selected Celiac disease epitopes in Glutenin**" is the result of an investigation carried out by **Jon Jyoti Kalita** (Registration Number - 156106013) under my supervision in the Department of Biosciences and Bioengineering, Indian Institute of Technology Guwahati, Kamrup 781039, Assam, India for the award of the degree of *Doctor of Philosophy in Biosciences and Bioengineering*.

This work has not been submitted elsewhere for any degree or diploma of any institute/university.

5/4/2023

April 2023

Prof. Utpal Bora
Supervisor

Dedicated to my Family

Acknowledgements

It's been a wonderful journey in the past few years that I have spent in Indian Institute of Technology Guwahati to carry out my doctoral research. This journey would not have been possible without the constant help and support from many people, to whom I will be indebted forever.

First and foremost, I express my deepest grateful to my thesis supervisor Prof. Utpal Bora for the opportunity to be a part of his research group, 'Bioengineering research laboratory (BERL)' and introducing me to the wonderful area of aptamer research. The guidance, support and encouragement received from him throughout my PhD journey has helped me immensely to stay motivated and finish this work. I had been fortunate enough to be involved in many scientific writing exercises and organizing conferences under his mentorship and learnt a great deal of skills.

I am extremely grateful to my Doctoral Committee members Prof. Ranjan Tamuli, Dr. Priyadarshi Satpati and Dr. Pankaj Kalita for their valuable suggestions, constant encouragement, and critical assessment of my Ph.D. work, which helped me in improving my critical thinking skills.

I would like to thank the Department of Biosciences and Bioengineering for providing the infrastructures and the DCIF facilities to carry out research activities effortlessly. I appreciate the staff members Nurul Sir, Prarthana Ma'am, Dipankar da, Niranjan da, Pankaj Da for their assistance.

I acknowledge the Centre for Central Instruments Facility, IIT Guwahati and Centre for the Environment, IIT Guwahati for providing access to various instrumentation facilities used in this thesis work.

I also appreciate the administration of IIT Guwahati for quickly reopening the research laboratories following the COVID lockdowns. Even under challenging conditions, access to the research facilities was maintained, enabling students to conduct experiments. Moreover, I acknowledge Indian Institute of Technology Guwahati for providing all the in-house facilities and for a healthy & well-maintained beautiful campus.

I acknowledge the Guwahati Biotech Park (GBP), Amingaon for providing access to their semi-preparative RP-HPLC.

I am sincerely thankful to Ministry of Human Resource Development, Govt. of India, for the financial support in the form of fellowship and Dept. of Biotechnology, Govt. of India, for research grants to my mentor.

I am thankful to my seniors in BERL, Dr. Ajoy Das, Dr. Arghya Sett, Dr. Dipika Singh, Dr. Sunita Ojha, Dr. Hasnahana Chetia, Dr. Papori Buragohain, Dr. Jintu Dutta, Dr. Vimal Mosahari and Dr. Debajyoti Kabiraj for their support morally and helps. I am extremely grateful to Dr. Arghya Sett for initial days of hands on training on aptamer technology. I am extremely thankful to my present lab mates Adhiraj, Dharitri, Biju, Pulak, Udangshree, Rounak, Pinky and Asma for their helps on numerous occasions, encouragements and providing an enjoyable working environment in the lab. I would also like to thank Dr. Pragya Sharma ma'am for the chance to work in collaboration and for the wonderful hospitality provided on numerous times.

I thank my friends, Dr. Avishek, Anurag, Aman, Dr. Angshuman, Dr. Nayan, Dr. Anupama, Dr. Madonna for making my stay at IIT Guwahati memorable. I am also thankful to the seniors and juniors from the BSBE department, Dr. Nandakishore Roy, Dr. Dibakar Gohain, Rahul, Darshana, Sosmita, Surabhi, Ambika for making the environment always cheerful.

I am extremely grateful to my parents Mr. Keshab Chandra Kalita and Mrs. Bina Kalita and siblings Mridul and Chandasmita for their unconditional love and tremendous support in the pursuit of fulfilling my dreams.

It would be hard to list everyone who has helped me in my academic endeavors. I sincerely appreciate each and every one of them for having faith in me.

Jon Jyoti Kalita *April 2023*

Table of Contents Page

Synopsis i

List of abbreviations and symbols vi

List of the figures ix

List of Tables xiv

Chapter 1: Introduction and literature review

1.1. Introduction 1

1.2. Literature Review 2

1.2.1. Pathogenesis of Celiac disease 2

1.2.2 Clinical features 5

1.2.3. Epidemiology of Celiac Disease 7

1.2.4 Genetic factor: Human Leukocyte Antigen (HLA) Locus 9

1.2.5 Gluten protein 12

1.2.5.1 Gliadin 15

1.2.5.2. Glutenins 16

1.2.6 Toxic peptides involved in Celiac Disease 18

1.2.6.1 Epitope Mapping of some known peptide epitopes in Gliadins, Glutenins, hordeins, secalins and avenins 21

1.2.7 Treatment of celiac disease 24

1.2.8 Analytical methods for detection of Gluten and celiac disease epitopes 24

1.2.8.1 Immunological method of gluten detection 25

1.2.8.2 Non-immunological method of gluten detection 28

1.2.9 Aptamers 30

1.2.9.1 Modified SELEX 32

1.2.9.2 Next Genome Sequencing - SELEX 34

1.2.9.3 Advantages of aptamer over antibodies 35

1.2.9.4 Aptamer based bioassays 36

1.2.9.5 Aptamer based biosensors 38

1.2.10 Application of aptamer in detection of food contaminants 39

1.2.10.1 Pathogenic microorganisms 39

1.2.10.2 Allergens 41

1.2.10.3 Biotoxin 43

1.2.10.4 Antibiotic residues 45

1.2.10.5 Pesticide 47

1.2.10.6 Heavy metals 48

1.2.10.7 Selective analyte extraction using aptamer 48
1.2.10.8 Application as target-responsive aptamer-cross-linked hydrogel 51
1.2.11 Challenges and opportunities in development of aptamer for gluten detection 53
1.2.12 Gap in the literature: 55
1.2.13 Objectives 56
1.2.14 References: 56

Chapter 2: Selection and characterisation of specific aptamers against toxic celiac disease epitopic peptide GQGQQGYYPTSPQQ

2.1 Introduction 86
2.2. Materials and Methods: 87
2.2.1. Chemicals and Reagents 87
2.2.2 Selection of the target peptide sequence 88
2.2.3 Synthesis of High Molecular Weight (HMW) Glutenin peptide 88
2.2.3.1 Fmoc solid phase synthesis 88
2.2.3.2 Cleavage of the peptide from the resin 89
2.2.3.3 Purification of the synthesized peptides 90
2.2.3.4 Characterisation of the synthesized peptides by mass spectroscopy 90
2.2.4 Secondary structure analysis by circular dichroism spectroscopy 91
2.2.5 Design of Aptamer library and PCR optimization 91
2.2.6 Immobilization of peptide sequence on magnetic beads 92
2.2.7 In-vitro selection of Aptamers against peptide GQGQQGYYPTSPQQ of HMW glutenin 93
2.2.8 Cloning and sequencing of the Aptamer sequences 94
2.2.9 *Insilico* analysis of aptamer sequences 96
2.2.10 Binding characterization of the aptamer with target peptide 96
2.2.10.1 Isothermal Titration Calorimetry (ITC) studies 96
2.2.10.2 Circular dichroism studies 97
2.2.10.3 Direct Enzyme linked aptamer-sorbent assay (ELAA) 97
2.3 Results 98
2.3.1 Selection of the target peptide sequence 98
2.3.2 Synthesis of High Molecular Weight (HMW) Glutenin peptide 99
2.3.2.1 Fmoc solid phase synthesis 99
2.3.2.2 Purification of the synthesized peptides 101
2.3.2.3 Characterisation of the synthesized peptides by mass spectroscopy 101
2.3.3 Secondary structure analysis by circular dichroism spectroscopy 102
2.3.4 Design of Aptamer library and PCR optimization 103
2.3.5 Immobilization of peptide sequence on magnetic beads 104

2.3.6 In-vitro selection of Aptamers against peptide GQGQQGYYPTSPQQ of HMW glutenin 105
2.3.7 Cloning and sequencing of the Aptamer sequences 106
2.3.8 *Insilico* analysis of aptamer sequences 107
2.3.9 Binding studies 109
2.3.9.1 Isothermal Titration Calorimetry (ITC) studies 109
2.3.9.2 Binding study through Circular Dichroism 113
2.3.9.3 Direct Enzyme linked aptamer-sorbent assay (ELAA) 115
2.4 Discussion: 116
2.5 Conclusion 119
2.6 References 119
Chapter 3: Selection and characterisation of specific aptamers against toxic celiac disease epitopic peptide SQQQPPFSQQQQPV
3.1. Introduction 124
3.2. Materials and Methods: 125
3.2.1 Chemicals and Reagents 125
3.2.2 Selection of the target peptide sequence 125
3.2.3 Characterisation of the synthesized peptides by mass spectroscopy 126
3.2.4 Secondary structure analysis by circular dichroism spectroscopy 126
3.2.5 Design of Aptamer library and PCR condition 127
3.2.6 Immobilization of peptide sequence on magnetic beads 128
3.2.7 *In-vitro* selection of Aptamers against peptide SQQQPPFSQQQQPV of LMW glutenin 128
3.2.8 Cloning and sequencing of the Aptamer sequences 130
3.2.9 *Insilico* analysis of aptamer sequences 132
3.2.10 Binding characterization of the aptamer with target peptide 132
3.2.10.1 Isothermal Titration Calorimetry (ITC) studies 132
3.2.10.2 Circular dichroism studies 133
3.2.10.3 Direct Enzyme linked aptamer-sorbent assay (ELAA) 133
3.3 Results 134
3.3.1 Selection of the target peptide sequence 134
3.3.2 Characterisation of the synthesized peptides by mass spectroscopy 135
3.3.3 Secondary structure analysis by circular dichroism spectroscopy 136
3.3.4 Design of Aptamer library and PCR optimization 138
3.3.5 Immobilization of peptide sequence on magnetic beads 138
3.3.6 *In-vitro* selection of Aptamers against peptide GQGQQGYYPTSPQQ of HMW glutenin 139
3.3.7 Cloning and sequencing of the Aptamer sequences 139
3.3.8 *Insilico* analysis of aptamer sequences 140

3.3.9 Binding studies 142
3.3.9.1 Isothermal Titration Calorimetry (ITC) studies 142
3.3.9.2 Binding study through Circular Dichroism 147
3.3.9.3 Direct Enzyme linked aptamer-sorbent assay (ELAA) 149
3.4 Discussion 149
3.5 Conclusion 152
3.6 References 152
Chapter 4: Development of aptassays for detection of CD epitopes in wheat gluten
4.1. Introduction 157
4.2. Materials and Methods 158
4.2.1. Chemicals and Reagents 158
4.2.2. Gold nanoparticle based calorimetric assay 158
4.2.2.1. Synthesis of gold nanoparticles 158
4.2.2.2 Calorimetric Assay using apt_J91P 159
4.2.2.3. Calorimetric Assay using apt_M09P 159
4.2.3. Magnetic bead based target extraction assay using biotinylated apt_J91P 159
4.3. Results 160
4.3.1. Gold nanoparticle based calorimetric assay 160
4.3.1.1. Synthesis of gold nanoparticles 160
4.3.1.2. Calorimetric Assay using apt_J91P 162
4.3.1.3. Calorimetric Assay using apt_M09P 163
4.3.5. Magnetic bead based target extraction assay using biotinylated apt_J91P 165
4.4. Discussion 167
4.5. Conclusion 168
4.6. References 168
Chapter 5: Summary and future prospects
5.1. Summary 171
5.1.1. Selection and characterization of specific aptamers against toxic celiac disease epitopic peptide GQGQQGYYPTSPQQ 171
5.1.2. Selection and characterization of specific aptamers against toxic celiac disease epitopic peptide SQQQPPFSQQQQPV 172
5.1.3. Development of aptassays for detection of CD epitopes in wheat gluten 172
5.2. Future prospects of this study 172
Curriculum Vitae 174
Appendix 175

Synopsis

The celiac disease (CD) or celiac sprue or Gluten sensitive enteropathy is an autoimmune enteropathy of small intestine characterized by a permanent intolerance to dietary gluten, a protein complex found in various types of cereals like wheat, rye, barley and oats (rarely) in genetically susceptible subjects of all ages (Alarida et al. 2011). It is the most common food intolerance in the world, affecting 1.4% and 0.7% of the world population based on serological and biopsy tests respectively (Singh et al., 2018). CD is attributed to the immune reaction to immunotoxic indigestible peptides present in glutenin and gliadin fractions of gluten trigger inflammation of the duodenal mucosa. This results in reduced intestinal villus height and hyperplastic cryptae which sometimes leads to complete villus atrophy (Shewry et al., 1992; Tonutti et al., 2014). The treatment of CD at present comprises of the restricting the consumption of gluten by the patients. Many advancements have been made with new therapies like the use of active proteases, gluten binder copolymer, and tight junction regulators etc., which are under initial states of clinical trial (Yoosuf & Makharia, 2019). The Codex Alimentarius (CODEX STAN 118, 1979) and the Regulation (EC) No 41/ 2009 specifies a highest gluten contamination of 20 mg/kg in gluten-free labelled products as a safe threshold for CD patients (Martín-Fernández et al., 2015). Therefore detection of gluten in food stuff is of upmost importance for management of the disease. Currently, antibody based immunological methods and non-immunological methods including mass-spectroscopy and Q-PCR are used for detection of gluten. While non-immunological methods are costly, not portable and need sophisticated equipment, the immunological methods suffers from disadvantages of high production cost, batch to batch variation, cross-reactivity and low heat stability of antibodies. Aptamers are emerging as a new class of bio-recognition element that can act as an alternative to the antibodies. Aptamers are short sequences of nucleic acid that can be selected against any type of analyte and form three dimensional structures for binding to the target analyte. They have the advantage of comparable level of specificity and affinity to antibodies, low batch to batch variation, and high thermal stability. Aptamers were developed recently against the gliadin fraction of gluten and the immunotoxic α2-gliadin peptide fragment (Miranda-Castro et al., 2016). However, there are large number of immunotoxic and immunodominant peptides present in the glutenin sunubit of gluten, detection of which is crucial for analysis of processed foods and in-terms of development of screening methods for the detection of immunotoxic wheat varieties. Based on the research gap

identified in the domain of analytical detection of gluten and immunotoxic peptide, the research objectives of this thesis are decided.

Objectives: To develop an aptamer based bioassays or biosensors for detection of toxic and immunodominant peptides of glutenin fraction of gluten protein, the following objectives were carried out-

1. Selection of specific aptamer ligands against the known peptide epitopes of celiac disease in high molecular weight glutenin subunit of wheat.
2. Selection of specific aptamer ligands against the known peptide epitopes of celiac disease in low molecular weight glutenin subunit of wheat.
3. Evaluation of the binding affinity of aptamer probes with the targets.
4. Development of aptaassays for detection of immunotoxic celiac epitopes of glutenin.

The thesis is organised into the following chapters as described below.

Chapter 1: Introduction and literature review

An extensive review of the literature was carried out on the state of the art of celiac disease pathogenesis by epitopes in gluten protein and analytical methods for gluten detection. This chapter describes in details about the pathogenesis, clinical features and etiology of the celiac disease, role of the indigestible immunogenic peptide sequences present in the gluten protein of wheat. The chapter further describes the existing analytical methods available for gluten detection in food sample and their advantages and limitations. Towards the end, it explains about the aptamers, the SELEX method and the recent advancements in application of aptamers in the detection of food contaminants with special reference to gluten.

Chapter 2: Selection and characterization of specific aptamers against toxic celiac disease epitopic peptide GQGQQGYYPTSPQQ

This chapter describes the *in-vitro* selection and characterization of aptamer against a 14 mer peptide sequence of the high molecular weight glutenin subunit 1Bx13 of wheat (Triticum aestivum), GQGQQGYYPTSPQQ, which contains a celiac disease epitope QGYYPTSPQ. A DNA aptamer apt_J91P of length 56 bp was selected through conventional SELEX method. The binding characterization by ITC reveals the dissociation constant of 2.26 μM and 4.385 mM for the primary and the secondary site of binding during the interaction of the aptamer and

the target in aptamer binding buffer respectively. The dissociation constant of 81.3 µM was determined for the interaction in water. The interactions were found to be both enthalpically and entropically driven. CD study reveals that the binding leads to local conformational change in the aptamer. The limit of detection (LOD) evaluated through direct-ELAA was found to be 16.0875 µM.

Chapter 3: Selection and characterization of specific aptamers against toxic celiac disease epitopic peptide SQQQPPFSQQQQPV

This chapter describes the *in-vitro* selection and characterization of aptamer against a 14 mer peptide sequence of the low molecular weight glutenin subunit of wheat (*Triticum aestivum*), SQQQPPFSQQQQPV, which contains a celiac disease epitope PFSQQQQPV. A DNA aptamer apt_M09P of length 76 bp was selected through conventional SELEX method. The binding characterization by ITC reveals the dissociation constant of 17.6 µM and 8.33 mM for the primary and the secondary site of binding during the interaction of the aptamer and the target in aptamer binding buffer respectively. The binding characterization reveals the binding is enthalpically favourable and entropically unfavourable. CD study reveals that the binding leads to local conformational change in the aptamer. The limit of detection (LOD) evaluated through direct-ELAA was found to be 20.00 µM.

Chapter 4: Development of aptassays for detection of CD epitopes in wheat gluten

This chapter describes the preliminary investigations carried out to check the applicability of the selected aptamers apt_J91P and apt_M09P in development of bioassays. The aptamers were used in the gold nanoparticle based aptamer assay and the aptamer mediated magnetic bead based extraction assay. The aptamers apt_J91P and apt_M09P were successful in detecting their respective target peptides GQGQQGYYPTSPQQ and SQQQPPFSQQQQPV in aptamer binding buffer demonstrating specificity. However, for detection of the target peptides in food matrix, further future investigation are needed to be carried out.

Chapter 5: Summary and future prospects

This chapter describes the summary of the findings of the work presented in this thesis and the scopes for future studies based on the present findings. The present work was carried out in an

attempt to develop aptamer against the two immunodominant peptide sequences of wheat that causes celiac disease in genetically predisposed population. The aptamers were successful in detecting the standard peptide targets in aptamer binding buffer. The present published literatures have focused on developing aptamer against the intact gliadin subunit and a selected 33mer immunodominant peptide from gliadin. This work is believed to be the first of its kind in terms of selecting the aptamers against the peptide sequences of glutenin. The future research focusing on the enhancement of the affinity of the selected aptamers will lead to development of successful bioassays and biosensors for glutenin detection.

Publications related to thesis work:

1. **Kalita, J. J.**, Sharma, P., & Bora, U. (2022). Recent developments in application of nucleic acid aptamer in food safety. Food Control, 109406. https://doi.org/10.1016/j.foodcont.2022.109406.
2. **Kalita, J. J**., Buragohain, P., Mosahari, P. V., & Bora, U. (2019). Food Allergens: Detection and Management. In Food Bioactives (pp. 243-279). Apple Academic Press.

Manuscript under preparation related to thesis work:

1. Kalita, J.J. & Bora. U. *In-vitro* selection and characterization of Aptamer against high molecular weight Glutenin peptide epitope of Celiac Disease (Research article)
2. Kalita, J.J. & Bora. U. *In-vitro* selection and characterization of Aptamer against low molecular weight Glutenin peptide epitope of Celiac Disease (Research article)

Publication from collaborative works:

1. Das, A. K., **Kalita, J. J.**, Borah, M., Bora, S., Sharma, M., Saharia D., Sarma, K. K., Das, D. & Bora, U., Papaya latex mediated synthesis of prism shaped proteolytic gold nanozymes. Scientific Reports. (*Accepted in March, 2023*).
2. Sharma, P., **Kalita, J. J**., Buragohain, P., & Deka, M. (2022). In Vitro Selection and Characterization of an Aptamer for Detection of the Epitopic Peptide Sequence of the Thermostable Direct Hemolysin (TDH) Toxin of Vibrio parahemolyticus. ACS Food Science & Technology, 2(5), 784-792. https://doi.org/10.1021/acsfoodscitech.1c00059.

3. Bhaskar, B., Dutta, J., Mosahari, P. V., **Kalita, J. J.,** Buragohain, P., & Bora, U. (2020). Nanoparticle-based antimicrobial coating on medical implants. In Nanostructures for Antimicrobial and Antibiofilm Applications (pp. 79-99). Springer, Cham.
4. Bharali, B., Chetia, H., **Kalita, J. J.**, Mosahari, P. V., Chhillar, A. K., & Bora, U. (2019). Engineered nanomaterials in plants: Sensors, carriers, and bio-imaging. In Comprehensive Analytical Chemistry (Vol. 87, pp. 133-157). Elsevier.
5. Mosahari, P. V., Singh, D., **Kalita, J. J**., Sharma, P., Chetia, H., Kabiraj, D., ... & Bora, U. (2018). Nanotoxicity: Impact on Health and Environment. In Environmental Toxicity of Nanomaterials (pp. 21-46). CRC Press.
6. Kabiraj, D., **Kalita, J. J.**, Chetia, H., Singh, D., & Bora, U. Expanding the frontiers of rice research through omics. J. Assam Sc. Soc. Vo. 56, No.2, December 2015; PP. 1-28

Conference proceedings:

1. **Kalita, J. J.,** Buragohain, P., Kabiraj, D., Mosahari, P.V., Bora, U. Future prospects of edible insects farming in North-East India. International Symposium on Biodiversity and Biobanking, BIODIVERSE 2018, at IIT Guwahati, North Guwahati, Assam, India, 27th to 29th January 2018.
2. **Kalita, J. J**., Kabiraj, D., Bharali, B., Saikia, D., Bora, U. Applications of aptamer-conjugated nanomaterials in biosensing and therapeutics. International Conference on Advances in Nanotechnology (ICAN-2017), at Assam Don Bosco University (ADBU), Azara, Guwahati, Assam, India, 9th to 13th January, 2017.

List of abbreviations and symbols

ΔG	Change in free energy
ΔH	Change in entropy
ΔS	Change in enthalpy
µM	Micromolar
ABB	Aptamer binding buffer
CD	Circular Dichroism
CFU	Colony forming unit
Da	Dalton
DCM	Dichloromethane
DIC	N,N′-Diisopropylcarbodiimide
DLS	Dynamic Light Scattering
DMAP	4-(Dimethylamino)pyridine
DMF	Dimethylformamide
EDC	1-ethyl-3-(3-dimethylaminopropyl) carbodiimide hydrochloride
ELAA	Enzyme linked aptamer-sorbent assay
ELISA	Enzyme-linked immunosorbent assay
FESEM	Field emission scanning electron microscopy
Fmoc	9-fluorenylmethoxycarbonyl
g	Relative centrifugal force (rcf)
GNP	Gold nanoparticle
GRAVY	Grand average of hydropathicity
h	Hour
HCCA	α-Cyano-4-hydroxycinnamic acid
HMW-GS	High molecular weight glutenin
HoBT	Hydroxybenzotriazole

HRP	Horse radish peroxide
HT voltage	High tension voltage
IPTG	Isopropyl ß-D-1-thiogalactopyranoside
ITC	Isothermal titration calorimetry
K_d	Dissociation constant
KDa	Kilodalton
LMW-GS	Low molecular weight glutenin
LOD	Limit of detection
m/z	mass to charge ratio
mAb	Monoclonal antibody
MALDI-TOF	Matrix-assisted laser desorption/ionization-time of flight
MES	2-[N-morpholino] ethane sulfonic acid
min	Minute
mM	Millimolar
mmol	Millimole
MS	Mass Spectroscopy
NRMSD	Normalized root mean square deviation
PAGE	Polyacrylamide gel electrophoresis
PCR	Polymerase chain reaction
pI	Isoelectric point
pM	Picomolar
PMT voltage	Photomultiplier voltage
ppb	Parts per billion
ppm	Parts per million
QL	Quantitation limit
RP-HPLC	Reverse phase high performance liquid chromatography
s	Second

SELEX	Systematic Evolution of Ligands by Exponential enrichment
ssDNA	Single stranded deoxyribonucleic acid
TFA	Trifluoroacetic acid
TG2	Tissue transglutamerase-2
Th2	Type II helper T cells
TJ	Tight junctions
TMB	3,3′,5,5′-Tetramethylbenzidine
UV-VIS	Ultraviolet-visible
V	Volt
X-Gal	5-Bromo-4-Chloro-3-Indolyl β-D-Galactopyranoside

List of the figures

Figure 1.1 A schematic representation of the mechanisms involved in celiac disease pathogenesis (Reprinted with permission from Catassi et al., 2022, copyright Elsevier 2022).

Figure 1.2 The celiac disease iceberg model (adopted from Lionetti & Catass, 2011)

Figure 1.3 Human leukocyte antigen (HLA) genotype and their associated magnitude of risk for coeliac disease (Reprinted with permission from Abadie et al., 2011, copyright Annual Reviews)

Figure 1.4 Classification of Prolamines (Reprinted from Tatham et al., 2000 with permission, copyright Springer, 2000)

Figure 1.5 Gliadin and glutenin loci in *Triticum aestivum* (AABBDD), 2n = 6x = 42. (Reprinted form Sharma et al., 2020, licensed with CC BY 4.0)

Figure 1.6 Schematic representation of SELEX process

Figure 1.7 Schematic diagram of aptamer based assay and biosensor. (A) Direct ELAA (B) Sandwich ELAA (C) Competitive direct ELAA and (D) Electrochemical Aptasensor, where eT is electron transfer rate. (Reprinted with permission from Kalita et al., 2022, copyright Elsivier, 2022)

Figure 2.1 The MALDI-TOF mass spectra of crude peptides (A) Fmoc-SPQQ (MW 680.28 Da) and (B) Fmoc-YYPTSPQQ (MW 1204.51 Da) with addition of adducts as [M+Na]+ and [M+K]+ , where M denotes the parent mass

Figure 2.2 Reverse phase-HPLC chromatogram of the purified peptide GQ-14 at retention time 13.52 min

Figure 2.3 The MALDI-TOF mass spectra of the purified peptide GQ-14 with dominant peaks of 1539.85 Da ($[M+H]^+$), 1561.767 ($[M+Na]^+$) and 1577.735 ($[M+K]^+$), where M denotes the parent mass of 1538.57 Da

Figure 2.4 Circular dichroism spectra of peptide GQ-14 recorded in the Far-UV wavelength 190-250 nm at 25 °C

Figure 2.5 Optimization of PCR conditions at 45 °C annealing temperature and 14 cycles. L1 is low molecular DNA ladder (NEB, 25-766 bp) and L2-l5 are PCR amplified aptamer library of 56 bp.

Figure 2.6 MALDI-TOF spectra of dynabead immobilised with peptide GQ-14 in linear negative mode where monoisotopic masses of 1537.49 Da ($[M-H]^-$) and 1653.76 Da ($[M+TFA]^{-1}$) are observed, where M denotes the parent mass of 1538.57 Da

Figure 2.7 2% agarose gel for 56 enriched N20 aptamer pool after SELEX rounds against peptide target GQ-14 from 3^{rd} to 12^{th} round (R3-R12), L-Small molecular DNA ladder (NEB, 25-766 bp)

Figure 2.8 Secondary structure of aptamer candidates as predicted by mfold; A) truncated aptamer Apt_J91 without flanking regions, B) aptamer Apt_J91P with flanking regions, C) truncated aptamer Apt_J94 without flanking regions, D) aptamer Apt_J94P with with flanking regions.

Figure 2.9 ITC isotherms for calorimetric titration between 30 μM aptamer apt_J91P with flanking regions and 1000 μM peptide GQ-14 at 25°C in aptamer binding buffer.

Figure 2.10 ITC isotherms for calorimetric titration between 30 μM aptamer apt_J91P with flanking region and 3000 μM peptide GQ-14 at 25°C in deionised water.

Figure 2.11 ITC isotherms for calorimetric titration between 30μM aptamer apt_J91P and 3000 μM peptide PV-12 at 25°C in 1x ABB.

Figure 2.12 Circular dichroism spectra of aptamer apt_J91P in 0.3x ABB buffer

Figure 2.13 Binding study of the aptamer-peptide complex by circular dichroism scanned from 190nm to 340 nm where the plot with red, blue and black denotes the

CD spectra of peptide GQ-14, aptamer apt_J91P and interaction between apt_J91P and peptide GQ-14

Figure 2.14 Analysis of the limit of detection of the aptamer by ELAA in the peptide concentration range of (40-200 μM).

Figure 3.1 The MALDI-TOF mass spectra of the purified peptide SV-14 obtained in (A) the mass range 100-3000 Da with dominant peaks of 1650.73 Da ([M+Na]+) and 1687.76 Da ([M+IsoProp+H, (B) the zoomed mass range 1600-1700 Da exhibiting the monoisotopic peaks of 1649.62 Da ([M+Na]+), 1665.69 Da ([M+K]+), 1668.71 ($[M+ACN+H]^+$) and 1687.70 Da ([M+IsoProp+H]+), where M denotes the parent mass of 1626.75 Da

Figure 3.2 Circular dichroism spectra of peptide SV-14 recorded in the Far-UV wavelength 190-250 nm at 25 °C

Figure 3.3 MALDI-TOF spectra of dynabead immobilised with peptide SQ-14 in linear positive ion mode where dominant monoisotopic mass of 1650.40 Da ([M+Na]+) is observed, where M denotes the parent mass of 1626.75 Da

Figure 3.4 15% native PAGE gel for 76 bp enriched N40 aptamer pool after SELEX rounds against peptide target SV-14 from round 4^{th} to 18^{th} (R4-R18). The PC is positive control by taking 76 bp aptamer library as template and L is small molecular DNA ladder (NEB, 25-766 bp)

Figure 3.5 Secondary structure of aptamer candidates as predicted by mfold; A) truncated aptamer Apt_M09 without flanking regions, B) aptamer Apt_M09P with flanking regions, C) truncated aptamer Apt_J51 without flanking regions, D) aptamer Apt_J51P with with flanking regions

Figure 3.6 ITC isotherms for calorimetric titration between 30 μM aptamer apt_M09P with flanking regions and 1000 μM peptide SV-14 at 25°C in aptamer binding buffer.

Figure 3.7 ITC isotherms for calorimetric titration between 30 μM aptamer apt_J51P with flanking region and 1000 μM peptide SV-14 at 25°C in 1x ABB

Figure 3.8 ITC isotherms for calorimetric titration between 30μM aptamer apt_M09 and 1000 μM peptide GQ-14 at 25°C in 1x ABB to check the specificity of aptamer apt_M09.

Figure 3.9 Circular dichroism spectra of aptamer apt_M09P with flanking regions in 0.3x aptamer binding buffer

Figure 3.10 Binding study of the aptamer-peptide complex by circular dichroism scanned from 200 nm to 340 nm where the plot with black, green and red lines denotes the CD spectra of aptamer apt_M09P, interaction between apt_M09P and peptide SV-14 and interaction between apt_M09 and peptide GQ-14 (negative control).

Figure 3.11 Analysis of the limit of detection of the aptamer by ELAA in the peptide concentration range of (40-200 μM)

Figure 4.1 Absorbance of synthesised gold nanoparticle at wavelength range 300-900nm

Figure 4.2 FESEM image of synthesized gold nanoparticles at 150.00K X magnification revealing average size between 30-50 nm

Figure 4.3 The distribution of hydrodynamic diameter of synthesized gold nanoparticles (GNP) before (red) and after (black) adsorption of aptamer (ApGNP) on nanoparticle's surface (J91P + GNP)

Figure 4.4 UV-VIS spectra of aptamer (J91P) based gold nanoparticle aggregation incubated with target peptide GQ-14 and control peptide SV-14

Figure 4.5 The distribution of hydrodynamic diameter of synthesized gold nanoparticles (GNP) before (red) and after (black) adsorption of aptamer on nanoparticle's surface (M09P + GNP)

Figure 4.6 UV-VIS spectra of aptamer (M09P) based gold nanoparticle aggregation incubated with target peptide SV-14 and control peptide PV-12

Figure 4.7 MALDI spectrum of elute from A) interaction between biotinylated aptamer J91P and GQ-14 showing the monoisotopic mass associated with the peptide GQ-14 B) interaction between biotinylated aptamer J91P and SV-14 showing the monoisotopic mass of the contaminates C) biotinylated aptamer without incubation with any target (as control experiment)

List of Tables

Table 1.1 Overview of T-cell stimulatory peptides in wheat gluten, hordeins, secalins (Sollid et al., 2012; Bodd et al., 2012).

Table 1.2 Description of method or principle used in some modified SELEX types

Table 1.3 The overview on aptamer and aptamer-based methods for detection of gluten

Table 2.1 Optimised conditions of PCR for amplifying N20 aptamer library

Table 2.2 Details of SELEX rounds with increasing stringency

Table 2.3 Components and amounts of Ligation reaction mixture

Table 2.4 Physiochemical property of the target peptide sequence GQGQQGYYPTSPQQ (GQ-14) of HMW-GS

Table 2.5 Distribution of secondary structure apt_J91 as predicted by Dichrowed

Table 2.6 Sequences of aptamer candidates of 56 bp containing 20 nucleotide random region with flanking primer regions selected against GQ-14

Table 2.7 Thermodynamic parameters of the aptamer sequences as calculated by mfold software

Table 2.8 List of dissociation constant and thermodynamic parameters calculated through ITC study of interaction between apt_J91P and GQ-14 in 1x ABB

Table 2.9 List of dissociation constant and thermodynamic parameters calculated through ITC study of interaction between apt_J91P with flanking region and GQ-14 in water

Table 3.1 Optimised conditions of PCR for amplifying N40 aptamer library

Table 3.2 Details of SELEX rounds with increasing stringency

Table 3.3 Components and amounts of Ligation reaction mixture

Table 3.4 Physiochemical property of the target peptide sequence SQQQPPFSQQQQPV (SV-14) of LMW-GS

Table 3.5 Estimation of secondary structure distribution of peptide SV-14 by Dichroweb

Table 3.6 Sequences of aptamer candidates of 76 bp containing 40 nucleotide random region with flanking primer regions selected against SV-14

Table 3.7 Thermodynamic parameters of the aptamer sequences as calculated by mfold software

Table 3.8 List of dissociation constant and thermodynamic parameters calculated through ITC study of interaction between apt_M09P and SV-14 in 1x ABB

Table 3.9 List of dissociation constant and thermodynamic parameters calculated through ITC study of interaction between apt_J51P with flanking region and GQ-14 in water

Chapter 1

Introduction and Literature Review

Chapter 1: Introduction and Literature Review

1.1. Introduction

The celiac disease (CD) or celiac sprue or Gluten sensitive enteropathy is an permanent autoimmune enteropathy of upper small intestine which is caused by ingestion of dietary gluten, a protein complex found in various types of cereals like wheat, rye, barley and rarely oats in genetically susceptible subjects of all ages (Alarida et al. 2011). It is affecting at least 1% of the Caucasian population (Marciano et al., 2006) which makes it one of the most common food intolerance in the world. Many indigestible peptides present in both the gliadin and glutenin fractions of the gluten or similar protein present in wheat, rye and barley trigger immune reactions and cause inflammation of the duodenal mucosa. It can lead to conditions like reduced enterocyte height, crypt hyperplasia, villous atrophy along with increased intraepithelial T lymphocytes (Shewry et al., 1992; Tonutti et al., 2014; Parzanese et al., 2017).

Celiac disease commonly appears in the early childhood, with sore symptoms including chronic diarrhoea and failure to thrive. The symptoms can also develop later in life, which includes diarrhoea, fatigue, and weight loss due to malabsorption and anaemia (Vilppula et al., 2011). Celiac disease is a lifelong disease, untreateble and associated with raised morbidity and mortality (Foschia et al., 2016). Celiac Disease is now recognised as multisystemic disorder (Malalgoda & Simsek, 2017). The dietary gluten contents proline and glutamine rich peptides which are resistance to intestinal digestive enzymes and gets modified by tissue transglutaminase enzymes. These immunogenic toxic peptides bind to MHC Class-II HLA-D2 or HLA-D8 molecules with high affinity to trigger immune reaction. The genetic predisposition associated with celiac disease is the specific HLA class II genes known as HLA-DQ2 and HLA-DQ8 located on chromosome 6p21 (Sollid, 2002). Once though as a western countries' disease, but recently it has been reported in almost all part of the world. Many studies have shown that India is also among the significantly high prevalence countries of celiac disease occurrence. Because of the common ancestry with European population and consumption of wheat in Northern India, 0.7% of Indian population is effected by celiac disease (Lionetti & Catassi, 2011). Consumption of a gluten free diet throughout life is the only treatment available for celiac disease till now. The presence of celiac disease epitopes in storage proteins of wheat, barley and rye makes the food products based on these cereals are not suitable for the patients (Kelly et al., 2015). The maintenance of gluten free diet is a challenge for both the celiac

disease patient and the food production companies as gluten gets contaminated into the food by many sources. Therefore the knowledge about safety of different wheat or rye or barley varieties for celiac patient is crucial. A robust analytical method for detection of celiac disease epitopes in food material is necessary. Although many analytical techniques of gluten detection are available, but each method has some disadvantages associated with. The most widely used method in gluten detection is ELISA based on monoclonal antibodies, the limitations associated with antibody such as high production cost, low shelf life, challenges in chemical modification, denaturation in gluten extrcation buffer etc. has raised demand for an alternative method (Scherf, & Poms, 2016). A novel non-protein receptor with enhanced affinity to the target while being stable and economical is crucial for development of new assays and advanced detection devices like biosensors (Amaya-González et al., 2013). Aptamers fulfil these criteria and researchs have been carried out extensively on use of aptamers for food safety applications.

1.2. Literature Review

1.2.1. Pathogenesis of Celiac disease

The pathogenesis of celiac disease is initiated by the combined influence of two factors, i.e. genetic and environmental. Genetic factor refers to the genetic predisposition due presence of several specific genes, while environmental factor solely is the ingestion of gluten. In 1950, William Karel Dicke was the first to recognise that ingestion of wheat may cause celiac disease (Malalgoda & Simsek, 2017). There are some peptide sequences present in the gluten protein resistant to digestion in the intestine due to high presence of proline and glutamine residues. The mixture of these undigested peptide fragments accumulates in the small intestine and they act as immunogenic and toxic epitopes to induce celiac disease. These epitopic peptides bind to the chemokine receptor CXCR3 present in intestine mucosa which causes the release of zonulin protein, a physiological modulator of intercellular intestinal tight junctions (TJ). Release of zonulin causes the disassembly of TJ, which increases intestinal permeability (Lammers et al., 2008). Celiac disease pathogenesis occurs by permeation of these toxic peptide through intestinal mucosa to reach the sub-epithelial lymphatic tissue (Fasano et al., 2012). Gluten peptides are involve in both adaptive and innate immune responses after reaching lamina propia (Gianfrani et al., 2005).

The presence of the genes HLA-DQ2 and HLA-DQ8 contribute strongly in development of the celiac disease in patients. About 90-95% of the celiac disease patients have the HLA-DQ2 gene, which also have two isoforms, the dominant HLA-DQ2.5 and the rare HLA-DQ2.2. In individuals with these genetic makeup, antigen presenting cells such as dendritic cells, macrophages and B cells express the two HLA-class II molecules, DQ2 and DQ-8 molecules on their cell surfaces. Although the presence of the HLA alleles for celiac disease initiation is well established, it is also found that non-HLA alleles may also contribute in the disease development. The characterization such non-HLA genes are not completely done yet, but about 39 non-HLA loci have been identified as a contributor for celiac disease development (Sollid et al., 2012). The both innate and adaptive immuno-response work to initiate the enteropathy in celiac disease. The adaptive immune response to the toxic gluten peptide starts when these peptides binds with the HLA-DQ2/DQ8 molecules and the APCs present HLA-DQ2/DQ8 bound peptides to the T-cell receptors in gluten sensitive $CD4^+$ T-cells causing an inflammatory T-cell response. The tissue transglutaminase enzyme converts the specific glutamine residues of the toxic peptides to glutamic acid through deamination reaction with water. Deamination of glutamine increases the affinity of the toxic peptide fragments for HLA-class II protein, although it is not necessary for activation of the T-Cells. The conversion of glutamine (Q) residues into glutamic acid (E) increases the overall negative charge of the peptide which is responsible for the increased in affinity (Malalgoda & Simsek, 2017; Caio et al., 2019). The presence of negative charge on amino acids at specific position enhances the interaction with basic amino acids residues present at the anchor position of the HLA-DQ2 and DQ8 molecules (Ciccocioppo et al., 2005). The interaction of gluten peptides and $CD4^+$ T-cells leads to the increased expression of cytokines Interferon (IFN)-γ, Interleukin (IL)-2 and Tumor Necrosis Factor (TNF)-α in the lamina propria. This is followed by the release and activation of matrix metalloproteinases (MMPs) that degrades the extracellular matrix proteins resulting in mucosal destruction and followed by epithelial apoptosis. Once the deaminated peptide fractions are recognised by the $DQ2/8^+$ antigen presenting cell, they are presented to the T helper cells. This also stimulates the activation and maturation of B-cells which produce antibodies IgM, IgG, and IgA against the gluten peptides, tissue transglutaminase and the peptide complexes formed due to the activity of the enzyme. T helper cells along with pro-inflammatory cytokines (interferon γ and tumor necrosis factor α) are involved in the damage of the epithelia cell. The $CD4^+$ T-cell mediated adaptive immune response is triggered by the upregulation of IL-15 during innate immune response (Malalgoda & Simsek, 2017; Caio et al., 2019). The innate immune response starts with secretion of cytokines such as interleukin (IL)-

15 and interferon-α by epithelial cells and lamina propria cells. Interleukin (IL)-15 specifically affects the proliferation, localisation and function of intraepithelial lymphocytes (IELs) and dendritic cells (Barone et al., 2015). Although the peptide epitopes are involved in adaptive immune-response; however, some epitopes induce the innate immune-response too. Some toxic peptides directly bind to enterocytes, macrophages and dendritic cells for induction of innate immune-response. The $CD3^+$ IELs may express the natural killer cell receptors, NKG2D and CD94 receptors while the epithelial cells express the ligand to NKG2D due to the trigger by overexpressing IL-15 and their interaction leads to destruction of the epithelial cells. During activation of innate immunity, celiac lesion are seen due to tissue remodelling as the toxic peptides induce IL-15 and epithelial growth factor (EGF)-dependent enterocyte proliferation and actin rearrangements leading to crypt hyperplasia (Malalgoda & Simsek, 2017; Caio et al., 2019).

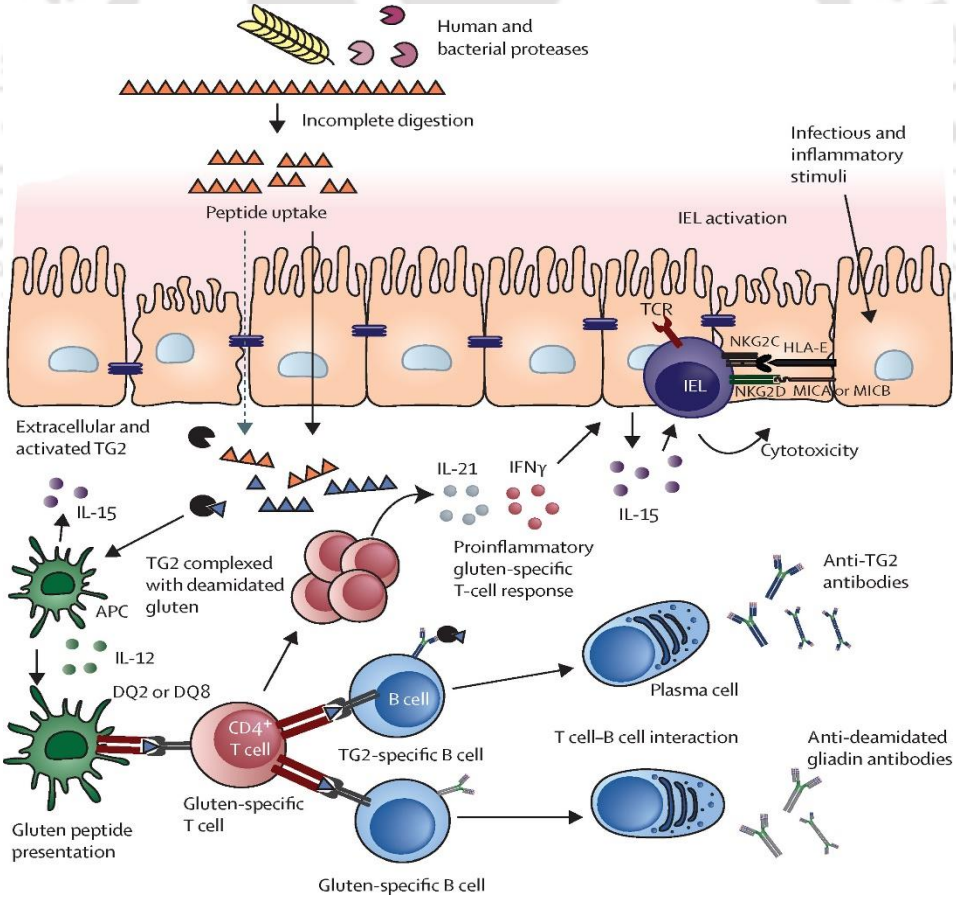

Figure 1.1 A schematic representation of the mechanisms involved in Celiac disease pathogenesis (Reprinted with permission from Catassi et al., 2022, copyright Elsevier 2022).

1.2.2 Clinical features

The most common symptoms of celiac disease are diarrhea, vomiting and abdominal pain (Scherf et al., 2016). Due to malabsorption of nutrients, conditions such as vitamin and mineral deficiencies, anemia, night blindness and weakness of bones could occur. Celiac disease is also reported to slower the growth of children and adolescents and cause issues in the reproductive health of women (Lauret & Rodrigo, 2013).

Immune response in celiac disease manifests mainly into degradation of the extracellular matrix proteins, damage of the mucosal epithelium and the production of antibodies against toxic peptide fractions of gluten, tissue transglutaminase and peptide complexes formed due to the activity of the enzyme. These result into the physiological symptoms in the celiac disease patients. The symptoms can be categorised into - intraintestinal and extraintestinal features.

In intraintestinal features, the classical symptoms of celiac disease mostly include diarrhoea, steatorrhea, vomiting, and abdominal pain. The patients can also develop non-classical symptoms like constipation, weight gain, and gastroesophageal reflux disease etc. Celiac disease is characterised by villous atrophy which is caused by mild partial damage to a total absence of villi, crypt hyperplasia, and increased lymphocyte infiltration of the epithelium damaging the mucosa of the upper small intestine. The extraintestinal features developed due to mucosal damage include development of symptoms from malabsorption of nutrients such as vitamin and mineral deficiencies leading to anaemia, decreased bone mineral density, bone pain and fractures, dental enamel defects, and night blindness. In addition to these, children and adolescence may suffer from slow growth rate and delayed puberty. Female patient of celiac disease may experience issue with mensuration and reproductive health. Celiac disease patients may also suffers from associated conditions arised due to autoimmune nature of the disease such as type 1 diabetes mellitus, autoimmune thyroid disease, juvenile chronic arthritis etc. Sometimes, psychiatric symptoms such as depression, anxiety, migraine, cerebellar ataxia, and epilepsy are also seen in a very small number of patients (Scherf et al., 2016; Newton & Singer, 2012).

Overall celiac disease is a heterogeneous systemic disorder that manifests in patients depending on their age, the duration and extend of the disease, and extraintestinal comorbidities associated with it. Depending on the clinical presentation of symptoms, the disease can be grouped into various subtypes (Scherf et al., 2016; Newton & Singer, 2012) -

a) Classical or typical form

It shows the common symptoms associated with celiac disease with villous atrophy and crypt hyperplasia that hinders the adsorption of nutrients in intestine. It arises at the infant stage during age of 6 to 18 months, after they start eating food containing prolamins.

b) Atypical form

In this form of celiac disease, the gastrointestinal symptoms are not detected; however, the extra-intestinal symptoms are prevalent in the patients. This form arises in older children and adults.

c) Silent or asymptomatic form

This form does not show any clinical symptoms associated with celiac disease. However, it is characterised by the serological and histological indicators of the disease. It is often detected in patients with a hereditary history of celiac disease or patients suffering with associated genetic disorders such as Down, Turner, or Williams's syndrome and autoimmune disease like type 1 diabetes.

d) Latent form

This form of celiac disease is detected after the disease has been resolved after occurrence at some point of time in past and reintroduction of gluten based diet has been started. Like the asymptotic form of celiac disease, it does not show any clinical manifestation; however, subtle morphometric abnormalities of the enterocyte can be detected along with elevated endomysial antibodies.

e) Potential form

This form of celiac disease is referred to the individuals that have no sign and symptoms and never been diagnosed with celiac disease, however they have genetic predisposition with presence of genes HLA-DQ2/DQ8. They may be also detected with serological indicators along with normal or minutely abnormal intestinal histology.

f) Refractory form

A very small number of celiac disease patients (2-5%) may have persistent or recurring malabsorptive symptoms and villous atrophy with elevated levels of IELs even after they are on a gluten-free diet till 6 months or one year. Based on the immunophenotype of IELs, refractory form of celiac disease can be classified as type 1 (normal IELs count) and type 2 (abnormal IELs count).

1.2.3. Epidemiology of Celiac Disease

Initially celiac Disease was thought to be only prevalent in European countries, but now it is known to be distributed throughout the world. Regions like Africa, the Middle East, Asia and South America were initially thought to be free of celiac disease, however with new epidemiological studies, it is clear that these regions also have a considerable number of population with celiac disease. The worldwide distribution of celiac disease indicates that the disease followed the path of spread of wheat as food item, along the route of migration of mankind (Gujral et al., 2012). The prevalence of the disease is increasing constantly and has increased over fourfold in the last half-century (Lerner et al. 2015). Celiac disease occurs in about 1% of the population worldwide, although most people with the condition are undiagnosed (Lebwohl et al., 2015). Celiac disease is highly prevalent in most of the developed European countries (2.0% in Finland, 1.2% in Italy, 0.9% in Northern Ireland, and 0.3% in Germany) as well as in the countries of individuals with European origin (like Australia, New Zealand and USA). The rate of prevalence of celiac disease in the developing world is almost comparable to the rates in Europe as it can be seen in North Africa (i.e., 0.53% in Egypt, 0.79% in Libya, and 0.6% in Tunisia), Middle East (i.e., 0.88% in Iran and 0.6% in Turkey), and India (i.e., 0.7%). (Lionetti & Catassi, 2011). It is also estimated that the prevalence of celiac disease is 0.4% in South America, 0.5% in Africa and North America together, 0.6% in Asia, and 0.8% in Europe and Oceania. The prevalence was found to be more in female population than in male (0.6% vs 0.4%; P <0.001) (Singh et al., 2018). Recent systematic reviews and meta-analysis reveal the prevalence of celiac disease at 1.4% tested by serological method and 0.7% by biopsy based method. Sex, age and location plays a role in difference in celiac disease prevalence. In the Italian children, celiac disease prevalence is found to be unusually increased in 2015-2016 to 1.58% compared to 25 years ago (0.88%, 1993-1995) (Gatti et al., 2019).

Preliminary Epidemiology data from Punjab, North India suggests prevalence as high as 1:310 in case of children (Sood A. et al., 2006). Study on urban and rural populations in the National Capital Region, Delhi, India has found out the overall prevalence of celiac disease in North India is 1.04% (1 in 96) (Makharia et al., 2011). In 1960, celiac disease was first recognized in northern Indian children (Ramakrishna et al., 2016). The prevalence of celiac disease primarily depends on two factors; the capability of population to express HLA-DQ 2 or 8 and consumption of gluten containing cereals (Lionetti & Catassi, 2011). In India, the north-western states such as Punjab, Delhi, Haryana, Rajasthan, Madhya Pradesh, Uttar

Pradesh and Bihar falls under the so-called "Celiac belt" as the consumption of wheat is higher in these places. Whereas, the frequency of DQ2 allele was found to be slightly higher in north India (38.1%) than south India (36.4%) and northeastern India (31.4%). Although, there is not much difference in the genetic background responsible for developing the disease in the three Indian region, the higher consumption of wheat is a factor due to which north Indian has a high prevalence of symptomatic celiac disease. The asymptomatic celiac disease is prevalent in both north and northeastern India, while in south India is much lower than the other two regions (Ramakrishna et al., 2016).

As number of population with asymptotic cases are more than the symptomatic celiac disease, the epidemiology of the disease is represented with a ''celiac disease iceberg'' model. The iceberg of this model represents the total population effected by celiac disease as result of combine influence of genetic predisposition and wheat consumption patterns. The 'tip' of the iceberg represents only the patients with visible syndrome while submerged portion represents the because of atypical patients. Undiagnosed celiac disease patients cannot receive timely treatment, and will have an elevated risk for developing secondary autoimmune disorders (Yuan et al., 2013; Lionetti et al., 2015).

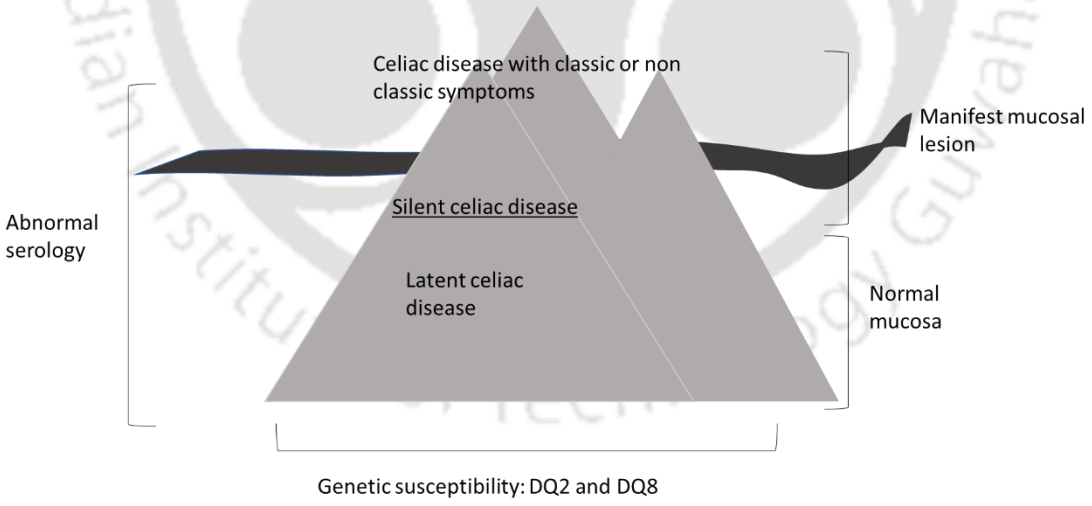

Figure 1.2 The celiac disease iceberg model (adopted from Lionetti & Catass, 2011)

1.2.4 Genetic factor: Human Leukocyte Antigen (HLA) Locus

The genetic background playing a deterministic role in the celiac disease development was elucidated from the fact that monozygotic twins have higher concordance rate of 83-86% than dizygotic twins with 11% concordance rate. The association of celiac disease with other autoimmune disease in individuals or in their first-degree relative also confirm that it has a common genetic predisposition related to autoimmunity (Megiorni & Pizzuti, 2012). In studies carried out by two groups (Strober and Cooke), the presence of HLA-B8 antigen was found in 88% celiac disease patients in United States and England, while it is 22–30% in control population. This established the link of HLA gene with celiac disease. The association was found to be stronger between celiac disease and HLA-DR3 and HLA-DQ2. Later through cloning of major histocompatibility (MHC) class II genes, it was established that celiac disease susceptibility is strongly influenced by genes encoding an HLA-DQ2 variant and HLA-DQ8 (Abadie et al., 2011).

Based on genetic linkage and genetic association studies, Human Leukocyte Antigen (HLA) system has been found to play a major role in development of celiac disease. The HLA super-locus is located on the short arm of the chromosome 6 (6p21.3) which is a 4000 kb wide genomic region. The HLA super-locus can be grouped into five regions, the extended class I, class I, class III, class II and extended class II regions (Martina et al., 2018). The HLA class I and class II genes encodes cell surface glycoproteins that are involved in antigen presentation to the immune cells, recognition of self and also few fundamental functions in cellular and molecular phenomenon. The HLA class II glycoproteins have a heterodimer structures necessary for antigen presentation composed of an alpha-heavy chain encoded by HLA-A, B or C loci and a small beta-2 microglobulin chain encoded by HLA-D region. The HLA-D region is located in chromosome 15 and contains HLA-DP (DPA1 and DPB1), HLA-DQ (DQA1 and DQB1) and HLA-DR (DRB1 and DRA) genes. These HLA class II glycoproteins can present the exogenous antigens to CD4+ lymphocytes to activate humoral immune response. The HLA class I glycoproteins are also structurally similar to class II and both classes resembles to Fab region of immunoglobulin. However, HLA class I glycoproteins presents endogenous antigens to CD8+ lymphocytes to trigger cytotoxic response (Megiorni & Pizzuti, 2012; Martina et al., 2018).

Celiac disease is characterised as polygenic disease with high inheritance of non-Mendelian pattern (Dieli-Crimi et al., 2015). The HLA locus inherited as haplotype where

many alleles are frequently transferred together due to extensive linkage disequilibrium (Martina et al., 2018).

Commonly celiac disease is strongly associated (about 90%) with HLA-DQ2.5 in individuals carrying DR3DQ2 haplotype (DRB1*03:01-DQA1*05:01-DQB1*02:01) and the expressed DQ2.5 molecule is encoded by alleles DQA1*05 and DQB1*02 located on the same chromosome i.e. *cis*-configuration. In case of heterozygous traits in individuals with DR5DQ7/DR7DQ2 haplotypes (DRB1*11/12-DQA1*05:05-DQB1*03:01; DRB1*07-DQA1*02:01-DQB1*02:02), it can be encoded by alleles located on opposite chromosomes, i.e. *trans*-configuration. The most of the remaining patients (5-10%) are affected by the presence of DR4DQ8 haplotypes (DRB1*04-DQA1*03:01-DQB1*03:02), where DQ8 heterodimer is encoded by DQA1*03 and DQB1*03:02. A very small portion of the celiac disease patients express either DQ2.2 molecule encoded by DQA1*02:01 and DQB1*02:01 or DQ7.5 molecule encoded by DQA1*05 and DQB1*03:01 in *trans*-configuration. These molecules are 'half' of DQ2.5 molecule and they expressed when celiac disease patients do not express either of DQ2.5 or DQ8 (Sollid et al., 2012). The **figure 1.3** shows Human leukocyte antigen (HLA) genotype and their associated magnitude of risk for coeliac disease. The susceptibility of celiac disease due to influence of HLA-DQ genes are explained by a gene-dose effect. The presence of specific alleles like DQA1*05 in HLA-DQA1 and DQB1*02 in HLA-DQB1 genes of an individual influences the number peptide the expressed heterodimer binds to initiate immune respond. Individuals with homozygous DQ2.5cis (DQ2.5/DQ2.5) and heterozygous DQ2.5cis (DQ2.5/DQ2.2) fall under highest risk group. Individuals with heterozygous DQ2.5cis (DQ2.5/DQ8) or heterozygous DQ2.5trans are grouped into intermediate risk group. Individuals with heterodimer HLA-DQ2.2 encoded by HLA-DQA1∗0201 and HLA-DQB1∗02 alleles is in the low risk group (Abadie et al., 2011; Dieli-Crimi et al., 2015; Martina et al., 2018). Although the risk of developing celiac disease may low due to presence of specific heterodimer, the clinical manifestation of the disease is same irrespective of the HLA-DQ type (Ting et al., 2020).

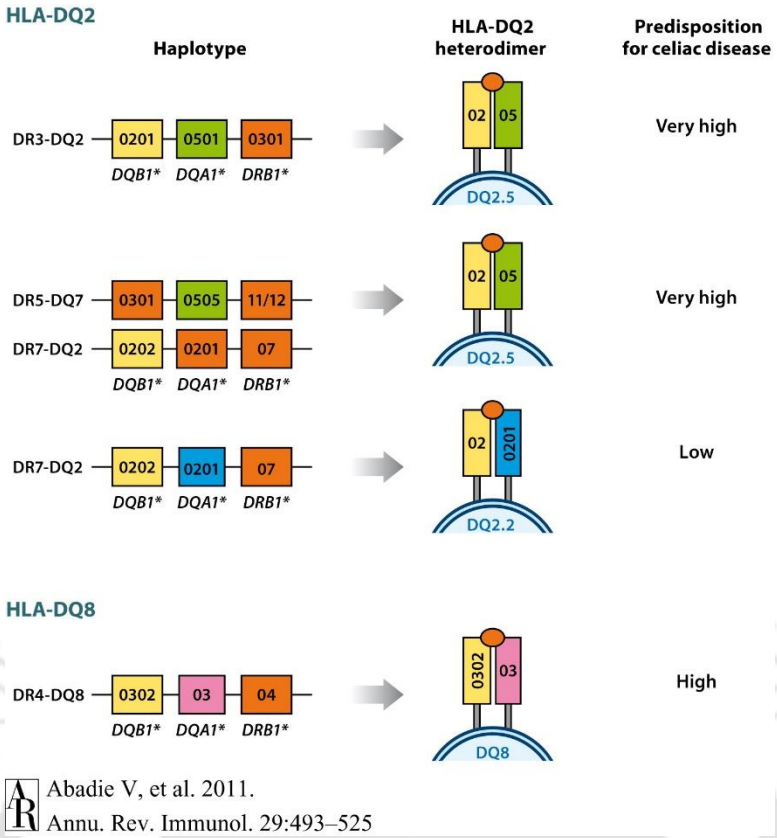

Figure 1.3 Human leukocyte antigen (HLA) genotype and their associated magnitude of risk for coeliac disease (Reprinted with permission from Abadie et al., 2011, copyright Annual Reviews)

The HLA-DQ gene locus has been named as *CELIAC1* by HUGO Gene Nomenclature Committee (http://www.genenames.org/), which is alone responsible for approximately 40% for the inheritance of the disease. New genome-wide association studies (GWAS) have identified other non-HLA gene locus such in chromosome locations 5q31-q33, 2q33 and 19p13 and termed as *CELIAC2*, *CELIAC3* and *CELIAC4* respectively as weak genetic predisposition factors (15%). The Th2 cytokine gene cluster and interleukin genes are located in CELIAC2 and the genes involved many autoimmune diseases such as Crohn's disease, type 1 diabetes, asthma, psoriasis and rheumatoid arthritis are located in *CELIAC3*, which make them shared risk variant for celiac disease. However, these locus are yet to be characterised fully to consider as risk factor in celiac disease (Koskinen et al., 2009; Megiorni & Pizzuti, 2012).

1.2.5 Gluten protein

Cereals are one of most widely used food grains worldwide for making homemade and industrial foods (G Chirdo & Arranz, 2015). Storage Protein in cereals have two different fractions - prolamins and glutenins. The prolamins of wheat are referred to as gliadins. The term 'Prolamin' was coined to reflect the high content of proline and glutamine (Shewry, 2019). Prolamins from other cereals also are considered to be gluten and are named according to their source (gluten in wheat, secalins from rye, hordeins from barley, avenins from oats, and zeins from corn) (Shewry, 1995). 'Gluten' is also commonly referred to the homologous prolamins present in rye, barley and oats. Cereals belonging to the *Triticeae* tribe such as wheat, rye and barley have a common ancestral origin. Therefore, prolamins from wheat, rye and barley possess the immune-reactive peptide sequences responsible for celiac disease. On the other hand, oat belongs to a separate *Aveneae* tribe which along with *Triticeae* is in the same sub-family called *Festucoideae*. Oat is closely related to *Triticeae* tribe, however, it is placed at little distance from wheat from phylogenetic point of view and this make oat's prolamin, called avenin, rarely immune-reactive to induce celiac disease. The hexaploid bread wheat (*Triticum aestivum* L.) with genome composition AABBDD, the tetraploid pasta wheat (*Triticum durum* L.) with genome composition AABB and diploid wheat (*Triticum monococcum* L.) with genome composition AA are well studied. The hexaploid and tetraploid wheat species have prolamins with diverse composition than the prolamins of diploid rye (*Secale cereale* L., genome composition RR) and barley (*Hordeum vulgare* L.) as the gene encoding these proteins are located in genomes A, B and D (Balakireva & Zamyatnin, 2016; Kilmartin et al., 2006). Oat contains lower quantity of storage protein and their proline content is also low when compared to the other cereals from *Triticeae* tribe (Wahab et al., 2012).

The prolamins from wheat, rye and barley along with those from oat, maize and rice together forms a prolamin superfamily. Prolamin superfamily protein shared a basic structure that contains- (i) signal peptide for translocation into cellular compartments, (ii) a non-repetitive N-terminal region, (iii) a non-repetitive C terminal region and (iv) a long repetitive central region (Balakireva & Zamyatnin, 2016). Depending on presence of sulphur-containing amino acids, Sherwy classified all prolamins into broad 'families'- sulphur-rich (S-rich), sulphur-poor (S-poor) and high molecular weight (HMW) prolamins (Sherwy, 2019). The central region has repeating units of glutamine-rich and proline-rich sequences unique to each prolamin. The S-rich and S-poor prolamins share similarities in the motifs of the central region,

while it is found that the position of cysteine is highly conserved between HMW proteins and S-rich prolamins (Balakireva & Zamyatnin, 2016).

Gluten has been defined as the "the rubbery mass that remains when wheat dough is washed to remove starch granules and water-soluble constituents" (Weiser, 2007). Codex Alimentarious Commission (Codex Alimentarious Commission, Foods for Special Dietary use for Persons Intolerant to Gluten., Rome, Italy, 2008.) defines gluten as 'the protein fraction from wheat, barley, rye, oats or their crossbred varieties and derivatives thereof, to which some persons are intolerant and that is insoluble in water and 0.5 M NaCl". No nutritional value has been attributed to gluten (Wieser, 2007). Wheat grain consist of 75%– 80% starch and 10%–15% protein (Woldemariam et al., 2022). As storage protein, gluten are found in the starchy endosperm of the grains and it constitute about 70-80% of the total protein content of the grain (Scherf et al., 2016). The glutamine and proline contents in gluten is about 35% and 15% of total amino acid respectively. The glutamine residues acts as nitrogen source for the seedlings developing from the wheat seed and the proline residues are suspected to be involved in the protection of the seedlings against drought (Koning et al., 2005).

Osborne used a fractionation method for isolation of wheat kernel proteins based on the solubility in different solvents, where he classified the water soluble fraction as albumins, saline soluble fractions as globulins, dilute acid or alkali soluble fraction as glutelins and alcohol-water soluble fraction as prolamins (Osborne & Voorhees, 1894). Based on the solubility in 60% ethanol (i.e. alcohol-water solution), the two constituent fractions of gluten proteins can be derived. The alcohol soluble fraction of gluten is known as gliadin while the alcohol insoluble fraction is glutenins (Wieser, 2007). Gliadin fraction is monomeric and glutenins are polymeric in nature formed by interchain disulfide bonds (Wieser, 2006). The gliadin fraction of gluten can be classified as α-, β-, γ-, and ω-gliadins from fastest to slowest based on their electrophoretic mobility in SDS-PAGE at low pH. The α- gliadin and β- gliadin show sequence similarity, therefore they are also placed in a single group, termed as α- type gliadin (Shewry, 2019). The glutenins are classified as the high molecular weight (HMW) glutenin and low molecular weight (LMW) glutenin. Both the gliadin and glutenin fractions are involved in the induction of celiac disease pathogenesis (Balakireva & Zamyatnin, 2016).

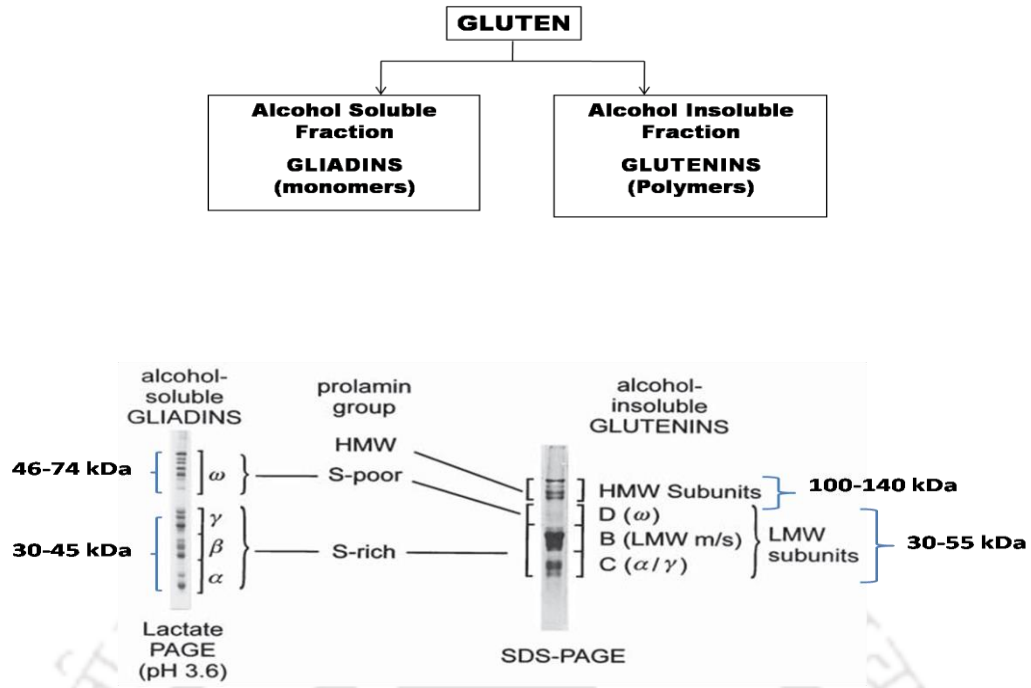

Figure 1.4 Classification of Prolamines (Reprinted from Tatham et al., 2000 with permission, copyright Springer, 2000)

The gliadin and glutenin content in wheat varieties vary which affect the dough making quality of the wheat variety in making products like breads, cookies, noodles etc. Glutenin contains a large number of cysteine residues that allows them to form disulphide bonds between the glutenin molecules. These bonds in glutenin are responsible for providing the elasticity and formation of the matrix in wheat dough. The gliadins molecules that link to these matrix can provide viscosity to the dough by binding to water (Koning et al., 2005). A viscoelastic matrix formed by gluten is mainly composed of 30% gliadins, 50% glutenins and 20% other proteins (Woldemariam et al., 2022). The glutamine residues are abundantly present in all types of gluten protein which makes the amino acid composition largely 'hydrophilic'. However due to formation of hydrogen bonds between same or other gluten subunits more favourably than with water result in the insolubility of the protein in water (Shewry & Lafiandra, 2022).

Due to the functional advantages in making food products, gluten is an indispensable part of diet for a huge portion of human population. However, it is also responsible for various disorders that certain percentage of the population with genetic predisposition suffers. Consumption of gluten may cause, (i) Autoimmune (IgG/IgA) diseases like celiac disease, gluten ataxia and dermatitis herpetiformis (ii) Allergic (IgE) disease like wheat-dependent

induced anaphylaxis (WDEIA) (iii) Non-autoimmune non-allergic (innate immune, IgG) disease like non-celiac gluten sensitivity (NCGS) (Woldemariam et al., 2022).

1.2.5.1 Gliadin

The gliadin proteins are a highly heterogeneous containing 40 components whose molecular weight ranges between 28-55 KDa (Malalgoda & Simsek, 2017). These constituent proteins can be assigned to the four sub-groups (α-, β-, γ- and ω-gliadins) based on electrophoretic mobility or the three updated types based on the N-terminal amino acid sequence similarities (α-, γ– and ω–types) (Ciccocioppo et al., 2005). In polyacrylamine gel electrophoresis at acidic pH (3.1), the bands of α-, β-, γ-, and ω- gliadins are obtained at 25–35 kDa, 30–35 kDa, 35–40 kDa and 55–75 kDa respectively (Asri et al., 2021).

The gliadin proteins are encoded by multigene, which are located on homologous loci *Gli-A1, -B1* and *-D1* on the short arm of chromosome 1 and *Gli-A2, -B2* and *-D2* loci on the short arm of chromosome 6. The gene are highly polymorphic as for some *Gli* loci more than 30 allelic variants have been identified. The γ- and ω-gliadins fractions are encoded by some of the *Gli-1* genes, while the α-/β- and some of the γ-gliadins fractions are encoded by *Gli-2* genes. Gli-1 genes also encode LMW-glutenin subunit, due to which strong associations between the γ - and ω-gliadins and LMW-glutenin are observed. Additionally, there are also some of the minor gliadin loci present on 1AS (*Gli-A3, -A5* and *-A6*), 1BS (*Gli-B3* and *-B5*) and 1DS (*Gli-D4* and *-D6*) (Balakireva & Zamyatnin et al., 2016; Asri et al., 2021). The gene copy numbers for α-gliadin are almost 25 to 150 per haploid genome and it has a highly diverse and complex gene family. Due to high copy number, α-gliadin encoded by *Gli-D2* loci of D-genome contains most immunogenic peptides. This is followed by γ-gliadins in terms of immunogenicity, which have gene copy number of about 15 to 40 per haploid genome. The α-gliadin encoded by the *Gli-B2* loci present in B-genome are least immunogenic containing few immunogenic celiac disease inducing peptides (Sharma et al., 2020).

The gliadins are monomeric protein. Each type of gliadin has a specific secondary structure formation. α/β- and γ-gliadins forms α-helices and β-sheets, while ω-gliadins remains as randomly coiled β-turns. The α-helices and β-sheets of α/β- and γ-gliadins are stabilised primarily by hydrogen bonds (Tatham et al., 1985). Stability is also obtained through intramolecular disulfide bonds and these bonds are converted into interchain disulfide bonds through SH–SS interchain reaction to attach with the glutenin molecules on heating (Schofield

et al., 1983). Majority of the celiac disease inducing toxic peptides have been identified and found to be located in the repetitive N-terminal domain of α-/β-gliadins which are rich in amino acid residues mainly glutamine, proline along with aromatic amino acids, such as phenylalanine and tyrosine (Malalgoda & Simsek, 2017).

1.2.5.2. Glutenins

The glutenins are called 'glutenin macropolymer', one of the largest protein group by size found in nature. Their molecular weight ranges from 60 to more than 10 million KDa. The exact determination of maximum size and size distribution of the polymeric glutenin protein is still to be done (Malalgoda & Simsek, 2017; Shewry & Lafiandra, 2022). The polymeric structure of glutenin protein is formed by the linkages with inter-and intramolecular disulfide bonds. The intramolecular disulphide bonds can be reduced with reducing agents such as 2-mercaptoethanol and dithiothreitol which release the subunits of glutenin. After reduction, the subunits are soluble in aqueous alcohol solution like the gliadin molecules (Wieser, 2007). The subunits can be separated based on their electrophoretic mobility in sodium dodecylsulphate polyacrylamide gel electrophoresis (SDS-PAGE). Subunit with mass range in about 60 to 100 KDa are called the high molecular weight glutenin subunits (HMW-GS) and about 30 to 50 KDa are low molecular weight glutenin subunits (LMW-GS). The HMW-GS and LMW-GS constitutes about 30–35% and 65–70% of the total glutenin fraction respectively (Shewry & Lafiandra, 2022), while HMW-GS and LMW-GS accounts for about 10% and 20% of the total gluten protein respectively (Wieser, 2007). The genes encoding HMW-GS are located in the homoeologous loci *Glu-A1*, *Glu-B1*, and *Glu-D1* of the long arms of group 1 chromosomes; while for LMW-GS, it is located in homoeologous loci *Glu-A3*, *Glu-B3*, and *Glu-D3* loci on the short arms of group 1 chromosomes (Sharma et al., 2020).

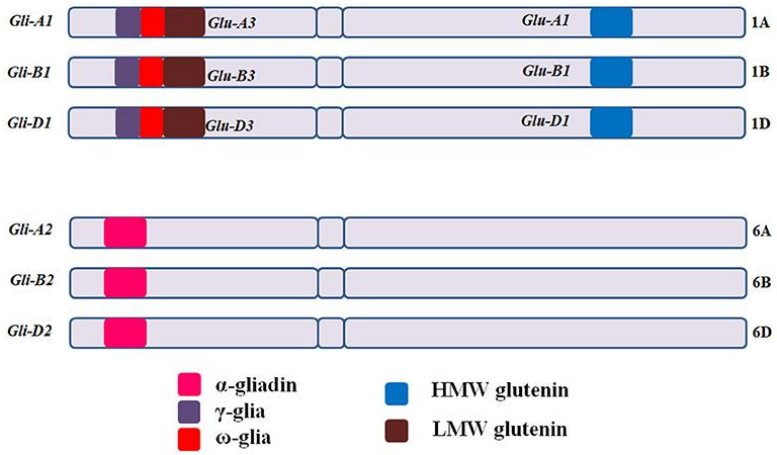

Figure 1.5 Gliadin and glutenin loci in *Triticum aestivum* (AABBDD), 2n = 6x = 42. (Reprinted form Sharma et al., 2020, licensed with CC BY 4.0)

The HMW-GS are further classified in sub-groups as x-type (MW= 83–88 KDa) and y-type MW= 67–74 KDa) subunits based on the molecular mass and electrophoretic mobility. The genes encoding the x- and y-types are present in the *Glu-1* loci, where each loci (*Glu-A1*, *Glu-B1*, and *Glu-D1*) contains two genes related to the both subunits (Asri et al., 2021). On the other hand, LMW-GS are grouped into B-, C-, and D-type subunits based on isoelectric point (pI) and electrophoretic mobility while HMW-GS is considered as A- type. The Glu-3 loci encoding LMW-GS contains several genes, each with more than one allele which makes it difficult to recognise the protein encoded from specific allelic form. The *Glu-3* loci is also linked with the *Gli-1* loci that encodes γ - and ω-gliadin genes and both the *Glu-3* and *Gli-1* loci have role on the LMW-GS expression. Therefore, the sequence similarity can be seen in the C- subunits of LMW-GS with α-/γ- gliadins and D subunits of LMW-GS with ω-gliadins (Asri et al., 2021).

Structurally, The LMW-GS are composed of two domains, the N-terminal domain and the C-terminal domain. The N-terminal domains composed of sequence section I possess glutamine- and proline-rich repeats (QQQPPFS). The C-terminal domain composed of sequence section III-V, have similarity with α-/β- and γ-gliadins in sequence section III and V (Weiser, 2007). The HMW-GS have three domains, which are- (i) a non-repetitive N terminal domain (A) containing about 80–105 amino acid residues (ii) a repetitive central domain (B) containing about 480–700 residues and (iii) a C-terminal domain (C) containing 42 residues. In B domain of x-type HMW-GS, the three priamary repetitive peptide units are present, which are tripeptides (GQQ), hexapeptides (PGQGQQ), and nonapeptides (GYYPTSPQQ). The tripeptide and hexapeptides are found to be present in tandem to each other in the x-type. The

primary repetitive peptide units present in the B domain of y-type HMW-GS are hexapeptides (PGQGQQ) and nonapeptides (GYYPTSLQQ). The domains A and C are mostly conserved, while variation between x- and y- types are seen in B domain. (Li et al., 2020). One of the characteristics of A and C domain is that they contain frequent charged amino acid residue and most of which are cysteine. The central domain is hydrophilic in nature and the N- and C-terminal domains are hydrophobic.

The cysteine residues which are involved in interchain or intrachain disulphide bond formations varies in the distribution across different subunits. It is noteworthy that the most of the cysteine residues in all the subunits (including gliadins) are located in the non-repetitive domains (Sherwy, 2019). In typical x-type subunit, there are four cysteine residues present. Out of which three are in domain A and one is in domain C. Two cysteines in domain A forms intrachain disulphide bonds, while two cysteines are involved in interchain disulphide bond. Exception are observed in the subunit Dx5 where there is an additional cysteine in the B domain and the 1Bx14 and 1Bx20 subunits possess only two cysteine residues in A and C domains. The additional cysteine in B domain of Dx may involve in another interchain disulphide bond formation. In y-type, cysteines are distributed as, five in A domains, one in the B domain, and one in the C domain. The cysteine in A domain of y-type forms interchain disulphite bonds with the parallel corresponding cysteine of A domain in another adjucent y-type subunit. The cysteine from B domain forms interchain disulphite bonds with a cysteine of LMW-GS. The LMW-GS has more abundance in cysteine content as it has total eight cysteines. Six cysteine residues are present in the region of LMW-GS homologous to a/b- and g-gliadins and two are in sequnece sections I and IV. These cysteine are involved in formation of interchain disulphide bonds. Despite the less abundance of cysteine, the HMW-GS is termed as “chain extender” of gluten network as it is extensively involved in formation of either intrachain disulphide bonds or interchain disulphide bonds with other HMW-GSs or LMW-GSs (Weiser, 2007; Li et al., 2020).

1.2.6 Toxic peptides involved in Celiac Disease

The unique composition of cereal proteins that contain high amounts of glutamine and proline residues is the basis of the toxicity of wheat, barley, and rye for patients with celiac disease. Of the total amino acids, the wheat gluten contents around 17–23% proline (P) and 30–36% glutamine (Q). This trend is also followed in hordein of barley and secalin of rye (Wahab et

al., 2012). The presence of the large number of proline (P) makes some polypeptide fractions of gliadin and glutenin resistant to digestion by gastrointestinal enzymes. The proline residues blocks the gastrointestinal post-proline cleaving proteases such as pepsin, trypsin, chymotrypsin, carboxypeptidases A and B, elastases that usually cleaves the polypeptide at a position next to proline residue. These relatively long indigested proline-rich gluten fragments with glutamine in key positions at primary structure are involved in the pathogenesis of celiac disease (Silano et al., 2009; Sollid et al., 2012).

Many studies have been done to screen out the toxic peptide sequences present in the wheat, barley, rye and oat cereals by various *in-vivo* or organ culture or T-cell tests (Ciccocioppo et al., 2005) and homology studies (Vader et al., 2003). Gluten peptides can be either 'toxic' or 'immunogenic'. The "toxic" peptide present in gluten can induce mucosal damage eliciting innate immune response if added *in-vitro* on an organ culture generated form duodenal mucosal biopsy or if administered to proximal and distal intestine through an *in-vivo* experiment. For a gluten peptide to be termed as 'immunogenic' or 'immunostimulatory' or 'immunodominant', it should able to trigger adaptive immune response either in HLA-DQ2- or DQ8- restricted T cell lines and jejunal mucosa derived T cell clones or in the peripheral blood cells collected from celiac disease patients (Ciccocioppo et al., 2005; Silano et al., 2009). For recognition of the toxic or immunogenic peptides by HLA-DQ2- or DQ8, their minimum length should be nine amino acids (Solid et al, 2002; Malalgoda & Simsek, 2017). Few important toxic celiac disease epitopes in cereals proteins are listed in **table 1.1**. The undigested toxic or immunogenic peptides may have amino acids flanking the 9 amino acids long core region at N- and C-terminal ends. These flanking amino acids also involved in the recognition process by CD^{4+} T cells. The peptides when contains same core region and different sequences of flanking region, they may elicit T-cell reactivity differently (Sollid et al., 2020). These peptides have been found in the in α-gliadins, γ-gliadins, and the LMW and HMW glutenins of wheat gluten. In α- gliadin, a 33 amino acid long peptide, resistant to the gastrointestinal enzymes has been identified. This peptide is found to have the highest immunogenicity among all celiac disease epitopes (Wahab et al., 2012). This single 33mer peptide contains three toxic epitopes, PFPQPQLPY, PQPQLPYPQ and PYPQPQLPY of celiac disease specific to CD^{4+} T-cell) (Malalgoda & Simsek, 2017). Apart from wheat gluten, several toxic and immunogenic peptides have also been identified in the similar proteins present in barley and rye, and to a lesser extent in oats (Koning et al., 2005).

The celiac disease inducing peptides in wheat gluten have a relationship with their presence in the protein domains of containing repetitive sequences. These repetitive sequence containing domains accounts for around 30-50% of the total protein sequence in the subunits S-rich gliadins and LMW-GS, around 75-85% in HMW-GS subunits, and almost all the protein sequences in ω-gliadin subunits. The three to nine amino acid sequence long short repeats may be present in tandem of one motif or interspersed as tandem of more than one motifs. Out of the identified celiac disease epitopes, around 31 peptides were found to be present in the repetitive domains of wheat and other cereals like rye, barley and oats and across subunits of gliadin and glutenin containing the epitopes (Shewry, 2019).

The gliadin derived peptides were evaluated initially, which established their role as toxic peptide in initiation of celiac disease. In 1999, van de Wal and his associates for first time also established though *in-vitro* T-cell reactivity assay with HLA-DQ8- restricted gluten-specific T cell clone (TCC) isolated from the small intestine of celiac disease patients that glutenin derived peptides can induce celiac disease. They identified immunogenic peptide SGQGQRPGQWLQPGQGQQGYYPTSPQQSGQGQQLGQ, termed as glt04 (residues 707–742) (Swiss Prot. Accession Number P08489) in domain B of the high molecular weight glutenin subunit. They determined the minimum sequence of amino acid for optimal stimulation of T-cell was QGYYPTSPQQS and identified the repetitive core motive QQGYYPT (van de Wal et al., 1999). The HMW-GS derived peptide GQQGYYPTSPQQS was also demonstrated to be bound preferentially by HLA-DQ8trans (encoded by DQA*0501/DQB*0302), a heterodimer formed by combination of the α-chain of HLA-DQ2 (DQA1*0501) and the β-chain of HLA-DQ8 (DQB1*0302) (Kooy-Winkelaar at al., 2011).

In 2002, Vader et al. used synthetic glutenin peptides to check reactivity of T-cell clones (TCCs) of intestinal biopsy of DQ2 (DQA1*0501/DQB1*02) positive patients against it and found that peptide GLT-156(40-59) with sequence QQQQPPFSQQQQSPFSQQQQ and GLT-17(46-60) with sequence QQPPFSQQQQQPLPQ from glutenin were able to elicit T-cell response when deaminated by tTG enzyme. Truncation of the peptides into varied length also led to identification of minimum length of peptide needed to elicit T-cell response are PFSQQQQSPF and PFSQQQQQ for GLT-156 and GLT-17 respectively (Vader et al., 2002).

In a study to examine the response of T cells of patients with HLA-DQ2.2 towards gluten, Bodd et al. used intestinal T-cell lines and clones from 7 patients with positive HLA-DQ2.2 and check their response through T-Cell Assays while adding enzyme hydrolysed gluten. It

was found that normal epitopes for DQ-2.5 and DQ-8 could not elicit response in T cells with form HLA-DQ2.2 positive patients. However, it was identified that a distinct epitope containing core 9mer amino acid sequence PFSQQQQPV initiated the T-cell response. This peptide is derived from low-molecular-weight glutenin protein and it was found that peptide fraction containing the 9mer core amino acid region with sequence QQP**PFSQQQQPV**LPQ showed highest level of T-cell reactivity (Bodd et al., 2012).

Dørum et al. used HLA-DQ molecules, DQ2.5 and DQ2.2 as an affinity matrix to identify the celiac disease specific T-cell epitopes present in gluten. The HLA-DQ molecules were incubated with enzymatic digest of gluten and treated with tissue transglutamerase-2 (TG2). The HLA-bound gluten peptides were eluted and analysed by mass spectroscopic technique MALDI-TOF and LC-MS/MS. It revealed that gluten peptide recognised by DQ2.5 molecules are well characterised, mostly from gliadin and two peptide sequences identified are PQQPEQIIPQQPQQP from LMW glutenin and QPQQPFPQQPQQPQQPFPQPQQPFP from ω-Gliadin and LMW glutenin. From the DQ2.2 molecule, a total of 34 peptides were identified that contained the 9-mer core amino acid sequence of the previously characterized DQ2.2-restricted epitope, PFSQQQQPV (DQ2.2-glut-L1) or it's homologous sequences. The peptides containing this epitope were found in the majority of the gel filtration fractions of digested gluten. For example, a 38mer long peptide PPFSQQQPPFSQQQQPVIPQQPSFSQQQLPPFSQQQPP and a short peptide QQPPFSQQQQPV were identified that contained the DQ2.2-glut-L1 peptide as underlined. Peptide PPFSQQQPPFSQQQQQPVL with the highly similar sequence to DQ2.2-glut-L1 with more than two time occurrence of the epitope was also detected. Apart from the other peptide fragments from gliadin, LMW glutenin derived peptides QQISQQQQPQISQ and QTFPHQSQQAFPQPQ were also identified as T-cell responsive epitopes of celiac disease (Dørum et al., 2014).

1.2.6.1 Epitope Mapping of some known peptide epitopes in Gliadins, Glutenins, hordeins, secalins and avenins

There are many celiac disease epitopes that have been reported in the various subunits of gliadins, glutenins, hordeins, secalins and avenins cereals protein (wheat, rye and barley). The position of these epitopes can be found in the amino acid sequences of various protein subunits

retrieved from various databases are listed below. An overview of the stimulatory peptides in wheat gluten, hordeins, secalins (Sollid et al., 2012; Bodd et al., 2012) can be seen in table 1.1.

>gi|7209265|emb|CAB76964.1| alpha-gliadin [Triticum aestivum]

MVRVPVPQLQPQNPSQQQPQEQVPLVQQQQFPGQQQPFPPQQPYPQPQPFPSQQPYLQLQ**PFPQPQLPY**PQPQLPYPQPQLPYPQPQP**FRPQQPYPQ**SQPQYSQPQQPISQQQQQQQQQQQQKQQQQQQQQILQQI LQQQLIPCRDVVLQQHSIAYGSSQVLQQSTYQLVQQLCCQQLWQIPEQSRCQAIHNVVHAIILHQQQQQ QQQQQQQPLSQVSFQQPQQQYPSG**QGSFQPSQQ**NPQAQGSVQPQQLPQFEEIRNLALETLPAMCNVYI PPYCTIAPVGIFGTNYR

>gi|170738|gb|AAA34289.1| gamma-gliadin [Triticum aestivum]

MKTLLILTILAMAITIGTANIQVDPSGQVQWLQQQLVPQLQQPLSQQPQQTFPQPQQTFPHQPQQQVPQ PQQPQQPFLQP(**QQPFP(QQPQ)QPFPQ)**T(**QQP(QQPFPQ)QPQ)**QPFPQT(**QQP(QQPFPQ)QPQ)**QPFP QT(**QQPQQPFPQ)**L(**QQPQQPFPQ)**PQQQLPQPQQ(**PQQSFPQQQ)**RPFIQPSLQQQLNPCKNILLQQSKP ASLVSSLWSIIWPQSDCQVMRQQCCQQLAQIPQQLQCAAIHSVVHSIIMQQQQQQQQQQGIDIFLPLSQ HEQVGQGSLVQGQGI(**IQPQQPAQL)**EAIRSLVLQTLPSMCNVYVPPECSIMRAPFASIVAGIGGQ

>gi|31415651|gb|AAP44989.1| low molecular weight glutenin [Triticum aestivum]

MKTFLVFALIAVVATSAIAQMETSCISGLERPWQQQPLPPQQSFSQQPPFSQQQQQPLPQQPSFSQQQPP FSQQQPILSQQP**PFSQQQQPV**LPQQSPFSQQQQLVLPPQQQQQQLVQQQIPIVQPSVLQQLNPCKVFLQ QQCSPVAMPQRLARSQMWQQSSCHVMQQQCCQQLQQIPEQSRYEAIRAIIYSIILQEQQQGFVQPQQQ QPQQSGQGVSQSQQQSQQQLGQCSFQQPQQQLGQQPQQQQQQVLQGTFLQPHQIAHLEAVTSIALRTL PTMCSVNVPLYSATTSVPFGVGTGVGAY

>tr|Q7Y074|Q7Y074_WHEAT Low molecular weight glutenin OS=Triticum aestivum subsp. tibeticum

MKTFLVFALLAVVATSAIAQMETSCIPGLERPWQQQPLQQKETFPQQPPSSQQQQPFPQQPPFLQQQPSF SQQPLFSQKQQPVL**PQQPPFSQQQQPV**LPPQQSPFPQQQQQHQQLVQQQIPVVQPSILQQLNPCKVFL QQQCNPVAMPQRLARSQMWQQSSCHVMQQQCCQQLPQIPEQSRYDAIRAITYSIILQEQQQGFVQPQQ QQPQQSVQGVYQPQQQSQQQLGQCSFQQPQQQLGQQPQQQQQVQKGTFLQPHQIARLEVMTSIALRTL PTMCSVNVPLYSSITSAPLGVGTGVGAY

>gi|146261040|gb|ABQ14770.1| HMW glutenin subunit 1Bx13 [Triticum aestivum]

MAKRLVLFAAVVVALVALTAAEGEASGQLQCERELEACQQVVDQQLRDVSPGCRPITVSPGTRQYER QPVVPSKAGSFYPSKTTPSQQLQQMIFWGIPALLRRYYPSVTSSQQGSYYPGQASPQQLGQGQQPGQG QQPRQEQQDQQPGQRQ**QGYYPTSPQ**QPGQGQQLGQGQPGYYPTSQQPGQKQQAGQGQQSGQGQ**QG YYPTSPQ**QSGQGQQPGQGQAGYYPTSPQQSGQWQQPGQGQQPGQGQQSGQGQQGQQPGQGQRPGQ GQ**QGYYPTSPQ**QPGQGQQSGQGQPGYYPTSLRQPGQWQQPGQGQQPGQGQQGQQPGQGQQPGQGQ QGYYPTSLQQPGQGQQPGQGQPGYYPTSQQSEQGQQPGQGKQPGQGQQGYYPTSSQQSGQGQQLGQ GQPGYYPTSPQQSGQGQQSGQGQ**QGYYPTSPQ**QSGQGQQPGQGQSGYFPTSRQQSGQGQQPGQGQQ SGQGQQGQQPGQGQQAYYPTSSQQSGQRQQAGQWQRPGQGQSGYYPTSPQQPGQEQQSGQAQQSGQ WQLVYYPTSPQQPGQLQQPAQGQQPAQGQQSAQEQQPGQAQQSGQWQLVYYPTSPQQPGQLQQPTQ GQ**QGYYPTSPQ**QSGQGQ**QGYYPTSPQ**QSGQGQ**QGYYPTSPQ**QSGQGQQPGQGRQPRQGQQGYYPI SPQQSGQGQQPGQGQ**QGYYPTSPQ**QSGQGQQPGHEQQPGQWLQLGQGQ**QGYYPTSPQ**QSGQGQQS GQGQQGYYPTSLWQPGQGQQPGQGQQGYDSPYHVSAEYQAARLKVAKAQQLAASLPAMCRLEGSD ALSTRQ

>tr|B5ANT6|B5ANT6_WHEAT LMW-glutenin OS=Triticum aestivum PE=2

MKTFLVFALLAVAATSAIAQMETRCIPGLERPWQQQPLPPQQTFPQQPPFSQQQQQPFPQQPPFSQQQP
PFSQQQQPVLPQQPSFSQQQLPPFSQQQP**PFSQQQQPV**LPQQPPFSQQQPVLPPQQSPFPQQQQHQQLV
QQQIPVVQPSILQQLNPCKLFLQQQCSPVAMPQRLARSQMLQQSSCHVMQQQCCQQLPQIPQQSRYEAI
RAIIYSIILQEQQQVQGSIQSQQQQPQQLGQCVSQPQQQSQQQLGQQPQQQQLAQGTFLQPHQIAQLEV
MTSIALRILPTMCSVNVPLYRTTTSVPFDVGTGVGAY

>gi|167042|gb|AAA32955.1| gamma-1 hordein precursor [Hordeum vulgare]

MKILIILTILAMATTFATSEMQVNPSVQVQPTQQQPYPESQQPFISQSQQQF(**PQP(QQPFPQ)QPQ)**QPFP
QSQQQCLQQPQHQFPQPTQQFPQRPLLPFTHPFLTFPDQLLPQPPHQSFPQPPQSYPQPPLQPFPQPPQQK
YPEQPQQPFPWQQPTIQLYLQQQLNPCKEFLLQQCRPVSLLSYIWSKIVQQSSCRVMQQQCCLQLAQIP
EQYKCTAIDSIVHAIFMQQGQRQGVQIVQQQPQPQQVGQCVLVQGQGVVQPQQLAQMEAIRTLVLQS
VPSMCNFNVPPNCSTIKAPFVGVVTGVGGQ

>gi|229610192|gb|ACQ83625.1| omega secalin [Secale cereale]

MKTFLIFVLAMTMSIITTARQLNPSEQELQSPQQPVPKEQSYPQQSYPSHQPFPTPQQYSPYQPQQPFPQP
QQPTPIQP**QQPFPQQPQQPF**PQPQQQLPLQPQQPFPQPQQPIRQQ**PQQSFPQQP**QRPEQQFPQQPQQIIP
QQTQQPFPLQP**QQPFPQQPQ**RPFAQQPEQIISQQPFPLQQQQPFSQPQQPFPQQPGQIIPQQPQQPSPLQP
QQPFSQQPQRP**QQPFPQQPQ**QIIPQQPQQPFPLQPQQPVPQQPQRPFGQQPEQIISQRPQQPFPLQPQQPF
SQPQQPFPQQPGQIIPQQPQQPFPLQPQQPFPQQPEQIISQQPQQPFPLQPQQPSPQQPQLPFPLPQQPFVV
VV

>gi|166557|gb|AAA32716.1| avenin [Avena sativa]

MKTFLIIALLAMAVATATATTTVQYNPSEQYQ**PYPEQQEPF**VQQQQPFVQQQQPFVQQQQMFLQPLL
QQQLNPCKQFLVQQCSPVAAVPFLRSQILRQAICQVTRQQCCRQLAQIPEQLRCPAIHSVVQSIILQQQQ
QQQQFIQPQLQQQVFQPQLQLQQQVFQPQLQQQVFQPQLQQVFNQPQMQGQIEGMRAFALQALPAMC
DVYVPPQCPVATAPLGGF

Table 1.1 Overview of T-cell stimulatory peptides in wheat gluten, hordeins, secalins (Sollid et al., 2012; Bodd et al., 2012).

Protein Source	HLA-DQ molecule	Cereal	Peptide Sequence
α- Gliadin	DQ2	Wheat	PQPQLPYPQ
α-Gliadin	DQ2	Wheat	PFPQPQLPY
α-Gliadin	DQ2	Wheat	FRPQQPYPQ
α-Gliadin	DQ8	Wheat	QGSFQPSQQ
γ-Gliadin	DQ2	Wheat	FPQQPQQPF
γ-Gliadin	DQ2	Wheat	PQQSFPQQQ
γ-Gliadin	DQ2	Wheat	IIQPQQPAQ
Hordein	DQ2	Barley	PQPQQPFPQ
Hordein	DQ2	Barley	PFPQPQQPF

Hordein	DQ2	Barley	FPPQQPFPQ
Secalin	DQ2	Rye	PQPQQPFPQ
Secalin	DQ2	Rye	PFPQPQQPF
Secalin	DQ2	Rye	PQQSFPQQP
LMW-glutenin	DQ2	Wheat	FSQQQQSPF
LMW-glutenin	DQ2	Wheat	PFSQQQQPV
LMW-glutenin	DQ2	Wheat	FSQQQQQPL
HMW-glutenin	DQ8	Wheat	QGYYPTSPQ

1.2.7 Treatment of Celiac disease

Currently there is no effective or approved treatment available of celiac disease except consumption of gluten free diet (GFD) throughout the life time of the patients. There are however few developments in treatment of celiac disease which are currently under clinical trials. One of such promising treatment is oral enzyme therapy that utilises gluten-degrading enzymes which includes enzymes such as prolyl endopeptidases, cysteine proteases and subtilisins. These enzymes can withstand the harsh gastro-duodenal conditions and cleave the digestion resistant gluten peptide fraction responsible for celiac disease pathogenesis (Wei et al., 2020). Other approach include use of tight junction regulators such as Larazotide acetate, also known as AT-1001. Larazotide acetate is a synthetic peptide which inhibiting the actin rearrangement caused by gluten peptides. It is currently under clinical trial (Khaleghi et al., 2016). There are also other prospective treatment that are also currently under study such gluten binders copolymer P(HEMAco-SS) (reduction of gluten immunogenicity), anti-CCR9 blockade CCX282-B agent (Lymphocyte recruitment blockade) and vaccination (Nexvax2) etc (Yoosuf & Makharia, 2019). However these treatment strategies have many challenges before they can be approve for application in the celiac disease patients and maintenance of celiac disease through GFD is the only option now.

1.2.8 Analytical methods for detection of Gluten and celiac disease epitopes

The maintenance of a Gluten free diet (GFD) is very crucial for both the celiac disease patient and Gluten free food product manufacturer. Food and beverage products such as bread, pasta

and beer made from wheat and related cereals like rye and barley are the obvious source of Gluten and it's hydrolysate containing the celiac disease epitopes. However, during the age of highly processed food products, gluten can be found in non-obvious sources like flavour enhancer, emulsifier, thickener, filler and fortification ingredient that are used not just in food products, but also in nutritional supplements, drugs and cosmetics (Westby, 2004). In addition to these, contamination of other gluten free cereals such as rice, maize, quinoa, buckwheat and amaranth with gluten usually occurs during crop rotation in farming, transportation or milling and processing due to use of common equipment. Therefore, the analytical detection of gluten is very important for quality control of raw material by gluten free food manufacturer and for personal disease care management of celiac disease patient (Scherf, & Poms, 2016). The Codex Alimentarius (CODEX STAN 118, 1979) and the Regulation (EC) No 41/2009 endorse a maximum gluten contamination of 20 mg/kg in gluten-free labelled products as a safe threshold (Martín-Fernández et al., 2015). Detection of gluten can be done by immunological methods and non-immunological methods.

1.2.8.1 Immunological method of gluten detection

The immunological methods of gluten detection are exclusively dependent on the high affinity antibodies or immunoglobulins specific for gluten protein or it's constituent peptides. Currently enzyme-linked immunosorbent assays (ELISAs) that employs antibodies are the most commonly and widely used method for the analysis of gluten in food products. ELISA offers high specificity, sensitivity and convenience for regular laboratory testing of gluten. There is no global independent reference method and reference material for testing of gluten at present. The PWG-gliadin is considered as the reference material for gluten analysis as recommended by Working Group on Prolamin Analysis and Toxicity (WGPAT). However, the gliadin subunit does not encompass the whole gluten protein. In such scenario, ELISA have been the most accepted method for analysis of gluten and the versions of ELISA that uses the anti-gluten antibodies, R5 and G12 were recommended by Codex Committee of Methods of Analysis and Sampling, 2015 (Scherf, & Poms, 2016). In past years, several gluten specific antibodies have been developed by several groups and many of these have been commercialised. The monoclonal antibodies that are most commonly used in the ELISA kits are Skerrit raised against heat-stable ω-gliadins, R5 obtained against ω-secalins, and G12 raised against a 33-mer peptide from α2-gliadin subunits of gluten (Miranda-Castro et al., 2016).

R5 ELISA primarily uses two types of ELISA methods, a sandwich ELISA to detect the whole native gluten protein and a competitive ELISA for detection of partially hydrolysed peptide products of gluten. The sandwich version uses two R5 antibodies, one being immobilised (capture antibody) and other one is free, but conjugated to HRP and therefore, this method require two binding epitopes in the gluten protein. The antibody in competitive version requires only one binding epitopes making it suitable for detecting the hydrolysed products. The sandwich ELISA is extensively studied and it is also approved as standard method by AACCI Method 38.50.01 and AOAC Official Method 2012.01. This method demonstrated the limit of detection of gliadins as 1.5 ng/ml (1.56 ppm gliadins and 3.2 ppm gluten) (Lacorn & Weiss, 2015; Garcia-Calvo et al., 2020). The R5 antibody can recognise the repetitive motif such as QQPFP, QQQFP, PQPFP, LQPFP, QQPYP, QLPYP present in the toxic peptides containing celiac disease epitopes such as Gliadin 33 mer peptide, Gliadin 26 mer peptide and Gliadin 25 mer peptide (Kahlenberg et al., 2006). Monoclonal antibodies G12 and A1 were raised against the most immunogenic 33 mer peptide present in α2-gliadin of wheat. Besides the 33 mer peptide of wheat, these antibodies can also recognised many immunogenic peptides of wheat, barley, rye, and varieties of oats with great specificity. Antibody G12 can recognise the peptide motifs such as QPQLPY, QPQLPF, QPQLPL, QPQQPY, QPELPY, while A1 can recognise QLPYPQP, QLPFPQP, QQPYPQP, QLPYPQS, QLSYPQP, QLPYSQP, QQPFPQP, QQPYPQE, ELPYPQP present in the prolamins of wheat and related cereals (Shan et al., 2002; Comino et al., 2013). The G12 mAb is considerably sensitive in detecting the prolamins while it's sensitive is low in detecting the glutenin subunits of gluten (Rallabhandi et al., 2015). On the other hand, the Skerrit monoclonal antibody raised against wheat gliadin could detect the HMW glutenins, HMW-secalins and D-hordeins with very high sensitivity. Skerrit mAb can also detect ω1-, ω2-gliadins and LMW-GS with relatively less sensitivity, however it cannot detect γ/ β-hordeins, γ-gliadins and α-gliadins sufficiently. Although Skerrit antibody was raised against ω-gliadin, it primarily recognises the QQGYYP motif which is present very repetitively in HMW-GS (Panda & Garber, 2019; Lexhaller et al., 2017). A competitive ELISA was developed involving monoclonal antibody PN3 raised against a 19 mer epitope of α-gliadin. PN3 mAb selectively recognises QQQPFP and can detect α- and γ-gliadins strongly, ω-gliadin, LMW-GS, hordeins and secalins moderately, but cannot detect HMW-GS, avenins, or zeins (Simón et al., 2017). ELISA has also been developed against many other celiac disease toxic peptides of wheat, barley and rice. Few polyclonal antibodies developed against gliadins have been used in many commercial ELISA kits and they offer advantage of possessing broad specificity towards gluten irrespective of cereal species, cultivar

and method of food processing used. However, polyclonal antibodies suffer from limited supply, less extensive characterization and batch to batch variation as they are directly extracted from sera of the immunised animal or chicken. Monoclonal antibodies being produced by hybridoma technology have the advantage of less batch to batch variation (Melini & Melini, 2018; Garcia-Calvo et al., 2020).

Based on the same antibodies that are used in ELISA, Immunosensors and Immunochromatographic assay method like dipstick or lateral-flow format have also been developed (Scherf, & Poms, 2016). Immunochromatographic assays are very convenient for use by the end user and they produce result that can be interpreted by visual inspection, however it does not give quantitative estimation of gluten (Garcia-Calvo et al., 2020). Immunosensors on the other hand provide quantitative estimation of gluten concentration.

Immunological methods like ELISA used to quantify the gluten concentration in a food sample, however there are few reported challenges that generally causes over- or underestimation of gluten in the sample. Since commercial ELISA kits involving different antibodies specific for different subunits of gluten, there is a lack of ELISA method that can comprehend the detection of all the fractions of gluten (Panda & Garber, 2019). Due to lack of a reference material, the individual ELISA kits may calibrate the gluten concentration based on gluten subunits which was not used in development of the antibody. This practice will lead to inaccurate gluten quantification. Although PWG-gliadin is considered as best and well characterised reference material recommended till now for ELISA testing of gluten, however it is not approved by Institute for Reference Material and Measurements of the European Commission (IRMM). The limitation associated with PWG-gliadin as reference material is that it cannot account for the glutenin content of the gluten protein until the ratio of prolamin to glutenin is known (Slot et al., 2016). The ratio of prolamin to glutenin content is generally considered as 1, but it varies considerably depending on the varieties of the cereals, growth condition and processing method applied. In addition to these, the extraction of gluten from food matrices is not a very efficient method due to structural complexities of the protein. Extraction of gluten in aqueous alcohol (60% ethanol or 50% propanol) is the most commonly used method, which can only isolate the prolamin fraction of the gluten from unprocessed food materials. However, the aqueous alcohol cannot solubilised the prolamin fraction from processed foods as heat treatment lead to aggregate formation of prolamins and glutelins through formation of inter-chain disulphide bonds. Use of an extraction ‘cocktail’ containing reducing agents like 2-mercaptoethanol which disrupts the disulphide bonds and

disaggregating agents to increase solubility like guanidine or SDS with aqueous alcohol solution leads to extraction of both prolamin and glutenins from raw and processed food. Such extraction solution are not suitable for some of the immunological methods as they denature the constituent proteins of assay. To tackle this problem recently a extraction solution named UPEX (universal prolamin and glutelin extractant solution) containing the reducing agent Tris(2-carboxyethyl)-phosphine and the disaggregating compound N-lauroylsarcosine has been designed to extract the total gluten from processed and raw food matrices (Scherf, & Poms, 2016; Miranda-Castro et al., 2016).

1.2.8.2 Non-immunological method of gluten detection

The non-immunological methods mainly include proteomics based methods and nucleic acid based methods. Proteomics based methods primarily use chromatographic separation techniques such as gel electrophoresis or HPLC along with mass spectroscopic techniques such as MALDI-TOF, ESI-MS etc. The nucleic acid based methods generally uses Q-PCR.

Following the purification and separation by HPLC, the mass spectroscopic methods profiles the protein and the peptides present in a sample through detection of the mass to charge (m/z) ratio of the ionised protein or peptide fragments. Apart from providing the mass of the peptide or protein, mass spectroscopy can also carry out *de novo* amino acid sequencing and analyse post translational modifications through tandem mass spectra obtained by post-source decay (PSD) or collision induced dissociation (Ferranti et al., 2007). The sample preparation generally involves extraction of gluten protein and it's enzymatic digestion to get a mixture of fragmented peptides. Mass spectroscopic method to carry out peptide identification can be either targeted or untargeted. Untargeted mass spectroscopy is done to generate a profile of peptides in the gluten. The m/z peaks obtained from MS profiling are searched into bioinformatics database (e.g., UniProt Knowledgebase or National Center for Biotechnology Information) to identify the unique marker peptide of gluten including immunogenic sequences and other peptide fraction of gluten. The marker peptides are later used in targeted mass spectroscopic analysis for detection of the pre-identified peptides and even for quantitation gluten (Xhaferaj et al., 2020). MALDI-TOF was successfully used to detect and quantify gliadins, secalins, hordeins, and avenins subunits from wheat, rye, barley, and oats cultivars through identification characteristic molecular mass of each without requirement of HPLC separation. MALDI-TOF however failed to detect at concentration below 100 mg gliadin/kg in

maize and rice based items contaminated with wheat gliadin. This was likely due to low sensitivity & accuracy in detecting higher mass, complexity of food matrix and reduced intensity of gliadin due to modification after heat treatment (Scherf & Poms, 2016). In many studies it is observed that MALDI-TOF mass spectroscopic method used for identification of the peptide epitopes in hydrolysed gluten in food sample such as beer failed considerably due to high heterogeneity of the sample. In some cases, only limited numbers of the toxic protein were identified. However, use of antibody based method after HPLC fractionation followed by elution of the peptides from antibody-target complexes and identification of peptides by mass spectroscopy significantly improved the identification of the celiac disease epitopic peptides (Comino et al., 2013). Although mass spectroscopic based methods are highly sensitive, accurate and selective, they are not routinely used for gluten analysis due to requirement of expensive and sophisticated instrument and expertise. Another disadvantage that mass spectroscopic based methods suffer like ELISA in quantitative detection of gluten is the unavailability of reference material. The publicly available gluten databases are not well curated for identification of peptide or proteins subunits, especially for glutenins which limits the application of mass spectroscopy (Scherf & Poms, 2016).

The PCR based methods are indirect method of gluten analysis. The PCR based methods use the genomic DNA extracted from food sample and the gene encoding gluten or species-specific regions of the genes are amplified using specific primer for detection and quantification of gluten or it's subunits. The amplified genes can be identified by gel electrophoresis, southern blotting or by sequencing (Simón et al., 2017). However, real time quantitative PCR (rt-qPCR) offers more convenience and allows quantification of the gluten concentration. The real time quantitative PCR can have higher sensitivity than ELISA. The rt-qPCR employs fluorescent dyes such as SYBR Green or TaqMan, which allows the real time monitoring of the amplification (Xhaferaj et al., 2020). The fluorescent signal specifies the amount of DNA present in the sample. The DNA concentration or copy number correlates with the concentration of the gluten in the sample of analysis (Simón et al., 2017).

The prerequisite of the PCR based method is availability of high quality genomic DNA, however food samples containing high levels of polyphenol may be present in the isolated DNA sample and hinder the polymerase chain reaction (Martín-Fernández et al., 2016). Application of the PCR-based method might be challenging in the highly hydrolysed food products such as beer, syrups and malt extract where DNA could be degraded to the extent that it cannot be amplified. Although DNA is stable in moderately high temperature, a very

aggressive heating process (200 °C/20 min) of the food sample can too degrade the DNA effecting accuracy of the PCR-based methods (García-García et al., 2019). Therefore, the PCR based methods are generally used as complimentary method to ELISA or proteomics based methods.

Considering the limitations of various analytical method for gluten analysis, there is scope for development of alternate methods. Currently ELISA is considered as the gold standard, however limitations associated with immunoglobulins such denaturation in gluten extraction buffer, comparatively higher cost of production and thermal instability can be overcome by an alternative non-protein receptor molecule such as aptamers.

1.2.9 Aptamers

Aptamers are artificial receptor molecules of oligonucleotide or peptide origin that can fold into distinctive three-dimensional conformations capable of binding to a target molecule with high affinity and specificity. The single stranded DNA or RNA aptamer can form a variety of complex three-dimensional structures such as stems, loops, bulges, hairpins, pseudoknots, triplexes, quadruplexes etc. With these three dimensional structures, aptamer can bind to a specific target molecule well fittingly through structure compatibility, stacking of aromatic rings, electrostatic interactions, van der Waals interactions, hydrogen bonding or through the involvement of combinations of these interactions (Stoltenburg et al., 2007). Aptamers are selected through a process known as Systematic Evolution of Ligands by Exponential Enrichment (SELEX) which is based on the principle of Darwinian evolution process of natural selection. SELEX is generally carried out as an *in-vitro* evolution process for selection and enrichment of the aptamer molecule (Wu et al. 2015). Aptamers were discovered in 1990 by two groups working independently, namely i) Craig Tuerk and Larry Gold and ii) Andy Ellington and Jack Szostak. Most commonly oligonucleotides, RNA and single stranded DNA (ssDNA) along with their unnatural base analogues are used as aptamer. The double stranded DNA and peptide aptamers are also used less frequently (Pinto, 2012). The aptamers are comparable with antibodies in terms of their performance and in many case, they offers advances over antibodies with potential to act as an alternative to antibodies.

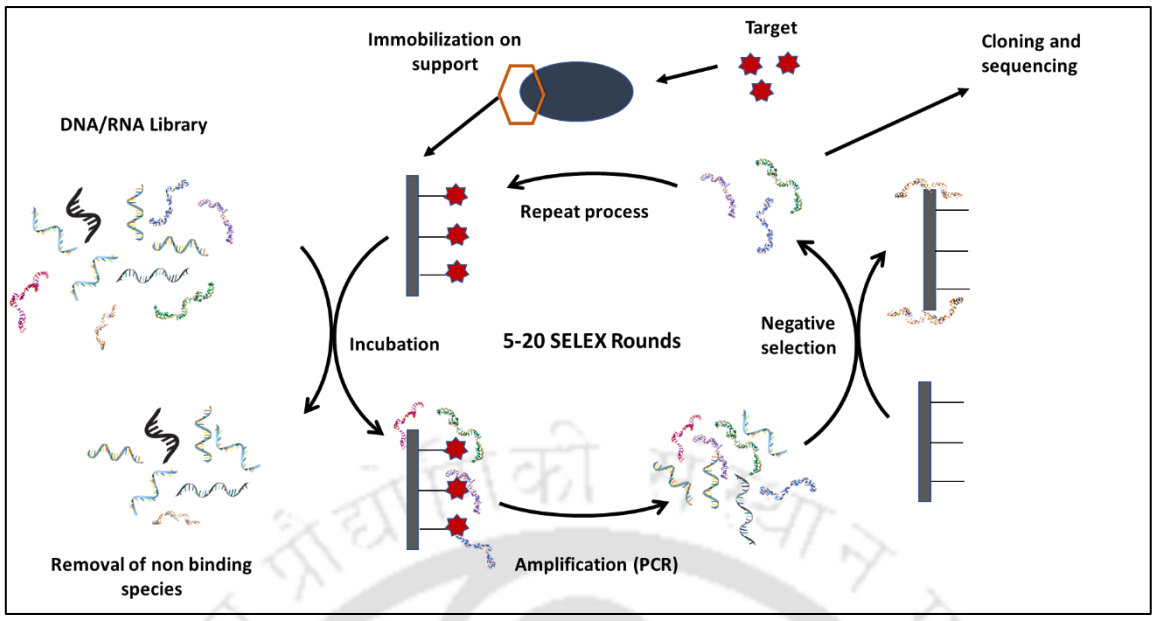

Figure 1.6 Schematic representation of SELEX process

After development of SELEX technology in 1990, it has been extensively used for selection aptamer against different kinds of target molecules ranging from peptides to proteins, small to large organic molecules (drug compounds) and even against metal ions. The initial focus of the aptamers based studies primarily were for applications as diagnostic or therapeutic tools (Gopinath 2007). The Food and Drug Administration (FDA) of USA approved a aptamer targeting vascular endothelial growth factor (VEGF) called Macugen as a therapeutic molecule for the treatment of wet (neovascular) age-related macular degeneration (ARMD). Thereafter, the applications of aptamer technology have increased rapidly and the technology becomes more effective and authoritative (Keefe et al. 2010).

The oligonucleotide aptamers are isolated from highly diverse starting libraries of synthetic Oligonucleotides of approximately 10^{12}–10^{15} combinatorial oligonucleotide libraries through SELEX (Djordjevic 2007). SELEX is based on the principle of Darwin's evolutionary process where among millions of random oligonucleotide sequences, the sequences with strongest binding affinity towards the target stand out (Tavitian & Haberkorn, 2009). The specific nucleotide sequence with the highest binding affinity is selected as a probe for target detection. SELEX process have three main steps. First, incubation of a random nucleotide sequences library or aptamer library (synthesised by combinatorial chemistry) with the target molecule. The aptamer library generally contains either RNA or DNA sequences of a specific length where a region of random nucleotide sequences is flanked by two defined primer binding regions. The second step is partitioning of oligonucleotides bound to the target from the

unbound sequences. The third step is enrichment of the bound oligonucleotide sequences with amplification by polymerase chain reaction (PCR). These three steps are carried out in iteration until the sequences with strongest binding affinity are obtained. Partitioning steps are always followed by a washing step where the loosely bound aptamer candidates are removed by washing with detergent based buffers. During subsequent iterative cycles, the stringency of the SELEX conditions e.g. binding time, salt concentration of buffer solution, amount of target used, temperature of the process etc. are increased to ensure elimination of weak binders. In conventional SELEX, the target is generally immobilised on a matrix which helps in partitioning of the unbound sequences in solution. A negative SELEX step is carried out mostly before the start of first round of SELEX. In negative SELEX step, the aptamer library is incubated with the bare matrix without immobilizing the target and unbound sequences are used in later SELEX step to eliminate the sequences that have affinity towards the material of matrix (Ellington & Szostak, 1992; Stoltenburg et al., 2007; J. Wu et al., 2014). The enrichment of aptamer molecules are monitored after each iterative cycle and once the enrichment is stable after several round, the amplified aptamer candidates are cloned and sequenced. Aptamer candidates identified by sequencing are synthesised and characterised for their binding affinity with target molecules by different physicochemical techniques like Isothermal Titration Calorimetry, Circular Dichroism, Surface Plasmon Resonance and Electrophoretic Mobility Shift Assay etc.

1.2.9.1 Modified SELEX

Based on the conventional steps of SELEX, there are many modifications done at various steps to make it more rapid, adaptable to nature of target, convenient and efficient. A modified version of conventional SELEX, named Cell-SELEX utilises a specific cell type as target where partitioning of candidate sequences is done by the cell itself without utilising any matrix material. In this case, the negative SELEX is done with a control cell line to eliminate the sequences binding to common and non-specific molecules on cells (Sefah et al., 2010). Cell SELEX or whole cell SELEX has been widely used in selection of aptamer candidates against various pathogenic bacteria in food samples (Dua et al., 2016; Moon et al., 2015; Teng et al., 2016). FluMag SELEX is another modification of SELEX process for more convenience where target is immobilised on magnetic beads for better partitioning and use of fluorescein-modified primers in PCR amplification renders easy and informative monitoring of enrichment.

Likewise Capillary electrophoresis-SELEX, Cross-linking SELEX, Mirror-image SELEX, Chimeric SELEX, Multi-stage SELEX, Toggle-SELEX, SPR-SELEX, Tailored SELEX, Artificially expanded genetic information systems (AEGIS)-SELEX etc. are examples of different variants of modified SELEX based on different principles adapted for the method (Darmostuk et al., 2014) . Some of these modified SELEX types are described in the **table 1.2**.

Table 1.2 Description of method or principle used in some modified SELEX types

SELEX type	Method/Principle	References
Capillary electrophoresis-SELEX	It employs capillary electrophoresis to partition bound aptamers from unbound free aptamers. It helps in reducing the number of SELEX cycle required.	Mendonsa & Bowser, 2004
Cross-linking or Photo SELEX	The aptamer library is modified with photosensitive nucleotides 5-bromo-2′-deoxyuridine, which upon UV irradiation forms covalent bond with sulphur containing and aromatic amino acid of target protein. It improves the aptamer-target interaction.	Jensen et al., 1995
Mirror-image SELEX/ Speigelmer Technology	The aptamers are selected through standard SELEX process, however the final aptamer candidates are synthesised with unnatural L-nucleotides which provides more stability and resistance to nucleases	Klußmann et al., 1996
Chimeric SELEX	Two separate aptamer libraries are used to select aptamers against two targets and letter they fused to form single aptamer sequence which can bind to dual targets independently	Burke and Willis, 1998
Multi-stage SELEX	It is modified version of chimeric SELEX where the longer fused aptamer is again selected through SELEX to achieve the allosteric binding activities of two targets	Wu and Curran, 1999

Toggle-SELEX	It uses two homologous molecules (e.g. human and porcine thrombins) alternatively during consecutive SELEX rounds to obtain the aptamer candidate with specificity to one and cross-reactivity to another	White et al., 2001
SPR-SELEX	The SELEX process utilises Surface Plasmon Resonance (SPR) assay for the monitoring of kinetics of interaction between aptamer library and target after each round. SELEX is carried out by immobilising the target on the SPR-chip and injecting aptamer library. This help in attaining aptamer with very high affinity.	Khati et al., 2003
Tailored SELEX	The SELEX is carried out using aptamer library devoid of primer sequences. Primer sequences are ligated to aptamer library after each SELEX round for amplification and cleavage before using in next round. It helps to select short aptamer sequences.	Vater et al., 2003
AEGIS -SELEX	Apart from the four natural nucleotides (A,T, G and C), it uses two nonstandard Artificially expanded genetic information systems (AEGIS) P and Z nucleotides in the aptamer library which increases the diversity of the aptamer sequences. It uses specialised tools for PCR and cloning of sequences. It improves the affinity of aptamer.	Sefah et al., 2014

1.2.9.2 Next Genome Sequencing - SELEX

Conventionally, Sanger sequencing is used to identify the potential aptamer candidate sequences that have been isolated at the last stage of SELEX process. Next genome sequencing (NGS) or high-throughput sequencing (HTS) is applied to sequence millions of aptamer sequences after each SELEX round which provides information on the most dominant sequence from the initial steps. This greatly reduces the amount of duration and experimental procedures required in conventional SELEX (Darmostuk et al., 2014). HTS with

bioinformatics analysis of aptamer helps in detailed characterization of functional or rare motifs, sequence clusters and binding motifs present across the dominant sequences (Valenzano et al., 2016).

1.2.9.3 Advantages of aptamer over antibodies

Antibodies are currently considered as gold standard in biochemical assays that have very high affinity, sensitivity and selectivity. Aptamers demonstrate a similar level of affinity comparable to antibodies with dissociation constants in the range of nanomolar (nM) and even picomolar (pM) for recognition of the target. Some of the aptamers have even achieved the dissociation constant in the range of picomolar–femtomolar. Besides, aptamer technology offers several other benefits over antibodies. Aptamers are chemically synthesised in a very rapid, simple and inexpensive process, whereas production of antibodies requires animals and a very laborious process. The process of SELEX and chemical synthesis of aptamer can be fully automated. The sequence based chemical synthesis allow the production of aptamers without any batch to batch variation. The production of polyclonal and monoclonal antibodies are often found with batch to batch variation (Toh et al., 2015). Chemical synthesis of aptamer also allows the convenient modification or labelling with reporter molecules, dyes, linkers and other functional groups at any desired position of a nucleotide in the sequence without effecting the binding affinity or selectivity. Although chemical modification of the antibodies are possible, the site specification modification in antigen molecule is not very easy task (Thiviyanathan & Gorenstein, 2012). Aptamers are more chemically stable and have a longer shelf life than antibodies. At room or higher temperature the protein based antibodies denatures irreversibly, however aptamer can unfold at higher temperature and regain it's original conformation when the temperature is set back to optimal level (Toh et al., 2015; Kusser, 2000). The comparatively smaller size of aptamer also allows higher membrane permeability to dense tissue for biomedical applications. The typical size of IgG antibodies are 150–170 kDa whereas aptamer molecules containing 30-80 nucleotides long sequence are around 12–30 kDa. Aptamers are essentially demonstrated to be non-immunogenic when applied as therapeutic molecule *in-vivo* (Kim et al., 2021). Aptamers can be selected against a wide varieties of target molecules ranging from small molecules to supramolecular. In case of antibodies a very small molecules do not elicit immune response in host animal body, therefore these are not suitable target for antibody development. *In-vitro* selection of aptamer is more suitable against toxins than antibody production as

involvement of toxins possess risk of harming the animal used for production (Thiviyanathan & Gorenstein, 2012). Further, aptamers can discriminate between the molecules with highly small difference in their structure. For example, aptamer can be specific to be either theophylline or caffeine, which are different by presence of only one methyl group (Toh et al., 2015). Once aptamer are selected their affinity can be enhanced by optimizing the length of the nucleotide sequences (Nery et al., 2009). Thus aptamer offers a lot more flexibility in production and application along with the prospect of cost effectiveness.

1.2.9.4 Aptamer based bioassays

Aptamers with good binding affinity are employed in assay development for detection of target analyte. Due to the versatility of oligonucleotide aptamer for chemical modifications, it can be used in different platforms. Assays involve multistep procedure to generate machine readable signal, therefore it is generally not rapid and portable. Although for signal measurement, assays involve instruments like UV-VIS spectrophotometer or fluorescence spectrophotometer, it does not require complex instrumentation like biosensors. Harnessing the power of selective and specific affinity towards the target, many aptamers have been successfully utilised in assays similar to immunoassays where antibodies act as prime recognition molecule. Inspired by the ELISA, Drolet et al. developed an assay called Enzyme-linked Oligonucleotide assay (ELONA) in 1996 utilising aptamer (Drolet et al., 1996). Similar assays have been carried out later by many investigators *viz*. Baldrich et al. termed it as Enzyme-Linked Aptamer Assay (ELAA) (Baldrich et al., 2005), Vivekananda and Kiel termed as Aptamer-Linked Immobilised Sorbent Assay (ALISA) (Vivekananda & Kiel, 2006), Narendran et al., 2012 termed as Enzyme-Linked Apta-Sorbent Assay (ELASA) etc. (Toh et al., 2015). Like ELISA, aptamer based enzyme linked sorbent assays can be done in direct, indirect or sandwich types (Jing et al., 2018). Generally in direct ELAA, the target is immobilised on the surface of a microtiter plate and an aptamer conjugated with biotin is incubated with it to bind in a suitable buffer. Unbound aptamers are washed off by washing buffer. A streptavidin conjugated enzyme is subsequently added to target-aptamer complex where streptavidin binds with biotin of conjugated aptamer. Enzymes such as Horseradish peroxidase are used in conjugation to streptavidin where adding of chromogenic substrate (e.g. TMB, ABTS or OPD etc.) forms colour which is measured in microplate reader for qualitative or quantitative detection of target. Indirect ELAA involves introduction of an antibody which binds to immobilised target and the

antibody is further detected by an enzyme linked aptamer (Frohnmeyer et al., 2018; Toh et al., 2015), although it is found that terms 'direct' and 'indirect' for ELAA are used interchangeably.

Competitive direct or indirect ELAA is widely used in various food contamination detection where aptamer is incubated with sample containing target before adding to a microtiter plate immobilised with standard target (Fig.1). The free target molecules compete with immobilised target molecules to bind with aptamer conjugated to enzyme (L. Sun & Zhao, 2018). Sandwich ELAA uses a capture antibody or aptamer immobilised on the surface of plate which binds a target and subsequently the target is recognised by another aptamer or antibody. Sandwich ELAA can be carried out in different configurations like aptamer-target-aptamer (Jing et al., 2018; Shin et al., 2018), aptamer-target-antibody, antibody-target-aptamer (W. Chen et al., 2020; Suh et al., 2018; Sundararaj et al., 2019) etc. Utilization of antibody and aptamer together in sandwich assays has been named as hetero-sandwich (W. Chen et al., 2020) or hybrid sandwich (Mudili et al., 2015) by investigators. Aptamers are also used in other type of assays like dot blot, nanoparticle aggregation assay, fluorescent based assays, Rolling Circle Amplification (RCA) assay. (Y. Jiang et al., 2017; Zhan et al., 2020).

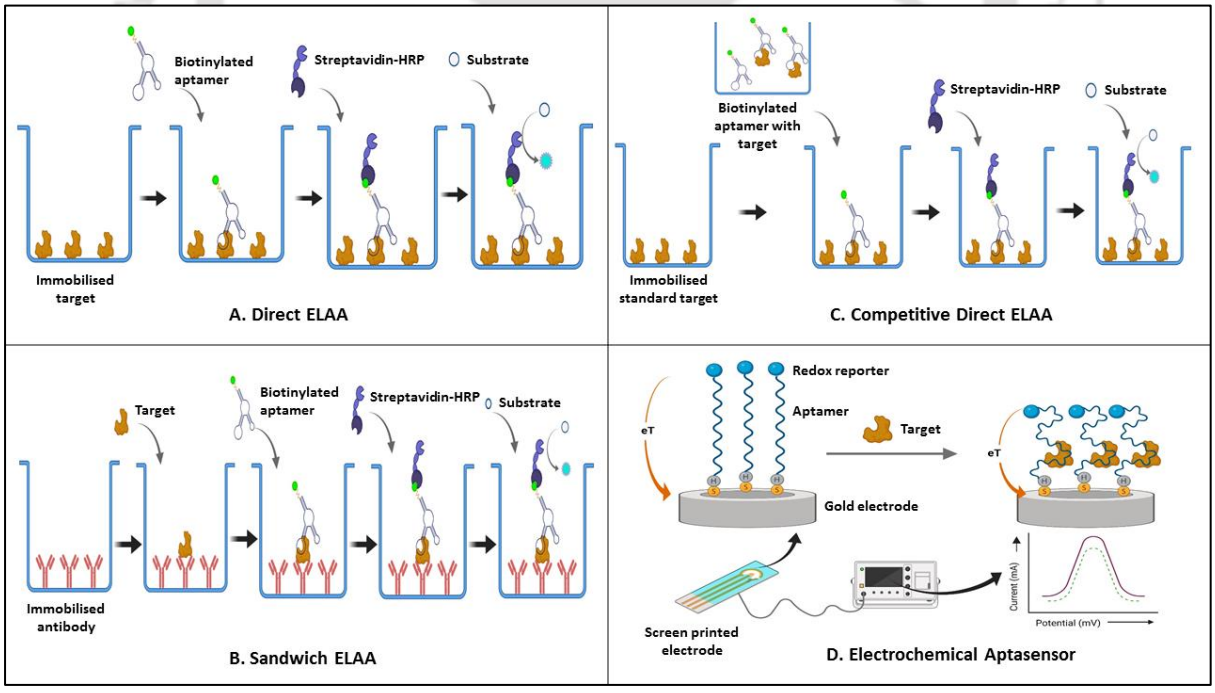

Figure 1.7 Schematic diagram of aptamer based assay and biosensor. **(A)** Direct ELAA **(B)** Sandwich ELAA **(C)** Competitive direct ELAA and **(D)** Electrochemical Aptasensor, where

eT is electron transfer rate. (Reprinted with permission from Kalita et al., 2022, copyright Elsivier, 2022)

1.2.9.5 Aptamer based biosensors

Aptamers are utilised as a recognition probe in different types of biosensor platform for detection of analyte. Biosensors offer high specificity, sensitivity, portability, miniaturisation, ease of use, rapidity, provision for on-line monitoring & automation and cost effectiveness (Ye et al., 2019). Biosensors generally contain a biorecognition element which interacts with target molecules, a transducer that converts the biochemical signals to an output electrical signal, a signal amplifier that amplifies the week electrical signals and a measurement or detection system (Gaudin, 2017; Neethirajan et al., 2017). Aptamer coupled on transducer surface when binds to a target molecule brings a change in the local environment of the transducer and it then generate an electrical or optical signal for quantification (Nehra et al., 2020). Based on the types of transducers used, the aptasensors can be categorised into electrochemical, optical, micromechanical and piezoelectric etc. Depending on electrochemical properties that influences a sensing electrode such as current generated, charge accumulated or conductance generated due to a biochemical reaction near the electrode surface, electrochemical sensors are termed as amperometric**,** potentiomentric or conductometric respectively (G. K. Mishra et al., 2018). Likewise optical biosensors take advantage of various optical phenomenon for generation of an optical signal while interacting with the analyte, which can be colorimetric, fluorescence, chemiluminescence and surface plasmon resonance (SPR) etc.(Jayan et al., 2020; Pirzada & Altintas, 2020). In a typical electrochemical aptasensor, the aptamer is immobilized on a gold electrode via thiol chemistry in one end while the other end can be labelled with a redox probe such as methylene blue or ferrocene. The aptamer conjugated on the electrode surface generally stays in an open conformation, therefore the redox probe maintains a distance from electrode surface. However, when the analyte molecule specific to aptamer comes into the close vicinity, the aptamer change it's conformation to fold into hairpin structure which results in the shortening of the distance between redox probe and electrode surface. This allows the increase efficiency of the electron transfer from the redox probe to the electrode surface as shown in the **figure 1.7 (D)**. The signal generated due to this change can be measured to calibrate with the concentration of the analyte to be detected (Ferapontova et al., 2008).

1.2.10 Application of aptamer in detection of food contaminants

1.2.10.1 Pathogenic microorganisms

Detection of foodborne microorganism with aptamer can be done through two approaches. Aptamers can be selected against the whole cell or against a part of cell surface e.g. Outer membrane proteins (Paniel & Noguer, 2019). Several aptamers have been selected mostly against the common foodborne bacteria, namely *Salmonella* (Ranjbar et al., 2018), *E.coli* (Abdelrasoul et al., 2020), *Listeria monocytogenes* (Lee et al., 2015), *Vibrio Parahaemolyticus* (L. Yao et al., 2017), *Staphylococcus aureus* (Cui et al., 2019), *Shigella sonnei* (M. S. Song et al., 2017) and food borne virus *Norovirus* (Weerathunge et al., 2019). Aptamers selected against pathogenic bacteria are incorporated into some of the innovative assays and biosensor platforms that can effectively detect the bacteria in food matrices.

Whole cell SELEX was applied against live *E. coli* O157:H7 pathogenic strain that was captured by an anti-*E. coli* antibody conjugated on magnetic bead. Capturing with antibody offers an advantage of aptamer binding to different binding sites without undergoing competition with antibody, which enables the development of aptamer-antibody sandwich assays. Counter SELEX performed with *Staphylococcus aureus, Listeria monocytogenes,* and *Salmonella Typhimurium* conferred the specificity to the aptamer selected (Yu et al., 2018).The whole bacterial cells without capturing can also be directly used in SELEX process, as it has been performed during aptamer selection against *Salmonella Enteritidis* (Z. Zhang et al., 2019). The drawback associated with the whole cell SELEX is that many of the surface epitopes are genus specific which leads to cross-reactivity with bacterium of same genus. Species level specificity was achieved while using an aptamer-based sandwich assay (ABSA) platform developed for sensitive detection of *L. monocytogenes* cells. It could detect concentration as low as 20 CFU/mL with good linearity in the 6log range (from 20 to 20×10^5 CFU/mL) (Lee et al., 2015).

Some bacteria are capable of causing illness with as minimum as 10 CFU counts in food sample. Analytical methods, therefore, should not only be very sensitive and also able to nullify the interference of food matrices in accurately measuring bacterial load for practical usage in real food sample. Aptasensors developed for detecting *Salmonella typhimurium* and *Staphylococcus aureus* have demonstrated excellent ability with a LOD as low as 1 CFU/mL (Majdinasab et al., 2018). Screen-printed carbon electrodes (SPEs) surface was modified with

diazonium salt to support denser aptamer immobilisation which allowed a labelled free impedimetric detection of *Salmonella typhimurium* with a LOD of 6 CFU/mL. Most importantly, this aptasensor could detect it in undiluted apple juice which was not possible in it's previous versions by the same authors (Bagheryan et al., 2016).

Aptamer based biosensor that could discriminate the live and the dead cells of bacteria were developed for detecting *Salmonella typhimurium* (S. Chen et al., 2020; P. Zhang et al., 2017). The selectivity to live bacterial cell arises from the heat degradation of the outer membrane proteins of dead *S. typhimurium* which the aptamer cannot recognise (S. Chen et al., 2020). Ranjbar et al., 2018 prepared nanoporous gold upon an Au coated GCE on which aptamers were immobilised to take the advantage of a higher surface to volume ratio. This aptasensor used for detection of *Salmonella typhimurium* in real egg samples able to obtain an excellent sensitivity and lower the LOD to 1 CFU/mL. The aptasensor was successful in discriminating dead and live bacterial cells while detecting, which was evident from change in the magnitude of charge transfer resistance (R_{ct} value) between dead and live cells (Ranjbar et al., 2018). To specifically remove interference of food matrix, an aptamer conjugated with magnetic bead was used to capture *Salmonella* cells in a model food (milk) matrix. This sensor has a very short processing time (less than 10 min). The capture bacteria were detected using a Quartz crystal microbalance (QCM) conjugated with same aptamer with a LOD of 100 CFU/mL (Ozalp et al., 2015). Aptamer functionalised reduced graphene oxide-carbon nanotubes (rGO-CNT) were used on a GCE surface for detection of *Salmonella enterica* serovar Typhimurium using differential pulse voltammetry (DPV) technique which showed a LOD of 10 CFU/mL and detection was rapidly completed within 10 min. The aptamer used in this study was reported previously by Joshi et al. which was selected against isolated outer membrane proteins (OMPs) of S. Typhimurium (Appaturi et al., 2020; Joshi et al., 2009). Aptamers have also been used to enumerate live cell of probiotic bacteria *Lactobacillus casei* present in different dairy drinks. A novel cell-SELEX method was employed, which used polyethyleneglycol (PEG) and chitosan functionalized graphene oxide (PC-GO) to eliminate nonspecific ssDNA sequences and a complementary ring-mediated rolling circle amplification method for aptamer enrichment. The detection strategy utilised an enriched aptamer conjugated to magnetic beads as *L. casei* capture probe, while detection aptamer conjugated to a fluorescent probe can qualitatively and quantitatively analyse viable cells in a linear range of 10^5 to 10^9 CFU/mL. The aptamer can discriminately bind to live cells and avoid dead cells on the basis of change in tertiary structure caused after death of the bacterium. Quantitative

analysis of the live bacterial cells was possible as florescence intensities directly proportionated with the number of cells in the linear range (S. Song et al., 2019).

Magnetic bead functionalised with aptamer as a capture probe was used along with cDNA-upconversion nanoparticles (UCNPs) as a florescent signal probe to detect *E.coli* in pork meat which showed a LOD of 10 CFU/mL. UCNPs were used as likely alternatives to quantum dots and organic fluorophores in florescent aptasensors (H. Li, Ahmad, et al., 2020). *Norovirus* is one of the foodborne viruses responsible for many outbreaks. Gold nanoparticles (Nanozyme) showing peroxide-like activity by catalysing oxidation of colorless TMB (3,3′,5,5′-tetramethylbenzidine) to a blue coloured product was used with a *murine norovirus* (MNV) specific aptamer to construct a colorimetric aptasensor. Surface passivation of gold nanoparticle with aptamer leads to loss of nanozyme-activity. In presence of MNV particles, the aptamers bind to it and release from the gold nanoparticle surface which results in reinstatement of nanozyme activity of GNP for calorimetric detection (Weerathunge et al., 2019). Shen et al., 2020 recently exploited the collateral catalytic activity of CRISPRCas13a, a new member of CRISPR-Cas family, with allosteric probe (AP) consisting three functional domains: aptamer domain, primer domain and T7 promoter domain for detection of *Salmonella Enteritidis* cells in milk samples. *S. enteriditidis* cells bind to aptamer domain initiating allosteric activation of other functional domains to transcribe ssRNA molecules complimentary to guide RNA of CRISPR-cas13a. Hybridization of transcribed ssRNA with guide RNA activates the collateral catalytic activity of CRISPR-Cas13a to cleave reporter RNA molecules for fluorescence signal generation (Fig.2). This strategy compared to RT-PCR reveals that it can detect lower level of *S. enteriditidis* than RT-PCR and more efficiently discriminate between contaminated milk from pasteurized milk (Shen et al., 2020).

1.2.10.2 Allergens

Food allergies are personalised trouble where individuals can be sensitive towards a specific molecule present in certain foods. Management of allergens needs detection not only in industrial level but also in a personal level. Aptamer based methods of detection have been reported against common allergens mainly found in milk, seafood, shellfish, nuts, eggs, wheat and soy (Khedri et al., 2018). Recently there has been development of few highly sensitive aptasensors against Beta-lactoglobulin (β-LG), a milk protein responsible for causing infant

milk allergy. DNA aptamers were integrated into electrochemical sensing platforms which adopted different strategies such as use of methylene blue functionalized aptamer as redox probe on Poly-L-Lysine modified graphite electrodes (LOD of 0.09 ppb) (Amor-Gutiérrez et al., 2020), ferrocyanide redox probe for aptamer functionalised graphene-modified screen printed carbon electrodes (GSPE) (LOD of 0.02 ppb) (Eissa & Zourob, 2017), flower-like bismuth vanadate ($BiVO_4$) microspheres as redox inducer along with Au nanoparticle-coated indium tin oxide modified conductive glass electrode (LOD of 0.007 ppb) (Xu et al., 2020). Shuo et al., 2021 used a high affinity β-LG specific aptamer to fabricate a novel fluorescence surface enhanced Raman scattering dual-mode aptasensor with LOD of 0.05 ppb (Qi et al., 2021). All these aptasensors were tested against spiked β-LG in real food samples where all showed at least 90% recovery rate. Although their performances cannot be conclusively compared as all aptasensors were tested in different food samples, the use of metal nanomaterials of large specific surface area with excellent electrochemical and peroxidase mimic catalytic activities in the aptasensor developed by Xu et al., 2020 certainly aided in lowering the limit of detection greatly. Au nanoparticle-coated indium tin oxide modified conductive glass electrode (AuNPs/ITO) is functionalised with a complimentary DNA strand (DNA1) which hybridizes with β-LG aptamer. In presence of analyte β-LG, the aptamer binds with it breaking the interaction with DNA1. Free DNA1 is then bound by Au@BiVO4 probe functionalised with another complimentary DNA strand (DNA2) where $BiVO_4$ catalyses the reaction of H_2O_2 with TMB giving rise to electrochemical signal. This aptasensor was compared with antibody based commercial sELISA kit, where aptasensor outperformed it in β-LG spiked concentration below 200 ng/mL. Eissa and Zourob, 2017 used graphene-modified screen printed carbon electrodes (GSPE) with aptamer physically absorbed on it and a ferrocyanide redox probe in solution for voltammetry based detection of β-LG, which is comparatively simple and label-free approach.

Several “on-off-on” fluorescence aptasensors based on fluorescence resonance energy transfer (FRET) against Arginine kinase, a major shellfish allergen (J. Zhou et al., 2020), tropomyosin, another major shrimp allergen (Chinnappan et al., 2020) and Ara h1, a homotrimeric allergenic protein of peanut (Weng & Neethirajan, 2016) have been developed. These aptasensors primarily use aptamer labelled with a fluorophore such as quantum dots or fluorescein which is attached to graphene oxide (GO) sensing platform through non-covalent interactions like π-π stacking and hydrophobic interactions. GO quenches florescence signal completely at this state, however subsequent introduction of analyte leads to binding of

fluorophore-labelled aptamer to it and detachment from GO surface recovers the florescence of the fluorophore (Fig.3). In case of the Ara h1 specific aptasensor, the aptamer/Qdot/GO assembly was fabricated into a microfluidic platform which allowed miniaturization, rapidity and minimization of reagent and sample usage (Weng & Neethirajan, 2016). The florescence aptasensor against tropomyosin had a LOD of 2.5 nM which is notable owing to the simplicity of the sensor's design, however it is not lower than previously reported ELISA methods (Chinnappan et al., 2020). Tabrizi et al., 2017 adopted a rather complex design while developing a photoelectric aptasensor which offered LOD of 0.23 ppb in real food sample by using graphitic carbon nitride and TiO_2 as photoactive nanomaterial along with electron donor, ascorbic acid (AA) and signal enhancer ruthenium (III) hexaammine (Amouzadeh Tabrizi et al., 2017). Apta-PCR or Aptamer-recombinase polymerase amplification (Apta-RPA) assays, a method similar to real time PCR uses amplification of bound aptamers to a target as template which allows quantification of target concentration in presence of a florescence dye. Apta-RPA, however does not require a thermocycler as it is an isothermal amplification method. Apt-RPA method was applied for detection of β-conglutin, sub-unit of allergen lupin found in seeds of leguminous plant, *Lupinus* which showed a limit of detection of 35 pM (Jauset-Rubio et al., 2017). In a colorimetric assay that follows competitive ELAA format where the targeted analyte Lysozyme, an antimicrobial agent considered as allergen, immobilised on magnetic beads was detected by biotinylated aptamer with subsequent binding of streptavidin-alkaline phosphate conjugate. On addition of Para-Nitrophenylphosphate, a chromogenic substrate of alkaline phosphate, it gives rise to the calorimetric signal (R. K. Mishra et al., 2017). Attempts have also been made to detect gluten protein present in wheat responsible for celiac disease using aptamers against immunotoxic 33-mer gliadin peptide segment of the protein (Amaya-González, de-los-Santos-Álvarez, et al., 2015; Amaya-González, López-López, et al., 2015).

1.2.10.3 Biotoxin

Aflatoxin B1 (AFB1) produced by fungus *Aspergillus* is one of the most harmful toxins labelled as group I carcinogen in humans by the International Agency for Research on Cancer (IARC) (Q. Wang et al., 2020). The maximum permissible limit of AFB1 set by European Union in foodstuff is 2ppb (2µg/Kg) (Setlem et al., 2020). A large number of aptamer based sensors and assays have been developed to detect AFB1 with limit of detection much lower than the EU specified limit (H. He et al., 2020; Y. Jia et al., 2020; H. Liu, Luan, et al., 2018;

Ma et al., 2016). A detection limit as low as 4.5×10^{-4} ppb was demonstrated in nanomaterial functionalised SERS aptasensor for AFB1 quantification in peanut oil samples. The sensor employed a capture probe of cDNA functionalised on gold-magnetic nanoparticle (Fe3O4@Au nanoflowers-cDNA) and a reporter probe of aptamer functionalised gold-silver nanosphere containing embedded Raman molecule 4-mercaptobenzoic acid (Au-4MBA@Ag NSs-Apt). The cDNA of reporter is complimentary to aptamer and they hybridised in absence of target AFB1. Competitive binding in presence of AFB1 leads to release of the aptamer conjugated reporter probe to solution while capture probes are isolated using external magnet. SERS analysis of capture probes shows linear decrease in intensity. Inverse relationship between AFB1 concentration and SERS intensity allows quantification (H. He et al., 2020) (Fig.4). A Florescent biosensor that uses fluorescence dye TAMRA labelled aptamer absorbed on a metal-organic frameworks (UiO-66-NH2) was developed for detection AFB1 in real food samples of corn, rice and milk with a LOD of 0.35 ppb. UiO-66-NH2 surface normally quenches the fluorescence of dye, while binding of the high affinity and specific aptamer to AFB1 results in emission of fluorescence (Y. Jia et al., 2020). Ochratoxin A (OTA) produced by *Aspergillus* and *Penicillium*, exhibiting nephrotoxic, teratogenic and carcinogenic activities, commonly found in livestock feeds and also in cereals, coffee, cocoa, wine, beer, cooking oil, soy products, grape juice and meat etc., is positioned just next to AFB1 in terms of toxicity (Han et al., 2021; K. Wu et al., 2019). High sensitive of sub-picomolar level in OTA detection was achieved by using nanoparticles for the strategy of magnetic separation and signal amplification. It used two DNA strands complimentary to OTA aptamer, one attached on Gold nanoparticle functionalised silica-coated iron oxide magnetic nanoparticles (mSiO2@Au-DNA1) and another on cadmium telluride quantum dots (CdTe QDs) modified graphene/AuNPs nanocomposites (GAu/CdTe-DNA2). Aptamers' base pairing to complementary DNAs joins the two complexes of nanomaterials, but presence of OTA leads to binding of aptamer with OTA and breaking of the bond between the complexes. mSiO2@Au is magnetically separated while GAu/CdTe is released to supernatants. CdTe QDs are dissolved by HNO_3 and it is detected by Squarewave voltammetry which in turns implies the concentration of OTA. This approach with LOD of 7×10^{-5} ppb was found to be one among the most sensitive OTA aptasensors. However the performance of this aptasensor needs to be evaluated in real food sample (Hao et al., 2016). Similar approach of employing separation technique using magnetic nanoparticle and signal generation by CdTe quantum dots in another OTA fluorescence aptasensor was validated in peanut sample with a limit of detection of 5.8×10^{-4} ppb (C. Wang et al., 2015).

Exonucleases which can cleave mononucleotide from oligonucleotide sequences are integrated into electrochemical aptasensors. A Methylene Blue (MB)-labelled DNA probes get exposed to exonuclease as a result of conformational change once analyte binds to aptamer sequence. MB-labelled electroactive mononucleotides (eT) produced from enzymatic cleavage can interact with Indium tin oxide (ITO) electrode surface to generate an signature electrochemical signal indicating quantity of analyte. This approach was applied for OTA detection with a LOD of 5.8×10^{-4} ppb (C. Liu et al., 2017) and 0.004 ppb (Y. Tan et al., 2015) and validated in wheat sample and corn samples respectively. Simultaneous detection of the two mycotoxins AFB1 and OTA in food stuffs was achieved by developing an aptamer-based microchip capillary electrophoresis coupled with laser induced fluorescence (MCE-LIF) detection method. Two aptamers, one specific to AFB1 and another specific to OTA initially remain in base pairing with two respective complementary DNA strands. Binding of the targets to aptamers releases the complementary DNA strands and aptamer-target complexes. These all types of oligonucleotides can be separated in MCE and detected in LIF unit. This simple detection method is very sensitive (with LOD of 0.026 ppb for AFB1 and 0.021 ppb for OTA) and fast which requires only 3 mins for analysis besides the 1 hour time required for aptamer-target binding (Xiao et al., 2018). Another major mycotoxin, T-2 toxin, produced by Fusarium was detected with an outstanding LOD of 1.79×10^{-6} ppb using a reduced graphene oxide-tetraethylene pentamine-gold@platinum (rGO-TEPAAu@Pt) nanorods based aptasensor in simulated beer samples (Zhong et al., 2019). Recently optical aptasensors based on attenuated internal reflection spectroscopic ellipsometry (AIR-SE) have been developed against biotoxins, Zearalenone (ZEN) produced by Fusarium species (Caglayan & Üstündağ, 2020a) and paralytic shellfish poisoning (PSP) toxin or Saxitoxin produced by marine dinoflagellates (Caglayan & Üstündağ, 2020b). Ellipsometry detects the variations in polarization state of reflected light from thin films occurring due to changes of dielectric constant. Aptamers when immobilised on the coupler of AIR-SE may result into change of the dielectric constant if the target binds. Combining AIR-SE with SPR increases the sensitivity of the detection system to a greater extent (Caglayan & Üstündağ, 2020a, 2020b).

1.2.10.4 Antibiotic residues

Directives of regulatory bodies like EU (Council Directive 96/23/EC) do not allow presence of an antibiotic residue beyond a specified concentration called Maximum Residual Levels

(MRL) in a specific food (Mehlhorn et al., 2018). For example, the MRL listed for Kanamycin in milk is 150 μg/kg (Yue et al., 2021). Aptasensors have been mostly developed against antibiotics kanamycin, chloramphenicol, tetracycline, and oxytetracycline (Mehlhorn et al., 2018). Aptasensors based on diverse signal generation and amplification strategies such as nanoparticle aggregation (Ramezani et al., 2015), electrochemical impedance spectroscopy (A. Sharma et al., 2017), microchip electrophoresis (L. Zhou et al., 2017), upconversion nanoparticles (UCNPs) based fluorescence (S. Wu et al., 2015), total internal reflection ellipsometry (Caglayan, 2020), fluorescence resonance energy transfer (FRET) (Ying Zhang et al., 2020), rolling circle amplification (RCA) reaction (Hong et al., 2021) etc. among others are applied for detection of various antibiotic residues in food samples (mostly in milk, fish and honey). An ultrasensitive calorimetric aptasensor was developed against chloramphenicol (CAP) that showed possibly the lowest LOD of 0.03pM with a wider linear range of 0.1 pM (0.0323 pg/mL) to 1000 pM (323 pg/mL) among the reported aptasensors for analysis of antibiotic in food (Luan et al., 2018). It used an aptamer sequence selected by Mehta et al., 2011, which had a dissociation constant of 0.77 μM (Mehta et al., 2011). Although the affinity of the aptamer is in micromolar level, the use of DNAzyme labelled Metal Organic Frame (Fe-MIL-88-Pt) as novel peroxidase mimic signal tags along with target-triggered circular strand-displacement polymerization (CSDP) strategy for enhanced signal amplification in the aptasensor has led to such low LOD level. In the sensing complex, a capture probe containing aptamer sequence immobilised on magnetic beads remains in partial hybridization with a complementary DNA sequence in DNAzyme of the signal tag (MIL-88-Pt-DNAzyme). In presence of CAP, capture probe binds to it more favourably releasing the signal tag. All the three components of the released signal tag can catalyse colourless 3,3′,5,5′-tetramethylbenzidine (TMB) to blue-coloured oxidized TMB (oxTMB) giving rise an output calorimetric signal. Further amplification of signal occurs with incorporation of oligonucleotide primer and Bst DNA polymerase that polymerises the cDNA of capture probe into double strands releasing CAP to interact with more sensing complexes and liberating signal tags. The applicability of the aptsensors was demonstrated in diluted milk samples (Luan et al., 2018).

There has also been some recent developments in construction of aptasensors that can multiplex analysis of more than one antibiotic residues in food samples. Microchip electrophoresis (MCE) is generally used for analysis of multiple analyte molecules. In a MCE based aptasensor, KAN and CAP specific aptamers as capture DNA (cDNA) functionalised on

magnetic beads were used for displacement of complimentary assistant DNA (A-DNA) on target binding. PCR amplification of A-DNA, separation and detection of PCR products of different length specifying the analyte on MCE enables quantification of KAN and CAP simultaneously with very low LODs of 0.0025 nM and 0.006 nM respectively (L. Zhou et al., 2018). For simultaneous detection of three different antibiotics, chloramphenicol (CAP), oxytocin (OTC), and kanamycin (KANA) with emission of specific colour fluorescence indicating each antibiotic residue, two-dimensional metal organic frameworks (2D MOFs) as quencher for fluorescent-dye-labelled aptamers were used in Double Stirring Bar Assisted Target Replacement (DSBATR) system. It showed extremely low LOD for each antibiotic residues, 1.5 pM for CAP, 2.4 pM for OTC and 1 pM for KANA. It was successfully used in multicolour imaging of the antibiotic residues in fish slice (Q. Yang et al., 2019).

1.2.10.5 Pesticide

Pesticides, applied during agriculture and farming, contaminate the foods of plant origin and also accumulate in animal based food products due to bioaccumulation and magnification. Apart from using various methodologies adopted for aptasensor development against small molecule like antibiotics as described earlier, combination of aptamer with other detection probe such as employing a double recognition methodology by combining aptamer with molecularly imprinted polymer receptors (MIPs) increases the sensitivity of the detection limit to femtomolar level. Electropolymerized aptamer-imprinted polymer along with nanogold was used to modify a glassy carbon electrode (GCE) to detect an organophosphate pesticide (OPP), chlorpyrifos (CPS) in apple and lettuce samples electrochemically (Roushani et al., 2018). A single aptamer which forms four loops in secondary structure that are likely to be involved in recognising four different organophosphorus pesticides viz, profenofos, isocarbophos, omethoate and phorate was functionalised on interdigitated microelectrodes (IDMEs) to fabricate an aptasensor which measures solid-liquid interfacial capacitance to quantify the pesticide levels in real time within 30 sec. This sensor has a limit of detection in the range 0.24–1.67 fM for the four different pesticides and it can be stored in room temperature at least for 14 days without loss of activity (J. Zhang et al., 2020). For aptamer based calorimetric detection of pesticide acetamiprid using gold nanoparticle aggregation strategy, the fine tuning of aptamer length or more specifically reducing the length by truncating the flaking regions for this specific small molecular target led to enhancement of the sensitivity (Tian et al., 2016).

1.2.10.6 Heavy metals

Heavy metals such as Mercury (Hg), Lead (Pb), Cadmium (Cd), Arsenic (As) etc. can get into food chain and cause multitude of adversities from organ damage, neurotoxicity to cancer when accumulate inside human body. There are weekly allowable intake standards established by different organisations for various heavy metals in foods. For instance, the Joint Food and Agriculture Organization (FAO)/World Health Organization (WHO) Expert Committee on Food Additives (JECFA) recommends a weekly allowable intake of methyl mercury not beyond 1.6 µg/kg (L. Wang et al., 2020). Along with formation of specific 3D tertiary structure, electrostatic attraction arises due to polyanionic nature of aptamer helps in binding to positively charged heavy metal ions, although simple structure and single binding site of heavy metal possess disadvantages in aptamer selection (Guo et al., 2021). Aptamer specific to Hg^{2+} are generally T-rich that selectively binds to it through formation of a stable T-Hg^{2+}-T base pair (Y. Liu et al., 2020). Such Hg^{2+} Specific aptamer has been utilised in development of a dual-channel biosensor that can simultaneously generate surface-enhanced Raman spectroscopy (SERS) and fluorescence signals for Hg^{2+} detection in spiked tap water and milk samples (H. Li, Huang, et al., 2020). Exploiting the T-Hg^{2+}-T hair pin structure formation of Hg^{2+} specific aptamer and induction of G-quadruplexes structure in a guanine (G)-rich Pb^{2+} specific aptamer upon binding of the respective targets, an electrochemiluminescence aptasensor that can detect both Hg^{2+} and Pb^{2+} was demonstrated in spiked fish and shrimp samples with recovery rates of 88-103% (Feng et al., 2020). An aptamer selected against Cd that binds through formation of a coordination bond between Cd(ii) and a T or G rich non-repeating segment of the aptamer (Y. Wu et al., 2014) was successfully incorporated in a gold interdigitated electrode (IDE) based aptasensor that measures interfacial capacitance. It could detect Cd in various matrices such as tap water, olive oil and rice leaching solution with extremely sensitive detection limit, a sub-femtomolar level of 253.16 aM (J. Zhang et al., 2021).

1.2.10.7 Selective analyte extraction using aptamer

Detection of analyte in food matrix is not always possible as food matrices interfere with the process and in some cases, the analyte concentration is so low that detectors fail to respond. Extraction of the analyte is generally employed as a pre-treatment step of sample preparation to enrich or pre-concentrate the analyte of interest and to reduce the amount of reagents

required during analysis (Płotka-Wasylka et al., 2016). Owing to the high specificity and affinity of aptamer towards target, aptamers have been conjugated to various sorbent materials for Solid Phase Extraction (SPE) process of analyte. Aptamers have been functionalised inside various types of affinity columns such as monolithic, material packed, spin, open tubular capillary columns; on magnetic materials such as magnetic nanoparticles (MNPs), magnetic beads (MBs) and magnetic microspheres (MMSs) and on surfaces of various micro/nanostructured materials such as carbon nanotubes, graphene oxide, gold and silica etc. (Du et al., 2015). The 5' or 3' end of aptamer can be modified with different chemical moieties very conveniently which enables the immobilization on solid sorbent surfaces. Immobilization can be achieved either by covalent or non-covalent binding depending on the nature of activated functional groups present on the solid supports. Streptavidin conjugated on solid materials like polystyrene, porous glass, and magnetic beads can non-covalently bind to biotinylated aptamer. Aptamers modified with functional groups like amino, thiol, carbonyl etc. can covalently bind to activated solid surfaces, e.g. gold, glass, magnetic beads or nanoparticles etc. (Pichon et al., 2015). In SPE methods, sample is first fed into an affinity column or exposed to sorbent in a vial where the bioaffinity ligands specifically bind to the analyte. Non-specifically bounded entities and other matrix components are removed by washing the sorbents with buffer solution. Bound analytes are eluted from sorbent by treating with an eluent solution and later the extracted analyte can be detected by a suitable analytical method like HPLC, LC-MS, GC-MS or Mass spectroscopy (MALDI-MS) etc. (H. Liu, Luan, et al., 2018). Oligosorbents or aptamer-based sorbents offer advantage of better reusability than immunosorbents as antibodies are prone to irreversible denaturation due to action of organic solvents, salts concentration and pH (Khodadadi et al., 2018). Reusability also depends on the method of aptamer immobilisation as non-covalent binding can be effected by organic solvents or some type of buffer, whereas covalently immobilized aptamers perform better (Acquah et al., 2015; Pichon et al., 2015).

An aptamer functionalised magnetic nanoparticle based solid-phase extraction procedure was developed by Khodadadi et al., 2018 for extraction of aflatoxin M1 (AFM1) from milk and dairy products matrices. Silica coated Fe_3O_4 magnetic nanoparticles functionalised with AFM1 specific aptamer offered excellent dispersion of the nano-sized sorbent in the sample and a large specific surface area for interaction with the targeted toxin which enabled efficient extraction. Extracted AFM1 was analysed with HPLC-FD with a detection limit of 0.2 $ng \cdot L^{-1}$ (Khodadadi et al., 2018). Aptamer was also conjugated to a

magnetic agarose microspheres (MAMs) through biotin–streptavidin interaction to perform magnetic solid-phase extraction (MSPE) of the aflatoxins AFB1 and AFB2 from maize sample as a rapid and convenient way prior to detection by HPLC-PCD-FLD (H. Liu, Lu, et al., 2018). Magnetic dispersive solid phase extraction was also successful in enrichment of three amphenicol antibiotics residues, Chloramphenicol (CAP), Thiamphenicol (TAP) and Florphenicol (FF) from milk by using specific aptamers conjugated to Silica-coated Fe_3O_4 magnetic nanoparticles through EDC/Sulfo NHS covalent coupling process. Pre-treatment by aptamer functionalised Silica-coated Fe_3O_4 magnetic nanoparticles enabled the detection of the three amphenicols by HPLC-DAD (Fig.5) which was not possible without pre-treatment (Huang et al., 2017). Aptamer functionalised magnetic particle (Fe_3O_4@SiO2@pGMA) was also employed in capture of pathogenic *Salmonella* cells from complex matrix of milk and entrapped bacterial cells were detected using another aptamer-gated MCM-41 silica nanoparticle loaded with reporter fluorescent molecule (Bayramoglu et al., 2018). Magnetic sorbents offer the advantages of dispersion throughout the sample, reversible agglomeration and redispersion in sample solutions and easy isolation from sample by applying external magnetic field. Ability of dispersion helps in better surface contact between sorbents and analyte which in turn increases mass-transfer. Separation of magnetic particles from sample does not require filtration or high speed centrifugation (H. L. Jiang et al., 2019; H. Liu, Lu, et al., 2018)

Aptamer based affinity column was used in selective extraction of mycotoxin aflatoxin B2 (AFB2) from peanut sample which used amino functionalised aptamer covalently conjugated to CNBr-activated Sepharose packed inside a 1mL SPE tube. HPLC with fluorometric detector was used for detection of extracted AFB2 with a limit of detection of 25 $pg \cdot mL^{-1}$ and efficient reusability up to 5 times (H. Liu, Luan, et al., 2018). AFB2 has also been enriched from lotus seed using aptamer functionalised Sepharose affinity column which showed better reusability and cheaper alternative than immunoaffinity chromatography (IAC) (Zhao et al., 2020). Ochratoxin A (OTA) was efficiently extracted from cornmeal samples using a aptamer functionalised Chitosan coated Fe_3O_4 magnetic nanoparticles where recovery rates were found to be very close to IAC while timing was faster (S. Wang et al., 2020).

Stir bar sorptive extraction (SBSE) technique holds 50-250 times higher coating amounts than solid-phase microextraction (SPME) fiber which enables enhanced recovery and extraction of analytes. Aptamers-functionalised SBSE was developed for selective enrichment

of poly chlorinated biphenyls (organic pollutant) 2,3′,5,5′-tetra-chlorobiphenyl (PCB72) and 2′,3′,4′,5,5′-pentachlorobiphenyl (PCB106) from complex matrix of fish samples and successively determined by coupled GC-MS (Lin et al., 2016). A gold nanoparticle based stir bar functionalised with thio-modified aptamer was used for extraction of antibiotic kanamycin residues in milk and fish sample. Aptamer on the stir bar was hybridised with a RCA primer which is released when kanamycin binds to the aptamer. This was conjugated to a Rolling Cycle Amplification and microfluidic chip-based ratiometric aptasensing platform for on-site quantification of the antibiotic residues (L. He et al., 2019). A dispersive SPE method was developed by using aptamer functionalised chitosan nanofibers (CNF) for extraction of a nonsteroidal estrogen, Zearalenone from corn, wheat, and beer samples. Aptamer-CNF was directly added to pre-treated samples at a shaking rate of 300rpm, removed and desorbed in acetonitrile and the desorbed analyte was analysed using HPLC (L. Liu et al., 2020).

1.2.10.8 Application as target-responsive aptamer-cross-linked hydrogel

Hydrogels are hydrophilic polymeric material with high water retention property (up to 99%) that forms a three dimensional network through cross-linking of monomers or polymer chains by covalent or noncovalent bonding. Hydrogels are widely used in biomedical applications for sensing and drug delivery (Di et al., 2020). Their utility has also been increasing in food sensing applications due to their advantageous target responsive and cost effective properties. They are easy to store, flexible, stable and portable for on-site detection (Di et al., 2020; Ma et al., 2016). Oligonucleotide based probes including aptamer can be exploit as a hydrogel material when used along with cross-linking oligonucleotide strands. Aptamer can also be incorporated with other polymeric material for functionality or stimuli responsive behaviour, while short oligonucleotide sequences are used as crosslinking supramolecular agent (Di et al., 2020; J. Li et al., 2016). Hydrogels when interact with a target molecule can swell by crosslinking or disintegrate. This property can be exploited for development of a simple and intelligent sensors with switch which could be either in ‘On’ or ‘Off’ state based on presence or absence of target (P. Wu et al., 2020). Aptamer based hydrogels are formed by using complimentary oligonucleotides that hybridises to cross-link the strands in a porous network. The presence of target can cause change in the conformation of aptamer to competitively bind with it over the complementary hybridization of oligonucleotides and this results in disintegration of the hydrogel. The hydrogel network can entrap or encapsulate dyes, colorimetric or fluorescence

agents such as nanoparticles or quantum dots which aids in optical detection upon collapse of hydrogel (Di et al., 2020).

Liu et al., 2015 used an aptamer-cross-linked hydrogel by using an Ochratoxin (OTA) specific aptamer and two complementary DNA strand grafted on linear polyacrylamide chains. The hydrogel entrapped gold AuNPs. Presence of OTA leads to interaction of aptamer with it and hydrogel collapses releasing the AuNPs which turns the colourless supernatant to red, enabling visual colorimetric analysis (R. Liu et al., 2015). Ma et al., 2016 also used similar strategy to detect aflatoxin B1 (AFB1) using aptamer-crosslinked-hydrogel preloaded with platinum nanoparticles (PtNPs) and they combined it with a distance-readout microfluidic volumetric bar chart chip (V-chip) for quantitative measurement of AFB1 concentration as well. The released PtNPs can be loaded to the distance-readout based microfluidic chip where PtNP catalyses decomposition of H_2O_2 to generate O_2. The pressure from generated O_2 moves a red ink bar in the V-chip and distance travelled by ink is directly proportional to the concentration of AFB1 (Ma et al., 2016). Zhao et al., 2018 used urease enzyme entrapped in aptamer-crosslinked-hydrogel which catalyses hydrolysis of urea on collapse of hydrogel to quantify AFB1 concentration in food through a handheld pH meter as readout (Zhao et al., 2018). Target recycling amplification with the help of Exonuclease I and electronic balances as a readout were also employed for aptamer-crosslinked-hydrogel based detection of AFB1 (Tang et al., 2020).

Target-responsive aptamer-cross-linked hydrogel was developed against toxin microcystin-LR for detection in food sample and it's calorimetric signal was amplified by released Cu/Au/Pt trimetallic nanoparticles which catalyses reaction of H_2O_2 with 3,3,5,5-tetramethylbenzidine (TMB) forming a coloured by-product (P. Wu et al., 2020). Aptamer was used with TiO_2 and poly(Nisopropylacrylamide-acrylic acid), P(NIPAM-AA) hydrogel to form a one-dimensional photonic crystals (1DPCs) for calorimetric detection of heavy metal mercury ions (Xuan et al., 2016). 1DPCs are formed from alternate stacking of materials with varying refractive indices in layer which finally exhibit specific optical property. The optical property of 1DPCs can be tuned by changing incident angles, periods, and the refractive index (C. Yao et al., 2014). The cross-linked single-stranded aptamers acting as stimuli-responsive element when bind to Hg^{2+} causes the shrinking of hydrogel and this leads to colour change of 1DPCs. From the blue shift value of Brag's diffraction peak of 1DPC, concentration of Hg^{2+} can be calculated (Xuan et al., 2016). A graphene oxide (GO) hydrogel was developed with

adenosine and aptamer acting together as co-cross linker, while the aptamer specific to antibiotic oxytetracycline (OTC) and responsible for target recognition was modified with a FAM tag. Florescence of FAM was quenched by GO sheet of hydrogel complex by the phenomenon of fluorescence resonance energy transfer (FRET). Presence of analyte changes confirmation of the aptamer, resulting in binding and detachment from hydrogel complex, which then induce florescence of FAM for quantification of OTC concertation (B. Tan et al., 2016). GO based hydrogels with aptamer have also been employed for detection of *Escherichia coli* by a luminol based electrochemiluminescence aptasensor (Hao et al., 2017), tetracycline by label-free photoelectrochemical aptasensor (Ge et al., 2018), chloramphenicol in honeycomb by photoelectrochemical aptasensor (D. Jiang et al., 2019).

1.2.11 Challenges and opportunities in development of aptamer for gluten detection

The advantages offered by aptamer over antibody motivated researchers to explore the development of aptamer based detection method for gluten. Aptamer based assays and sensors have been developed recently by many groups as listed in the **table 1.3**. The initial trials to select aptamer against gliadin fractions and it's immunodominant small peptide epitopes were faced with failures (Pinto et al., 2014). Considering the hydrophobic nature of gluten protein, it has been challenging to come up with an effective aptamer molecule due the hydrophilic nature of nucleic acid. Targets devoid of positively charge groups in selection buffer condition, plane aromatic rings and groups that can form hydrogen bonds are generally not very ideal for aptamer selection (Amaya-Gonzalez et al., 2014). Besides, the proline-rich hydrophobic gliadin fraction of the gluten is difficult to dissolve in aqueous media and immobilization of it on solid support through covalent bond is generally not achieved. In case of selecting aptamers against hydrophobic targets, the approach of attaching using unnatural nucleotide with the hydrophobic base 7-(2-thienyl)imidazo[4,5-b]pyridine (Ds) along with the natural bases in the aptamer library helps in obtaining high affinity aptamer (Kimoto et al., 2013). Pinto et al., however, were able to select unmodified aptamer G33 with natural bases using a different immobilization tactic. They immobilised the hydrophobic gliadin (Sigma gliadin) on polystyrene microtitre plates through hydrophobic interactions which allowed the less hydrophobic moieties of gliadin to interact with oligonucleotide library. They carried out conventional SELEX for 8 rounds to select the aptamer candidate and determined the LOD of 2 nM (100 ng ml^{-1}) with apta-PCR based assay. This aptamer was not evaluate in real food

sample for it's applicability (Pinto et al., 2014; Miranda-Castro et al., 2016). Amaya-Gonzalez et al. were able to select a panel of aptamers against the apolar and most immunodominant 33 mer peptide of α2-gliadin using conventional SELEX method. The peptide was immobilised on a Ni^{2+}-nitrilotriacetic acid magnetic beads through a polyhistidine tag attached to C-terminal with a spacer peptide in between to avoid the steric hindrance by magnetic bead. Negative SELEX was carried out against spacer-polyhistidin tag to remove non-specific binders. Selected through this method one specific aptamer Gli4 could bind to PWG-gliadin with a LOD of 0.5 ppb determined through an electrochemical competitive enzyme-linked assay on magnetic particles. The LOD reported for this aptamer was found to be 6 times lower than the standard R5 Sandwich ELISA assay (Amaya-Gonzalez et al. 2014). Further, another aptamer Gli1 was found to be suitable in detecting peptides of gluten in hydrolysed food samples. (Amaya-González et al., 2015). An electrochemical based aptasensor has been also developed to detect gluten in food sample which has the sensitivity comparable with ELISA based gluten detection method (López-López et al., 2017). To overcome the problem of poor solubility of gluten protein and for gaining higher numbers of confirmation of DNA aptamers, a deep eutectic solvent has recently been used as aptamer selection buffer which increase the probability of selecting high affinity aptamer against gluten (Svigelj et al., 2018). DES allows the formation of different and diverse number of DNA functional shapes than in aqueous solvents (Svigelj et al., 2017). Utilisation of DES as selection buffer in SELEX process of aptamer against target like poorly soluble gluten proteins enabled the selection of aptamer candidates in less number of SELEX cycles than in aqueous buffer (Svigelj et al., 2018; Svigelj et al., 2020).

Table 1.3 The overview on aptamer and aptamer-based methods for detection of gluten

Aptamer	Target	Section method	K_d Value	Application platform	LOD	References
Gli1 (DNA)	Immunotoxic α2-gliadin fragment, 33-mer	Conventional SELEX	102 nM	Electrochemical Aptamer-Based Assay	4.9 ppm	Amaya-González et al., 2015
Gli5 (DNA)	Immunotoxic α2-gliadin fragment, 33-mer	Conventional SELEX	61 nM	Electrochemical Aptamer-Based Assay	0.5 ppm	Amaya-González et al., 2014

Gli1 (DNA)	PWG gliadin	Conventional SELEX	6.66 nM	Label-free Impedimetric Aptasensor	5 ppm	Malvano et al., 2017
G33 (DNA)	Gliadin	Conventional SELEX	_	Real-time Apta-PCR Assay	2 nM	Pinto et al., 2014
Gli2D and Gli3D (DNA)	Immunotoxic α2-gliadin fragment, 33-mer	SELEX in deep Eutectic Solvent	1.3 µM	Bioassay	_	Svigelj et al., 2018

1.2.12 Gap in the literature:

The detection of whole gluten and hydrolysed products of gluten is important as both are widely used in food processing industries. The extensive literature review shows the current analytical methods employed for detection of gluten suffer from certain limitations. Most of the commercial antibodies used in ELISA exist presently for detection of gluten are developed only to detect the celiac disease epitopes in the gliadin fraction. The antibodies also suffers from the disadvantages of getting denatured due to use of protein reducing agents for enhance extraction of total gluten which raises a necessity to use alternative non-protein probes for gluten detection. Alcoholic beverages such as beer and whiskey often contain a hydrolysed form of gluten protein which includes the peptides responsible for celiac disease. Apart from alcoholic beverages, there are other processing techniques which causes hydrolysis of intact food proteins. The mass spectroscopic methods are generally used to detect and quantify these protein fractions which is a very tedious and costly exercise along with requirement of trained laboratory technicians. Aptamer are considered as an alternative to antibodies due to several advantages and they have been recently explored for application into gluten detection. There have been development of a few successful aptamers for detection of gluten, which however is focused on the gliadin subunit of the gluten protein. Apart from the protein subunit, detection of the epitope peptide fragments of gluten is very important to obtain a greater resolution and advantages in terms of determining the safety of the food product containing hydrolysed gluten (Mitea et al., 2008). The anti-epitopic peptide aptamer candidates have been developed against only a 33 mer immunogenic peptide faction of gliadin. The glutenin subunit also contains immunogenic peptides which are harmful for celiac patients. Currently, glutenin specific

aptamers for detection of the immunogenic peptide epitopes of celiac disease in glutenin are not found to be reported in literature. Development of aptamer against the epitopes in glutenin can be promising in order to develop the multiplexing aptamer based method along with aptamer candidates selected against the epitopes in gliadin fraction. For accurate estimation of gluten and the toxic peptides, it is essential to develop detection probes with greater utility against all the available epitopes of celiac disease for development of a reliable and cost-effective analytical method.

1.2.13 Objectives

1. Selection of specific aptamer ligands against the known peptide epitopes of celiac disease in high molecular weight glutenin subunit of wheat.
2. Selection of specific aptamer ligands against the known peptide epitopes of celiac disease in low molecular weight glutenin subunit of wheat.
3. Evaluation of the binding affinity of aptamer probes with the targets.
4. Development of aptaassays for detection of immunotoxic celiac epitopes of glutenin.

(*Part of this chapter has been published as 'Kalita, J. J., Sharma, P., & Bora, U. (2022). Recent developments in application of nucleic acid aptamer in food safety. Food Control, 109406.'*)

1.2.14 References:

1. Abadie, V., Sollid, L. M., Barreiro, L. B., & Jabri, B. (2011). Integration of genetic and immunological insights into a model of celiac disease pathogenesis. Annual review of immunology, 29, 493-525
2. Abdelrasoul, G. N., Anwar, A., MacKay, S., Tamura, M., Shah, M. A., Khasa, D. P., Montgomery, R. R., Ko, A. I., & Chen, J. (2020). DNA aptamer-based non-faradaic impedance biosensor for detecting E. coli. Analytica Chimica Acta, 1107, 135–144.
3. Acquah, C., Agyei, D., Obeng, E. M., Pan, S., Tan, K. X., & Danquah, M. K. (2020). Aptamers: an emerging class of bioaffinity ligands in bioactive peptide applications. Critical Reviews in Food Science and Nutrition, 60(7), 1195–1206.

4. Acquah, C., Danquah, M. K., Yon, J. L. S., Sidhu, A., & Ongkudon, C. M. (2015). A review on immobilised aptamers for high throughput biomolecular detection and screening. Analytica Chimica Acta, 888, 10–18.
5. Amaya-Gonzalez, S., de-Los-Santos-Álvarez, N., Miranda-Ordieres, A. J., & Lobo-Castanon, M. J. (2014). Aptamer binding to celiac disease-triggering hydrophobic proteins: a sensitive gluten detection approach. Analytical chemistry, 86(5), 2733-2739.
6. Amaya-González, S., de-los-Santos-Álvarez, N., Miranda-Ordieres, A. J., & Lobo-Castañón, M. J. (2013). Aptamer-based analysis: A promising alternative for food safety control. Sensors (Switzerland), 13(12), 16292–16311.
7. Amaya-González, S., López-López, L., Miranda-Castro, R., de-los-Santos-Álvarez, N., Miranda-Ordieres, A. J., & Lobo-Castañón, M. J. (2015). Affinity of aptamers binding 33-mer gliadin peptide and gluten proteins: Influence of immobilization and labeling tags. Analytica chimica acta, 873, 63-70.
8. Amor-Gutiérrez, O., Giulia, S. M., Fernández-Abedul, T., De La, A., Muñiz, E., & Marrazza, G. (2020). Folding-based electrochemical aptasensor for the determination of β-lactoglobulin on poly-l-lysine modified graphite electrodes. Sensors (Switzerland), 20(8).
9. Amouzadeh Tabrizi, M., Shamsipur, M., Saber, R., Sarkar, S., & Ebrahimi, V. (2017). A high sensitive visible light-driven photoelectrochemical aptasensor for shrimp allergen tropomyosin detection using graphitic carbon nitride-TiO2 nanocomposite. Biosensors and Bioelectronics, 98(June), 113–118.
10. Appaturi, J. N., Pulingam, T., Thong, K. L., Muniandy, S., Ahmad, N., & Leo, B. F. (2020). Rapid and sensitive detection of Salmonella with reduced graphene oxide-carbon nanotube based electrochemical aptasensor. Analytical Biochemistry, 589(October 2019), 113489.
11. Asri, N., Rostami-Nejad, M., Anderson, R. P., & Rostami, K. (2021). The gluten gene: unlocking the understanding of gluten sensitivity and intolerance. The application of clinical genetics, 37-50.
12. Bagheryan, Z., Raoof, J. B., Golabi, M., Turner, A. P. F., & Beni, V. (2016). Diazonium-based impedimetric aptasensor for the rapid label-free detection of Salmonella typhimurium in food sample. Biosensors and Bioelectronics, 80, 566–573.
13. Balakireva, A. V., & Zamyatnin Jr, A. A. (2016). Properties of gluten intolerance: gluten structure, evolution, pathogenicity and detoxification capabilities. Nutrients, 8(10), 644.

14. Baldrich, E., Restrepo, A., & O'Sullivan, C. K. (2005). Aptasensor development: Elucidation of critical parameters for optimal aptamer performance. Analytical Chemistry, 76(23), 7053–7063..
15. Barone, M. V., Zanzi, D., Maglio, M., Nanayakkara, M., Santagata, S., Lania, G., ... & Auricchio, S. (2011). Gliadin-mediated proliferation and innate immune activation in celiac disease are due to alterations in vesicular trafficking. PLoS One, 6(2), e17039.
16. Bayramoglu, G., Ozalp, V. C., Dincbal, U., & Arica, M. Y. (2018). Fast and Sensitive Detection of Salmonella in Milk Samples Using Aptamer-Functionalized Magnetic Silica Solid Phase and MCM-41-Aptamer Gate System. ACS Biomaterials Science and Engineering, 4(4), 1437–1444.
17. Bodd, M., Kim, C. Y., Lundin, K. E., & Sollid, L. M. (2012). T-cell response to gluten in patients with HLA-DQ2. 2 reveals requirement of peptide-MHC stability in celiac disease. Gastroenterology, 142(3), 552-561.
18. Bruno, J. G. (2015). Predicting the uncertain future of aptamer-based diagnostics and therapeutics. Molecules, 20(4), 6866–6887.
19. Bruno, J. G., Sivils, J. C., & Phillips, T. (2017). Aptamer-magnetic bead quantum dot sandwich assays for foodborne pathogen detection: Pros, cons, and lessons learned. Journal of AOAC International, 100(4), 895–899.
20. Burke, D. H., & Willis, J. H. (1998). Recombination, RNA evolution, and bifunctional RNA molecules isolated through chimeric SELEX. Rna, 4(9), 1165-1175.
21. Caglayan, M. O. (2020). Aptamer-based ellipsometric sensor for ultrasensitive determination of aminoglycoside group antibiotics from dairy products. Journal of the Science of Food and Agriculture, 100(8), 3386–3393.
22. Caglayan, M. O., & Üstündağ, Z. (2020a). Detection of zearalenone in an aptamer assay using attenuated internal reflection ellipsometry and it's cereal sample applications. Food and Chemical Toxicology, 136(September 2019).
23. Caglayan, M. O., & Üstündağ, Z. (2020b). Saxitoxin aptasensor based on attenuated internal reflection ellipsometry for seafood. Toxicon, 187(September), 255–261.
24. Caio, G., Volta, U., Sapone, A., Leffler, D. A., De Giorgio, R., Catassi, C., & Fasano, A. (2019). Celiac disease: a comprehensive current review. BMC medicine, 17(1), 1-20.
25. Castillo, G., Spinella, K., Poturnayová, A., Šnejdárková, M., Mosiello, L., & Hianik, T. (2015). Detection of aflatoxin B1 by aptamer-based biosensor using PAMAM dendrimers as immobilization platform. In Food Control (Vol. 52, pp. 9–18).

26. Catassi, C., & Yachha, S. (2008). The global village of celiac disease. In Frontiers in celiac disease (pp. 23-31). Karger Publishers.
27. Catassi, C., Verdu, E. F., Bai, J. C., & Lionetti, E. (2022). Coeliac disease. The Lancet.
28. Chen, C., Feng, S., Zhou, M., Ji, C., Que, L., & Wang, W. (2019). Development of a structure-switching aptamer-based nanosensor for salicylic acid detection. Biosensors and Bioelectronics, 140, 111342.
29. Chen, J., Ying, G. G., & Deng, W. J. (2019). Antibiotic Residues in Food: Extraction, Analysis, and Human Health Concerns. Journal of Agricultural and Food Chemistry, 67(27), 7569–7586.
30. Chen, S., Yang, X., Fu, S., Qin, X., Yang, T., Man, C., & Jiang, Y. (2020). A novel AuNPs colorimetric sensor for sensitively detecting viable Salmonella typhimurium based on dual aptamers. Food Control, 115(March), 107281.
31. Chen, W., Teng, J., Yao, L., Xu, J., & Liu, G. (2020). Selection of Specific DNA Aptamers for Hetero-Sandwich-Based Colorimetric Determination of Campylobacter jejuni in Food. Journal of Agricultural and Food Chemistry, 68(31), 8455–8461.
32. Chinnappan, R., Rahamn, A. A., AlZabn, R., Kamath, S., Lopata, A. L., Abu-Salah, K. M., & Zourob, M. (2020). Aptameric biosensor for the sensitive detection of major shrimp allergen, tropomyosin. Food Chemistry, 314(January 2019), 126133.
33. Ciccocioppo, R., Di Sabatino, A., & Corazza, G. R. (2005). The immune recognition of gluten in coeliac disease. Clinical & Experimental Immunology, 140(3), 408-416.
34. Comino, I., Real, A., de Lourdes Moreno, M., Montes, R., Cebolla, A., & Sousa, C. (2013). Immunological determination of gliadin 33-mer equivalent peptides in beers as a specific and practical analytical method to assess safety for celiac patients. Journal of the Science of Food and Agriculture, 93(4), 933-943.
35. Cui, F., Sun, J., De Dieu Habimana, J., Yang, X., Ji, J., Zhang, Y., Lei, H., Li, Z., Zheng, J., Fan, M., & Sun, X. (2019). Ultrasensitive Fluorometric Angling Determination of Staphylococcus aureus in Vitro and Fluorescence Imaging in Vivo Using Carbon Dots with Full-Color Emission. Analytical Chemistry, 91(22), 14681–14690.
36. Darmostuk, M., Rimpelova, S., Gbelcova, H., & Ruml, T. (2014). Current approaches in SELEX: An update to aptamer selection technology. In Biotechnology Advances (Vol. 33, Issue 6, pp. 1141–1161).
37. Das, R., Chaterjee, B., Kapil, A., & Sharma, T. K. (2020). Aptamer-NanoZyme mediated sensing platform for the rapid detection of *Escherichia coli* in fruit juice. Sensing and Bio-Sensing Research, 27(August 2019), 100313.

38. Di, Y., Wang, P., Li, C., Xu, S., Tian, Q., Wu, T., Tian, Y., & Gao, L. (2020). Design, Bioanalytical, and Biomedical Applications of Aptamer-Based Hydrogels. Frontiers in Medicine, 7(October), 1–15.
39. Dieli-Crimi, R., Cénit, M. C., & Nunez, C. (2015). The genetics of celiac disease: A comprehensive review of clinical implications. Journal of autoimmunity, 64, 26-41.
40. Dieterich, W., Ehnis, T., Bauer, M., Donner, P., Volta, U., Riecken, E. O., & Schuppan, D. (1997). Identification of tissue transglutaminase as the autoantigen of celiac disease. Nature medicine, 3(7), 797-801.
41. Djordjevic, M. (2007). SELEX experiments: new prospects, applications and data analysis in inferring regulatory pathways. Biomolecular engineering, 24(2), 179-189.
42. Dong, N., Hu, Y., Yang, K., & Liu, J. (2016). Development of aptamer-modified SERS nanosensor and oligonucleotide chip to quantitatively detect melamine in milk with high sensitivity. Sensors and Actuators B: Chemical, 228, 85-93.
43. Dørum, S., Arntzen, M. Ø., Qiao, S. W., Holm, A., Koehler, C. J., Thiede, B., ... & Fleckenstein, B. (2010). The preferred substrates for transglutaminase 2 in a complex wheat gluten digest are peptide fragments harboring celiac disease T-cell epitopes. PLoS One, 5(11), e14056
44. Dørum, S., Bodd, M., Fallang, L. E., Bergseng, E., Christophersen, A., Johannesen, M. K., ... & Sollid, L. M. (2014). HLA-DQ molecules as affinity matrix for identification of gluten T cell epitopes. The Journal of Immunology, 193(9), 4497-4506.
45. Drolet, D. W., Moon-McDermott, L., & Romig, T. S. (1996). An enzyme-linked oligonucleotide assay. Nature Biotechnology, 14(8), 1021–1025.
46. Du, F., Guo, L., Qin, Q., Zheng, X., Ruan, G., Li, J., & Li, G. (2015). Recent advances in aptamer-functionalized materials in sample preparation. TrAC - Trends in Analytical Chemistry, 67, 134–146.
47. Dua, P., Ren, S., Lee, S. W., Kim, J. K., Shin, H. S., Jeong, O. C., Kim, S., & Lee, D. K. (2016). Cell-SELEX based identification of an RNA aptamer for *escherichia coli* and its use in various detection formats. Molecules and Cells, 39(11), 807–813..
48. Eissa, S., & Zourob, M. (2017). In vitro selection of DNA aptamers targeting β-lactoglobulin and their integration in graphene-based biosensor for the detection of milk allergen. Biosensors and Bioelectronics, 91(October 2016), 169–174.
49. Ellington, A. D., & Szostak, J. W. (1992). Selection in vitro of single-stranded DNA molecules that fold into specific ligand-binding structures. Nature, 355(6363), 850-852.

50. Fasano, A. (2012). Zonulin, regulation of tight junctions, and autoimmune diseases. Annals of the New York Academy of Sciences, 1258(1), 25-33.
51. Feng, D., Li, P., Tan, X., Wu, Y., Wei, F., Du, F., Ai, C., Luo, Y., Chen, Q., & Han, H. (2020). Electrochemiluminescence aptasensor for multiple determination of Hg2+ and Pb2+ ions by using the MIL-53(Al)@CdTe-PEI modified electrode. Analytica Chimica Acta, 1100, 232–239.
52. Ferapontova, E. E., Olsen, E. M., & Gothelf, K. V. (2008). An RNA aptamer-based electrochemical biosensor for detection of theophylline in serum. Journal of the American Chemical Society, 130(13), 4256-4258.
53. Ferranti, P., Mamone, G., Picariello, G., & Addeo, F. (2007). Mass spectrometry analysis of gliadins in celiac disease. Journal of mass spectrometry, 42(12), 1531-1548.
54. Foschia, M., Horstmann, S., Arendt, E. K., & Zannini, E. (2016). Nutritional therapy–Facing the gap between coeliac disease and gluten-free food. International Journal of Food Microbiology, 239, 113-124.
55. Freeman, H. J., Chopra, A., Clandinin, M. T., & Thomson, A. B. (2011). Recent advances in celiac disease. World J Gastroenterol, 17(18), 2259-2272.
56. Friedman, M., & Gumbmann, M. R. (1986). Nutritional Improvement of Soy Flour Through Inactivation of Trypsin Inhibitors by Sodium Sulfite. Journal of Food Science, 51(5), 1239–1241.
57. Frohnmeyer, E., Frisch, F., Falke, S., Betzel, C., & Fischer, M. (2018). Highly affine and selective aptamers against cholera toxin as capture elements in magnetic bead-based sandwich ELAA. Journal of Biotechnology, 269(December 2017), 35–42.
58. G Chirdo, F., & Arranz, E. (2015). Cereal Proteins: Immunostimulatory and Toxic Peptides. OmniaScience Monographs
59. Garcia-Calvo, E., García-García, A., Madrid, R., Martin, R., & García, T. (2020). From polyclonal sera to recombinant antibodies: A review of immunological detection of gluten in foodstuff. Foods, 10(1), 66.
60. García-García, A., Madrid, R., Sohrabi, H., de la Cruz, S., García, T., Martín, R., & González, I. (2019). A sensitive and specific real-time PCR targeting DNA from wheat, barley and rye to track gluten contamination in marketed foods. Lwt, 114, 108378.
61. Gatti, S., Lionetti, E., Balanzoni, L., Verma, A. K., Galeazzi, T., Gesuita, R. & Team, C. S. (2019). Increased Prevalence of Celiac Disease in School-age Children in Italy. Clinical Gastroenterology and Hepatology.

62. Gaudin, V. (2017). Advances in biosensor development for the screening of antibiotic residues in food products of animal origin – A comprehensive review. Biosensors and Bioelectronics, 90(December 2016), 363–377.
63. Ge, L., Li, H., Du, X., Zhu, M., Chen, W., Shi, T., Hao, N., Liu, Q., & Wang, K. (2018). Facile one-pot synthesis of visible light-responsive BiPO4/nitrogen doped graphene hydrogel for fabricating label-free photoelectrochemical tetracycline aptasensor. Biosensors and Bioelectronics, 111(April), 131–137.
64. Gianfrani, C., Auricchio, S., & Troncone, R. (2005). Adaptive and innate immune responses in celiac disease. Immunology letters, 99(2), 141-145.
65. Gianibelli, M. C., Larroque, O. R., MacRitchie, F., & Wrigley, C. W. (2001). Biochemical, genetic, and molecular characterization of wheat glutenin and its component subunits. Cereal Chemistry, 78(6), 635-646.
66. Gopinath, S. C. B. (2007). Methods developed for SELEX. Analytical and bioanalytical chemistry, 387(1), 171-182.
67. Green, P. H., Rostami, K., & Marsh, M. N. (2005). Diagnosis of coeliac disease. Best Practice & Research Clinical Gastroenterology, 19(3), 389-400.
68. Gu, C., Lan, T., Shi, H., & Lu, Y. (2015). Portable detection of melamine in milk using a personal glucose meter based on an in vitro selected structure-switching aptamer. Analytical chemistry, 87(15), 7676-7682.
69. Gu, C., Xiang, Y., Guo, H., & Shi, H. (2016). Label-free fluorescence detection of melamine with a truncated aptamer. Analyst, 141(14), 4511-4517.
70. Gujral, N., Freeman, H. J., & Thomson, A. B. (2012). Celiac disease: prevalence, diagnosis, pathogenesis and treatment. World journal of gastroenterology: WJG, 18(42), 6036.
71. Guo, W., Zhang, C., Ma, T., Liu, X., Chen, Z., Li, S., & Deng, Y. (2021). Advances in aptamer screening and aptasensors' detection of heavy metal ions. Journal of Nanobiotechnology, 19(1), 1–19.
72. Han, B., Fang, C., Sha, L., Jalalah, M., Al-Assiri, M. S., Harraz, F. A., & Cao, Y. (2021). Cascade strand displacement reaction-assisted aptamer-based highly sensitive detection of ochratoxin A. Food Chemistry, 338(August 2020), 127827.
73. Hao, N., Jiang, L., Qian, J., & Wang, K. (2016). Ultrasensitive electrochemical Ochratoxin A aptasensor based on CdTe quantum dots functionalized graphene/Au nanocomposites and magnetic separation. In Journal of Electroanalytical Chemistry (Vol. 781, pp. 332–338).

74. Hao, N., Zhang, X., Zhou, Z., Hua, R., Zhang, Y., Liu, Q., Qian, J., Li, H., & Wang, K. (2017). AgBr nanoparticles/3D nitrogen-doped graphene hydrogel for fabricating all-solid-state luminol-electrochemiluminescence *Escherichia coli* aptasensors. Biosensors and Bioelectronics, 97(May), 377–383.
75. He, H., Sun, D. W., Pu, H., & Huang, L. (2020). Bridging Fe3O4@Au nanoflowers and Au@Ag nanospheres with aptamer for ultrasensitive SERS detection of aflatoxin B1. Food Chemistry, 324(August 2019).
76. He, L., Shen, Z., Cao, Y., Li, T., Wu, D., Dong, Y., & Gan, N. (2019). A microfluidic chip based ratiometric aptasensor for antibiotic detection in foods using stir bar assisted sorptive extraction and rolling circle amplification. Analyst, 144(8), 2755–2764.
77. Heiat, M., Najafi, A., Ranjbar, R., Latifi, A. M., & Rasaee, M. J. (2016). Computational approach to analyze isolated ssDNA aptamers against angiotensin II. Journal of biotechnology, 230, 34-39.
78. Herrmann, S. S., Duedahl-Olesen, L., & Granby, K. (2015). Occurrence of volatile and non-volatile N-nitrosamines in processed meat products and the role of heat treatment. In Food Control (Vol. 48, pp. 163–169).
79. Hong, C., Zhang, X., Ye, S., Yang, H., Huang, Z., Yang, D., Cai, R., & Tan, W. (2021). Aptamer-Pendant DNA Tetrahedron Nanostructure Probe for Ultrasensitive Detection of Tetracycline by Coupling Target-Triggered Rolling Circle Amplification. ACS Applied Materials and Interfaces, 13(17), 19695–19700.
80. Hu, Q., Wang, R., Wang, H., Slavik, M. F., & Li, Y. (2018). Selection of acrylamide-specific aptamers by a quartz crystal microbalance combined SELEX method and their application in rapid and specific detection of acrylamide. Sensors and Actuators B: Chemical, 273, 220-227.
81. Huang, S., Gan, N., Liu, H., Zhou, Y., Chen, Y., & Cao, Y. (2017). Simultaneous and specific enrichment of several amphenicol antibiotics residues in food based on novel aptamer functionalized magnetic adsorbents using HPLC-DAD. Journal of Chromatography B: Analytical Technologies in the Biomedical and Life Sciences, 1060(June), 247–254.
82. Jauset-Rubio, M., Sabaté del Río, J., Mairal, T., Svobodová, M., El-Shahawi, M. S., Bashammakh, A. S., Alyoubi, A. O., & O'Sullivan, C. K. (2017). Ultrasensitive and rapid detection of B-conglutin combining aptamers and isothermal recombinase polymerase amplification. Analytical and Bioanalytical Chemistry, 409(1), 143–149.

83. Jayan, H., Pu, H., & Sun, D. W. (2020). Recent development in rapid detection techniques for microorganism activities in food matrices using bio-recognition: A review. Trends in Food Science and Technology, 95(November 2019), 233–246.
84. Jensen, K. B., Atkinson, B. L., Willis, M. C., Koch, T. H., & Gold, L. (1995). Using in vitro selection to direct the covalent attachment of human immunodeficiency virus type 1 Rev protein to high-affinity RNA ligands. Proceedings of the National Academy of Sciences, 92(26), 12220-12224.
85. Jia, J., Yan, S., Lai, X., Xu, Y., Liu, T., & Xiang, Y. (2018). Colorimetric aptasensor for detection of malachite green in fish sample based on RNA and gold nanoparticles. Food Analytical Methods, 11(6), 1668-1676.
86. Jia, M., Sha, J., Li, Z., Wang, W., & Zhang, H. (2020). High affinity truncated aptamers for ultra-sensitive colorimetric detection of bisphenol A with label-free aptasensor. In Food Chemistry (Vol. 317).
87. Jia, Y., Zhou, G., Wang, X., Zhang, Y., Li, Z., Liu, P., Yu, B., & Zhang, J. (2020). A metal-organic framework/aptamer system as a fluorescent biosensor for determination of aflatoxin B1 in food samples. Talanta, 219(March), 121342.
88. Jiang, D., Du, X., Liu, Q., Hao, N., & Wang, K. (2019). MoS 2 /nitrogen doped graphene hydrogels p-n heterojunction: Efficient charge transfer property for highly sensitive and selective photoelectrochemical analysis of chloramphenicol. Biosensors and Bioelectronics, 126(November 2018), 463–469.
89. Jiang, H. L., Li, N., Cui, L., Wang, X., & Zhao, R. S. (2019). Recent application of magnetic solid phase extraction for food safety analysis. TrAC - Trends in Analytical Chemistry, 120.
90. Jiang, Y., Zou, S., & Cao, X. (2017). A simple dendrimer-aptamer based microfluidic platform for *E. coli* O157:H7 detection and signal intensification by rolling circle amplification. In Sensors and Actuators, B: Chemical (Vol. 251, pp. 976–984).
91. Jing, L., Li, J., Qin, M., Song, Y., Zhang, J., Chen, Q., Xia, X., & Han, Q. (2018). Development and characterization of sandwich-type enzyme-linked aptamer assay for the detection of rongalite in food. Analytical Biochemistry, 563(June), 25–34.
92. Joshi, R., Janagama, H., Dwivedi, H. P., Senthil Kumar, T. M. A., Jaykus, L. A., Schefers, J., & Sreevatsan, S. (2009). Selection, characterization, and application of DNA aptamers for the capture and detection of Salmonella enterica serovars. In Molecular and Cellular Probes (Vol. 23, Issue 1, pp. 20–28).

93. Kabbani, T. A., Goldberg, A., Kelly, C. P., Pallav, K., Tariq, S., Peer, A., ... & Leffler, D. A. (2012). Body mass index and the risk of obesity in coeliac disease treated with the gluten-free diet. Alimentary pharmacology & therapeutics, 35(6), 723-729.
94. Kahlenberg, F., Sanchez, D., Lachmann, I., Tuckova, L., Tlaskalova, H., Méndez, E., & Mothes, T. (2006). Monoclonal antibody R5 for detection of putatively coeliac-toxic gliadin peptides. European Food Research and Technology, 222(1-2), 78-82.
95. Keefe, A. D., Pai, S., & Ellington, A. (2010). Aptamers as therapeutics. Nature reviews Drug discovery, 9(7), 537-550.
96. Kelly, C. P., Bai, J. C., Liu, E., & Leffler, D. A. (2015). Advances in diagnosis and management of celiac disease. Gastroenterology, 148(6), 1175-1186. Chicago
97. Khaleghi, S., Ju, J. M., Lamba, A., & Murray, J. A. (2016). The potential utility of tight junction regulation in celiac disease: focus on larazotide acetate. Therapeutic advances in gastroenterology, 9(1), 37-49.
98. Khati, M., Schüman, M., Ibrahim, J., Sattentau, Q., Gordon, S., & James, W. (2003). Neutralization of infectivity of diverse R5 clinical isolates of human immunodeficiency virus type 1 by gp120-binding 2′ F-RNA aptamers. Journal of virology, 77(23), 12692-12698.
99. Khedri, M., Ramezani, M., Rafatpanah, H., & Abnous, K. (2018). Detection of food-born allergens with aptamer-based biosensors. TrAC - Trends in Analytical Chemistry, 103, 126–136.
100. Khodadadi, M., Malekpour, A., & Mehrgardi, M. A. (2018). Aptamer functionalized magnetic nanoparticles for effective extraction of ultratrace amounts of aflatoxin M1 prior its determination by HPLC. Journal of Chromatography A, 1564, 85–93.
101. Kilmartin, C., Wieser, H., Abuzakouk, M., Kelly, J., Jackson, J., & Feighery, C. (2006). Intestinal T cell responses to cereal proteins in celiac disease. Digestive diseases and sciences, 51(1), 202-209.
102. Kim, D. H., Seo, J. M., Shin, K. J., & Yang, S. G. (2021). Design and clinical developments of aptamer-drug conjugates for targeted cancer therapy. Biomaterials Research, 25, 1-12.
103. Kimoto, M., Yamashige, R., Matsunaga, K. I., Yokoyama, S., & Hirao, I. (2013). Generation of high-affinity DNA aptamers using an expanded genetic alphabet. Nature biotechnology, 31(5), 453-457.
104. Klußmann, S., Nolte, A., Bald, R., Erdmann, V. A., & Fürste, J. P. (1996). Mirror-image RNA that binds D-adenosine. Nature biotechnology, 14(9), 1112-1115.

105. Koning, F., Gilissen, L., & Wijmenga, C. (2005, June). Gluten: a two-edged sword. Immunopathogenesis of celiac disease. In Springer Seminars in Immunopathology (Vol. 27, pp. 217-232). Springer-Verlag.
106. Kooy-Winkelaar, Y., van Lummel, M., Moustakas, A. K., Schweizer, J., Mearin, M. L., Mulder, C. J., ... & Koning, F. (2011). Gluten-specific T cells cross-react between HLA-DQ8 and the HLA-DQ2α/DQ8β transdimer. The Journal of Immunology, 187(10), 5123-5129.
107. Koskinen, L. L. E., Einarsdottir, E., Korponay-Szabo, I. R., Kurppa, K., Kaukinen, K., Sistonen, P., ... & Saavalainen, P. (2009). Fine mapping of the CELIAC2 locus on chromosome 5q31-q33 in the Finnish and Hungarian populations. Tissue Antigens, 74(5), 408-416.
108. Kumar, P., Lambadi, P. R., & Navani, N. K. (2015). Non-enzymatic detection of urea using unmodified gold nanoparticles based aptasensor. Biosensors and Bioelectronics, 72, 340-347.
109. Kusser, W. (2000). Chemically modified nucleic acid aptamers for in vitro selections: evolving evolution. Reviews in Molecular Biotechnology, 74(1), 27-38.
110. Lacorn, M., & Weiss, T. (2015). Partially hydrolyzed gluten in fermented cereal-based products by R5 competitive ELISA: collaborative study, first action 2015.05. Journal of AOAC International, 98(5), 1346-1354.
111. Lammers, K. M., Lu, R., Brownley, J., Lu, B., Gerard, C., Thomas, K., ... & Fasano, A. (2008). Gliadin induces an increase in intestinal permeability and zonulin release by binding to the chemokine receptor CXCR3. Gastroenterology, 135(1), 194-204.
112. Lau, O. W., & Wong, S. K. (2000). Contamination in food from packaging material. Journal of Chromatography A, 882(1–2), 255–270.
113. Lauret, E., & Rodrigo, L. (2013). Celiac disease and autoimmune-associated conditions. BioMed research international, 2013.
114. Lebwohl, B., Ludvigsson, J. F., & Green, P. H. (2015). State of the Art Review: Celiac disease and non-celiac gluten sensitivity. BMJ: British Medical Journal, 351.
115. Lee, S. H., Ahn, J. Y., Lee, K. A., Um, H. J., Sekhon, S. S., Sun Park, T., Min, J., & Kim, Y. H. (2015). Analytical bioconjugates, aptamers, enable specific quantitative detection of Listeria monocytogenes. Biosensors and Bioelectronics, 68, 272–280.
116. Lerner, A., Jeremias, P., & Matthias, T. (2015). The world incidence of celiac disease is increasing: a review. Int J Recent Scient Res, 7, 5491-5496.

117. Lexhaller, B., Tompos, C., & Scherf, K. A. (2017). Fundamental study on reactivities of gluten protein types from wheat, rye and barley with five sandwich ELISA test kits. Food Chemistry, 237, 320-330.
118. Li, H., Ahmad, W., Rong, Y., Chen, Q., Zuo, M., Ouyang, Q., & Guo, Z. (2020). Designing an aptamer based magnetic and upconversion nanoparticles conjugated fluorescence sensor for screening *Escherichia coli* in food. Food Control, 107(July 2019), 106761.
119. Li, H., Huang, X., Mehedi Hassan, M., Zuo, M., Wu, X., Chen, Y., & Chen, Q. (2020). Dual-channel biosensor for Hg2+ sensing in food using Au@Ag/graphene-upconversion nanohybrids as metal-enhanced fluorescence and SERS indicators. Microchemical Journal, 154(September 2019), 104563.
120. Li, J., Mo, L., Lu, C. H., Fu, T., Yang, H. H., & Tan, W. (2016). Functional nucleic acid-based hydrogels for bioanalytical and biomedical applications. Chemical Society Reviews, 45(5), 1410–1431.
121. Li, L., Xu, S., Yan, H., Li, X., Yazd, H. S., Li, X., Huang, T., Cui, C., Jiang, J., & Tan, W. (2021). Nucleic Acid Aptamers for Molecular Diagnostics and Therapeutics: Advances and Perspectives. Angewandte Chemie - International Edition, 60(5), 2221–2231.
122. Li, Y., Fu, J., Shen, Q., & Yang, D. (2020). High-molecular-weight glutenin subunits: Genetics, structures, and relation to end use qualities. International Journal of Molecular Sciences, 22(1), 184.
123. Li, Y., Xu, J., Wang, L., Huang, Y., Guo, J., Cao, X., ... & Sun, C. (2016). Aptamer-based fluorescent detection of bisphenol A using nonconjugated gold nanoparticles and CdTe quantum dots. Sensors and Actuators B: Chemical, 222, 815-822.
124. Lin, S., Gan, N., Zhang, J., Qiao, L., Chen, Y., & Cao, Y. (2016). Aptamer-functionalized stir bar sorptive extraction coupled with gas chromatography-mass spectrometry for selective enrichment and determination of polychlorinated biphenyls in fish samples. Talanta, 149, 266–274.
125. Lionetti, E., & Catassi, C. (2011). New clues in celiac disease epidemiology, pathogenesis, clinical manifestations, and treatment. International reviews of immunology, 30(4), 219-231.
126. Lionetti, E., Gatti, S., Pulvirenti, A., & Catassi, C. (2015). Celiac disease from a global perspective. Best Practice & Research Clinical Gastroenterology, 29(3), 365-379.

127. Liu, C., Guo, Y., Luo, F., Rao, P., Fu, C., & Wang, S. (2017). Homogeneous Electrochemical Method for Ochratoxin A Determination Based on Target Triggered Aptamer Hairpin Switch and Exonuclease III-Assisted Recycling Amplification. Food Analytical Methods, 10(6), 1982–1990.
128. Liu, H., Lu, A., Fu, H., Li, B., Yang, M., Wang, J., & Luan, Y. (2018). Affinity capture of aflatoxin B1 and B2 by aptamer-functionalized magnetic agarose microspheres prior to their determination by HPLC. Microchimica Acta, 185(7).
129. Liu, H., Luan, Y., Lu, A., Li, B., Yang, M., & Wang, J. H. (2018). An oligosorbent-based aptamer affinity column for selective extraction of aflatoxin B2 prior to HPLC with fluorometric detection. Microchimica Acta, 185(1).
130. Liu, L., Ma, Y., Zhang, X., Yang, X., & Hu, X. (2020). A dispersive solid phase extraction adsorbent based on aptamer modified chitosan nanofibers for zearalenone separation in corn, wheat, and beer samples. Analytical Methods.
131. Liu, R., Huang, Y., Ma, Y., Jia, S., Gao, M., Li, J., Zhang, H., Xu, D., Wu, M., Chen, Y., Zhu, Z., & Yang, C. (2015). Design and synthesis of target-responsive aptamer-cross-linked hydrogel for visual quantitative detection of ochratoxin A. ACS Applied Materials and Interfaces, 7(12), 6982–6990.
132. Liu, Y., Cai, Z., Sheng, L., Ma, M., & Wang, X. (2020). A magnetic relaxation switching and visual dual-mode sensor for selective detection of Hg2+ based on aptamers modified Au@Fe3O4 nanoparticles. Journal of Hazardous Materials, 388(July 2019), 121728.
133. Liu, Y., Tuleouva, N., Ramanculov, E., & Revzin, A. (2010). Aptamer-based electrochemical biosensor for interferon gamma detection. Analytical chemistry, 82(19), 8131-8136.
134. Long, L., Han, Y., Yuan, X., Cao, S., Liu, W., Chen, Q., Wang, K., & Han, Z. (2020). A novel ratiometric near-infrared fluorescent probe for monitoring cyanide in food samples. Food Chemistry, 331(June), 127359.
135. López-López, L., Miranda-Castro, R., de-Los-Santos-Alvarez, N., Miranda-Ordieres, A. J., & Lobo-Castañón, M. J. (2017). Disposable electrochemical aptasensor for gluten determination in food. Sensors and Actuators B: Chemical, 241, 522-527.
136. Luan, Q., Xiong, X., Gan, N., Cao, Y., Li, T., Wu, D., Dong, Y., & Hu, F. (2018). A multiple signal amplified colorimetric aptasensor for antibiotics measurement using DNAzyme labeled Fe-MIL-88-Pt as novel peroxidase mimic tags and CSDP target-triggered cycles. Talanta, 187(September 2017), 27–34.

137. Luo, X., Chen, Z., Li, H., Li, W., Cui, L., & Huang, J. (2019). Exploiting the application of l-aptamer with excellent stability: An efficient sensing platform for malachite green in fish samples. Analyst, 144(14), 4204–4209.
138. Ma, Y., Mao, Y., Huang, D., He, Z., Yan, J., Tian, T., Shi, Y., Song, Y., Li, X., Zhu, Z., Zhou, L., & Yang, C. J. (2016). Portable visual quantitative detection of aflatoxin B1 using a target-responsive hydrogel and a distance-readout microfluidic chip. Lab on a Chip, 16(16), 3097–3104.
139. Mairal Lerga, T., Jauset-Rubio, M., Skouridou, V., Bashammakh, A. S., El-Shahawi, M. S., Alyoubi, A. O., & O'Sullivan, C. K. (2019). High affinity aptamer for the detection of the biogenic amine histamine. Analytical chemistry, 91(11), 7104-7111.
140. Majdinasab, M., Hayat, A., & Marty, J. L. (2018). Aptamer-based assays and aptasensors for detection of pathogenic bacteria in food samples. TrAC - Trends in Analytical Chemistry, 107, 60–77.
141. Makharia, G. K., Verma, A. K., Amarchand, R., Bhatnagar, S., Das, P., Goswami, A., ... & Anand, K. (2011). Prevalence of celiac disease in the northern part of India: a community based study. Journal of gastroenterology and hepatology, 26(5), 894-900.
142. Malalgoda, M., & Simsek, S. (2017). Celiac disease and cereal proteins. Food Hydrocolloids, 68, 108-113.
143. Marciano, F., Savoia, M., & Vajro, P. (2016). Celiac disease-related hepatic injury: Insights into associated conditions and underlying pathomechanisms. Digestive and Liver Disease, 48(2), 112-119.
144. Martina, S., Fabiola, F., Federica, G., Chiara, B., Gioacchino, L., & Gian, L. D. A. (2018). Genetic susceptibilty and celiac disease: what role do HLA haplotypes play?. Acta Bio Medica: Atenei Parmensis, 89(Suppl 9), 17.
145. Martín-Fernández, B., Costa, J., Oliveira, M. B. P. P., López-Ruiz, B., & Mafra, I. (2016). Combined effects of matrix and gene marker on the real-time PCR detection of wheat. International Journal of Food Science & Technology, 51(7), 1680-1688.
146. Martín-Fernández, B., Costa, J., Oliveira, M. B. P., López-Ruiz, B., & Mafra, I. (2015). Screening new gene markers for gluten detection in foods. Food Control, 56, 57-63.
147. Megiorni, F., & Pizzuti, A. (2012). HLA-DQA1 and HLA-DQB1 in Celiac disease predisposition: practical implications of the HLA molecular typing. Journal of biomedical science, 19, 1-5

148. Mehlhorn, A., Rahimi, P., & Joseph, Y. (2018). Aptamer-based biosensors for antibiotic detection: A review. Biosensors, 8(2).
149. Mehta, J., Van Dorst, B., Rouah-Martin, E., Herrebout, W., Scippo, M. L., Blust, R., & Robbens, J. (2011). In vitro selection and characterization of DNA aptamers recognizing chloramphenicol. In Journal of Biotechnology (Vol. 155, Issue 4, pp. 361–369).
150. Meirinho, S. G., Dias, L. G., Peres, A. M., & Rodrigues, L. R. (2016). Voltammetric aptasensors for protein disease biomarkers detection: A review. Biotechnology advances.
151. Melini, F., & Melini, V. (2018). Immunological methods in gluten risk analysis: A snapshot. Safety, 4(4), 56.
152. Mendonsa, S. D., & Bowser, M. T. (2004). In vitro evolution of functional DNA using capillary electrophoresis. Journal of the American Chemical Society, 126(1), 20-21.
153. Miranda-Castro, R., De-los-Santos-Álvarez, N., Miranda-Ordieres, A. J., & Lobo-Castañón, M. J. (2016). Harnessing aptamers to overcome challenges in gluten detection. Biosensors, 6(2), 16.
154. Mishra, G. K., Sharma, V., & Mishra, R. K. (2018). Electrochemical aptasensors for food and environmental safeguarding: A review. Biosensors, 8(2), 1–13.
155. Mishra, R. K., Hayat, A., Mishra, G. K., Catanante, G., Sharma, V., & Marty, J. L. (2017). A novel colorimetric competitive aptamer assay for lysozyme detection based on superparamagnetic nanobeads. Talanta, 165(October 2016), 436–441.
156. Monošík, R., Streďanský, M., & Šturdík, E. (2012). Biosensors-classification, characterization and new trends. Acta Chimica Slovaca, 5(1), 109-120.
157. Moon, J., Kim, G., Park, S. B., Lim, J., & Mo, C. (2015). Comparison of whole-cell SELEX methods for the identification of Staphylococcus Aureus-specific DNA aptamers. Sensors (Switzerland), 15(4), 8884–8897.
158. Mudili, V., Makam, S. S., Sundararaj, N., Siddaiah, C., Gupta, V. K., & Rao, P. V. L. (2015). A novel IgY-Aptamer hybrid system for cost-effective detection of SEB and its evaluation on food and clinical samples. Scientific Reports, 5(October), 1–12.
159. Neethirajan, S., Ahmed, S. R., Chand, R., Buozis, J., & Nagy, É. (2017). Recent advances in biosensor development for foodborne virus detection. Nanotheranostics, 1(3), 272–295.

160. Nehra, M., Lettieri, M., Dilbaghi, N., Kumar, S., & Marrazza, G. (2019). Nano-biosensing platforms for detection of cow's milk allergens: An overview. Sensors, 20(1), 32.
161. Nerín, C., Aznar, M., & Carrizo, D. (2016). Food contamination during food process. Trends in Food Science and Technology, 48, 63–68.
162. Nery, A. A., Wrenger, C., & Ulrich, H. (2009). Recognition of biomarkers and cell-specific molecular signatures: Aptamers as capture agents. Journal of separation science, 32(10), 1523-1530.
163. Newton, K. P., & Singer, S. A. (2012, July). Celiac disease in children and adolescents: special considerations. In Seminars in Immunopathology (Vol. 34, No. 4, pp. 479-496). Springer-Verlag.
164. Ogilvie, O., Roberts, S., Sutton, K., Domigan, L., Larsen, N., Gerrard, J., & Demarais, N. (2020). Proteomic modelling of gluten digestion from a physiologically relevant food system: A focus on the digestion of immunogenic peptides from wheat implicated in celiac disease. Food Chemistry, 333, 127466
165. Osborne, T. B., & Voorhees, C. L. (1894). Proteids of the wheat kernel. Journal of the American Chemical Society, 16(8), 524-535.
166. Ozalp, V. C., Bayramoglu, G., Erdem, Z., & Arica, M. Y. (2015). Pathogen detection in complex samples by quartz crystal microbalance sensor coupled to aptamer functionalized core-shell type magnetic separation. Analytica Chimica Acta, 853(1), 533–540.
167. Panda, R., & Garber, E. A. (2019). Detection and quantitation of gluten in fermented-hydrolyzed foods by antibody-based methods: Challenges, progress, and a potential path forward. Frontiers in Nutrition, 6, 97.
168. Paniel, N., & Noguer, T. (2019). Detection of salmonella in food matrices, from conventional methods to recent aptamer-sensing technologies. Foods, 8(9).
169. Parzanese, I., Qehajaj, D., Patrinicola, F., Aralica, M., Chiriva-Internati, M., Stifter, S., ... & Grizzi, F. (2017). Celiac disease: From pathophysiology to treatment. World journal of gastrointestinal pathophysiology, 8(2), 27.
170. Patel, P. D. (2002). (Bio) sensors for measurement of analytes implicated in food safety: a review. TrAC Trends in Analytical Chemistry, 21(2), 96-115.
171. Phopin, K., & Tantimongcolwat, T. (2020). Pesticide aptasensors—State of the art and perspectives. Sensors, 20(23), 6809.

172. Pichon, V., Brothier, F., & Combès, A. (2015). Aptamer-based-sorbents for sample treatment - A review. Analytical and Bioanalytical Chemistry, 407(3), 681–698.
173. Pinto, A. (2012). Real-time AptaPCR: a Novel Approach Exploiting Nucleic Acid Aptamers for Ultrasensitive Detection of Analytes in Clinical Diagnostics and in Food Analysis: Doctoral Thesis (Doctoral dissertation, Universitat Rovira i Virgili).
174. Pinto, A., Polo, P. N., Henry, O., Redondo, M. C. B., Svobodova, M., & O'Sullivan, C. K. (2014). Label-free detection of gliadin food allergen mediated by real-time apta-PCR. Analytical and bioanalytical chemistry, 406, 515-524.
175. Pirzada, M., & Altintas, Z. (2020). Recent progress in optical sensors for biomedical diagnostics. Micromachines, 11(4), 356.
176. Płotka-Wasylka, J., Szczepańska, N., de la Guardia, M., & Namieśnik, J. (2016). Modern trends in solid phase extraction: New sorbent media. TrAC - Trends in Analytical Chemistry, 77, 23–43.
177. Poonia, A., Jha, A., Sharma, R., Singh, H. B., Rai, A. K., & Sharma, N. (2017). Detection of adulteration in milk: A review. International Journal of Dairy Technology, 70(1), 23–42.
178. Qi, S., Duan, N., Sun, Y., Zhou, Y., Ma, P., Wu, S., & Wang, Z. (2021). High-affinity aptamer of allergen β-lactoglobulin: Selection, recognition mechanism and application. Sensors and Actuators, B: Chemical, 340(February), 129956.
179. Rallabhandi, P., Sharma, G. M., Pereira, M., & Williams, K. M. (2015). Immunological characterization of the gluten fractions and their hydrolysates from wheat, rye and barley. Journal of agricultural and food chemistry, 63(6), 1825-1832.
180. Ramakrishna, B. S., Makharia, G. K., Chetri, K., Dutta, S., Mathur, P., Ahuja, V., ... & Das, A. (2016). Prevalence of adult celiac disease in India: regional variations and associations. The American journal of gastroenterology.
181. Ramezani, M., Mohammad Danesh, N., Lavaee, P., Abnous, K., & Mohammad Taghdisi, S. (2015). A novel colorimetric triple-helix molecular switch aptasensor for ultrasensitive detection of tetracycline. Biosensors and Bioelectronics, 70, 181–187.
182. Ranjbar, S., Shahrokhian, S., & Nurmohammadi, F. (2018). Nanoporous gold as a suitable substrate for preparation of a new sensitive electrochemical aptasensor for detection of Salmonella typhimurium. Sensors and Actuators, B: Chemical, 255, 1536–1544.

183. Rather, I. A., Koh, W. Y., Paek, W. K., & Lim, J. (2017). The sources of chemical contaminants in food and their health implications. Frontiers in Pharmacology, 8(NOV).
184. Roushani, M., Nezhadali, A., & Jalilian, Z. (2018). An electrochemical chlorpyrifos aptasensor based on the use of a glassy carbon electrode modified with an electropolymerized aptamer-imprinted polymer and gold nanorods. Microchimica Acta, 185(12).
185. Ruscito, A., & DeRosa, M. C. (2016). Small-molecule binding aptamers: Selection strategies, characterization, and applications. Frontiers in Chemistry, 4(MAY), 1–14.
186. Scherf, K. A., & Poms, R. E. (2016). Recent developments in analytical methods for tracing gluten. Journal of Cereal Science, 67, 112-122.
187. Scherf, K. A., Koehler, P., & Wieser, H. (2016). Gluten and wheat sensitivities–An overview. Journal of Cereal Science, 67, 2-11.
188. Schilling, K. B., DeGrasse, J., & Woods, J. W. (2018). The influence of food matrices on aptamer selection by SELEX (systematic evolution of ligands by exponential enrichment) targeting the norovirus P-Domain. Food Chemistry, 258(October 2017), 129–136.
189. Schofield, J. D., Bottomley, R. C., Timms, M. F., & Booth, M. R. (1983). The effect of heat on wheat gluten and the involvement of sulphydryl-disulphide interchange reactions. Journal of Cereal Science, 1(4), 241-253.
190. Sefah, K., Shangguan, D., Xiong, X., O'Donoghue, M. B., & Tan, W. (2010). Development of DNA aptamers using cell-selex. Nature Protocols, 5(6), 1169–1185.
191. Sefah, K., Yang, Z., Bradley, K. M., Hoshika, S., Jiménez, E., Zhang, L., ... & Benner, S. A. (2014). In vitro selection with artificial expanded genetic information systems. Proceedings of the National Academy of Sciences, 111(4), 1449-1454.
192. Setlem, K., Mondal, B., Shylaja, R., & Parida, M. (2020). Dual Aptamer-DNAzyme based colorimetric assay for the detection of AFB1 from food and environmental samples. Analytical Biochemistry, 608(April), 113874.
193. Shan, L., Molberg, Ø., Parrot, I., Hausch, F., Filiz, F., Gray, G. M., ... & Khosla, C. (2002). Structural basis for gluten intolerance in celiac sprue. Science, 297(5590), 2275-2279.
194. Sharma, A., Istamboulie, G., Hayat, A., Catanante, G., Bhand, S., & Marty, J. L. (2017). Disposable and portable aptamer functionalized impedimetric sensor for

detection of kanamycin residue in milk sample. In Sensors and Actuators, B: Chemical (Vol. 245, pp. 507–515).

195. Sharma, N., Bhatia, S., Chunduri, V., Kaur, S., Sharma, S., Kapoor, P., ... & Garg, M. (2020). Pathogenesis of celiac disease and other gluten related disorders in wheat and strategies for mitigating them. Frontiers in Nutrition, 7, 6.
196. Shen, J., Zhou, X., Shan, Y., Yue, H., Huang, R., Hu, J., & Xing, D. (2020). Sensitive detection of a bacterial pathogen using allosteric probe-initiated catalysis and CRISPR-Cas13a amplification reaction. Nature Communications, 11(1), 1–10.
197. Shewry, P. (2019). What is gluten—why is it special?. Frontiers in Nutrition, 101.
198. Shewry, P. R. (1995). Plant storage proteins. Biological Reviews, 70(3), 375-426.
199. Shewry, P. R., & Lafiandra, D. (2022). Wheat glutenin polymers 1. structure, assembly and properties. Journal of Cereal Science, 103486.
200. Shewry, P. R., Tatham, A. S., & Kasarda, D. D. (1992). Cereal proteins and coeliac disease. Coeliac disease. Oxford: Blackwell Scientific Publications, 305, 348.
201. Shin, W. R., Sekhon, S. S., Kim, S. G., Rhee, S. J., Yang, G. N., Won, K., Rhee, S. K., Ryu, H., Kim, K., Min, J., Ahn, J. Y., & Kim, Y. H. (2018). Aptamer-based pathogen monitoring for salmonella enterica ser. Typhimurium. Journal of Biomedical Nanotechnology, 14(11), 1992–2002.
202. Silano, M., Vincentini, O., & De Vincenzi, M. (2009). Toxic, immunostimulatory and antagonist gluten peptides in celiac disease. Current medicinal chemistry, 16(12), 1489-1498.
203. Simón, E., Larretxi, I., Churruca, I., Lasa, A., Bustamante, M. Á., Navarro, V., ... & del Pilar Fernández-Gil, M. (2017). Techniques for Analyzing Gluten. Nutritional and Analytical Approaches of Gluten-Free Diet in Celiac Disease, 29-46.
204. Singh, P., Arora, A., Strand, T. A., Leffler, D. A., Catassi, C., Green, P. H. & Makharia, G. K. (2018). Global prevalence of celiac disease: systematic review and meta-analysis. Clinical Gastroenterology and Hepatology, 16(6), 823-836.
205. Slot, I. B., Van Der Fels-Klerx, H. J., Bremer, M. G., & Hamer, R. J. (2016). Immunochemical detection methods for gluten in food products: where do we go from here?. Critical reviews in food science and nutrition, 56(15), 2455-2466.
206. Sollid, L. M. (2002). Coeliac disease: dissecting a complex inflammatory disorder. Nature Reviews Immunology, 2(9), 647-655.

207. Sollid, L. M., Qiao, S. W., Anderson, R. P., Gianfrani, C., & Koning, F. (2012). Nomenclature and listing of celiac disease relevant gluten T-cell epitopes restricted by HLA-DQ molecules. Immunogenetics, 64, 455-460.
208. Sollid, L. M., Tye-Din, J. A., Qiao, S. W., Anderson, R. P., Gianfrani, C., & Koning, F. (2020). Update 2020: nomenclature and listing of celiac disease–relevant gluten epitopes recognized by CD4+ T cells. Immunogenetics, 72, 85-88.
209. Song, M. S., Sekhon, S. S., Shin, W. R., Kim, H. C., Min, J., Ahn, J. Y., & Kim, Y. H. (2017). Detecting and discriminating shigella sonnei using an aptamer-based fluorescent biosensor platform. Molecules, 22(5).
210. Song, S., Wang, X., Xu, K., Ning, L., & Yang, X. (2019). Rapid identification and quantitation of the viable cells of Lactobacillus casei in fermented dairy products using an aptamer-based strategy powered by a novel cell-SELEX protocol. Journal of Dairy Science, 102(12), 10814–10824.
211. Sood, A., Midha, V., Sood, N., Avasthi, G., & Sehgal, A. (2006). Prevalence of celiac disease among school children in Punjab, North India. Journal of gastroenterology and hepatology, 21(10), 1622-1625.
212. Spano, G., Russo, P., Lonvaud-Funel, A., Lucas, P., Alexandre, H., Grandvalet, C., Coton, E., Coton, M., Barnavon, L., Bach, B., Rattray, F., Bunte, A., Magni, C., Ladero, V., Alvarez, M., Fernández, M., Lopez, P., de Palencia, P. F., Corbi, A., … Lolkema, J. S. (2010). Biogenic amines in fermented foods. European Journal of Clinical Nutrition, 64, S95–S100.
213. Stoltenburg, R., Reinemann, C., & Strehlitz, B. (2007). SELEX-A (r)evolutionary method to generate high-affinity nucleic acid ligands. Biomolecular Engineering, 24(4), 381–403.
214. Su, R., Zheng, H., Dong, S., Sun, R., Qiao, S., Sun, H., ... & Sun, C. (2019). Facile detection of melamine by a FAM–aptamer–G-quadruplex construct. Analytical and bioanalytical chemistry, 411(12), 2521-2530.
215. Suh, S. H., Choi, S. J., Dwivedi, H. P., Moore, M. D., Escudero-Abarca, B. I., & Jaykus, L. A. (2018). Use of DNA aptamer for sandwich type detection of Listeria monocytogenes. Analytical Biochemistry, 557(February), 27–33.
216. Sun, L., & Zhao, Q. (2018). Competitive horseradish peroxidase-linked aptamer assay for sensitive detection of Aflatoxin B1. In Talanta (Vol. 179, pp. 344–349).
217. Sun, Y., Li, Z., Huang, X., Zhang, D., Zou, X., Shi, J., Zhai, X., Jiang, C., Wei, X., & Liu, T. (2019). A nitrile-mediated aptasensor for optical anti-interference detection of

acetamiprid in apple juice by surface-enhanced Raman scattering. Biosensors and Bioelectronics, 145(September), 111672.

218. Sundararaj, N., Kalagatur, N. K., Mudili, V., Krishna, K., & Antonysamy, M. (2019). Isolation and identification of enterotoxigenic Staphylococcus aureus isolates from Indian food samples: evaluation of in-house developed aptamer linked sandwich ELISA (ALISA) method. Journal of Food Science and Technology, 56(2), 1016–1026.
219. Svigelj, R., Bortolomeazzi, R., Dossi, N., Giacomino, A., Bontempelli, G., & Toniolo, R. (2017). An effective gluten extraction method exploiting pure choline chloride-based deep eutectic solvents (ChCl-DESs). Food Analytical Methods, 10(12), 4079-4085.
220. Svigelj, R., Dossi, N., Pizzolato, S., Toniolo, R., Miranda-Castro, R., de-los-Santos-Álvarez, N., & Lobo-Castañón, M. J. (2020). Truncated aptamers as selective receptors in a gluten sensor supporting direct measurement in a deep eutectic solvent. Biosensors and Bioelectronics, 112339.
221. Svigelj, R., Dossi, N., Toniolo, R., Miranda-Castro, R., de-los-Santos-Álvarez, N., & Lobo-Castañón, M. J. (2018). Selection of Anti-gluten DNA Aptamers in a Deep Eutectic Solvent. Angewandte Chemie, 130(39), 13032-13036.
222. Tan, B., Zhao, H., Du, L., Gan, X., & Quan, X. (2016). A versatile fluorescent biosensor based on target-responsive graphene oxide hydrogel for antibiotic detection. Biosensors and Bioelectronics, 83, 267–273.
223. Tan, Y., Wei, X., Zhang, Y., Wang, P., Qiu, B., Guo, L., Lin, Z., & Yang, H. H. (2015). Exonuclease-Catalyzed Target Recycling Amplification and Immobilization-free Electrochemical Aptasensor. Analytical Chemistry, 87(23), 11826–11831.
224. Tang, L., Huang, Y., Lin, C., Qiu, B., Guo, L., Luo, F., & Lin, Z. (2020). Highly sensitive and selective aflatoxin B1 biosensor based on Exonuclease I-catalyzed target recycling amplification and targeted response aptamer-crosslinked hydrogel using electronic balances as a readout. Talanta, 214(December 2019), 120862.
225. Tatham, A. S., Drake, A. F., & Shewry, P. R. (1985). A conformational study of a glutamine-and proline-rich cereal seed protein, C hordein. Biochemical Journal, 226(2), 557-562.
226. Tatham, A. S., Gilbert, S. M., Fido, R. J., & Shewry, P. R. (2000). Extraction, separation, and purification of wheat gluten proteins and related proteins of barley, rye, and oats. Celiac Disease: Methods and Protocols, 55-73.

227. Tavitian, B., & Haberkorn, U. (2009). Darwinian molecular imaging. European Journal of Nuclear Medicine and Molecular Imaging, 36(9), 1475–1482.
228. Teng, J., Yuan, F., Ye, Y., Zheng, L., Yao, L., Xue, F., Chen, W., & Li, B. (2016). Aptamer-based technologies in foodborne pathogen detection. Frontiers in Microbiology, 7(SEP), 1–11.
229. Thiviyanathan, V., & Gorenstein, D. G. (2012). Aptamers and the next generation of diagnostic reagents. PROTEOMICS–Clinical Applications, 6(11-12), 563-573.
230. Tian, Y., Wang, Y., Sheng, Z., Li, T., & Li, X. (2016). A colorimetric detection method of pesticide acetamiprid by fine-tuning aptamer length. Analytical Biochemistry, 513, 87–92.
231. Ting, Y. T., Dahal-Koirala, S., Kim, H. S. K., Qiao, S. W., Neumann, R. S., Lundin, K. E., ... & Rossjohn, J. (2020). A molecular basis for the T cell response in HLA-DQ2. 2 mediated celiac disease. Proceedings of the National Academy of Sciences, 117(6), 3063-3073.
232. Toh, S. Y., Citartan, M., Gopinath, S. C., & Tang, T. H. (2015). Aptamers as a replacement for antibodies in enzyme-linked immunosorbent assay. Biosensors and bioelectronics, 64, 392-403.
233. Tonutti, E., & Bizzaro, N. (2014). Diagnosis and classification of celiac disease and gluten sensitivity. Autoimmunity reviews, 13(4), 472-476.
234. Vader, L. W., Stepniak, D. T., Bunnik, E. M., Kooy, Y. M., De Haan, W., Drijfhout, J. W., ... & Koning, F. (2003). Characterization of cereal toxicity for celiac disease patients based on protein homology in grains. Gastroenterology, 125(4), 1105-1113.
235. Valenzano, S., Girolamo, A. De, Derosa, M. C., Mckeague, M., Schena, R., Catucci, L., & Pascale, M. (2016). Screening and Identification of DNA Aptamers to Tyramine Using in Vitro Selection and High-Throughput Sequencing.
236. Van Belzen, M. J., Meijer, J. W., Sandkuijl, L. A., Bardoel, A. F., Mulder, C. J., Pearson, P. L., ... & Wijmenga, C. (2003). A major non-HLA locus in celiac disease maps to chromosome 19. Gastroenterology, 125(4), 1032-1041.
237. van de Wal, Y., Kooy, Y. M., van Veelen, P., Vader, W., August, S. A., Drijfhout, J. W., ... & Koning, F. (1999). Glutenin is involved in the gluten-driven mucosal T cell response. European journal of immunology, 29(10), 3133-3139.

238. Vater, A., Jarosch, F., Buchner, K., & Klussmann, S. (2003). Short bioactive Spiegelmers to migraine-associated calcitonin gene-related peptide rapidly identified by a novel approach: Tailored-SELEX. Nucleic acids research, 31(21), e130-e130.
239. Verma, N., & Bhardwaj, A. (2015). Biosensor technology for pesticides—a review. Applied biochemistry and biotechnology, 175(6), 3093-3119.
240. Verma, N., & Singh, M. (2003). A disposable microbial based biosensor for quality control in milk. Biosensors and bioelectronics, 18(10), 1219-1224.
241. Vilppula, A., Kaukinen, K., Luostarinen, L., Krekelä, I., Patrikainen, H., Valve, R., ... & Collin, P. (2011). Clinical benefit of gluten-free diet in screen-detected older celiac disease patients. BMC gastroenterology, 11(1), 1.
242. Viswanathan, S., & Radecki, J. (2008). Nanomaterials in electrochemical biosensors for food analysis-a review. Polish Journal of Food and Nutrition Sciences, 58(2).
243. Vivekananda, J., & Kiel, J. L. (2006). Anti-Francisella tularensis DNA aptamers detect tularemia antigen from different subspecies by Aptamer-Linked Immobilized Sorbent Assay. Laboratory Investigation, 86(6), 610–618.
244. Wahab, W. A., Šuligoj, T., Ellis, H. J., & Ciclitira, I. N. P. J. (2012). 5.2 Coeliac disease immunogenicity studies of barley hordein and rye secalin derived peptides. Working group on prolamin analysis and toxicity, 75.
245. Wang, C., Qian, J., Wang, K., Wang, K., Liu, Q., Dong, X., Wang, C., & Huang, X. (2015). Magnetic-fluorescent-targeting multifunctional aptasensorfor highly sensitive and one-step rapid detection of ochratoxin A. In Biosensors and Bioelectronics (Vol. 68, pp. 783–790).
246. Wang, J., Zhao, C., Hong, C., Lin, Z., & Huang, Z. (2021). Rapid detection of malachite green in fish and water based on the peroxidase-like activity of Fe3O4NPs enhanced with aptamer. Journal of Food Composition and Analysis, 104, 104162.
247. Wang, L., Peng, X., Fu, H., Huang, C., Li, Y., & Liu, Z. (2020). Recent advances in the development of electrochemical aptasensors for detection of heavy metals in food. Biosensors and Bioelectronics, 147(October 2019), 111777.
248. Wang, Q., Yang, Q., & Wu, W. (2020). Progress on Structured Biosensors for Monitoring Aflatoxin B1 From Biofilms: A Review. Frontiers in Microbiology, 11(March), 1–15.
249. Wang, S., Niu, R., Yang, Y., Zhou, X., Luo, S., Zhang, C., & Wang, Y. (2020). Aptamer-functionalized chitosan magnetic nanoparticles as a novel adsorbent for

selective extraction of ochratoxin A. In International Journal of Biological Macromolecules (Vol. 153, pp. 583–590).

250. Weerathunge, P., Ramanathan, R., Torok, V. A., Hodgson, K., Xu, Y., Goodacre, R., Behera, B. K., & Bansal, V. (2019). Ultrasensitive Colorimetric Detection of Murine Norovirus Using NanoZyme Aptasensor. Analytical Chemistry, 91(5), 3270–3276.
251. Wei, G., Helmerhorst, E. J., Darwish, G., Blumenkranz, G., & Schuppan, D. (2020). Gluten degrading enzymes for treatment of celiac disease. Nutrients, 12(7), 2095.
252. Weng, X., & Neethirajan, S. (2016). A microfluidic biosensor using graphene oxide and aptamer-functionalized quantum dots for peanut allergen detection. Biosensors and Bioelectronics, 85, 649–656.
253. Wenzl, T., Lachenmeier, D. W., & Gökmen, V. (2007). Analysis of heat-induced contaminants (acrylamide, chloropropanols and furan) in carbohydrate-rich food. Analytical and Bioanalytical Chemistry, 389(1), 119–137.
254. Westby, P. (2014). The Effects of Modern Day Wheat. Nutritional Perspectives: Journal of the Council on Nutrition, 37(2).
255. White, R., Rusconi, C., Scardino, E., Wolberg, A., Lawson, J., Hoffman, M., & Sullenger, B. (2001). Generation of species cross-reactive aptamers using "toggle" SELEX. Molecular Therapy, 4(6), 567-573.
256. Wieser, H. (2007). Chemistry of gluten proteins. Food microbiology, 24(2), 115-119.
257. Wieser, H., & Koehler, P. (2008). The biochemical basis of celiac disease. Cereal Chemistry, 85(1), 1-13.
258. Wieser, H., Bushuk, W., & MacRitchie, F. (2006). The polymeric glutenins. Gliadin and glutenin: The unique balance of wheat quality, 213-240.
259. Woldemariam, K. Y., Yuan, J., Wan, Z., Yu, Q., Cao, Y., Mao, H., ... & Sun, B. (2022). Celiac disease and immunogenic wheat gluten peptides and the association of gliadin peptides with HLA DQ2 and HLA DQ8. Food Reviews International, 38(7), 1553-1576.
260. Wrigley, C. W., & Shepherd, K. W. (1973). Electrofocusing of grain proteins from wheat genotypes. Annals of the New York Academy of Sciences, 209(1), 154-162.
261. Wu, J., Zhu, Y., Xue, F., Mei, Z., Yao, L., Wang, X., Zheng, L., Liu, J., Liu, G., Peng, C., & Chen, W. (2014). Recent trends in SELEX technique and its application to food safety monitoring. Microchimica Acta, 181(5–6), 479–491.

262. Wu, K., Ma, C., Zhao, H., Chen, M., & Deng, Z. (2019). Sensitive aptamer-based fluorescene assay for ochratoxin A based on RNase H signal amplification. Food Chemistry, 277(October 2018), 273–278.
263. Wu, L., & Curran, J. F. (1999). An allosteric synthetic DNA. Nucleic acids research, 27(6), 1512-1516.
264. Wu, P., Li, S., Ye, X., Ning, B., Bai, J., Peng, Y., Li, L., Han, T., Zhou, H., Gao, Z., & Ding, P. (2020). Cu/Au/Pt trimetallic nanoparticles coated with DNA hydrogel as target-responsive and signal-amplification material for sensitive detection of microcystin-LR. Analytica Chimica Acta, 1134, 96–105.
265. Wu, S., Zhang, H., Shi, Z., Duan, N., Fang, C. C., Dai, S., & Wang, Z. (2015). Aptamer-based fluorescence biosensor for chloramphenicol determination using upconversion nanoparticles. In Food Control (Vol. 50, pp. 597–604).
266. Wu, X., Chen, J., Wu, M., & Zhao, J. X. (2015). Aptamers: active targeting ligands for cancer diagnosis and therapy. Theranostics, 5(4), 322-44.
267. Wu, Y., Zhan, S., Wang, L., & Zhou, P. (2014). Selection of a DNA aptamer for cadmium detection based on cationic polymer mediated aggregation of gold nanoparticles. Analyst, 139(6), 1550–1561.
268. Xhaferaj, M., Alves, T. O., Ferreira, M. S., & Scherf, K. A. (2020). Recent progress in analytical method development to ensure the safety of gluten-free foods for celiac disease patients. Journal of Cereal Science, 96, 103114.
269. Xiao, M. W., Bai, X. L., Liu, Y. M., Yang, L., & Liao, X. (2018). Simultaneous determination of trace Aflatoxin B1 and Ochratoxin A by aptamer-based microchip capillary electrophoresis in food samples. Journal of Chromatography A, 1569, 222–228.
270. Xu, D., Xu, D., Yu, X., Liu, Z., He, W., & Ma, Z. (2005). Label-free electrochemical detection for aptamer-based array electrodes. Analytical Chemistry, 77(16), 5107-5113.
271. Xu, S., Dai, B., Zhao, W., Jiang, L., & Huang, H. (2020). Electrochemical detection of β-lactoglobulin based on a highly selective DNA aptamer and flower-like Au@BiVO4 microspheres. Analytica Chimica Acta, 1120, 1–10.
272. Xuan, H., Ren, J., Zhu, Y., Zhao, B., & Ge, L. (2016). Aptamer-functionalized P(NIPAM-AA) hydrogel fabricated one-dimensional photonic crystals (1DPCs) for colorimetric sensing. RSC Advances, 6(43), 36827–36833.

273. Xue, J., Liu, J., Wang, C., Tian, Y., & Zhou, N. (2016). Simultaneous electrochemical detection of multiple antibiotic residues in milk based on aptamers and quantum dots. Analytical Methods, 8(9), 1981–1988.
274. Yang, Q., Hong, J., Wu, Y. X., Cao, Y., Wu, D., Hu, F., & Gan, N. (2019). A Multicolor Fluorescence Nanoprobe Platform Using Two-Dimensional Metal Organic Framework Nanosheets and Double Stirring Bar Assisted Target Replacement for Multiple Bioanalytical Applications. ACS Applied Materials and Interfaces, 11(44), 41506–41515.
275. Yang, Y., Yin, S., Li, Y., Lu, D., Zhang, J., & Sun, C. (2017). Application of aptamers in detection and chromatographic purification of antibiotics in different matrices. TrAC - Trends in Analytical Chemistry, 95, 1–22.
276. Yao, C., Ren, J., Liu, C., Yin, T., Zhu, Y., & Ge, L. (2014). Hydrogel improved the response in the titania/graphene oxide one-dimensional photonic crystals. ACS Applied Materials and Interfaces, 6(19), 16727–16733.
277. Yao, L., Ye, Y., Teng, J., Xue, F., Pan, D., Li, B., & Chen, W. (2017). In Vitro Isothermal Nucleic Acid Amplification Assisted Surface-Enhanced Raman Spectroscopic for Ultrasensitive Detection of Vibrio parahaemolyticus. Analytical Chemistry, 89(18), 9775–9780.
278. Ye, W., Liu, T., Zhang, W., Zhu, M., Liu, Z., Kong, Y., & Liu, S. (2019). Marine toxins detection by biosensors based on aptamers. Toxins, 12(1), 1–22.
279. Yu, X., Chen, F., Wang, R., & Li, Y. (2018). Whole-bacterium SELEX of DNA aptamers for rapid detection of *E.coli* O157:H7 using a QCM sensor. Journal of Biotechnology, 266(December 2017), 39–49.
280. Yuan, J., Gao, J., Li, X., Liu, F., Wijmenga, C., Chen, H., & Gilissen, L. J. (2013). The tip of the "celiac iceberg" in China: a systematic review and meta-analysis. PLoS One, 8(12), e81151.
281. Yue, F., Li, F., Kong, Q., Guo, Y., & Sun, X. (2021). Recent advances in aptamer-based sensors for aminoglycoside antibiotics detection and their applications. Science of the Total Environment, 762(12), 143129.
282. Yoosuf, S., & Makharia, G. K. (2019). Evolving therapy for celiac disease. Frontiers in pediatrics, 7, 193.
283. Zhan, Z., Li, H., Liu, J., Xie, G., Xiao, F., Wu, X., Aguilar, Z. P., & Xu, H. (2020). A competitive enzyme linked aptasensor with rolling circle amplification (ELARCA)

assay for colorimetric detection of Listeria monocytogenes. In Food Control (Vol. 107).

284. Zhang, D., Yang, J., Ye, J., Xu, L., Xu, H., Zhan, S., ... & Wang, L. (2016). Colorimetric detection of bisphenol A based on unmodified aptamer and cationic polymer aggregated gold nanoparticles. Analytical biochemistry, 499, 51-56.
285. Zhang, J., Fang, X., Wu, J., Hu, Z., Jiang, Y., Qi, H., Zheng, L., & Xuan, X. (2020). An interdigitated microelectrode based aptasensor for real-time and ultratrace detection of four organophosphorus pesticides. Biosensors and Bioelectronics, 150(August 2019), 111879.
286. Zhang, J., Zhang, Y., Wu, J., Qi, H., Zhao, M., Yi, M., Li, Z., & Zheng, L. (2021). Real-time Cd2+ detection at sub-femtomolar level in various liquid media by an aptasensor integrated with microfluidic enrichment. Sensors and Actuators, B: Chemical, 329(November 2020), 129282.
287. Zhang, P., Liu, H., Li, X., Ma, S., Men, S., Wei, H., Cui, J., & Wang, H. (2017). A label-free fluorescent direct detection of live Salmonella typhimurium using cascade triple trigger sequences-regenerated strand displacement amplification and hairpin template-generated-scaffolded silver nanoclusters. Biosensors and Bioelectronics, 87(September 2016), 1044–1049.
288. Zhang, Ying, Duan, B., Bao, Q., Yang, T., Wei, T., Wang, J., Mao, C., Zhang, C., & Yang, M. (2020). Aptamer-modified sensitive nanobiosensors for the specific detection of antibiotics. Journal of Materials Chemistry B, 8(37), 8607–8613.
289. Zhang, Youxiong, Wu, Q., Sun, M., Zhang, J., Mo, S., Wang, J., Wei, X., & Bai, J. (2018). Magnetic-assisted aptamer-based fluorescent assay for allergen detection in food matrix. Sensors and Actuators, B: Chemical, 263, 43–49.
290. Zhang, Z., Liu, D., Bai, Y., Cui, Y., Wang, D., & Shi, X. (2019). Identification and characterization of two high affinity aptamers specific for Salmonella Enteritidis. Food Control, 106(March).
291. Zhao, M., Wang, P., Guo, Y., Wang, L., Luo, F., Qiu, B., Guo, L., Su, X., Lin, Z., & Chen, G. (2018). Detection of aflatoxin B1 in food samples based on target-responsive aptamer-cross-linked hydrogel using a handheld pH meter as readout. Talanta, 176(July 2017), 34–39.
292. Zhao, Y., Wang, N., Gao, H. L., Guo, Z. X., Lu, A. X., Guo, X. J., Lu, J. H., & Luan, Y. X. (2020). Determination of Aflatoxin B1 in Lotus Seed by High Performance

Liquid Chromatography with Aptamer Affinity Column for Purification and Enrichment. Chinese Journal of Analytical Chemistry, 48(5), 662–669.

293. Zhong, H., Yu, C., Gao, R., Chen, J., Yu, Y., Geng, Y., Wen, Y., & He, J. (2019). A novel sandwich aptasensor for detecting T-2 toxin based on rGO-TEPA-Au@Pt nanorods with a dual signal amplification strategy. Biosensors and Bioelectronics, 144(August), 111635.
294. Zhou, J., Ai, R., Weng, J., Li, L., Zhou, C., Ma, A., Fu, L., & Wang, Y. (2020). A "on-off-on" fluorescence aptasensor using carbon quantum dots and graphene oxide for ultrasensitive detection of the major shellfish allergen Arginine kinase. Microchemical Journal, 158(June), 105171.
295. Zhou, L., Gan, N., Hu, F., Li, T., Cao, Y., & Wu, D. (2018). Microchip electrophoresis array-based aptasensor for multiplex antibiotic detection using functionalized magnetic beads and polymerase chain reaction amplification. Sensors and Actuators, B: Chemical, 263, 568–574.
296. Zhou, L., Gan, N., Zhou, Y., Li, T., Cao, Y., & Chen, Y. (2017). A label-free and universal platform for antibiotics detection based on microchip electrophoresis using aptamer probes. Talanta, 167(December 2016), 544–549.
297. Zhu, Y., Cai, Y., Xu, L., Zheng, L., Wang, L., Qi, B., & Xu, C. (2015). Building an aptamer/graphene oxide FRET biosensor for one-step detection of bisphenol A. ACS applied materials & interfaces, 7(14), 7492-7496.
298. Zuker, M. (2003). Mfold web server for nucleic acid folding and hybridization prediction. Nucleic acids research, 31(13), 3406-3415.

Chapter 2

Selection and characterization of specific aptamers against toxic Celiac disease epitopic peptide GQGQQGYYPTSPQQ

Chapter 2: Selection and characterization of specific aptamers against toxic celiac disease epitopic peptide GQGQQGYYPTSPQQ

Abstract

***Introduction**: This chapter describes the in-vitro selection and characterization of aptamer against a 14 mer peptide sequence of the high molecular weight glutenin subunit 1Bx13 of wheat (Triticum aestivum), GQGQQGYYPTSPQQ, which contains a celiac disease epitope QGYYPTSPQ.*

***Methods**: The peptide GQGQQGYYPTSPQQ was synthesised manually by fmoc solid phase synthesis method. A conventional SELEX method was carried out by immobilising the peptide GQGQQGYYPTSPQQ on a magnetic beads to select DNA aptamer from 56 bp long aptamer library. The binding characteristics of interaction between selected aptamer and the target was studied by using Isothermal Titration Calorimetry and Circular Dichroism. The limit of detection (LOD) evaluated through direct-ELAA.*

***Results**: A DNA aptamer apt_J91P of length 56 bp was successfully selected. The binding characterization by ITC reveals the dissociation constant of 2.26 µM and 4.385 mM for the primary and the secondary site of binding during the interaction of the aptamer and the target in aptamer binding buffer respectively. The dissociation constant of 81.3 µM was determined for the interaction in water. The LOD evaluated through direct-ELAA was found to be 16.0875 µM.*

***Discussion**: The interactions were found to be both enthalpically and entropically driven as evaluated through ITC. The CD study reveals that the binding leads to local conformational change in the aptamer.*

2.1 Introduction

The high molecular weight glutenin (HMW-GS) subunit of gluten is responsible for providing the viscoelastic property necessary for dough formation in order to prepare different food products and also forms polymeric aggregates (Zhang et al., 2018). The HMW-GS are present as a macro-polymer forming disulphide bond with LMW-GS and gliadin subunit of gluten. Due to the advantageous technical properties offered by HMW-GS, it is an indispensable entity in the modern food processing industries. There has always been an attempt to identify wheat varieties that lacks celiac disease epitopes. Some studies have indicated that ancient wheat variety such as *Triticum monococcum* has lower expression of the D-genome which encodes the most toxic α-gliadins subunit. However, D-genome is also responsible for the expression of HMW-GS, therefore the ancient varieties are not suitable for making products like pasta with superior dough making and baking quality. Modern hexaploid wheat varieties (e.g. *Triticum aestivum* L) that are obtained through selective breeding contains higher amount of starch along with an increased amount of HMW-GS which gives the characteristic property to the wheat based products such as bread, pasta or noodle etc. (Malalgoda & Simsek, 2017). Therefore while evaluating the toxicity associated with gluten protein, it is necessary to evaluate the toxicity of the HMW-GS subunit in addition to gliadin.

Due to complexities of isolating glutenin subunit during the initial period of gluten research, the majority works were concentrated on evaluating the toxicity of gliadin subunit and therefore, exploration of glutenin started comparatively little late. Molberg et al. determined the toxicity of HMW-GS fraction through *in vitro* studies using T-cell line derived from small intestinal biopsy of CD patients. Recombinant HMW-GS with 1Dx5 and 1Dy10 subunits, important for dough formation, expressed in *E.coli* were added to the intestinal T-cells and established the proliferation of T-cells. The study also revealed the TG2 sensitivity and DQ2 restriction displayed by the HMW-GS (Molberg et al., 2003). The toxicity of HMW-GS has also been confirmed by Dewar et al., 2006 through an *in-vivo* HMW-GS challenge study in patient volunteers (Dewar et al., 2006).

Earlier Mitea & group developed monoclonal antibodies against two variants of CD epitope from HMW-GS, QGQQGYYPTSPQQ(P/S). They used synthetic peptides of the two variants of the epitope and immunized them into Balb/c mice. The mAb raised recognised and had the highest reactivity against the peptide sequences PGQGQQGYYPTSPQ and GQGQQGYYPTSPQQ that contained the minimal peptide sequence QGYYPTSPQ for T-Cell stimulation (Mitea et al., 2008). Bonilla & group have also developed antibody against the

immunogenic peptide sequence QGQSGYYPTSPQ of HMW-GS. This reparative peptide sequence has a very high frequency of occurrence in the amino acid sequences of HMW-GS. It is partially soluble in water which allowed binding of the antibody to it in the native glutenin subunit (Bonilla et al., 2018).

Considering the importance of detecting the CD epitope present in HMW-GS and advantages of aptamer over antibody, we have attempted to develop an aptamer candidate against the peptide containing epitope QGYYPTSPQ in the present study. To the best of our knowledge no aptamer candidate has been developed till now against peptide sequence of HMW-GS containing epitope QGYYPTSPQ by other groups.

2.2. Materials and Methods:

2.2.1. Chemicals and Reagents

Wang resin and Nα-(9-Fluorenylmethoxycarbonyl)-amino acids (Fmoc-AA) were purchased from Advanced ChemTech, Louisville, Kentucky, USA. Analytical grade peptide synthesis chemicals, dichloromethane (DCM), N, N-dimethylformamide (DMF), tri-isopropylsilane (TIS), piperidine, and HPLC-grade solvents, trifluoroacetic acid (TFA) and acetonitrile (CH3CN) were purchased from Merck, India. All other analytical grade chemicals, 1-hydroxybenzotriazole (HOBt), N,N,N',N'-Tetramethyl-O-(1H-benzotriazol-1-yl) uranium hexafluorophosphate (HBTU), 4-(N,N dimethylamino)-pyridine (DMAP), N,N-diisopropylethylamine (DIPEA), N,N'-diisopropylcarbodimide (DIC), p-chloranil, acetic anhydride and α-Cyano-4-hydroxycinnamic acid (4-HCCA) MALDI-matrix were procured from Sigma-Aldrich Chemicals Pvt. Ltd., India. The degenerated single-stranded DNA (aptamer) library and the primers were procured from Integrated DNA Technologies (USA). Dynabeads M270 carboxylic acid, SYBR Gold nucleic acid stain and InsTA clone PCR cloning kit were purchased from Invitrogen Thermo Scientific (USA). Streptavidin magnetic beads and Low molecular weight (LMW) DNA ladder were procured from New England Biolabs (USA). IPTG (Isopropyl β-Dthiogalactopyranoside) and X-Gal (5-bromo-4-chloro-3-indolyl-β-dgalactopyranopside) were purchased from Himedia (India). Miniprep plasmid isolation kit and, Sigma Readymix and agarose were procured from Sigma Aldrich (India). All other chemicals were analytical grade and cited wherever necessary.

2.2.2 Selection of the target peptide sequence

The peptides responsible for celiac disease is selected from the amino acid sequence data of HMW-GS of wheat (*Triticum aestivum*) available in database. The amino acid sequences of the high molecular weight glutenin with accession number ABQ14770.1 (HMW glutenin subunit 1Bx13) and P10388 (HMW glutenin subunit Dx5) were retrieved from Genbank (https://www.ncbi.nlm.nih.gov/genbank/) and Uniprot (https://www.uniprot.org/) respectively. The immunostimulatory peptide sequence QGYYPTSPQ is reported as a DQ8 restricted epitope for celiac disease. The target peptide was selected considering the presence of repetitive and immunostimulatory peptide motif QGYYPTSPQ, avoiding the negative net charge of the peptide to escape electrostatic repulsion with the polyanionic oligonucleotides, higher pI value than the working pH of the experimental condition (i.e. pH 7-8). The physiochemical properties of the selected peptide were determined by using the online tool Protparam (https://web.expasy.org/protparam/) (Gasteiger et al., 2005).

2.2.3 Synthesis of High Molecular Weight (HMW) Glutenin peptide

The celiac disease toxic epitopic peptide GQGQQGYYPTSPQQ (GQ-14) of HMW glutenin subunit 1Bx13 and DX5 of wheat (*Triticum aestivum*) was synthesised manually by fmoc solid phase synthesis method (Hansen & Oddo, 2015).

2.2.3.1 Fmoc solid phase synthesis

200mg of Wang resin with a loading capacity of 1.2 mmol/g was used as the solid support for the synthesis of the peptide. The resins in a concentration of 10-15 mg/ml were swollen in a reaction vessel by dipping in a solution of 9:1 (v/v) DCM (dichloromethane)/DMF (dimethylformamide) for 8-9 hours. The first fmoc-amino acid is activated for coupling to the Wang resin. 5 equivalent (relative to resin loading capacity) of the amino acid taken in a round bottom flask is dissolved in DMF. An equal equivalent of HoBT was added to the amino acid solution, which was followed by addition of enough DMF to dissolve the mixture completely. An equal equivalent of DIC was added to the amino acid solution which was followed by addition of DMAP solution. The DMAP solution was prepared separately in another flask by dissolving 0.3 equivalent of DMAP in DMF. The reaction mixture of the amino acid was incubated for 8-10 min at 0°C before adding to the reaction vessel containing pre-swollen

Wang resins. The addition of the activated amino acid solution to Wang resin was followed by sparging of Nitrogen gas into the reaction vessel immediately to maintain an inert environment for the stability of the coupling reactants. It was then incubated at room temperature for 2-3 h with agitation. The coupling reaction was repeated one more time to ensure the maximum attachment of amino acid to the resin. The resins were then washed three times with DMF followed by washing with 1:1 (v/v) DMF/DCM once and with DCM three times. After coupling of the amino acids, the deprotection by removing the fmoc group was done by adding 20% piperidine in DMF and incubating for 20-30 min at room temperature. Then the solution was filtered out, washed in DMF and the deprotection step repeated once again. For coupling of the subsequent amino acid, 5 equivalent of Fmoc-amino acid, 5 equivalent of HBTU and 10 equivalents of DIPEA dissolved in DMF was added to the Wang resin with the first amino acid attached in the reaction vessel. Further, 5 equivalent of HOBT was added to the reaction mixture in order to decrease racemisation. The inert environment inside reaction vessel was maintained and the reaction was allowed to run for 1-1.5 h with agitation. It was followed by the deprotection step. By following the process of coupling, deprotection and washing are followed in cycle until all the amino acids in the desired peptide sequence were attached one after another. The choranil test, a qualitative colorimetric test was performed to monitor the coupling of amino acids to the resins. The free amino acids develops colour in the chloranil reaction, by turning primary free amines dark red and secondary free amines dark blue. However, absence of the free amino acids in case of coupling give colourless to yellowish beads indicating a successful coupling reaction. The choranil test was also performed to check the success of deprotection, where the dark red and dark blue colour indicates positive deprotection. The progress of the peptide synthesis was monitored through mass spectroscopic analysis by matrix assisted laser desorption/ionization mass spectrometry (Autoflex Speed MALDI-TOF/TOF mass analyser, Bruker) after coupling of amino acids with the fmoc group ($C_{15}H_{11}O_2$) attached.

2.2.3.2 Cleavage of the peptide from the resin

Once the desired length of the peptide was synthesised and confirmed by MALDI-TOF, the peptide was cleaved from the resin by adding 1ml of freshly prepared cleavage cocktail (TFA/water/Triisopropylsilane: 95/2.5/2.5) and incubating for 2-3 h. The cleaved peptides were separated from resins by filtering through glass wood plugged in a disposable

polypropylene syringe. The resins were washed twice with fresh cocktail solution and the filtrate was recovered in centrifuged tube. The peptides were then precipitated by adding 10x cold (-20ºC) diethyl ether and incubating at 4 ºC overnight. The precipitated was washed three times with fresh diethyl ether by homogenization and resuspension to remove residual scavengers. The peptides were dissolved in 1:1 acetonitrile/water (v/v).

2.2.3.3 Purification of the synthesized peptides

The synthesised crude peptides were purified using semi-preparative Reverse Phase-HPLC (1260 Infinity, Agilent Technologies, USA in Guwahati Biotech Park) that used a C18 column. A linear gradient of water and acetonitrile (10–100%) in the presence of 0.1% trifluoroacetic acid was used. The mobile phase used was 10% Acetonitrile, 0.1% TFA in water as Solvent A and 0.1% TFA in Acetonitrile as Solvent B. The flow rate maintained was 4ml/min and the volume of injection was 200 µl. The column temperature was adjusted at room temperature and a UV detector at 280 nm was used. The most dominant peaks after elution at specific retention time were collected, lyophilised to powder form and stored at -20 ºC.

2.2.3.4 Characterisation of the synthesized peptides by mass spectroscopy

The purified and dried peptide was dissolved in deionised water. The concentration of the peptide was estimated through a nanodrop spectrophotometer using the molar extinction coefficient of 2980 $M^{-1}cm^{-1}$ at 280 nm (calculated using https://web.expasy.org/protparam/). The synthesised peptide was characterised by matrix assisted laser desorption/ionization mass spectrometry (Autoflex Speed MALDI-TOF/TOF mass analyser, Bruker). The MALDI matrix was prepared by dissolving α-Cyano-4-hydroxycinnamic acid (HCCA) in a solution of 60:40 (v/v) 0.3% trifluoroacetic acid (TFA) in water and acetonitrile at a concentration of 15 mg/ml. An equal volume of MALDI matrix and 20 µM of the synthesised peptide were mixed and 2 µl of the mixture is spotted on the MALDI steel sample plate and allowed to dry for 1 h. The samples were ionized with 500 laser shots (a nitrogen laser of 337 nm) operated in a linear positive ion mode. The mass spectra were analysed using the in-built Flex control analysis software.

2.2.4 Secondary structure analysis by circular dichroism spectroscopy

CD spectroscopy was used for secondary structural analysis of the peptide GQ-14. For secondary structure analysis, 20µM GQ-14 peptide in deionised water was used to record the CD spectra in a Jasco J-1500 spectropolarimeter in a 1 mm path length quartz-cuvette and using 1 nm bandwidth. The spectrum was recorded in the far-UV wavelength of 190-250 nm at a scan-rate of 100 nm/min, wavelength interval of 0.5 nm, integration time (time constant) of 2 s and an average of 4 scans at 25℃ maintaining PMT voltage (HT voltage) <500 V. The baseline was corrected by subtracting the spectrum of the water. The spectra were smoothed using the Savitzky-Golay algorithm (Savitzky & Golay, 1964). For analysis of the CD spectra of the peptide, algorithms viz. CONTINLL, CDSSTR SELCON3 and K2D offered by online softwares Dichrowave (http://dichroweb.cryst.bbk.ac.uk/html/home.shtml) was used (Whitmore & Wallace, 2004).

2.2.5 Design of Aptamer library and PCR optimization

A 56 nucleotide long degenerate oligo-deoxynucleotide library, 5′ATACCAGTCTATTCAATT–N20–AGATAGTATGTGCAATCA3′ that contained 20 random nucleotides and flanked by 18 nucleotide long invariant primer annealing sites at both the 5′ and 3′ ends was used. The primer sequences used for this aptamer library were designed by our group in a previous study (Sett et al., 2017). The aptamer library and the three different primers used for PCR amplification, unmodified forward primer, F1: 5′-ATACCAGTCTATTCAATT-3′, 5′ Biotin conjugated reverse primer, R2: Biotin-5′-TGATTGCACATACTATCT-3′ and Unmodified reverse primer, R1: 5′-TGATTGCACATACTATCT-3′ were purchased from IDT Technologies (USA). The primer sequences used were chosen by following the research work by Ogasawara et al., 2007. The aptamer library was synthesised at 1 µM synthesis scale and PAGE purified while the labelled and unlabelled primers were synthesized at 100 nM synthesis scale. The aptamer library and the primers were reconstituted in Tris-EDTA buffer, pH 7.5. The PCR condition used for amplification of the aptamer library were optimised at mentioned in **table 2.1** for 14 cycle.

Table 2.1 Optimised conditions of PCR for amplifying N20 aptamer library

PCR Cycle		Temperature	Time
Initial Denaturation		94 °C	6 min
Denaturation	14 cycles	94 °C	30 s
Annealing		45 °C	30 s
Extension		72 °C	50 s
Final Extension		72 °C	10 min

2.2.6 Immobilization of peptide sequence on magnetic beads

The GQGQQGYYPTSPQQ peptide was immobilised on magnetic beads (Dynabeads® M-270 Carboxylic Acid with binding capacity of about 700 pmol peptide per mg, Invitrogen) as per the manufacture's instruction. The immobilization of peptide on the dynabeads works on the principle of carbodiimide chemistry, where the presence of a carbodiimide leads to formation of an amide bond between the carboxylic acid functional group of the magnetic bead and the primary amine of the peptide. Briefly, for immobilization, 3 mg (100 µl) Dynabeads were first washed with 100 µL 0.01 M NaOH. Then it was activated by mixing with a cold 100 µl solution of 0.4 M 1-ethyl-3-(3-dimethylaminopropyl) carbodiimide hydrochloride (EDC) by vortexing and followed by incubation for 30 min at room temperature with slow tilt rotation. Activated dynabeads, after washing once with 50 mM 2-[N-morpholino] ethane sulfonic acid (MES) buffer, pH 5 were mixed with an excess amount (>2100pmol) peptide (based on the binding capacity of the Dynabeads) in 50 mM MES buffer and incubated for 2 h in 4 °C with slow tilt rotation. The coated dynabeads were washed by incubating in 50 mM Tris, pH 7.4 for 15 min to remove excess peptides and quench unreacted carboxyl groups, followed by washing once with aptamer binding buffer (ABB: 50 mM Tris-HCL, pH 7.5, 250 mM NaCl, 5 mM MgCl2). The immobilization of the dynabeads with the GQ-14 peptide was confirmed by mass spectrometry analysis using a MALDI-TOF mass analyser.

2.2.7 In-vitro selection of Aptamers against peptide GQGQQGYYPTSPQQ of HMW glutenin

2000 pmole of ssDNA aptamer library was activated in 500 µl of aptamer binding buffer by heating at 95 °C for 10 min, quickly cooled on ice for 10 min for favouring secondary structure formation of ssDNA and then allowed to stand at room temperature for 10 min. The ssDNA aptamer library was used as an initial pool for the SELEX process. It was added to 50 µl of peptide immobilised dynabeads (1.5 mg beads = 1050 pmole of peptide) and incubated at room temperature for 2 h with mixing by tilt rotation in a rotary mixture. After the incubation, the beads were washed with 1x aptamer washing buffer (Aptamer binding buffer + 0.01% Tween 20) to remove unbound and weakly bound DNA. Binding conditions for the first four round were made relaxed to allow binding of aptamer candidates ranging from weak to strong affinity of binding. The aptamer candidates bound to the peptide immobilised magnetic beads were eluted by heating at 95°C for 8 min in 75 µl nuclease free water (Sigma). The eluted ssDNA was PCR amplified using F1 primer (unmodified forward primer) and R2 primer (biotinylated reverse primer).

The PCR amplified biotinylated double stranded aptamer pool was separated into single strands using streptavidin magnetic bead (New England Biolabs). 80 µl of streptavidin magnetic beads were activated by washing three times in streptavidin magnetic bead washing buffer (0.5 M NaCl, 20 mM Tris-Hcl pH 7.5, and 1 mM EDTA). PCR amplified aptamer pools were added to the activated streptavidin magnetic beads and allowed to react by incubating for 1 h with gentle stirring in room temperature. After incubation beads were washed three times by 1x ABB and finally re-suspended in 100 µl sigma water. The strands were separated by alkaline denaturation by adding 10 µl of 0.1 M NaOH and incubating for 5 min. The immobilised complementary biotinylated strand was then removed by applying a magnet and the non-biotinylated strand was eluted. The eluted solution is neutralised by adding 5 µl of 0.2 M HCl. This eluted solution containing ssDNA serve as the new enriched aptamers pool for next SELEX rounds.

In the subsequent round, the bound aptamers from the previous round were used as the aptamer pool and the process was repeated for 12 iterative rounds. The stringency of the SELEX process were increased from 4th round as shown in the **table 2.2**. Enrichment of the aptamer pools after each round was checked by running the PCR amplified aptamers in 2% agarose gel.

Two Negative SELEX rounds were performed before the starting of the 1st SELEX round and after 5th SELEX round to remove the aptamer pool binding specifically to the materials of dynabead. The ssDNA aptamer pool in 500 µl ABB after activation by heating at 95 °C for 10 min, quickly cooled on ice for 10 min and allowed to stand at room temperature for 10 min was incubated with the 1.5 mg of bare dynabeads (without immobilization of the peptide) for 30 min. After incubation, the supernatant was collected and used as aptamer pool for the next SELEX round. The the SELEX process is represented schematically in **figure no. 1.6 in** chapter 1.

Table 2.2 Details of SELEX rounds with increasing stringency

SELEX Round	**Beads(mg)/Peptide(pmole)**	**Binding time**	**Washing steps + Volume**
NS	1.5 mg + 0	30 min	
1st	1.5 mg + 1050 pmole	120 min	1 x 500µl
2nd	1.5 mg + 1050 pmole	120 min	1 x 500µl
3rd	1.5 mg + 1050 pmole	120 min	1 x 500µl
4th	1.5 mg + 1050 pmole	120 min	2 x 500µl
5th	1.5 mg + 1050 pmole	120 min	2 x 500µl
NS	1.5 mg + 0	30 min	
6th	1.5 mg + 1050 pmole	120 min	2 x 500µl
7th	1.5 mg + 1050 pmole	120 min	2 x 500µl
8th	1.5 mg + 1050 pmole	60 min	2 x 500µl
9th	1.5 mg + 1050 pmole	60 min	2 x 500µl
10th	1.5 mg + 1050 pmole	60 min	2 x 500µl
11th	1.0 mg + 700 pmol	60 min	2 X 500 µl
12th	1.0 mg + 700 pmol	60 min	2 X 500 µl

NS- Negative SELEX

2.2.8 Cloning and sequencing of the Aptamer sequences

The aptamer candidates from the final 12th SELEX round were PCR amplified by using F1 (unmodified forward) and R1 (unmodified reverse) primers. The PCR products were purified by the electroelution technique. 100 µl of the PCR products were run in a 15% native PAGE gel. The band of aptamer candidate corresponding to 56 bp were excised and put inside a dialysis tubing (3 KDa cut-off) containing 300 µl 0.1x TAE buffer. The dialysis tubing with

both ends tightly clipped was placed in the horizontal electrophoresis tank filled with 0.1x TAE running buffer and a power 80 V was applied. After running for 30-40 min under 80 V and polarity of the electrophoresis tank was reversed and run further for 5 min. The aptamer eluted to the 0.1xTAE solution inside the dialysis tubing was collected, precipitated adding 3M sodium acetate ($1/10^{th}$ of the sample volume) and chilled 100% ethanol (3 times the total sample volume). The precipitated DNA is air-dried and reconstituted in 10 µl TE buffer.

The purified dsDNA aptamer candidates were cloned by using a PCR TA cloning kit (InsTA Clone PCR Cloning Kit, Thermo Scientific). The dsDNA aptamer candidates were ligated into a specialised TA cloning vector pTZ57R/T by mixing the components of the reaction mixture mentioned in the **table 2.3** and incubating it for 16 h at 4°C as per manufacturer's instructions. The amount of insert (in ng) used in the ligation reaction was calculated by the standard formula,

Amount of Insert (ng) = {Amount of vector (ng) x size of insert (kb)/Size of vector (kb)} x molar ratio of Insert: vector.

Table 2.3 Components and amounts of Ligation reaction mixture

Reaction components	**Volume**
10X Ligation buffer	1.0 µl
Vector pTZ57R/T (50ng)	1.0 µl (55 ng)
Purified Aptamer pool	added in ratio 3:1 (insert/vector ratio)
T4 DNA ligase (3 units/µl)	1.0 µl
Nuclease free water	Volume made to 10 µl
Total Volume	10 µl

The ligated vector pTZ57R/T was transformed into chemically competent *E.Coli* DH5α host cells and grown in the LB (Luria Bertani) agar plates containing ampicillin, X-gal and IPTG. The positively transformed colonies were screened on the basis of blue white selection.

About 100 positively transformed white colonies were picked up randomly and grown overnight in LB broth. The plasmids were isolated from overnight grown cultures by a miniprep plasmid isolation kit (Sigma Aldrich, Germany). Isolated plasmids were checked in 0.8% Agarose gel. Presence of aptamer insert in the plasmid was confirmed by PCR amplification using unmodified forward and reverse primers. The positive plasmids were sequenced by

Sanger sequencing method using the M13 forward and reverse primers and the sequencing process was outsourced to AgriGenome Labs Pvt. Ltd., India. Multiple sequence alignment through Clustal Omega (https://www.ebi.ac.uk/Tools/msa/clustalo/) was carried out to find any homology between the sequences.

2.2.9 *Insilico* analysis of aptamer sequences

The aptamer sequences obtained from Sanger sequencing were preliminarily analysed for free energy comparison and structural stability using the mfold web server (http://unafold.rna.albany.edu/?q=mfold) to find out the most potent aptamer candidate against the peptide target (Zuker M, 2003). The Gibbs free energy (ΔG) and secondary structure for the aptamer sequences were predicted by setting the ionic condition used in aptamer binding buffer of 250 mM NaCl and 5 mM $MgCl_2$ and temperature at 25 ºC. The secondary structure of the aptamer sequences was predicted by a free energy minimization algorithm in the mfold software.

2.2.10 Binding characterization of the aptamer with target peptide

2.2.10.1 Isothermal Titration Calorimetry (ITC) studies

Isothermal titration calorimetry was carried out to study the binding affinity between aptamer candidates and the target peptide. The truncated aptamer candidates Apt_J91 and Apt_94 (both without flanking regions) and their respective whole sequences with flanking regions viz. Apt_J91P and Apt_J94P were studied for their affinity towards the target GQ-14 peptide. The experiments were performed at 25 °C using a MicroCal iTC200 (GE Healthcare, UK). 200 µl of aptamer was loaded into the calorimetric cell. Typically, 25 serial injections (1.5 µl/injection) of the peptide from the syringe were injected at the spacing of 120 s with the continuous stirring of the solution in the calorimetric cell at 200 rpm. To compensate the heat of dilution, a control experiment was carried out without aptamer in the syringe. To attain the saturation in binding between, different concentrations of aptamer (10-40 µM) and peptide (1000-3000 µM) were tried for optimization. The aptamer and the peptide interaction was allowed to carry out in the aptamer binding buffer which was used in SELEX and in deionised water. The aptamers were also analysed for their specificity by studying binding characteristics between the aptamer candidate and an unrelated peptide PV-12 (PQQPPFQQQQPV).

2.2.10.2 Circular dichroism studies

CD spectroscopy was used for the structural analysis of the aptamer apt_J91P. 4µM of aptamer apt_J91P in 0.3x ABB was activated by heating at 95 ℃ for 10 min, followed by cooling in ice for 10 min and then incubating at room temperature for 10 min. The spectrum was recorded in the wavelength range of 190-340 nm at a scan-rate of 100 nm/min, wavelength interval of 0.5 nm, integration time (time constant) of 2 s and an average of 4 scans at 25℃ maintaining PMT voltage (HT voltage) <500 V in a Jasco J-1500 spectropolarimeter with 1 mm path length quartz-cuvette and using 1 nm bandwidth. The baseline was corrected by subtracting the spectrum of the buffer. The spectra were smoothed using the Savitzky-Golay algorithm (Savitzky & Golay, 1964).

For studying interaction between the aptamer and the peptide, the aptamer was activated as mention above. The activated aptamer was added to the peptide and the interaction was allowed to occur in 0.3x ABB by incubating in room temperature for 1h 30 min at rotospin. For acquisition of the CD spectrum in a Jasco J-1500 spectropolarimeter, the parameters used and baseline correction and smoothening performed were similar as mentioned above.

2.2.10.3 Direct Enzyme linked aptamer-sorbent assay (ELAA)

The direct Enzyme linked aptamer-sorbent assay was carried out to determine the affinity of Apt_91P to the target peptide GQ-14. The peptide immobilised dynabeads were taken in five Eppendorf tube in an increasing concentration of 40-200 µM. Dynabeads without immobilising the peptide on it was taken as control. The experiment was carried out in duplicates. Aptamer Apt_J91P biotinylated at the 5’ end (5'-Biotin-ATACCAGTCTATTCAATTCTCCTGAGCTATCTGGAAAGAGATAGTATGTGCAATCA-3') at concentration of 0.5 µM was added to each tube. The reaction was carried out in 200 µL of 1x aptamer binding buffer (50mM Tris-HCl, 0.25 M NaCl, 5mM MgCl2, pH 7.4) and incubated for 1 h in rotation at room temperature. The unbound aptamers were washed away with 1x aptamer washing buffer (aptamer binding buffer + 0.01% Tween 20). 200 µL Streptavidin-HRP conjugate (1:1000 dilution from 1 mg/ml) as detection probe was added to each tube and incubated for 1 h with tilt rotation at room temperature, followed by washing with 1x aptamer washing buffer. 50 µL of 3,3′,5,5′-Tetramethylbenzidine/H_2O_2 solution

(Sigma, USA) was added to it. After 15 min of incubation in dark, 50 µL stop solution of 1 M H_2SO_4 was added. The supernatant was separated from magnetic beads and transferred to a microtiter plate for measurement of intensity at 490 nm in a microplate reader (Tecan, Switzerland).

2.3 Results

2.3.1 Selection of the target peptide sequence

Considering the presence of repetitive and immunostimulatory peptide motif QGYYPTSPQ, avoiding the negative net charge of the peptide to escape electrostatic repulsion with negatively charged oligonucleotides and a higher pI value than the working pH of the experimental condition of SELEX, a 14 amino acid long peptide sequence from the protein sequence of HMW-GS subunits 1Bx13 and DX5 were selected for the development of aptamer candidate against it. The selected peptide sequence is highlighted in red with underlining the immunostimulatory motif of celiac disease in the protein sequence below.

>gi|146261040|gb|ABQ14770.1| HMW glutenin subunit 1Bx13 [Triticum aestivum]

MAKRLVLFAAVVVALVALTAAEGEASGQLQCERELEACQQVVDQQLRDVSPGCRPITVSPGTRQYERQPVVPSKAGSFYPSKTTPSQQLQQMI
FWGIPALLRRYYPSVTSSQQGSYYPGQASPQQLGQGQQPGQGQQPRQEQQDQQPGQRQQGYYPTSPQQPGQGQQLGQGQPGYYPTSQQ
PGQKQQAGQGQQSGQGQQGYYPTSPQQSGQGQQPGQGQAGYYPTSPQQSGQWQQPGQGQQPGQGQQSGQGQQGQQPGQGQRPG
GQGQQGYYPTSPQQPGQGQQSGQGQPGYYPTSLRQPGQWQQPGQGQQPGQGQQGQQPGQGQQPGQGQQGYYPTSLQQPGQGQQPG
QGQPGYYPTSQQSEQGQQPGQGKQPGQGQQGYYPTSSQQSGQGQQLGQGQPGYYPTSPQQSGQGQQSGQGQQGYYPTSPQQPGQEQ
QPGQGQSGYFPTSRQQSGQGQQPGQGQQSGQGQQGQQPGQGQQAYYPTSSQQSGQRQQAGQWQRPGQGQSGYYPTSPQQPGQEQ
QSGQAQQSGQWQLVYYPTSPQQPGQLQQPAQGQQPAQGQQSAQEQQPGQAQQSGQWQLVYYPTSPQQPGQLQQPTQGQQGYYPTSP
QQSGQGQQGYYPTSPQQSGQGQQGYYPTSPQQSGQGQQPGQGRQPRQGQQGYYPISPQQSGQGQQPGQGQQGYYPTSPQQSGQGQQ
PGHEQQPGQWLQLGQGQQGYYPTSPQQSGQGQQSGQGQQGYYPTSLWQPGQGQQPGQGQQGYDSPYHVSAEYQAARLKVAKAQQLA
ASLPAMCRLEGSDALSTRQ

The physiochemical properties of the selected peptide sequence is determined by Protoparam (https://web.expasy.org/protparam/) and listed below in **the table 2.4**.

Table 2.4 Physiochemical property of the target peptide sequence GQGQQGYYPTSPQQ (GQ-14) of HMW-GS

Physiochemical properties	
Molecular weight	1538.57 g/mol
Extinction coefficient	2980 M^{-1} cm^{-1}
Iso-electric point (pI)	pH 5.52
Net charge at pH 7	0
Grand average of hydropathicity (GRAVY)	-1.857

2.3.2 Synthesis of High Molecular Weight (HMW) Glutenin peptide

2.3.2.1 Fmoc solid phase synthesis

The target peptide GQGQQGYYPTSPQQ (MW of 1538.57 g/mol) was synthesised by fmoc solid phase synthesis method using Wang resin as the solid support. The process of coupling of fmoc-amino acid and deprotection of fmoc group from the attached amino acid was monitored through qualitative Chloranil test. Analysis of molecular weight of the growing peptide sequence through MALDI-TOF confirmed the status of positive attachment during the synthesis process. Mass analysis of the crude peptide sequence after attachment of the 4^{th} amino acid (Fmoc-SPQQ) and 8^{th} amino acid (Fmoc-YYPTSPQQ) showed the expected m/z ratio in mass spectra. The f**igure 2.1** shows the corresponding m/z peaks to the fmoc attached peptide fragments with adducts. The dominant m/z peaks of 704.225 ($[M+Na]^+$) and 720.308 ($[M+K]^+$) correspond to the monoisotopic mass of Fmoc-SPQQ along with Sodium and Potassium ions as adducts respectively. Similarly, the dominant m/z peaks of 1228.714 ($[M+Na]^+$) and 1244.699 ($[M+K]^+$) correspond to the monoisotopic mass of Fmoc-YYPTSPQQ along with Sodium and Potassium ions as adducts respectively.

A

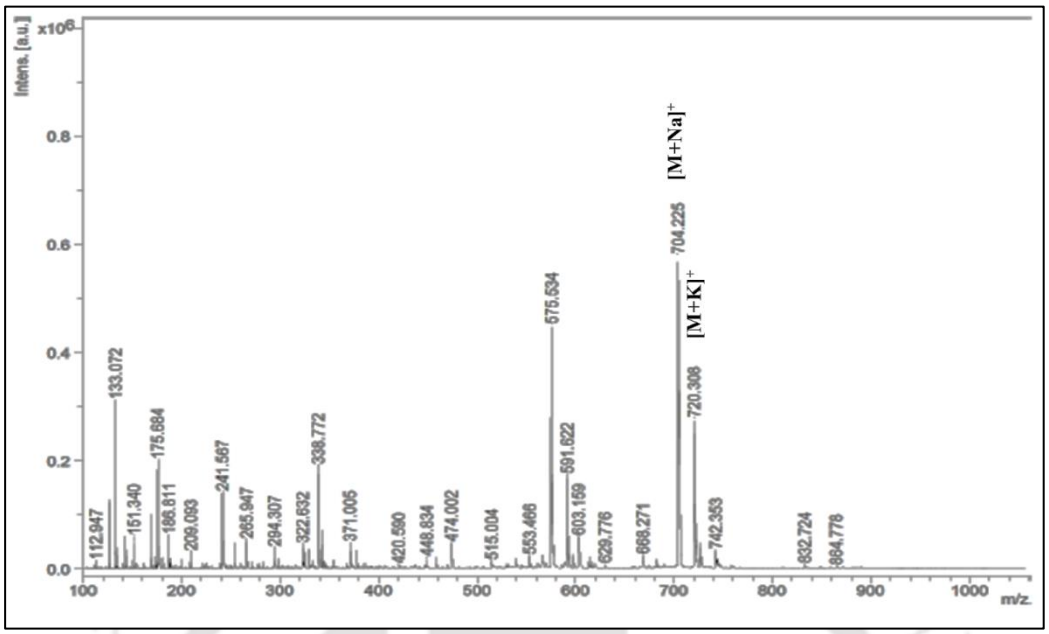

B

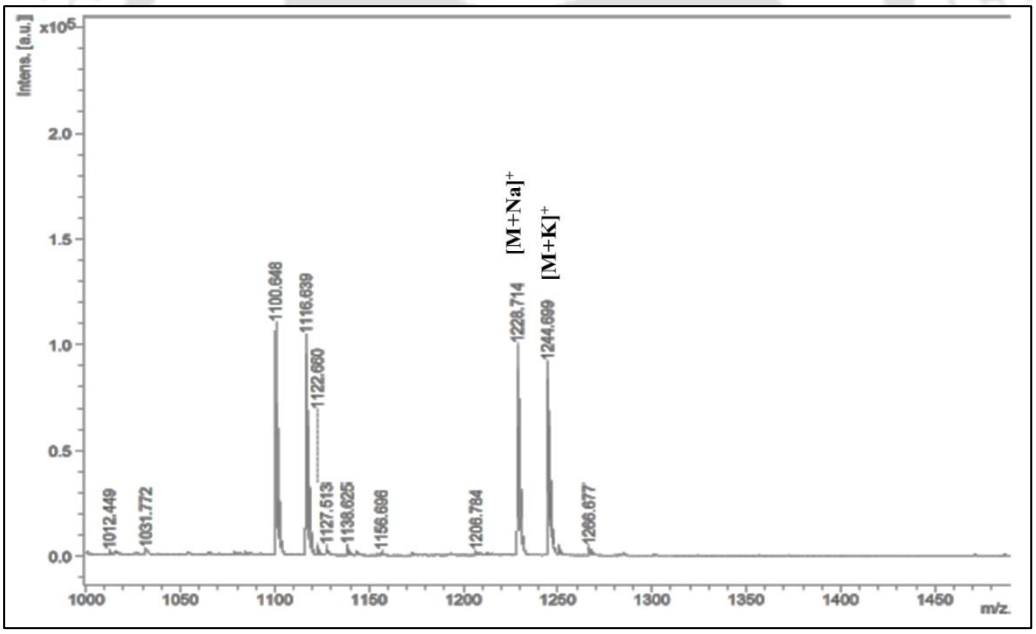

Figure 2.1 The MALDI-TOF mass spectra of crude peptides (A) Fmoc-SPQQ (MW 680.28 Da) and (B) Fmoc-YYPTSPQQ (MW 1204.51 Da) with addition of adducts as $[M+Na]^+$ and $[M+K]^+$, where M denotes the parent mass

2.3.2.2 Purification of the synthesized peptides

For purification of the crude peptide cleaved from Wang resin, it was dissolved in 1:1 acetonitrile/water (v/v). With a linear gradient of mobile phase water and acetonitrile (10–100%) with 0.1% trifluoroacetic acid, the crude peptide sample was purified with a C18 reverse phase HPLC. The HPLC chromatograms were recorded with UV-Vis detector at wavelength 280 nm which showed a dominant peak at retention time 13.52 min along with other few small peaks as shown in **figure 2.2**. The HPLC fractions at different retention times were collected and mass spectroscopic analysis of each fraction was carried out. Peptide fraction retained at 13.52 min was found to correspond to the expected mass of peptide GQ-14 thorough mass spectroscopic analysis. The fraction containing the purified target peptide is then lyophilised to a powder form.

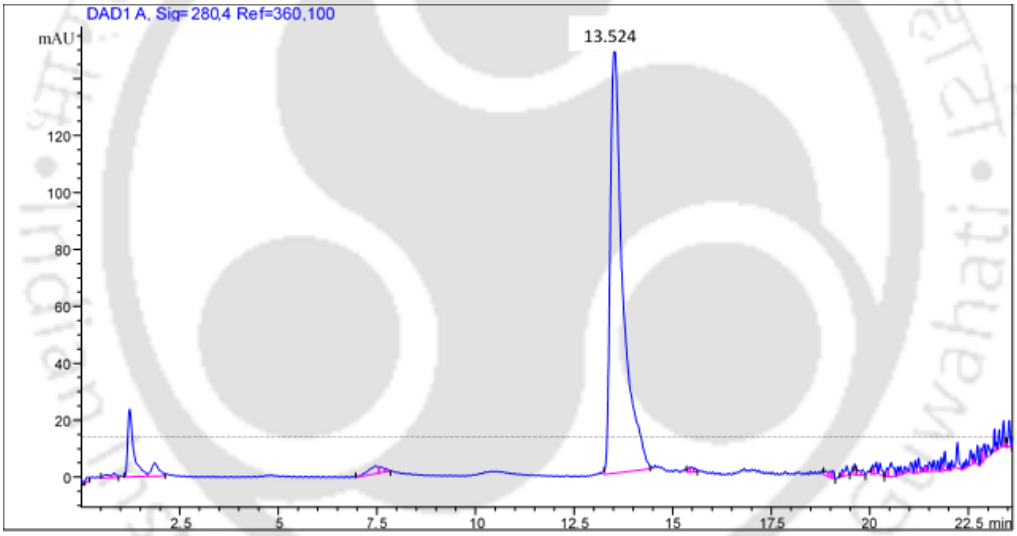

Figure 2.2 Reverse phase-HPLC chromatogram of the purified peptide GQ-14 at retention time 13.52 min

2.3.2.3 Characterisation of the synthesized peptides by mass spectroscopy

The MALDI-TOF mass spectroscopy was used to obtain the characteristic molecular weight of the synthesised peptide. The matrix assisted laser desorption/ionization technique involves the hitting of the uniformly mixed analyte with energy-absorbent matrix compound with UV ray of the wavelength 337 nm (nitrogen laser light) which leads to generation of singly protonated ions of the analyte. The ions are separated on the basis of their mass-to-charge ratio (m/z) under a fixed potential in the time-of-flight analyser and the characteristic mass spectra

(m/z) of the all the constituent compounds of the analyte are obtained. The **figure 2.3** shows the characteristic mass spectrum of the purified peptide GO-14. The dominant monoisotopic mass obtained are found to be the mass of the peptide GQ-14 along with different adducts. The m/z peaks of 1539.85 Da, 1561.767 and 1577.735 correspond to the mass of peptide with Hydrogen $[M+H]^+$, Sodium $[M+Na]^+$ and Potassium $[M+K]^+$ as adducts respectively. The mass spectra confirm the successful purification of the synthesised peptide GQ-14.

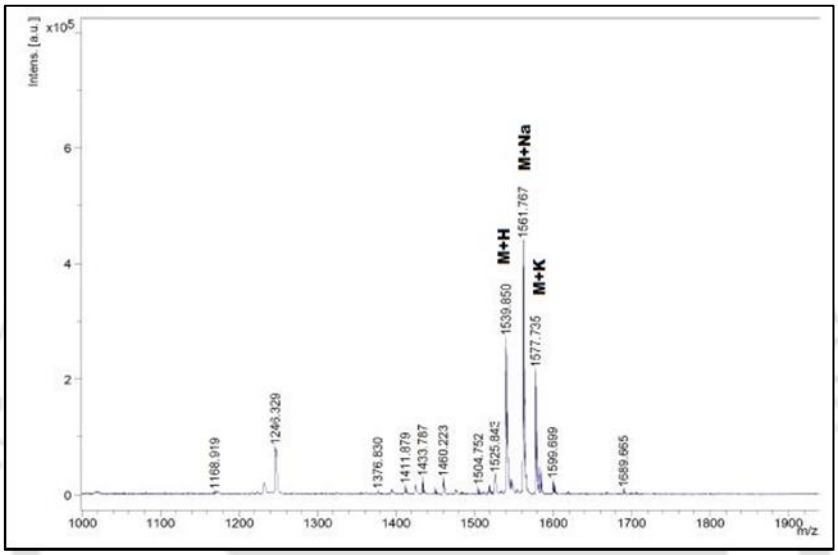

Figure 2.3 The MALDI-TOF mass spectra of the purified peptide GQ-14 with dominant peaks of 1539.85 Da ($[M+H]^+$), 1561.767 ($[M+Na]^+$) and 1577.735 ($[M+K]^+$), where M denotes the parent mass of 1538.57 Da

2.3.3 Secondary structure analysis by circular dichroism spectroscopy

The circular dichroism (CD) spectra of the peptide GQ-14 was recorded in far-UV wavelength of 190-250 nm at 25 °C. The peptide shows a characteristics strong minima near between 196 nm and 200 nm confirming their random coil secondary structure shown in the **figure 2.4**. The CD spectra were analysed by using the online analysis tool Dichrowave which performs quantitative estimation of the secondary structure using methods CONTINLL, SELCON3, CDSSTR, VARSLC and K2D. These methods compare the experimental CD spectral data with reference database of a protein whose secondary structure is known from X-ray crystallography and calculate fraction of each type secondary structure contributing to the net experimental CD spectral data (Whitmore &. Wallace, 2004). Out of all the methods used, the CONTINLL with use of the reference set, SP175 exhibits the lowest normalized root mean square deviation

(NRMSD) value which indicates the goodness-of-fit of experimental data with the reference data and it is listed in the **table 2.5.** The secondary structure of peptide GQ14 is estimated to be around 35% random structure (unordered).

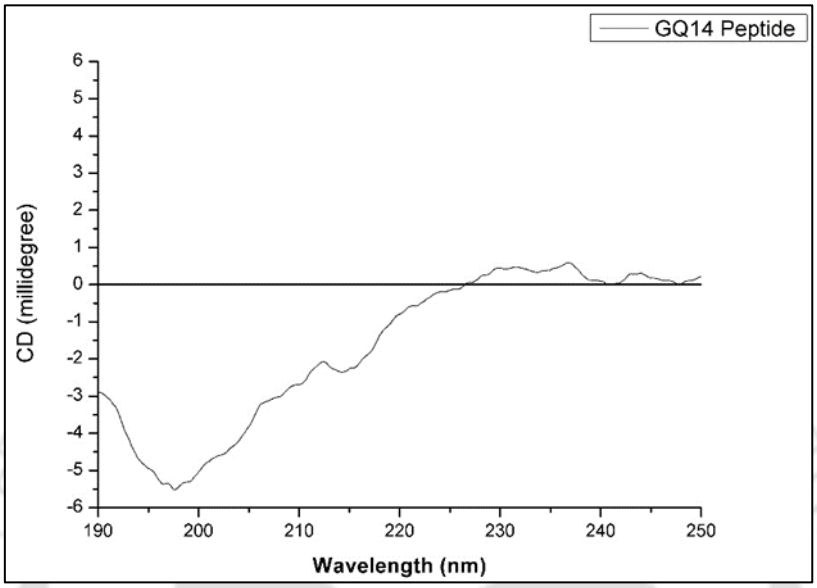

Figure 2.4 Circular dichroism spectra of peptide GQ-14 recorded in the Far-UV wavelength 190-250 nm at 25 °C

Table 2.5 Distribution of secondary structure apt_J91 as predicted by Dichrowed

	Secondary structure predicted by Dichroweb							
Peptide	Algorthim	Helix1	Helix2	Strand1	Strand2	Turns	Unordered	NRMSD
GQ-14	Contin-LL	0.003	0.016	0.277	0.138	0.215	**0.351**	0.7

2.3.4 Design of Aptamer library and PCR optimization

The aptamer library of length 56 nucleotide containing a 20 nucleotide long central random region flanked by two primer binding regions was dissolved in Tris-EDTA buffer, pH 7.5. The amplification of the library is crucial for SELEX. The melting temperature of the aptamer library is 65.7 °C. The PCR conditions to amplify the aptamer library were optimised as

mentioned in the **table 2.1**. The amplified aptamer library was run in 2% agarose gel, the size of the amplified library was found to be intact at 56 bp with 14 PCR cycle.

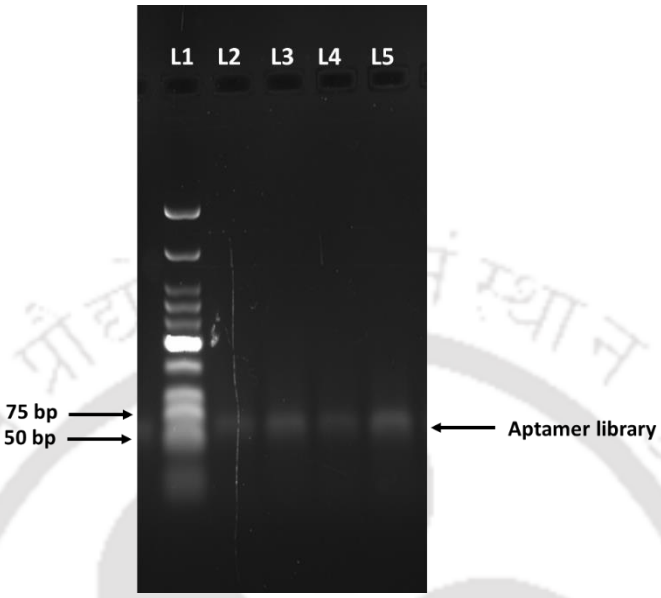

Figure 2.5 Optimization of PCR conditions at 45 °C annealing temperature and 14 cycles. L1 is low molecular DNA ladder (NEB, 25-766 bp) and L2-l5 are the PCR amplified aptamer library of 56 bp.

2.3.5 Immobilization of peptide sequence on magnetic beads

Immobilization of the peptide GQ-14 on dynabeads was successfully confirmed by MALDI-TOF analysis of the beads. The MALDI mass spectra were acquired in linear negative ion mode, while linear positive ion mode yielded a very noisy mass spectra likely due to presence of materials of dynabead. The characteristic mass of the peptide with addition of adducts 1537.49 ($[M-H]^-$) and 1653.76 ($[M+TFA]^{-1}$) are observed in mass spectra as shown in the **figure 2.7**.

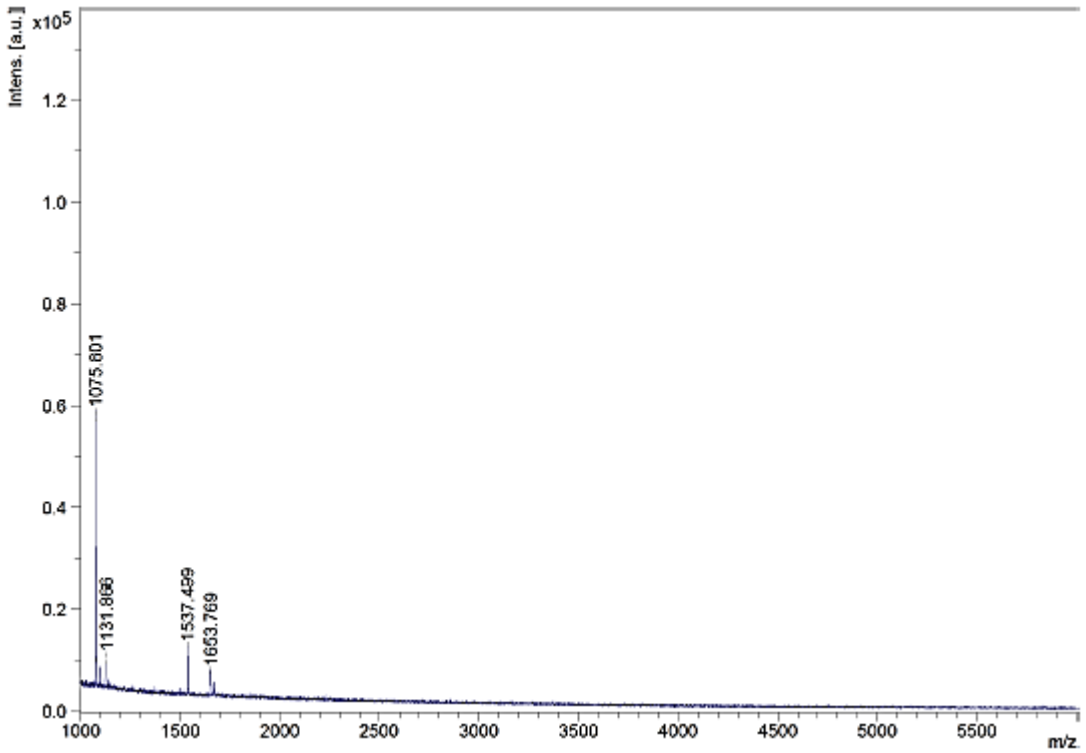

Figure 2.6 MALDI-TOF spectra of dynabead immobilised with peptide GQ-14 in linear negative mode where monoisotopic masses of 1537.49 Da ($[M-H]^-$) and 1653.76 Da ($[M+TFA]^{-1}$) are observed, where M denotes the parent mass of 1538.57 Da

2.3.6 In-vitro selection of Aptamers against peptide GQGQQGYYPTSPQQ of HMW glutenin

The SELEX rounds were carried out for 12 cycles with two negative SELEX rounds at the beginning and after the 5th round. The initial pool of the aptamer library should theoretically contain 10^{12} distinct aptamer sequences and the process of incubation of the library with the target peptide in iteration in SELEX process should select the aptamer sequence with high affinity for the target. The stringency of the SELEX process was increased in each round after 4th round and continued till the 11th round. The enrichment of the aptamer candidate after each rounds was monitored through 2% agarose gel electrophoresis as shown in the **figure 2.8**. The SELEX was successfully carried out till 12th round and the enriched sequences retrieved were cloned and sequenced.

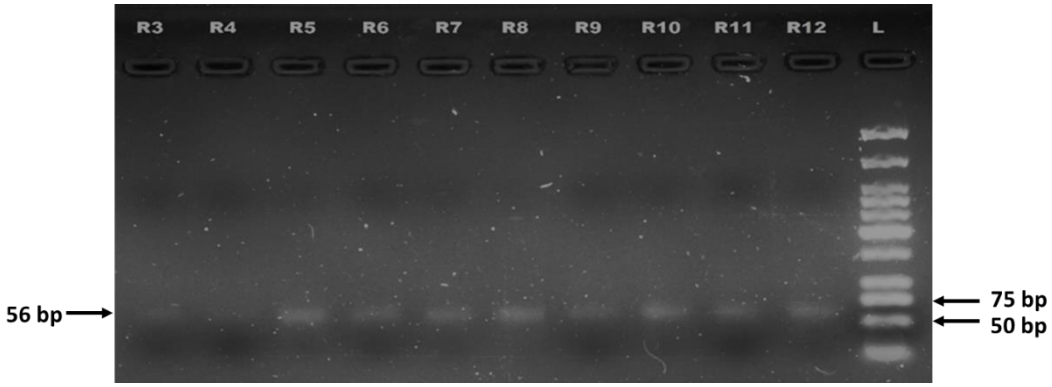

Figure 2.7 2% agarose gel for 56 enriched N20 aptamer pool after SELEX rounds against peptide target GQ-14 from 3rd to 12th round (R3-R12), L-Small molecular DNA ladder (NEB, 25-766 bp)

2.3.7 Cloning and sequencing of the Aptamer sequences

Around 100 positively transformed colonies were selected based on the blue white screening after the growth of the cloned *E.Coli* DH5α cells in LB-ampicillin plates. The plasmid were isolated successfully from the positively transformed cells and insertion of the aptamer sequences in the plasmid vector was analysed by PCR amplification using primer sequences, unmodified forward primer (5′-ATACCAGTCTATTCAATT-3′) and unmodified reverse primer (5′-TGATTGCACATACTATCT-3′). A total of 25 plasmids with positive insertion of the aptamer sequence were sequenced by Sanger method. Out of 25 sequences received, only 15 sequences were found be correctly inserted aptamer sequences which are listed in the **table 2.6**. The multiple sequence alignment did not shown any homology or any consensus motif between the sequences as each sequence contain a unique primary structure.

Table 2.6 Sequences of aptamer candidates of 56 bp containing 20 nucleotide random region with flanking primer regions selected against GQ-14

Sl. No.	*Name of Aptamer*	*Sequence*
1	Apt_J85	TGATTGCACATACTATCT**GGCTTTGATCCGTGCGCTCG**AATTGAATAGACTGGTAT
2	Apt_J86	ATACCAGTCTATTCAATT**CCAATCGGCAAATGTTGTTG**AGATAGTATGTGCAATCA
3	Apt_J87	ATACCAGTCTATTCAATT**TCAAGGTTTTTAAGCAATTA**AGATAGTATGTGCAATCA
4	Apt_J88	ATACCAGTCTATTCAATT**CCATTCTGCATGAAGCGTCC**AGATAGTATGTGCAATCA
5	Apt_J89	ATACCAGTCTATTCAATT**AGTGGCAGCCCCGACTTAAG**AGATAGTATGTGCAATCA

6	Apt _J91	ATACCAGTCTATTCAATT**CTCCTGAGCTATCTGGAAAG**AGATAGTATGTGCAATCA
7	Apt _J93	ATACCAGTCTATTCAATT**CCAATGTCCTGGCTTACTCG**AGATAGTATGTGCAATCA
8	Apt _J94	ATACCAGTCTATTCAATT**AGATGGAGATACTCCCCTTA**AGATAGTATGTGCAATCA
9	Apt _J123	ATACCAGTCTATTCAATT**CACTCGGCTCTGTCGTCTGT**AGATAGTATGTGCAATCA
10	Apt _J125	ATACCAGTCTATTCAATT**TGCATCAATTCGGGCCGGTG**AGATAGTATGTGCAATCA
11	Apt _J128	ATACCAGTCTATTCAATT**CCTCGCCCGGGTGATGGTTC**AGATAGTATGTGCAATCA
12	Apt _J129	ATACCAGTCTATTCAATT**AGGGATGAGTGCTTGATGAT**AGATAGTATGTGCAATCA
13	Apt _J130	TGATTGCACATACTATCT**AGGCGGGTCTATACATGGCG**AATTGAATAGACTGGTAT
14	Apt _J131	TGATTGCACATACTATCT**GGATGTGGAACCACCGAGGT**AATTGAATAGACTGGTAT
15	Apt _J134	ATACCAGTCTATTCAATT**GCCGATAATGTCACACTTAC**AGATAGTATGTGCAATCA

2.3.8 *Insilico* analysis of aptamer sequences

The 15 aptamer sequences obtained from Sanger sequencing were preliminary analysed for the free energy comparison and the structural stability using mfold web server. The thermodynamic parameters like change in enthalpy (ΔH), change in entropy (ΔS) and change in Gibb's free energy (ΔG) were determined for each of the 15 aptamer candidate sequences. The lowest value of change in Gibb's free energy (ΔG) indicates the most stable structure formation. The sequences with lowest Gibb's free energy (ΔG) are listed in the **table 2.7** and they are consider for further analysis. Although the aptamer candidates with and without the primer sequences have different values of Gibb's free energy (ΔG), they can be arrange in same order when lowest to highest values are considered. The secondary structure of the selected aptamer candidates were predicted by mfold web server which generated more than one secondary structure for each sequence with different values of Gibb's free energy (ΔG). The structure of the aptamer sequences predicted with lowest Gibb's free energy (ΔG) are presented in the **figure 2.9**. The secondary structure of the aptamer sequences is predicted by a free energy minimization algorithm in mfold software. At minimum Gibbs free energy, the thermodynamically stable secondary structure formed by both truncated aptamers Apt_J91 and Apt_J94 are predicted to take a stem-loop shape. The aptamer candidates with primer regions attached, Apt_J91P and Apt_J94P are predicted to have dumbbell-shaped structure with stem-loop extending outward.

Table 2.7 Thermodynamic parameters of the aptamer sequences as calculated by mfold software

Name	Sequence (Random Region)	Gibb's Free Energy (ΔG) (Kcal/Mol At 25℃)	Enthalpy Change (ΔH) (Kcal/Mol)	Entropy Change (ΔS) (Kcal/K.Mol)
APT_J91	CTCCTGAGCTATCTGGAAAG	**-2.87**	-35.00	-107.7×10^{-3}
APT_J94	AGATGGAGATACTCCCCTTA	**-2.68**	-31.50	-96.6×10^{-3}

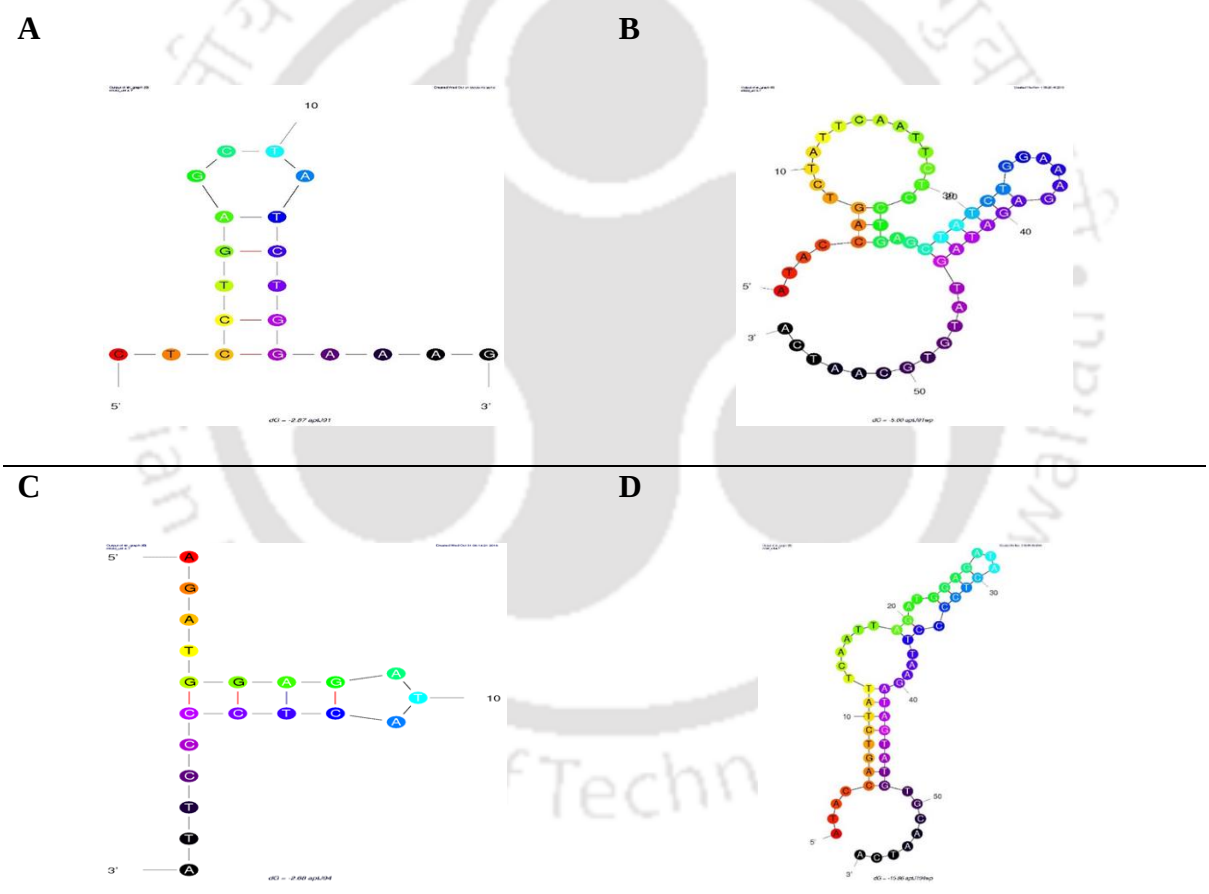

Figure 2.8 Secondary structure of aptamer candidates as predicted by mfold; A) truncated aptamer Apt_J91 without flanking regions, B) aptamer Apt_J91P with flanking regions, C) truncated aptamer Apt_J94 without flanking regions, D) aptamer Apt_J94P with with flanking regions.

2.3.9 Binding studies

2.3.9.1 Isothermal Titration Calorimetry (ITC) studies

Binding affinity in terms of dissociation constant (K_d) and other thermodynamic parameters were evaluated by isothermal titration calorimetry (ITC) studies. From the homogenous binding events between aptamer and peptide, a binding isotherm of the aptamer-peptide complex is generated from the heat exchange data of binding. The amount of heat exchanged during the interaction of the peptide and the aptamer after each injection is plotted against the molar ratio of concentrations of peptide and aptamer. The calorimetric cell records the amount of heat exchanged after each injection derived from the amount of power required to maintain the cell at a constant temperature. The each injection in calorimetry cell generates a heat-burst curve (µcal/s) as a function of time (min). From the thermogram, the values of association constant (K_a), change in enthalpy (ΔH), change in entropy (ΔS), dissociation constant (K_d) and stochiometry of the binding (N) are derived. The change in enthalpy (ΔH) can be directly measured from thermogram while the change in entropy (ΔS) and the Gibb's free energy change (ΔG) and the dissociation constant (K_d) are calculated from the following equations, where R is the universal gas constant (1.986 cal K^{-1} mol^{-1}) and T is the temperature of the reaction.

$$\Delta G = -RT \ln K_a$$

$$\Delta G = \Delta H - T\Delta S$$

$$K_a = 1/K_d$$

The interaction of 1000 µM apt_J91P with flanking regions with 30 µM peptide GQ-14 in buffer 1x ABB was first studied through ITC. The peaks of the isotherm of their interaction were integrated and fitted into a two sites sequential binding model in Origin 5.0 software (Microcal, Inc) as shown in **figure 2.10**. The dissociation constant and the other thermodynamic parameter of the interaction is listed out in **table 2.8**.

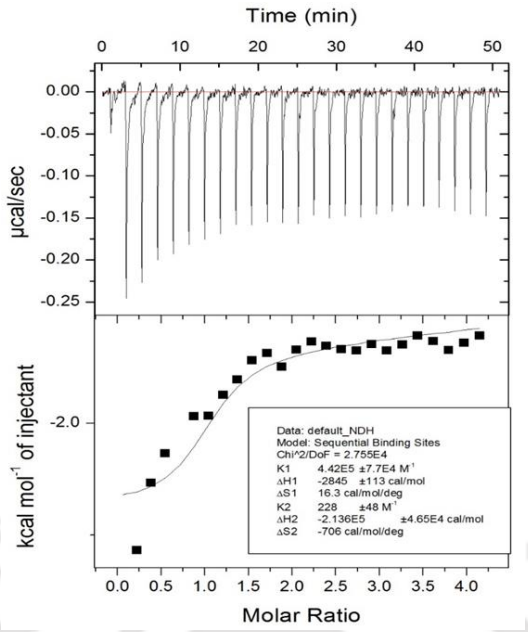

Figure 2.9 ITC isotherms for calorimetric titration between 30 µM aptamer apt_J91P with flanking regions and 1000 µM peptide GQ-14 at 25°C in aptamer binding buffer.

Table 2.8 List of dissociation constant and thermodynamic parameters calculated through ITC study of interaction between apt_J91P and GQ-14 in 1x ABB

1^{st} site	
Dissociation constant, K_d1	2.26 µM
Change in Enthalpy, ΔH1	-2845 cal/mol
Change in Entropy, ΔS1	16.3 cal/mol/deg
TΔS1	407.5 cal/mol
Gibb's free energy change, ΔG1	-3252.5 cal/mol
2^{nd} site	
Dissociation constant K_d2	4.385 mM
Change in Enthalpy, ΔH2	-2.136×10^5 cal/mol
Change in Entropy, ΔS2	-706 cal/mol/deg
TΔS2	-17650 cal/mol
Gibb's free energy change, ΔG2	-1.9×10^5 cal/mol

From the ITC binding isotherm of between apt_J91P and GQ-14, it is seen that the reactions of binding are exothermic. The binding is found to be favoured by both enthalpy, ΔH (-2845 cal/mol) and entropy, TΔS (407.5 cal/mol) at temperature 25°C for the first site of binding. The exothermic enthalpy generally indicates the binding of the peptide molecule in

the DNA major groove (Kuo et al., 2013). The favorable entropy change indicates the desolvation process or removal of water molecules from the complex interface (Amaya-González et al., 2015). The dissociation constant was determined to be 2.26 µM for the interaction between apt_91P and the target peptide GQ-14. The aptamer also contained a low affinity binding site with dissociation constant of 4.385 mM.

The interaction between the apt_J91P and GQ-14 was also studied by performing ITC while dissolving both the aptamer and peptide in deionized water. The isotherm of interaction (**figure 2.10**) between 30 µM aptamer apt_J91P and 3000 µM GQ14 interaction in deionized water was fitted to a one site binding model in Origin 5.0 software (Microcal, Inc). The dissociation constant and the other thermodynamic parameter of the interaction are listed out in **table 2.9**.

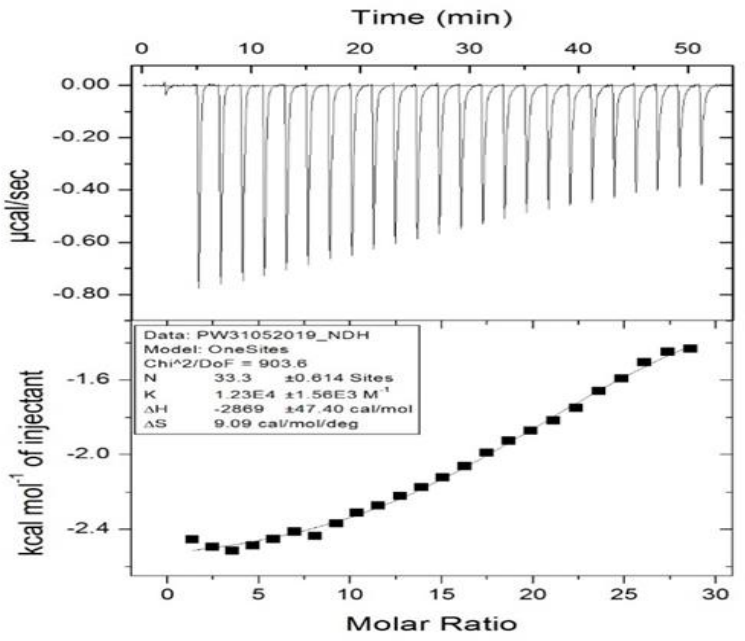

Figure 2.10 ITC isotherms for calorimetric titration between 30 µM aptamer apt_J91P with flanking region and 3000 µM peptide GQ-14 at 25°C in deionised water.

Table 2.9 List of dissociation constant and thermodynamic parameters calculated through ITC study of interaction between apt_J91P with flanking region and GQ-14 in water

Single site binding model	
Dissociation constant K_d	0.0813 mM
Change in Enthalpy, ΔH	-2869 cal/mol
Change in Entropy, ΔS	9.09 cal/mol/deg
TΔS	227.25 cal/mol
Gibb's free energy change, ΔG	-3096.25 cal/mol

The binding characteristics of the apt_J91P and target GQ-14 in deionised water was found to be similar with their interaction in 1x ABB buffer, however, the dissociation constant was found to be higher in this case with 0.0813 mM.

ITC was carried out to check the specificity of apt_J91P with flanking region with a peptide PV-12 (PQQPPFQQQQPV) which contains different amino acid sequence than GQ-14 in 1x ABB buffer. The isotherm for apt_J91P-PV-12 interaction were tried to fit to a sequential binding model in Origin 5.0 software (Microcal, Inc) as shown **figure 2.12**. The binding isotherm of apt_J91 with PV-12 shows no saturation, which establishes that apt_J91P is specific to peptide GQ-14.

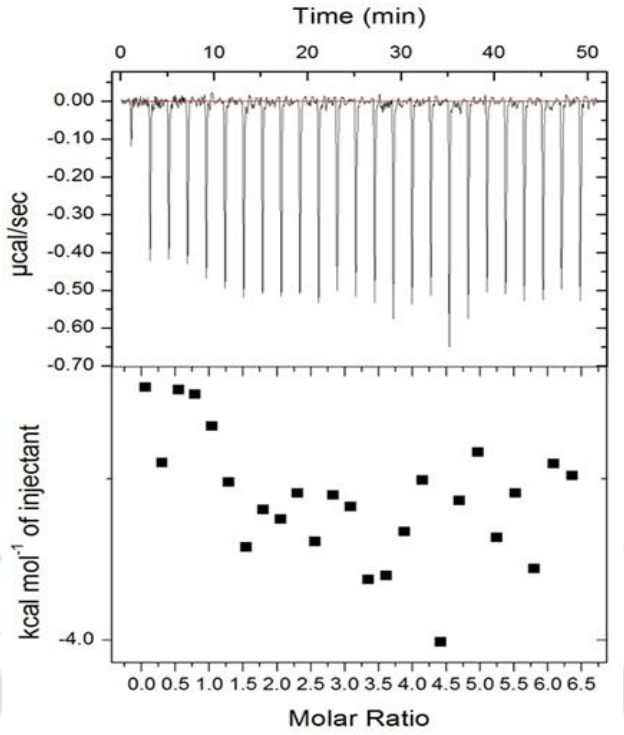

Figure 2.11 ITC isotherms for calorimetric titration between 30µM aptamer apt_J91P and 3000 µM peptide PV-12 at 25°C in 1x ABB.

The ITC binding experiments were also carried out to check the interaction of aptamer candidate apt_J91 without flanking region and apt_J94 with and without flanking region. These interaction did not yield any saturation during the titration in the isotherms, likely due to very low affinity. This also proves that the flanking regions (primer binding regions) of the aptamer sequence apt_J91P are strongly involved in the binding with the target peptide along with the random region.

2.3.9.2 Binding study through Circular Dichroism

The secondary structure of the aptamer candidate Apt_J91P with the flanking regions were studied before the interaction with target in 0.3x ABB buffer through CD spectrometry. The buffer concentration is reduced as use of 1x ABB buffer increases the HT voltage beyond 500 V in the CD experiments. The signature peaks of maxima near 280 nm and a minima near 245 nm as shown in the **figure 2.12** indicates the duplex B-form DNA of the aptamer sequence. The presence of maximum peak at ~277 nm and a minimum at ~245 nm are also associated with self-associative conformations of aptamer formed through Watson–Crick base pairing

such as stem-loop secondary structures (Serrano et al., 2019). The nature of the secondary structure inferred from CD study is in accordance with the predicted structure of apt_J91P by mfold.

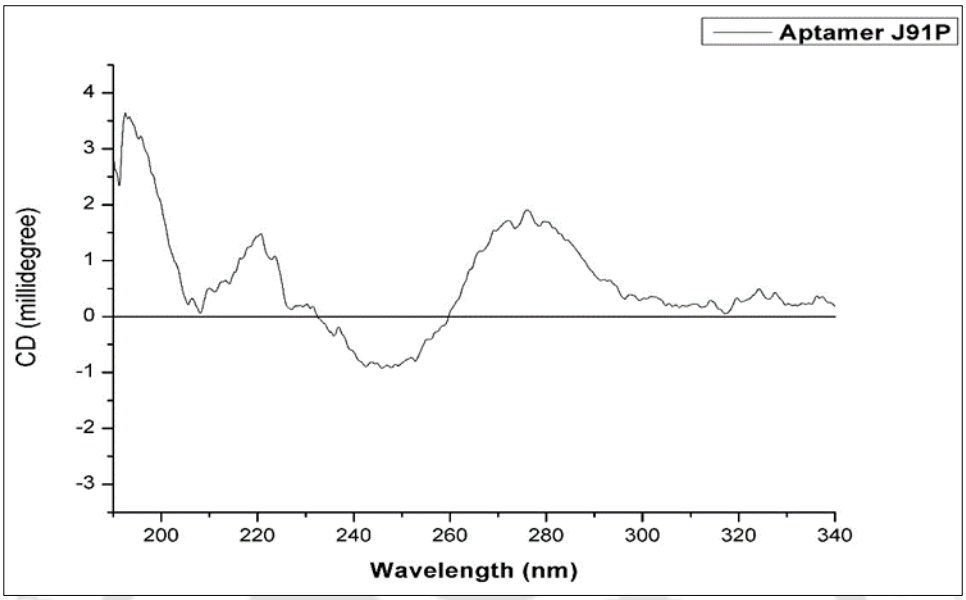

Figure 2.12 Circular dichroism spectra of aptamer apt_J91P in 0.3x ABB buffer

The CD spectra of interaction between apt_J91P and the target peptide GQ-14 in 0.3x ABB was recorded in the wavelength range of 190-340 nm. The CD spectra of the interaction was compared with the spectra of apt_J91P without the presence of target peptide in the **figure 2.13**. There was no change in ellipticity observed in the CD spectra of interaction when compared to the spectra of only aptamer indicating no structural reassembling of the aptamer. However, the binding of ligands to the aptamer molecule led to the change in magnitude of the ellipticity in CD spectra of interaction indicating binding (Prante et al., 2019).

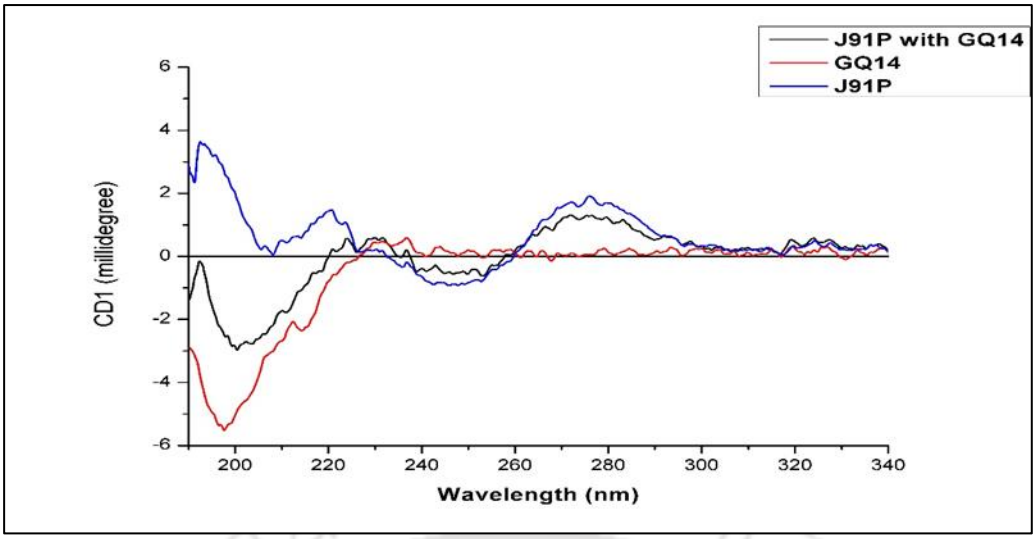

Figure 2.13 Binding study of the aptamer-peptide complex by circular dichroism scanned from 190nm to 340 nm where the plot with red, blue and black denotes the CD spectra of peptide GQ-14, aptamer apt_J91P and interaction between apt_J91P and peptide GQ-14

2.3.9.3 Direct Enzyme linked aptamer-sorbent assay (ELAA)

The binding of aptamer J91P to the standard target peptide GQ-14 in increasing concentration is measured by the intensities developed. As visualised from the **figure 2.14** absorbance is found to be increasing in very small scales with the increase in concentration of peptide. Blank sample contributing to detectable absorbance is probably due to unspecific binding, which is considerable as background noise. The limit of detection of the aptamer was calculated from linear regression curve (y=0.0004x+0.1058) using the equation LOD=3.3 x standard deviation of the regression line (σ) /Slope(S) is found to be 16.0875 µM. The quantitation limit (QL) expressed as (10Xstandrd deviation of low concentration/ slope of the calibration line) is found to be 48.75 µM

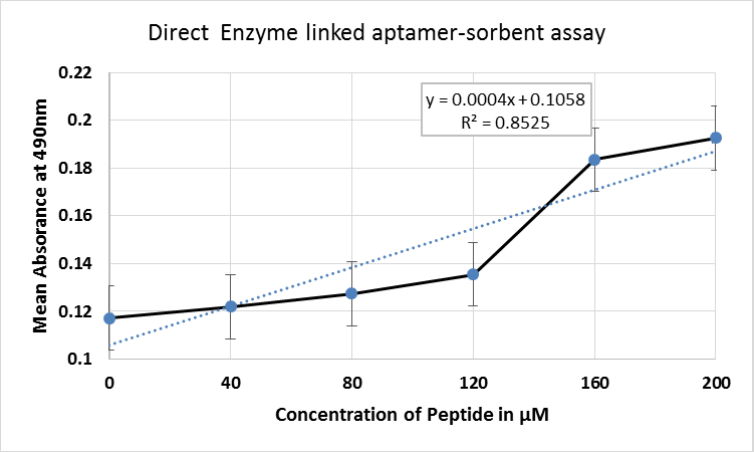

Figure 2.14 Analysis of the limit of detection of the aptamer by ELAA in the peptide concentration range of (40-200 µM).

2.4 Discussion:

The chapter addresses the objective of *in-vitro* selection of an aptamer candidate that would be able to detect the peptide sequence containing immunostimulatory epitope QGYYPTSPQ of celiac disease present in HMW-GS subunit of glutenin. For the selection of the aptamer candidate against this epitope, we have chosen a degenerated oligonucleotide library that contained 20 nucleotides long central portion which provides the required heterogeneity of oligonucleotide sequences in the order of 10^{12}. Along with the two primer binding regions the length of the whole oligonucleotide sequence is 56 nucleotides. Generally, the aptamer library with 40 nucleotides long random region is widely used in SELEX. However, for the selection of aptamers against a target molecule of comparatively small size, it is suggested to use library of shorter size as it reduces the size gap between the target and aptamer and increases the efficiency of SELEX by reducing the overcrowding of sequences (Ruscito, & DeRosa, 2016). Since the peptide target of our choice is significantly smaller than the other protein targets, we opted for the aptamer library of 56 nucleotides long. The choice of developing DNA aptamer over RNA due to the stability DNA offers, the lower cost and the reduction of a few processes such as *in-vitro* transcription and reverse transcription. The nature of the target is a factor that strongly influences the success of aptamer selection. Recent studies have established that the molecular weight of the target species is proportional to the binding affinity of the aptamer selected, therefore the high molecular weight targets have a lower value of dissociation constant (K_d) (McKeague & DeRosa, 2012). The target peptide selection was motivated by the necessity to detect the immunostimulatory motif QGYYPTSPQ. The addition of flanking

amino acids on either end of the QGYYPTSPQ in our target peptide was done to increase the molecular weight for a successful selection of aptamer with high affinity. The peptide fragment selected had a relatively hydrophilic nature with a grand average of hydropathicity index (GRAVY) of -1.857. GRAVY signifies the hydrophobicity of a peptide with average values of hydropathy calculated from the constituent amino acids of the peptide. A positive GRAVY values indicates the hydrophobic nature of the peptide while negative values indicate the hydrophilic (Chang & Yang, 2013). The peptide was also found to be dissolved in deionised water.

The aptamer candidates were selected against the target peptide GQ-14 through a 12 rounds conventional SELEX process where the peptide was immobilised on magnetic beads as solid support to aid in the partitioning of the strongly bound aptamer sequences. Negative SELEX were also carried out before the start of the first round of SELEX and after 5th round of SELEX in order the remove the aptamer sequences that binds with materials of magnetic beads and sequences only specific to the peptide immobilised was retained. Through SELEX followed by cloning and sequences, 15 numbers of potential aptamer sequences were obtained. Based on the *in-silico* studies, only two aptamers with the lowest Gibb's free energy change values which implies the highest structural stability in selection buffer among the 15 sequences were selected for further studies.

The binding characterization of the aptamer candidates through ITC reveals that aptamer apt_J91P with flanking regions had the affinity for GQ-14 peptide with a dissociation constant of 2.26 μM and 4.385 mM for the primary and secondary sites of binding of the aptamer respectively in the aptamer selection buffer. Specificity of the aptamer apt_J91P was also demonstrated through ITC when allowed to interact with a non-target peptide PV-12 which didn't form complex. The ITC revealed that interaction between apt_J91P and GQ-14 is driven by both favourable enthalpy and entropy which has also been observed in the case of studying binding characteristics of an aptamer candidate against small molecular targets amodiaquine, chloroquine and mefloquine by Slavkovic et al. They suspected that this was be due to slight hydrophobic nature of these molecules and possible formation of stacking interactions owing to the presence of an aromatic ring especially in amodiaquine, although other factors like molecular shape and hydration and solvation effects may as well contributed (Slavkovic et al., 2018). The presence of tyrosine containing an aromatic ring and the presence of few hydrophobic amino acid residues such as glycine and proline in the GQ-14 target peptide may explain the thermodynamic characteristics of binding between Apt_J91P and GQ-14. In case

of the 33mer gliadin peptide target, the aptamer developed by Amaya-González et al. showed a favourable entropy and unfavourable enthalpy of binding with target. This was likely due to the comparatively more hydrophobic nature of the target peptide (GRAVY -1.079) (Amaya-González et al., 2015). The ITC thermogram was best fitted to a two site binding model in our study between apt_J91P and GQ-14. One of the binding site was of high affinity while the other one is low. The aptamer with one high and another low affinity sites are not uncommon in the case of small molecular target, it was observed in an aptamer selected against cocaine (Slavkovic et al., 2018).

The ITC experiment involving apt_J91P and GQ in deionised water was carried out to check if the absence of the salts influence the binding affinity, which reveal successful binding while the affinity of the binding is lower than in the aptamer binding buffer. In an experiment, the affinity of aptamer evaluated by Slavkovic et al. reported that depending on the nature of the target molecule the affinity of binding between the aptamer and target may increase or decrease if the salt concentration of the buffer is reduced. The aptamer MN4 had reduced affinity for amodiaquine, chloroquine and mefloquine when NaCl and KCL were not added (Slavkovic et al., 2018).

The various type of folds in the secondary structure of aptamer determines characteristics of binding mechanism such as hydrophobicity, molecular shape complementarity or intercalation of small molecular targets in double-stranded regions of the aptamer involved during it's binding with the target molecule (Serrano et al., 2019). The Circular dichroism study was carried out to investigate the secondary structure formation of aptamer, peptide and during their interaction in 0.3x aptamer binding buffer. The concentration of buffer was reduced while recording CD spectra of aptamer as high (1x ABB) salt concentration increased the HT voltage beyond 500 V. The CD study revealed that the apt_J91P likely forms stem-loop shape in aptamer binding buffer. CD spectra of aptamers at maxima ~260 nm and 210 nm, minimum ~240 nm indicates the presence of aptamer forming G-quadruplex structures which offers more chemical and thermal stability than the aptamers with other secondary structure (Pearce et al., 2014). However, as inferred from CD spectra, G-quadruplex structures are absent in apt_91P. During the interaction of aptamer and target, the change in ellipticity in the CD spectra indicate conformational reshuffling of the aptamer upon binding with the target. For instance, a prominent increase in the amplitude of the maxima in CD spectra of B-form DNA indicates target induce structural change or induce fit type of binding of target with aptamer. However, in case of binding of the target to the native structure

of aptamer does not exhibit such changes (Sharma et al., 2017). In our study, during the interaction between apt_J91 and target GQ-14, a slight decrease in the amplitude of the minima and maxima was observed. A similar trend was also observed in case of interaction of aptamer VDBA14 with target 25-hydroxyvitamin D (Prante et al., 2019), interaction of aptamer R12.45 Trunc with it's target atrazine (Abraham et al., 2018) and interaction of aptamer H2 with histamine (Mairal et al., 2019). The binding of these aptamer with their respective target was confirmed by other biophysical characterization techniques.

2.5 Conclusion

In this chapter, we report the successful selection of aptamer candidate apt_J91 against toxic celiac disease epitopic peptide GQGQQGYYPTSPQQ present in the subunit of 1Bx13 and 1Dx5 of high molecular weight glutenin. The binding affinity in terms of the dissociation constant (K_d) of the aptamer candidate selected was found to be 2.26 µM for primary site of binding and 4.385 mM in the secondary site of binding for the target GQGQQGYYPTSPQQ in aptamer binding buffer. It has a binding affinity of 81.3 µM (K_d) while interacting in deionized water. The aptamer has been found to form a stem-loop secondary structure. The binding characterization reveals the binding is both enthalpically and entropically driven and local conformational change occurs in aptamer during binding. The limit of detection (LOD) evaluated through direct-ELAA was found to be 16.0875 µM.

2.6 References

1. Abraham, K. M., Roueinfar, M., Ponce, A. T., Lussier, M. E., Benson, D. B., & Hong, K. L. (2018). In vitro selection and characterization of a single-stranded DNA aptamer against the herbicide atrazine. Acs Omega, 3(10), 13576-13583.
2. Amaya-González, S., López-López, L., Miranda-Castro, R., de-los-Santos-Álvarez, N., Miranda-Ordieres, A. J., & Lobo-Castañón, M. J. (2015). Affinity of aptamers binding 33-mer gliadin peptide and gluten proteins: Influence of immobilization and labeling tags. Analytica Chimica Acta, 873, 63-70.
3. Bonilla, J. C., Ryan, V., Yazar, G., Kokini, J. L., & Bhunia, A. K. (2018). Conjugation of specifically developed antibodies for high-and low-molecular-weight glutenins with fluorescent quantum dots as a tool for their detection in wheat flour dough. Journal of agricultural and food chemistry, 66(16), 4259-4266.

4. Chang, K. Y., & Yang, J. R. (2013). Analysis and prediction of highly effective antiviral peptides based on random forests. PloS one, 8(8), e70166.
5. Dewar, D. H., Amato, M., Ellis, H. J., Pollock, E. L., Gonzalez-Cinca, N., Wieser, H., & Ciclitira, P. J. (2006). The toxicity of high molecular weight glutenin subunits of wheat to patients with coeliac disease. European journal of gastroenterology & hepatology, 18(5), 483-491.
6. Gasteiger, E., Hoogland, C., Gattiker, A., Duvaud, S. E., Wilkins, M. R., Appel, R. D., & Bairoch, A. (2005). Protein identification and analysis tools on the ExPASy server (pp. 571-607). Humana press.
7. Hansen, P. R., & Oddo, A. (2015). Fmoc solid-phase peptide synthesis. Peptide antibodies: Methods and protocols, 33-50.
8. Kuo, T. C., Lee, P. C., Tsai, C. W., & Chen, W. Y. (2013). Salt bridge exchange binding mechanism between streptavidin and its DNA aptamer–thermodynamics and spectroscopic evidences. Journal of Molecular Recognition, 26(3), 149-159.
9. Mairal Lerga, T., Jauset-Rubio, M., Skouridou, V., Bashammakh, A. S., El-Shahawi, M. S., Alyoubi, A. O., & O'Sullivan, C. K. (2019). High affinity aptamer for the detection of the biogenic amine histamine. Analytical chemistry, 91(11), 7104-7111.
10. McKeague, M., & DeRosa, M. C. (2012). Challenges and opportunities for small molecule aptamer development. Journal of nucleic acids, 2012
11. Mitea, C., Kooy-Winkelaar, Y., van Veelen, P., de Ru, A., Drijfhout, J. W., Koning, F., & Dekking, L. (2008). Fine specificity of monoclonal antibodies against celiac disease–inducing peptides in the gluteome. The American journal of clinical nutrition, 88(4), 1057-1066.
12. Ogasawara, D., Hasegawa, H., Kaneko, K., Sode, K., & Ikebukuro, K. (2007). Screening of DNA aptamer against mouse prion protein by competitive selection. Prion, 1(4), 248-254
13. Pearce, T. R., Waybrant, B., & Kokkoli, E. (2014). The role of spacers on the self-assembly of DNA aptamer-amphiphiles into micelles and nanotapes. Chemical Communications, 50(2), 210-212.
14. Prante, M., Schüling, T., Roth, B., Bremer, K., & Walter, J. (2019). Characterization of an Aptamer directed against 25-hydroxyvitamin D for the development of a competitive aptamer-based Assay. Biosensors, 9(4), 134.
15. Ruscito, A., & DeRosa, M. C. (2016). Small-molecule binding aptamers: Selection strategies, characterization, and applications. Frontiers in chemistry, 4, 14.

16. Serrano, C. M., Freeman, R., Godbe, J., Lewis, J. A., & Stupp, S. I. (2019). DNA-peptide amphiphile nanofibers enhance aptamer function. ACS applied bio materials, 2(7), 2955-2963.
17. Sharma, T. K., Bruno, J. G., & Dhiman, A. (2017). ABCs of DNA aptamer and related assay development. Biotechnology advances, 35(2), 275-301.
18. Slavkovic, S., Churcher, Z. R., & Johnson, P. E. (2018). Nanomolar binding affinity of quinine-based antimalarial compounds by the cocaine-binding aptamer. Bioorganic & Medicinal Chemistry, 26(20), 5427-5434.
19. Sreerama, N., & Woody, R. W. (2000). Estimation of protein secondary structure from circular dichroism spectra: comparison of CONTIN, SELCON, and CDSSTR methods with an expanded reference set. Analytical biochemistry, 287(2), 252-260.
20. Whitmore, L., & Wallace, B. A. (2004). DICHROWEB, an online server for protein secondary structure analyses from circular dichroism spectroscopic data. Nucleic acids research, 32(suppl_2), W668-W673.
21. Zhang, Y., Hu, M., Liu, Q., Sun, L., Chen, X., Lv, L., ... & Li, H. (2018). Deletion of high-molecular-weight glutenin subunits in wheat significantly reduced dough strength and bread-baking quality. BMC plant biology, 18(1), 1-12

Chapter 3

Selection and characterization of specific aptamers against toxic celiac disease epitopic peptide SQQQPPFSQQQQPV

Chapter 3: Selection and characterization of specific aptamers against toxic celiac disease epitopic peptide SQQQPPFSQQQQPV

Abstract

***Introduction**: This chapter describes the in-vitro selection and characterization of aptamer against a 14 mer peptide sequence of the low molecular weight glutenin subunit of wheat (Triticum aestivum), SQQQPPFSQQQQPV, which contains a celiac disease epitope PFSQQQQPV.*

***Methods**: A conventional SELEX method was carried out by immobilising the peptide SQQQPPFSQQQQPV on a magnetic beads to select DNA aptamer from 76 bp long aptamer library. The binding characteristics of interaction between selected aptamer and the target was studied by using Isothermal Titration Calorimetry (ITC) and Circular Dichroism (CD). The limit of detection (LOD) evaluated through direct-ELAA.*

***Results**: A DNA aptamer apt_M09P of length 76 bp was selected succesfully. The binding characterization by ITC reveals the dissociation constant of 17.6 μM and 8.33 mM for the primary and the secondary site of binding during the interaction of the aptamer and the target in aptamer binding buffer respectively. The LOD evaluated through direct-ELAA was found to be 20.00 μM.*

***Discussion**: The binding characterization through ITC reveals the binding is enthalpically favourable and entropically unfavourable. The CD study reveals that the binding leads to local conformational change in the aptamer.*

3.1. Introduction

The low molecular weight subunit (LMW-GS) of glutenin is encoded by the genes present at Glu-3 loci. It has a molecular weight of 30−80 kD and contains three three sub-units. The LMW-GS accounts for about 40% of the total gluten protein (Wang et al., 2023). The LMW-GS forms inter-molecular disulphide bonds with each other or with the HMW-GS to form a polymeric structure of glutenin. The amino acid sequences of LMW-GS are closely related to the gliadin subunit due the loci Glu-3 loci and Gli-1 (encodes gliadin) are associated genetically. Both LMW-GS and gliadin are responsible for providing volume to loaf in bread making processes; however, only the LMW-GS effects positively on the dough strength. However, the positive effect of the LMW-GS on the elasticity of dough is found to be milder than that of HMW-GS (Bonilla et al., 2018). The LMW-GS is a complex of highly polymorphic proteins which causes difficulties in separating to individual protein for characterization (D'Ovidio & Masci, 2004).

According to studies based on database comparison and identification of new epitopes, about 5% of the sequences in LMW-GS contain epitope of celiac disease (Woldemariam et al., 2022). Vader et al. identified the immunostimulatory peptide GLT-156 and GLT-17 with minimum core sequences PFSQQQQSPF and PFSQQQQQ respectively which are found to elicit the T-cell response in celiac disease patients (Vader et al., 2002). Bodd et al., also demonstrated that peptide fraction QQPPFSQQQQPVLPQ that contains epitope PFSQQQQPV can elicit T-cell response (Bodd et al., 2012). Many immunostimulatory peptides identified have been found to be present in both γ-Gliadin and LMW glutenin (Woldemariam et al., 2022).

Mitea et al. developed monoclonal antibodies against the immunostimulatory peptide, PPFSQQQQSPFS of LMW-GS, where the underlined sequence is the minimum core epitope of celiac disease. They immunised Balb/c mice with synthetic version of this peptide for development of the monoclonal antibodies. The developed anti-LMW-glt (1) monoclonal antibodies were found to be specific for the minimum amino acid sequence, PPFSQQ of the immunised peptide and were able to detect the several peptide fragments containing this 6 amino acid long sequence in pepsin/trypsin digest of wheat flour (Mitea et al., 2008). The Skerritt mAb, which was mainly developed against ω-gliadins that recognises epitope QQGYYP, was found to detect LMW-GS with high specificity along with other subunits of gluten such as HMW-GS and ω1/2-gliadins (Lexhaller et al., 2017). Bonilla et al. developed

an antibody against the peptide fraction PVLPQQPPFSQQ of LMW-GS which contains the epitopes of celiac disease (Bonilla et al., 2018).

Till now, for detection of the CD epitopes in the LMW-GS, mass spectroscopy have been extensively used and only a few antibodies have been developed against them to use in immunoassays or biosensors. Aptamers being an emerging alternative to the antibodies and less laborious and sophisticated than mass spectroscopic methods, we attempted to developed aptamer candidates against the celiac disease epitopic peptide SQQQPPFSQQQQPV of LMW-GS subunit of glutenin. This peptide contains the minimum amino acid sequence PFSQQQQPV that can stimulate T-cells in the celiac disease patients. We have carried out a conventional SELEX process by immobilising the target peptide in a magnetic bead based solid support.

3.2. Materials and Methods:

3.2.1 Chemicals and Reagents

α-Cyano-4-hydroxycinnamic acid (4-HCCA) MALDI-matrix was procured from Sigma-Aldrich Chemicals Pvt. Ltd., India. The degenerated single-stranded DNA (aptamer) library and the primers were procured from Integrated DNA Technologies (USA). Dynabeads MyOne carboxylic acid, SYBR Gold nucleic acid stain and InsTA clone PCR cloning kit were purchased from Invitrogen Thermo Scientific (USA). Streptavidin magnetic beads and Low molecular weight (LMW) DNA ladder were procured from New England Biolabs (USA). IPTG (Isopropyl β-Dthiogalactopyranoside) and X-Gal (5-bromo-4-chloro-3-indolyl-β-dgalactopyranopside) were purchased from Himedia (India). Peptide SV-14 was purchased from Biotechdesk, India. Miniprep plasmid isolation kit and, Sigma Readymix and agarose were procured from Sigma Aldrich (India). All other chemicals were analytical grade and cited wherever necessary.

3.2.2 Selection of the target peptide sequence

The peptides responsible for the celiac disease is selected from the amino acid sequence data of LMW-GS of wheat (*Triticum aestivum*) available in database. The amino acid sequences of the low molecular weight glutenin subunit with accession number B5ANT6 were retrieved

from Uniprot (https://www.uniprot.org/). The immunostimulatory peptide sequence PFSQQQQPV is reported as a DQ2.2 restricted epitope of celiac disease. The target peptide was selected considering the presence of repetitive and immunostimulatory peptide motif PFSQQQQPV, avoiding the negative net charge of the peptide to escape electrostatic repulsion with polyanionic oligonucleotides, higher pI value than the working pH of the experimental condition (i.e. pH 7-8) and possibility of generation of the peptide by enzymatic cleavage of glutenin. The physiochemical property of the selected peptide SQQQPPFSQQQQPV (SV-14) was determined by using online tool Protparam (https://web.expasy.org/protparam/) (Gasteiger et al., 2005). The selected peptide was synthesised by solid phase synthesis with >95% purity at Biotechdesk, India.

3.2.3 Characterisation of the synthesized peptides by mass spectroscopy

The purified and dried peptide was dissolved in deionised water. Since the selected peptide is devoid of Trp, Tyr or Cys, the concentration of the peptide were estimated through a nanodrop spectrophotometer using Scopes's method (Scopes, 1974). The synthesised peptide was characterised by matrix assisted laser desorption/ionization mass spectrometry (Autoflex Speed MALDI-TOF/TOF mass analyser, Bruker). The MALDI matrix was prepared by dissolving α-Cyano-4-hydroxycinnamic acid (HCCA) in a solution of 60:40(v/v) 0.3% trifluoroacetic acid (TFA) in water and acetonitrile at a concentration of 15 mg/ml. An equal volume of MALDI matrix and 20 µM of the synthesised peptide were mixed and 2 µl of the mixture was spotted on the MALDI steel sample plate and allowed to dry for 1 h. The samples were ionized with 500 laser shots (a nitrogen laser of 337 nm) operated in a linear positive ion mode. The mass spectrum were analysed using the in-built Flex control analysis software.

3.2.4 Secondary structure analysis by circular dichroism spectroscopy

The CD spectroscopy was used for secondary structural analysis of the peptide SV-14. For secondary structure analysis, 20 µM SV-14 peptide in deionised water was used to record the CD spectra in a Jasco J-1500 spectropolarimeter in a 1 mm path length quartz-cuvette using 1 nm bandwidth. The spectrum was recorded in the far-UV wavelength of 190-250 nm at a scan-rate of 100 nm/min, wavelength interval of 0.5 nm, integration time (time constant) of 2 s and an average of 4 scans at 25 ℃ maintaining PMT voltage (HT voltage) <500 V. The baseline

was corrected by subtracting the spectrum of the water. The spectra were smoothed using the Savitzky-Golay algorithm (Savitzky & Golay, 1964). For analysis of the CD spectra of the peptide through algorithm CONTINLL, CDSSTR SELCON3 and K2D offered by online softwares Dichrowave (http://dichroweb.cryst.bbk.ac.uk/html/home.shtml) was used (Whitmore & Wallace, 2004).

3.2.5 Design of Aptamer library and PCR condition

A 76 nucleotides long degenerate oligo-deoxynucleotide library, 5′ATACCAGTCTATTCAATT–N40–AGATAGTATGTGCAATCA3′ that contained 40 random nucleotides and flanked by 18 nucleotides long invariant primer annealing sites at both the 5′ and 3′ ends. The primer sequences used for this aptamer library were designed by our group in a previous study. The optimised PCR conditions used are listed in **table 3.1** (Sett et al., 2017). The aptamer library and the three different primers used for PCR amplification, unmodified forward primer, F1: 5′-ATACCAGTCTATTCAATT-3′, 5′ Biotin conjugated reverse primer, R2: Biotin-5′-TGATTGCACATACTATCT-3′, Unmodified reverse primer, R1: 5′-TGATTGCACATACTATCT-3′ were purchased from purchased from IDT Technologies (USA). The aptamer library was synthesised at 1 μM synthesis scale and PAGE purified while the labelled and unlabelled primers were synthesized at 100 nM synthesis scale. The aptamer library and the primers were reconstituted in Tris-EDTA buffer, pH 7.5.

Table 3.1 Optimised conditions of PCR for amplifying N40 aptamer library

PCR Cycle		Temperature	Time
Initial Denaturation		94 °C	6 min
Denaturation	14 Cycles	94 °C	30 s
Annealing		45 °C	30 s
Extension		72 °C	60 s
Final Extension		72 °C	7 min

3.2.6 Immobilization of peptide sequence on magnetic beads

The SQQQPPFSQQQQPV peptide was immobilised on magnetic beads (Dynabeads® MyOne Carboxylic Acid with the binding capacity of 1800 pmol peptide per mg, Invitrogen) as per the manufacture's instruction. The immobilization of peptide on the dynabeads works on the principle of carbodiimide chemistry, where the presence of a carbodiimide leads to formation of an amide bond between the carboxylic acid functional group of the magnetic bead and the primary amine of the peptide. The exact molecular mass of the Dynabeads are not provided by the manufacturer. However, the MALDI of the dynabeads shows a polymeric mass profile ranging from 568 Da to 2018 Da while using matrix α-Cyano-4-hydroxycinnamic acid (HCCA). Briefly, for immobilization, 3 mg (300 µl) dynabeads were first washed with 300 µL 0.01 M NaOH. Then it was activated by mixing with a cold 200 µl solution of 0.4 M 1-ethyl-3-(3-dimethylaminopropyl) carbodiimide hydrochloride (EDC) by vortexing and followed by incubation for 30 min at room temperature with slow tilt rotation. The activated dynabeads are washed once with 300 µl deionised water followed by another washing with 25 mM 2-[N-morpholino] ethane sulfonic acid (MES) buffer, pH 6. Then they are mixed with an excess amount (>5400pmol) peptide (based on the binding capacity of the dynabeads) in 25 mM MES buffer and incubated for 2 h in 4 °C with slow tilt rotation. The coated dynabeads were washed by incubating in 50 mM Tris, pH 7.4 for 15 min to remove excess peptides and quench unreacted carboxyl groups, followed by washing once with aptamer binding buffer (ABB: 50 mM Tris-HCL, pH 7.5, 250 mM NaCl, 5 mM MgCl2). The immobilization of the dynabeads with the SV-14 peptide was confirmed by mass spectrometry analysis using a MALDI-TOF mass analyser.

3.2.7 *In-vitro* selection of Aptamers against peptide SQQQPPFSQQQQPV of LMW glutenin

2000 pmole of ssDNA aptamer library was activated in 500 µl of aptamer binding buffer by heating at 95 °C for 10 min, quickly cooled on ice for 10 min for favouring the secondary structure formation of ssDNA and then allowed to stand at room temperature for 10 min. The ssDNA aptamer library was used as an initial pool for SELEX process. It was added to 55 µl of peptide immobilised dynabeads (0.55 mg beads = 1000 pmole of peptide) and incubated at room temperature for 2 h with mixing by tilt rotation in a rotary mixture. After incubation, the beads were washed with 1x aptamer washing buffer (Aptamer binding buffer + 0.01% Tween

20) to remove unbound and weakly bound DNA. Binding conditions for the first four round were made relaxed to allow binding of aptamer candidates ranging from weak to strong affinity of binding. The aptamer candidates bounded to the peptide immobilised magnetic beads were eluted by heating at 95°C for 8 min in 75 µl nuclease free water (Sigma). The eluted ssDNA was PCR amplified using F1 primer (unmodified forward primer) and R2 primer (biotinylated reverse primer). The concentration of the dsDNA was measured using UV nano-spectrophotometer.

The PCR amplified biotinylated double stranded aptamer pool was separated into single strand using streptavidin magnetic bead (New England Biolabs). 80 µl of streptavidin magnetic beads were activated by washing three times in streptavidin magnetic bead washing buffer (0.5 M NaCl, 20 mM Tris-Hcl pH 7.5, and 1 mM EDTA). The PCR amplified aptamer pools were added to the activated streptavidin magnetic beads and allowed to react by incubating for 1 h with gentle stirring in room temperature. After incubation, the beads were washed three times with 1x ABB and finally re-suspended in 100 µl sigma water. The strands were separated by alkaline denaturation by adding 10 µl of 0.1 M NaOH and incubating for 5 min. The immobilised complementary biotinylated strands were then removed by applying an external magnet and the non-biotinylated strands were eluted. The eluted solution is neutralised by adding 5 µl of 0.2 M HCl. This eluted solution containing ssDNA serves as the new enriched aptamers pool for next SELEX rounds.

In the subsequent round, the bound aptamers from the previous round were used as the aptamer pool and the process was repeated for 18 iterative rounds. The stringency of the SELEX process were increased from 4th round as shown in the **table no. 3.2**. Enrichment of the aptamer pools after each round were checked by running the PCR amplified aptamers in a 15 % native PAGE gel.

Two Negative SELEX rounds were performed before the starting of the 1st SELEX round and after the 6th SELEX round to remove the aptamer pool binding specifically to the materials of dynabead. The ssDNA aptamer pool in 500 µl ABB after activation by heating at 95 °C for 10 min, quickly cooled on ice for 10 min and allowed to stand at room temperature for 10 min was incubated with the 0.55 mg of bare dynabeads (without immobilization of the peptide) for 30 min. After incubation, the supernatant was collected and used as aptamer pool for the next SELEX round.

Table 3.2 Details of SELEX rounds with increasing stringency

SELEX Round	Beads(mg)/Peptide(pmole)	Binding time	Washing steps + Volume
NS	0.55 mg + 0	30 min	
1st	0.55 mg + 1000 pmole	120 min	1 x 500µl
2nd	0.55 mg + 1000 pmole	120 min	1 x 500µl
3rd	0.55 mg + 1000 pmole	120min	1 x 500µl
4th	0.55 mg + 1000 pmole	120 min	2 x 500µl
5th	0.55 mg + 1000 pmole	120 min	3 x 500µl
6th	0.55 mg + 1000 pmole	120 min	3 x 500µl
NS	0.55 mg + 0	30 min	
7th	0.55 mg + 1000 pmole	90 min	3 x 500µl
8th	0.50 mg + 900 pmole	90 min	3 x 500µl
9th	0.50 mg + 900 pmole	60 min	3 x 500µl
10th	0.50 mg + 900 pmole	45 min	3 x 500µl
11th	0.50 mg + 900 pmol	45 min	3 x 500 µl
12th	0. 45 mg + 810 pmol	45 min	3 x 500 µl
13th	0. 45 mg + 810 pmol	30min	3 x 500 µl
14th	0. 40 mg + 810 pmol	30min	4 x 500 µl
15th	0. 35 mg + 630 pmol	30min	4 x 500 µl
16th	0. 35 mg + 630 pmol	20min	4 x 500 µl
18th	0. 20 mg + 3600 pmol	20min	4 x 500 µl

NS- Negative SELEX

3.2.8 Cloning and sequencing of the Aptamer sequences

The aptamer candidates from the 16th SELEX round were PCR amplified by using F1 (unmodified forward) and R1 (unmodified reverse) primers. The PCR products were purified by the electroelution technique. 100 µl of the PCR products were run in a 15% native PAGE gel. The band of aptamer candidate corresponding to 76 bp was excised and put inside a dialysis tubing (3KDa cut-off) containing 300 µl 0.1xTAE buffer. The dialysis tubing with both ends tightly clipped was place in the horizontal electrophoresis tank filled with 0.1x TAE running

buffer and a power 80 V was applied. After running for 30-40 min under 80 V and polarity of the electrophoresis tank was reversed and run further for 5 min. The aptamers eluted to the 0.1xTAE solution inside the dialysis tubing were collected, precipitated using 3M sodium acetate and 100% ethanol and reconstituted in 10µl TE buffer.

The purified dsDNA aptamer candidates were cloned by using a PCR TA cloning kit (InsTA Clone PCR Cloning Kit, Thermo Scientific). The dsDNA aptamer candidates were ligated into a specialised TA cloning vector pTZ57R/T by mixing the components of the reaction mixture mentioned in the **table 3.3** and incubating it for 16 hours at 4°C as per manufacturer's instructions. The amount of insert (in ng) used in the ligation reaction was calculated by the standard formula,

Amount of Insert (ng) = {Amount of vector (ng) x size of insert (kb)/Size of vector (kb)} x molar ratio of Insert: vector.

Table 3.3 Components and amounts of Ligation reaction mixture

Reaction components	**Volume**
10X Ligation buffer	1.0 µl
Vector pTZ57R/T (50ng)	1.0 µl (55 ng)
Purified Aptamer pool	added in ratio 3:1 (insert/vector ratio)
T4 DNA ligase (3 units/µl)	1.0 µl
Nuclease free water	Volume made to 10 µl
Total Volume	10 µl

The ligated vector pTZ57R/T was transformed into chemically competent *E.Coli* DH5α host cells and grown in LB (Luria Bertani) agar plates containing ampicillin, X-gal and IPTG. The positively transformed colonies were screened on the basis of the blue white selection.

About 80 positively transformed white colonies were picked up randomly and grown overnight in LB broth. The plasmids were isolated from overnight grown cultures by a miniprep plasmid isolation kit (Sigma Aldrich, Germany). The isolated plasmids were checked in a 0.8% agarose gel. The presence of aptamer insert in plasmid was confirmed by PCR amplification using the unmodified forward and reverse primers. The positive plasmids were sequenced by Sanger sequencing method using the M13 forward and reverse primers and the sequencing process was outsourced to AgriGenome Labs Pvt. Ltd., India. Multiple sequence alignment

through Clustal Omega (https://www.ebi.ac.uk/Tools/msa/clustalo/) was carried out to find any homology between the sequences.

3.2.9 *Insilico* analysis of aptamer sequences

The aptamer sequences obtained from sanger sequencing were preliminary analysed for the free energy comparison and the structural stability using mfold web server (http://unafold.rna.albany.edu/?q=mfold) to find out the most potent aptamer candidate against the peptide target (Zuker M, 2003). The Gibbs free energy (ΔG) and secondary structure for the aptamer sequences were predicted by setting the ionic condition used in aptamer binding buffer of 250 mM NaCl and 5 mM $MgCl_2$ and temperature at 25 ºC. The secondary structures of the aptamer sequences were predicted by a free energy minimization algorithm in the mfold software.

3.2.10 Binding characterization of the aptamer with target peptide

3.2.10.1 Isothermal Titration Calorimetry (ITC) studies

Isothermal titration calorimetry was carried out to study the binding affinity between aptamer candidates and the target peptide. The truncated aptamer candidates Apt_M09 and Apt_J51 (both without flanking regions) and their respective whole sequences with flanking regions viz. Apt_M09P and Apt_J51P were studies for their affinity towards target SV-14 peptide. The experiments were performed in 25 °C using a MicroCal iTC200 (GE Healthcare, UK). 200 µl of aptamer was loaded into the calorimetric cell. Typically, 25 serial injections (1.5 µl/injection) of the peptide from the syringe were injected at spacing of 120 s with the continuous stirring of the solution in the calorimetric cell at 200 rpm. To compensate the heat of dilution, a control experiment was carried out without aptamer in the syringe (with 1x ABB). To attain the saturation in binding between, different concentrations of aptamer (10-40 µM) and peptide (1000-3000 µM) was tried for optimization. The aptamer and the peptide interaction was allowed to carry out in the aptamer binding buffer which was used in SELEX. The aptamer were also analysed for their specificity by studying binding characteristics between aptamer candidate and an unrelated peptide GQ-14 (GQGQQGYYPTSPQQ).

3.2.10.2 Circular dichroism studies

CD spectroscopy was used for structural analysis of the aptamer apt_M09J. 4µM of aptamer apt_M09 in 0.3x ABB was activated by heating at 95 ℃ for 10 min, followed by cooling in ice for 10 mins and then incubating at room temperature for 10 min. The spectrum was recorded in the wavelength range of 190-340 nm at a scan-rate of 100 nm/min, wavelength interval of 0.5 nm, integration time (time constant) of 2 s and an average of 4 scans at 25℃ maintaining PMT voltage (HT voltage) <500 V in a Jasco J-1500 spectropolarimeter with 1 mm path length quartz-cuvette using 1 nm bandwidth. The baseline was corrected by subtracting the spectrum of the buffer. The spectra were smoothed using the Savitzky-Golay algorithm (Savitzky & Golay, 1964).

For studying interaction between the aptamer and the peptide, the aptamer was activated as mention above. The activated aptamer was added to the peptide and the interaction was allowed to occur in 0.3x ABB by incubating in room temperature for 1h 30 min at rotospin. For acquisition of the CD spectrum in a Jasco J-1500 spectropolarimeter, the parameters used and baseline correction and smoothening performed are similar as mentioned above.

3.2.10.3 Direct Enzyme linked aptamer-sorbent assay (ELAA)

The direct Enzyme linked aptamer-sorbent assay was carried out to determine the affinity of Apt_M09P to the target peptide SV-14. The peptide immobilised dynabeads were taken in five Eppendorf tube in an initial increasing concentration of 40-200 µM. A control was taken without immobilising the peptide on dynabeads. The experiment was carried out in duplicates. Aptamer Apt_J91P biotinylated at the 5’ end (5'-Biotin-ATACCAGTCTATTCAATTCCCACACGTCTTATTATTAATGGGTATCCGTACACCG GGGAGATAGTATGTGCAATCA-3') at concentration of 0.5 µM was added to each tube. The reaction was carried out in 200 µL of 1x aptamer binding buffer (50mM Tris-HCl, 0.25 M NaCl, 5mM MgCl2, pH 7.4) and incubated for 1 h in rotation at room temperature. The unbound aptamers were washed away with 1x aptamer washing buffer (Aptamer binding buffer + 0.01% Tween 20). 200 µL Streptavidin-HRP conjugate (1:1000 dilution from 1mg/ml) as detection probe was added to each tube and incubated for 1 h with tilt rotation at room temperature, followed washing with 1x aptamer washing buffer. 50 µL of 3,3′,5,5′-Tetramethylbenzidine/H_2O_2 solution (Sigma, USA) was added. After 15 min of incubation in dark, 50 µL stop solution of 1M H_2SO_4 was added. The supernatant was separated from

magnetic beads and transferred to a microtiter plate for measurement of intensity at 490 nm in microplate reader (Tecan, Switzerland).

3.3 Results

3.3.1 Selection of the target peptide sequence

Considering the presence of repetitive and immunostimulatory peptide motif PFSQQQQPV, avoiding the negative net charge of the peptide to escape electrostatic repulsion with negatively charged oligonucleotides and higher pI value than the working pH of the experimental condition of SELEX; SQQQPPFSQQQQPV, a 14 amino acid long peptide sequence from the protein sequence of LMW-GS subunit selected for development of aptamer candidate against it. This peptide SQQQPPFSQQQQPV is also reported to be generated in the enzymatic hydrolysis of whole gluten when treated with a cocktail of enzymes containing pepsin, trypsin, chymotrypsin, elastase and carboxypeptidase (Dørum et al., 2010). The selected peptide sequence is highlighted in red with underlining the immunostimulatory motif of celiac disease in the protein sequence below.

>tr|B5ANT6|B5ANT6_WHEAT LMW-glutenin OS=Triticum aestivum PE=2

MKTFLVFALLAVAATSAIAQMETRCIPGLERPWQQQPLPPQQTFPQQPPFSQQQQQPFPQQPPFSQQQ
PPFSQQQQPVLPQQPSFSQQQLPPFSQQQPPFSQQQQPVLPQQPPFSQQQPVLPPQQSPFPQQQQHQ
QLVQQQIPVVQPSILQQLNPCKLFLQQQCSPVAMPQRLARSQMLQQSSCHVMQQQCCQQLPQIPQQS
RYEAIRAIIYSIILQEQQQVQGSIQSQQQQPQQLGQCVSQPQQQSQQQLGQQPQQQQLAQGTFLQPHQ
IAQLEVMTSIALRILPTMCSVNVPLYRTTTSVPFDVGTGVGAY

The physiochemical properties of the selected peptide sequence is determined by Protoparam (https://web.expasy.org/protparam/) and listed below in **the table 3.4**.

Table 3.4 Physiochemical property of the target peptide sequence SQQQPPFSQQQQPV (SV-14) of LMW-GS

Physiochemical properties	
Molecular weight	1626.75 g/mol
Extinction coefficient	0 $M^{-1}cm^{-1}$
Iso-electric point (pI)	pH 5.24
Net charge at pH 7	0
Grand average of hydropathicity (GRAVY)	-1.707

3.3.2 Characterisation of the synthesized peptides by mass spectroscopy

The MALDI-TOF mass spectroscopy was used to obtain the characteristic molecular weight (1626.75 g/mol) of the synthesised peptide. The matrix assisted laser desorption/ionization technique involves the hitting of the uniformly mixed analyte with energy-absorbent matrix compound with UV ray of wavelength 337 nm (nitrogen laser light) which leads to generation of singly protonated ions of the analyte. The ions are separated on the basis of their mass-to-charge ratio (m/z) under a fixed potential in the time-of-flight analyser and the characteristic mass spectra (m/z) of the all the constituent compounds of the analyte is obtained. The **figure 3.1** shows the characteristic mass spectrum of the purified peptide SV-14. The dominant monoisotopic mass obtained are found to be the mass of the peptide SV-14 along with different adducts. The m/z peaks of 1649.62 Da, 1665.69 Da, 1668.71 and 1687.70 Da corresponds to the mass of the peptide with Sodium ($[M+Na]^+$), Potassium ($[M+K]^+$), Acetonitrile ($[M+ACN+H]^+$) and Isopropanol ($[M+IsoProp+H]^+$) as adducts respectively.

A

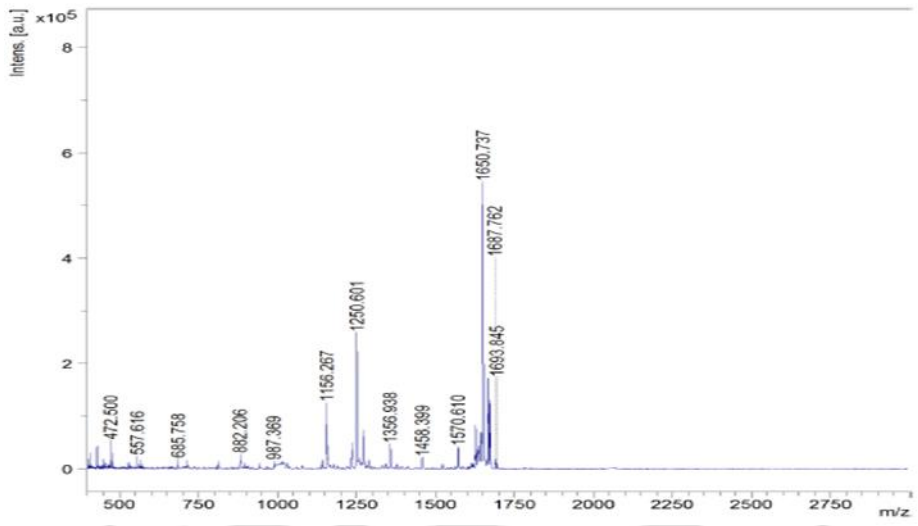

B

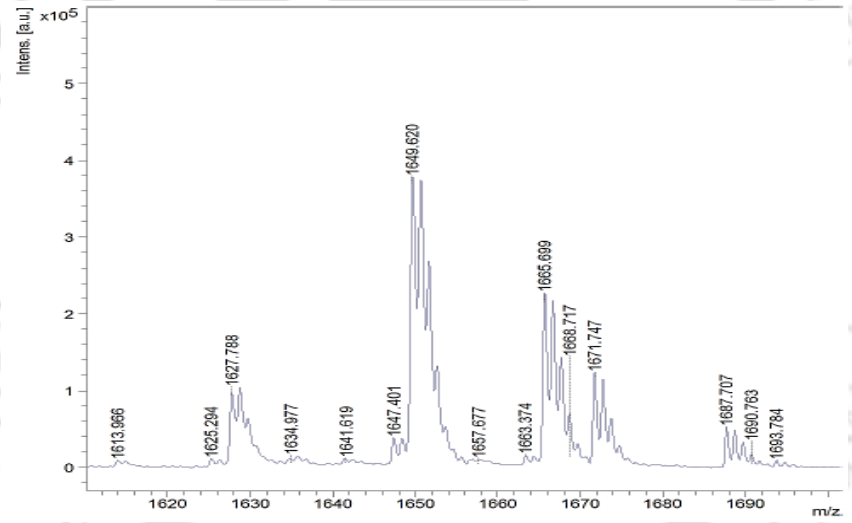

Figure 3.1 The MALDI-TOF mass spectra of the purified peptide SV-14 obtained in **(A)** the mass range 100-3000 Da with dominant peaks of 1650.73 Da ([M+Na]+) and 1687.76 Da ([M+IsoProp+H, **(B)** the zoomed mass range 1600-1700 Da exhibiting the monoisotopic peaks of 1649.62 Da ([M+Na]+), 1665.69 Da ([M+K]+), 1668.71 ([M+ACN+H]$^{+}$) and 1687.70 Da ([M+IsoProp+H]+), where M denotes the parent mass of 1626.75 Da

3.3.3 Secondary structure analysis by circular dichroism spectroscopy

The circular dichroism (CD) spectra of the peptides SV-14 in buffer 0.3x ABB was recorded in far-UV wavelength of 190-250 nm at 25 °C. The peptide shows a characteristics strong

minima near between 196 nm 200 nm confirming the random coil secondary structure shown in the **Figure 3.2**. The CD spectra were analysed by using the online analysis tool Dichrowave which performs quantitative estimation of the secondary structure using methods CONTINLL, SELCON3, CDSSTR, VARSLC and K2D. These methods compare the experimental CD spectral data with reference database of a protein whose secondary structure is known from X-ray crystallography and calculate fraction of each type secondary structure contributing to the net experimental CD spectral data (Whitmore &. Wallace, 2004). Out of all the methods used, the CONTINLL with use of reference set SP175 exhibits the lowest normalized root mean square deviation (NRMSD) value which indicates the goodness-of-fit of experimental data with the reference data and it is listed in the **table no 3.5.** The secondary structure of peptide SV14 is estimated to be around 39% random structure (unordered).

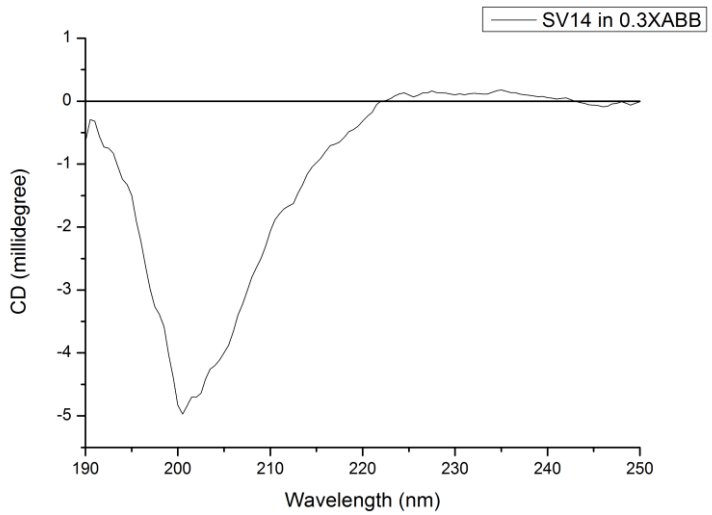

Figure 3.2 Circular dichroism spectra of peptide SV-14 recorded in the Far-UV wavelength 190-250 nm at 25 °C

Table 3.5 Estimation of secondary structure distribution of peptide SV-14 by Dichroweb

Secondary structure predicted by Dichroweb								
Peptide	Algorthim	Helix1	Helix2	Strand1	Strand2	Turns	Unordered	NRMSD
SV-14	Contin-LL	0.000	0.063	0.275	0.141	0.123	**0.388**	0.9

3.3.4 Design of Aptamer library and PCR optimization

The aptamer library of length 76 nucleotide containing a 20 nucleotide long central random region flanked by two primer binding regions was dissolved in Tris-EDTA buffer, pH 7.5. The amplification of the library is crucial for SELEX. The melting temperature of the aptamer library is 69.1 °C which makes it feasible for denaturation during PCR. The PCR condition to amplify the aptamer library was optimised as mentioned in the **table 3.3**.

3.3.5 Immobilization of peptide sequence on magnetic beads

Immobilization of the peptide SV-14 with dynabead was successful which was confirmed by MALDI-TOF analysis of the peptide immobilised beads. The MALDI mass spectra were acquired in linear negative ion mode. The characteristic mass of the peptide with addition of adducts 1650.40 Da ($[M+Na]^+$) is observed in mass spectra as shown in the **figure 3.3**.

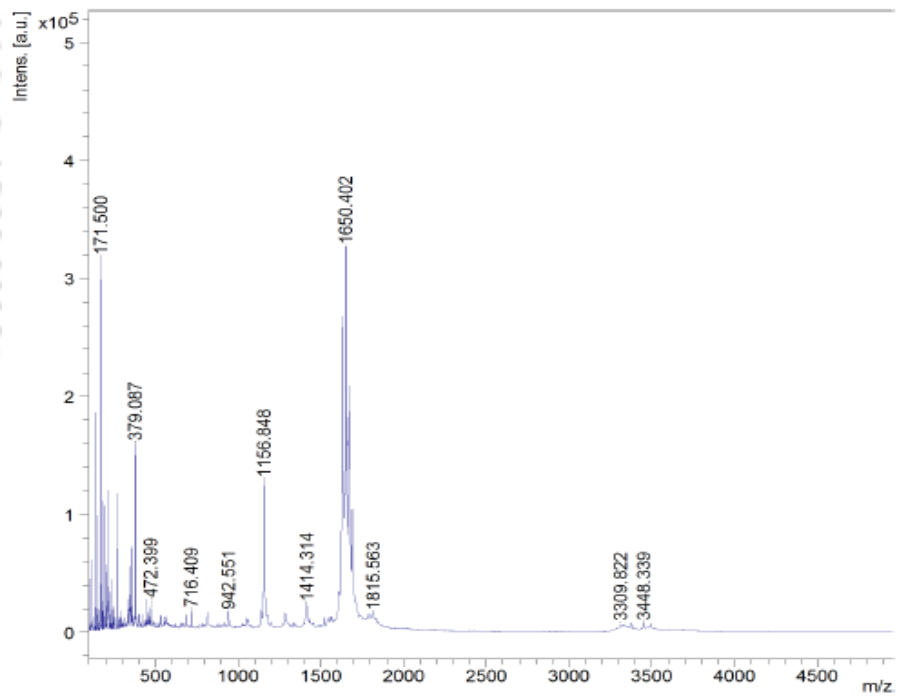

Figure 3.3 MALDI-TOF spectra of dynabead immobilised with peptide SQ-14 in linear positive ion mode where dominant monoisotopic mass of 1650.40 Da ([M+Na]+) is observed, where M denotes the parent mass of 1626.75 Da

3.3.6 *In-vitro* selection of Aptamers against peptide GQGQQGYYPTSPQQ of HMW glutenin

The SELEX rounds were carried for 18 cycles with two negative SELEX round at the beginning and after the 6th round. The initial pool of the aptamer library should theoretically contain 10^{24} distinct aptamer sequences and the incubation of the library with the target peptide in iteration in SELEX process should select the aptamer sequence with high affinity for the target. The stringency of the SELEX process were increased in each round after 4th round and continued till 18th round. The enrichment of the aptamer candidate after each rounds was monitored in a 15% native PAGE as shown in the **Figure 3.4**. The enrichment of the aptamer candidates were observed till 16th round, while high stringency in 18th round did not enriched the aptamer candidates. The SELEX was successfully carried out till 16th round and the enriched sequences after this round were retrieved, cloned and sequenced.

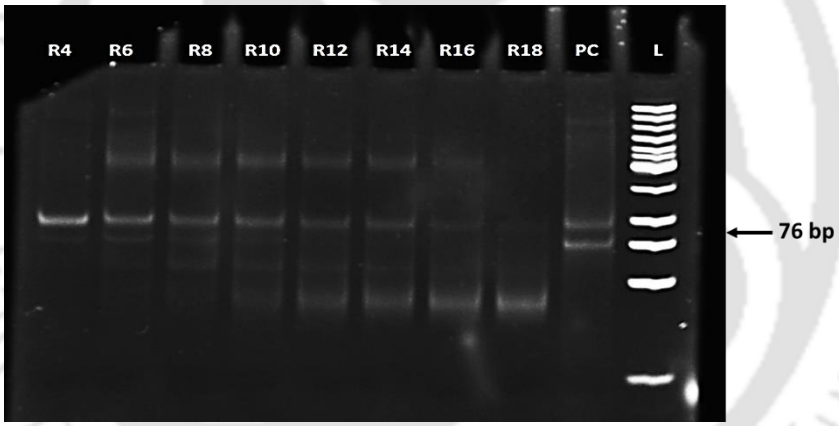

Figure 3.4 15% native PAGE gel for 76 bp enriched N40 aptamer pool after SELEX rounds against peptide target SV-14 from round 4th to 18th (R4-R18). The PC is positive control by taking 76 bp aptamer library as template and L is small molecular DNA ladder (NEB, 25-766 bp)

3.3.7 Cloning and sequencing of the Aptamer sequences

Around 80 positively transformed colonies were selected based on the blue-white screening after growth of the cloned *E.Coli* DH5α cells in LB-ampicillin plates. The plasmid were isolated successfully from the positive transformed cell and insertion of the aptamer sequences in the plasmid vector was analysed by PCR amplification using the primer sequences,

unmodified forward primer (5′-ATACCAGTCTATTCAATT-3′) and unmodified reverse primer (5′-TGATTGCACATACTATCT-3′). A total of 25 plasmids with positive insertion of aptamer sequence were sequenced by Sanger method. Out of 20 sequence received, only 10 sequences were found be correctly inserted with aptamer sequences which are listed in the **table 3.6**. The multiple sequence alignment did not shown any homology or any consensus motif between the sequences as each sequence contain a unique primary structure.

Table 3.6 Sequences of aptamer candidates of 76 bp containing 40 nucleotide random region with flanking primer regions selected against SV-14

Sl. No.	Name of Aptamer	Sequence
1	J47P	ATACCAGTCTATTCAATT**CAAACGGAGATGATGAGTATTTCACTTTTGATA GTATGGG**AGATAGTATGTGCAATCA
2	J48P	ATACCAGTCTATTCAATT**CCCTACGCACTAATAAGTAATCCAAATGCTCTCT TATCCG**AGATAGTATGTGCAATCA
3	J51P	ATACCAGTCTATTCAATT**CATGCGAGGTGGAATGAGCGGATTATCTATAAT GTCGTCT**AGATAGTATGTGCAATCA
4	M09P	ATACCAGTCTATTCAATT**CCCACACGTCTTATTATTAATGGGTATCCGTACAC CGGGG**AGATAGTATGTGCAATCA
5	M06P	TGATTGCACATACTATCT**TACAGGAGGGTATATGAGTTGGTAATTGAATAG ACGGGTT**AATTGAATAGACTGGTAT
6	M13P	ATACCAGTCTATTCAATT**CACACACGTCTTATTATTCCCGGGTATCCGTTATC CGGGG**AGATAGTATGTGCAATCA
7	M19P	TGATTGCACATACTATCT**TACAGGAGGGTATATGAGTTGGTAATTGAATAG ACGGGT**AATTGAATAGACTGGTAT
8	M20P	ATACCAGTCTATTCAATT**CACACACCGTTTATTATTAATGGGTATCCCTTCAC CGATG**AGATAGTATGTGCAATCA
9	M21P	ATACCAGTCTATTCAATT**CGTCTTATTATGCTTACTAATGGGTATGCGTACAC CGGGG**AGATAGTATGTGCAATCA
10	M22	ATACCAGTCTATTCAATT**CAGGTGCAGGGGAGTACTGTTTCACTATATATTA TGGCAG**AGATAGTATGTGCAATCA

3.3.8 *Insilico* analysis of aptamer sequences

The 10 aptamer sequences obtained from Sanger sequencing were preliminary analysed for free energy comparison and structural stability using mfold web server. The thermodynamic

parameters like change in enthalpy (ΔH), change in entropy (ΔS) and change in Gibb's free energy (ΔG) were determined for each of the 10 aptamer candidate sequences. The lowest value of change in Gibb's free energy (ΔG) indicates the most stable structure formation. The sequences with lowest Gibb's free energy (ΔG) are listed in the **table 3.7** and they are consider for further analysis. Although the aptamer candidates with and without the primer sequences have different values of Gibb's free energy (ΔG), they can be arrange in same order when lowest to highest values are considered. The secondary structure of the selected aptamer candidates were predicted by mfold web server which generated more than one secondary structure for each sequence with different values of Gibb's free energy (ΔG). The structure of the aptamer sequences predicted with lowest Gibb's free energy (ΔG) are shown in the **figure 3.5**. The secondary structure of the aptamer sequences is predicted by a free energy minimization algorithm in mfold software. At minimum Gibbs free energy, the thermodynamically stable secondary structure formed by truncated aptamers Apt_M09 takes two stem-loop structure, one with another extended stem-loop. With flanking regions aptamer Apt_M09J exhibits three stem-loops. The truncated Apt_J51 is predicted to take two stem-loop shape with extended loop in one and another extended loop in the other. Aptamer Apt_J51J with flanking region contains two stem-loops with a small bulge in each of the stem-loop.

Table 3.7 Thermodynamic parameters of the aptamer sequences as calculated by mfold software

Name	**Sequence (Random region)**	**Gibb's free energy (ΔG)** (Kcal/mol at 25℃)	**Enthalpy change (ΔH)** (Kcal/mol)	**Entropy change (ΔS)** (Kcal/K.mol)
Apt_M09	CCCACACGTCTTATTATTAATGGGTATCCGTACACCGGGG	**-6.67**	-92.00	-286.1×10^{-3}
Apt_J51	CATGCGAGGTGGAATGAGCGGATTATCTATAATGTCGTCT	**-5.34**	-107.20	-341.6×10^{-3}

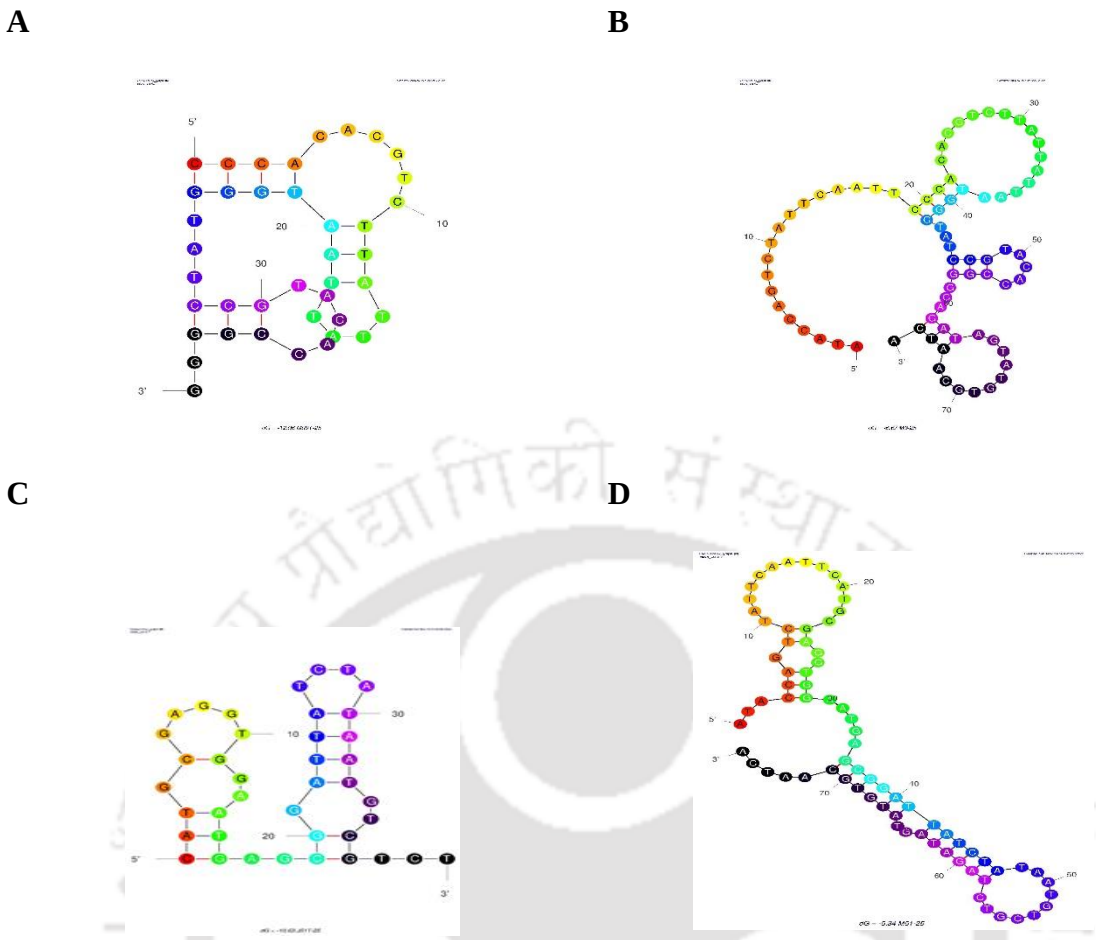

Figure 3.5 Secondary structure of aptamer candidates as predicted by mfold; A) truncated aptamer Apt_M09 without flanking regions, B) aptamer Apt_M09P with flanking regions, C) truncated aptamer Apt_J51 without flanking regions, D) aptamer Apt_J51P with flanking regions

3.3.9 Binding studies

3.3.9.1 Isothermal Titration Calorimetry (ITC) studies

Binding affinity in terms of dissociation constant (K_d) and other thermodynamic parameters were evaluated by isothermal titration calorimetry (ITC) studies. From the homogenous binding events between aptamer and peptide, a binding isotherm of the aptamer-peptide complex is generated from the heat exchange data of binding. The amount of heat exchanged during the interaction of peptide and aptamer after each injection is plotted against the molar ratio of the concentrations of peptide and aptamer. The calorimetric cell records the amount of heat exchanged after each injection derived from amount of power required to maintain the cell

at a constant temperature. The each injection in calorimetry cell generates a heat-burst curve (µcal/s) as a function of time (min). From the thermogram, the values of association constant (K_a), change in enthalpy (ΔH), change in entropy (ΔS), dissociation constant (K_d) and stochiometry of the binding (N) are derived. The change in enthalpy (ΔH) can be directly measured from thermogram while the change in entropy (ΔS) and the Gibb's free energy change (ΔG) and the dissociation constant (K_d) are calculated from the following equations, where R is the universal gas constant (1.986 cal K^{-1} mol^{-1}) and T is the temperature of the reaction.

$\Delta G = -RT \ln K_a$

$\Delta G = \Delta H - T\Delta S$

$K_a = 1/K_d$

The interaction of 1000 µM apt_M09P with flanking regions with 30 µM peptide SQ-14 in buffer 1x ABB was first studied through ITC. The peaks of the isotherm of their interaction were integrated and fitted into a two sites sequential binding model in Origin 5.0 software (Microcal, Inc) as shown in **Figure 3.6**. The dissociation constant and the other thermodynamic parameter of the interaction is listed out in **table no 3.8**.

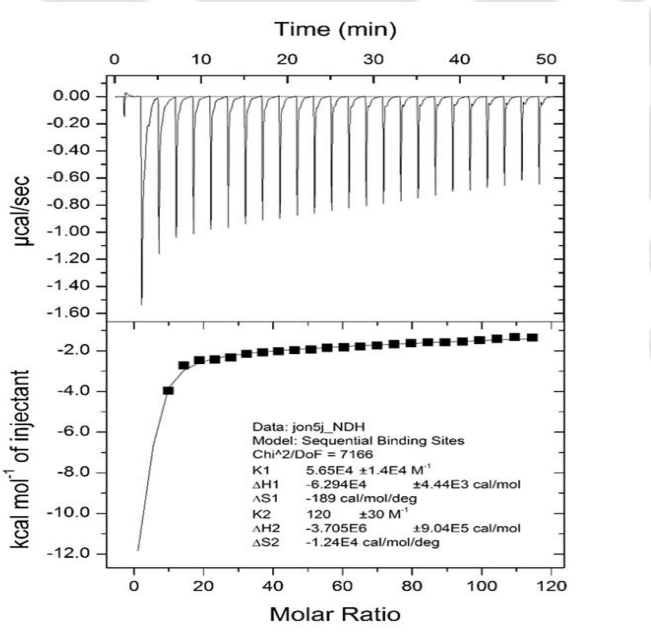

Figure 3.6 ITC isotherms for calorimetric titration between 30 µM aptamer apt_M09P with flanking regions and 1000 µM peptide SV-14 at 25°C in aptamer binding buffer.

Table 3.8 List of dissociation constant and thermodynamic parameters calculated through ITC study of interaction between apt_M09P and SV-14 in 1x ABB

1^{st} site	
Dissociation constant, K_d1	17.6 µM
Change in Enthalpy, ΔH1	- 6294 cal/mol
Change in Entropy, ΔS1	- 189 cal/mol/deg
TΔS1	- 4725 cal/mol
Gibb's free energy change, ΔG1	-1569 cal/mol
2^{nd} site	
Dissociation constant K_d2	8.33 mM
Change in Enthalpy, ΔH2	-3.705×10^{6} cal/mol
Change in Entropy, ΔS2	-1240 cal/mol/deg
TΔS2	-3.10×10^{6} cal/mol
Gibb's free energy change, ΔG2	-3.39×10^{5} cal/mol

From the ITC binding isotherm of between apt_JM09P with flanking region and SV-14, it is seen that the reactions of binding are exothermic. The binding is found to be favourable by change in enthalpy ΔH (- 6294 cal/mol) and unfavourable by change in entropy TΔS (- 4725 cal/mol) at temperature 25°C for the first site of binding. The favourable enthalpy ($\Delta H < 0$) arises due to effective surface complementarity likely formed by electrostatic interaction, hydrogen bonding and van der Waals interactions. The unfavourable enthalpy ($\Delta S < 0$) is contributed by the decrease conformational degree of freedom of both the molecules in bound state or/and decrease in the solvation entropy (Amaya-González et al., 2015; Amano et al., 2016). In sequential binding mechanism, generally there is a presence of another low affinity site apart from the primary high affinity site. In this case, the aptamer apt_M09J also contains a low affinity binding site with dissociation constant of 8.33 mM.

The interaction between the apt_J51P with flanking region and SV-14 was also studied by performing ITC while dissolving both the aptamer and peptide in 1x ABB. The isotherm of interaction (**figure 3.7**) between 1000µM aptamer apt_J51P and 30 µM SV-14 interaction in 1x ABB water was fitted to a one site binding model in Origin 5.0 software (Microcal, Inc).

The dissociation constant and the other thermodynamic parameter of the interaction are listed out in **table 3.9**.

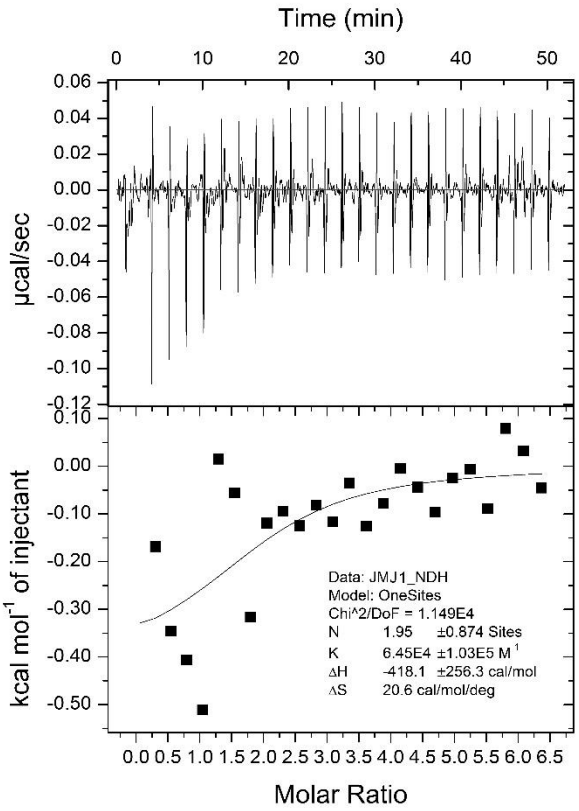

Figure 3.7 ITC isotherms for calorimetric titration between 30 µM aptamer apt_J51P with flanking region and 1000 µM peptide SV-14 at 25°C in 1x ABB

Table 3.9 List of dissociation constant and thermodynamic parameters calculated through ITC study of interaction between apt_J51P with flanking region and GQ-14 in 1xABB

Single site binding model	
Dissociation constant K_d	0.155 µM
Change in Enthalpy, ΔH	-418.10 cal/mol
Change in Entropy, ΔS	20.6 cal/mol/deg
TΔS	515 cal/mol
Gibb's free energy change, ΔG	-933.10 cal/mol

The binding characteristics of the apt_J51P and target SV-14 in aptamer binding buffer was found to be favoured by both change in enthalpy and change in entropy. The similar trend was observed in the interaction between aptamer apt_J91P with flanking region and the target GQ-14 as described in the chapter 2. The dissociation constant (K_d) for this interaction was found to be 0.155 µM, which is lower than the interaction between apt_M09P and SV-14. However, by considering the goodness of fitting, the Chi^2/DoF value of the thermogram of interaction between apt_J51P and SV-14 was found to be higher than the interaction between apt_M09P and SV-14, therefore apt_J51 is not considered for further analysis.

ITC was carried out to check the specificity of apt_M09P with flanking region with peptide GQ-14 (GQGQQGYYPTSPQQ) from HMW-GS which contains different amino acid sequence than SV-14 in 1x ABB buffer. The isotherm for apt_M09P and GQ-14 interaction were tried to fit to a sequential binding model in Origin 5.0 software (Microcal, Inc) as shown **figure 3.8**. The binding isotherms of apt_M09P with GQ-14 show no saturation, which establishes that apt_M09P is specific to peptide SV-14.

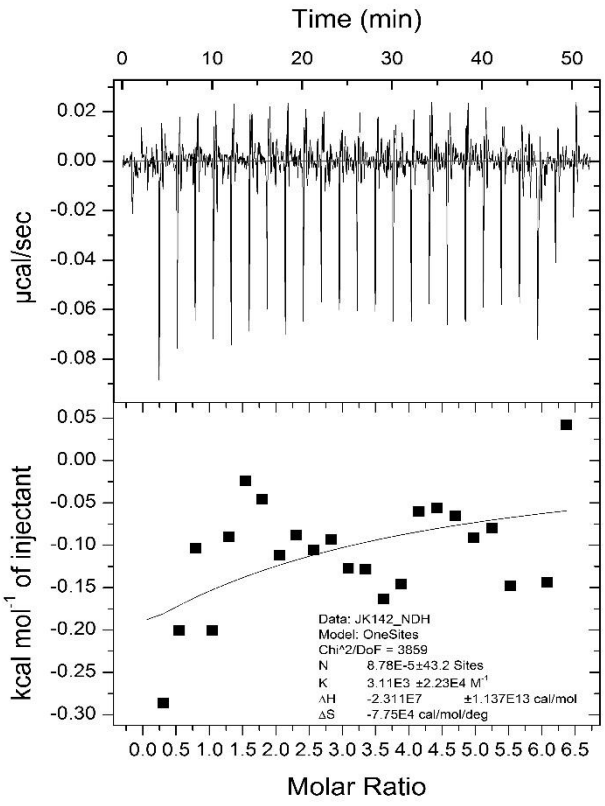

Figure 3.8 ITC isotherms for calorimetric titration between 30µM aptamer apt_M09P and 1000 µM peptide GQ-14 at 25°C in 1x ABB to check the specificity of aptamer apt_M09.

The ITC binding experiments were also carried out to check the interaction of aptamer candidate apt_M09 without flanking region and apt_J51 without flanking region. These interaction did not yield any saturation during the titration in the isotherms, likely due to very low affinity. This also proves that the flanking regions (primer binding regions) of the aptamer sequence apt_M09P and apt_J51P strongly involve in the binding with the target peptide along with the random region.

3.3.9.2 Binding study through Circular Dichroism

The secondary structure of the aptamer candidate Apt_M09P with the flanking regions were studied before the interaction with target in 0.3x ABB buffer through CD spectrometry. The buffer concentration is reduced as use of 1x ABB buffer increases the HT voltage beyond 500 V in the CD experiments. The signature peaks of maxima near 280 nm and a minima near 245 nm as shown in the **figure 3.9** indicates the duplex B-form DNA of the aptamer sequence. The presence of maximum peak at ~277 nm and a minimum at ~245 nm are also associated with self-associative conformations of aptamer formed through Watson–Crick base pairing such as stem-loop secondary structures (Serrano et al., 2019). The nature of the secondary structure inferred from CD study is in accordance with the predicted structure of apt_M09P by mfold.

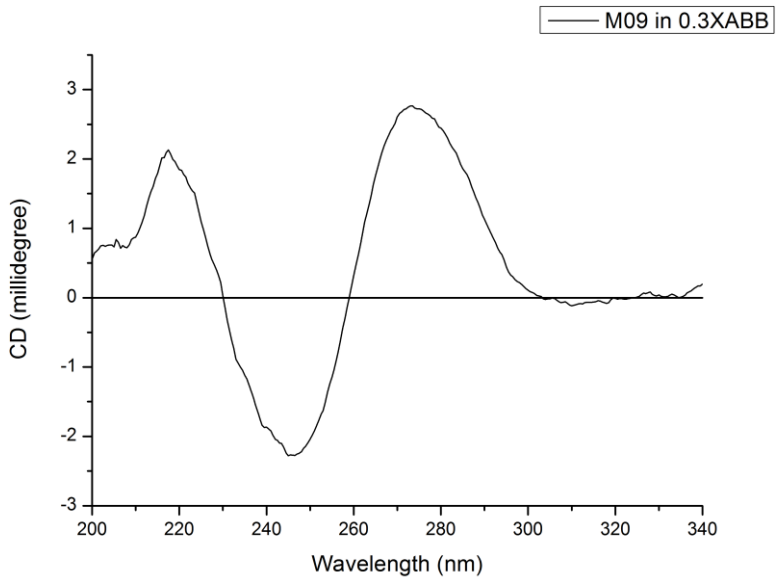

Figure 3.9 Circular dichroism spectra of aptamer apt_M09P with flanking regions in 0.3x aptamer binding buffer

The CD spectra of interaction between apt_M09P and the target peptide SV-14 in 0.3x ABB was recorded in the wavelength range of 190-340 nm. The CD spectra of the interaction was compared with the spectra of apt_M09P without the presence of target peptide in the **figure 3.10**. The CD spectra of interaction between apt_M09P with an unrelated peptide GQ-14 (GQGQQGYYPTSPQQ) from HMW-GS is used as negative control of the experiment. There was no change in ellipticity observed in the CD spectra of interaction when compared to the spectra of only aptamer indicating no structural reassembling of the aptamer. However, the increase in the amplitude of the ellipticity in CD spectra of interaction indicates target induce structural change or induce fit type of binding of the target with aptamer (Sharma et al., 2017).

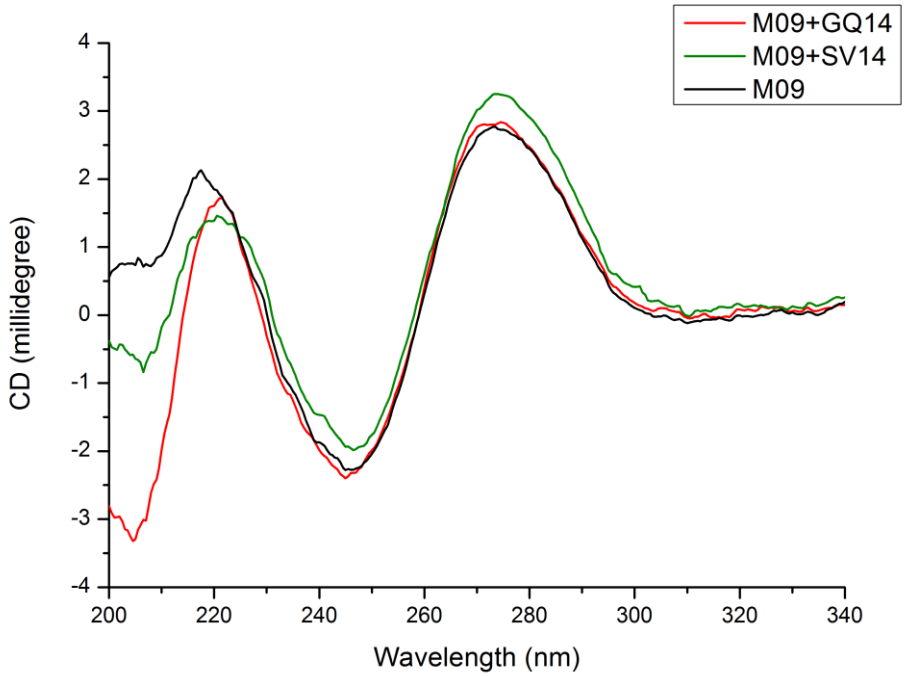

Figure 3.10 Binding study of the aptamer-peptide complex by circular dichroism scanned from 200 nm to 340 nm where the plot with black, green and red lines denotes the CD spectra of aptamer apt_M09P, interaction between apt_M09P and peptide SV-14 and interaction between apt_M09P and peptide GQ-14 (negative control).

3.3.9.3 Direct Enzyme linked aptamer-sorbent assay (ELAA)

The binding of aptamer apt_M09P to the standard target peptide SQ-14 in increasing concentration is measured by the intensities developed. As seen in the **figure 3.11,** the absorbances are found to be increasing in very small scales with the increased in concentration of the peptide. Blank sample contributing to detectable absorbance probably due to unspecific binding is considerable as background noise. The limit of Detection of the aptamer was calculated from linear regression curve (y=0.0008x+0.0965) using the equation LOD=3.3 x standard deviation of the regression line (σ) /Slope(S) is found to be 20.00 µM. The quantitation limit (QL) can be expressed as (10 x standard deviation of low concentration/ slope of the calibration line) is found to be 60.06 µM

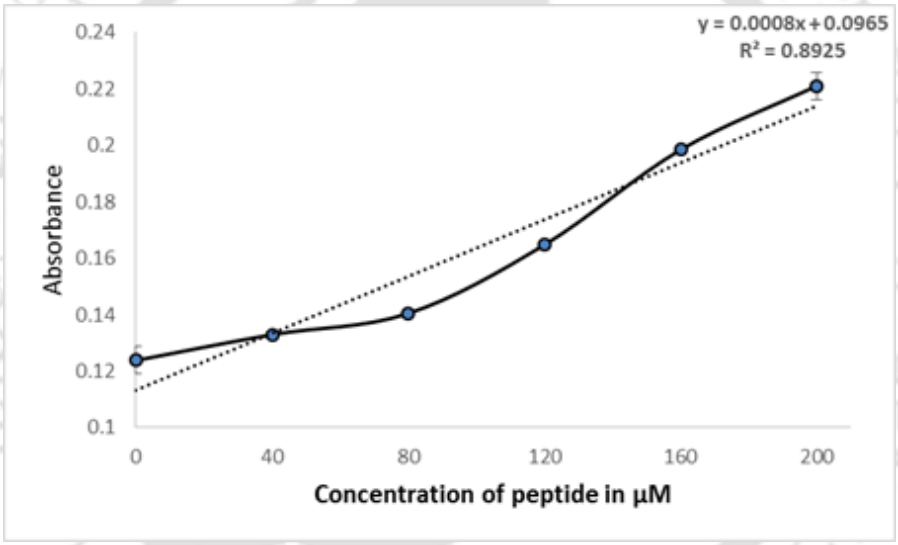

Figure 3.11 Analysis of the limit of detection of the aptamer by ELAA in the peptide concentration range of (40-200 µM)

3.4 Discussion

The focus of this chapter is to select an aptamer candidate that would be able to detect a peptide fraction, SQQQPPFSQQQQPV of low molecular weight glutenin subunit of wheat gluten protein containing the HLA-DQ2.2 restricted celiac disease epitope PFSQQQQPV. In order to select the aptamer candidate, we have carried out conventional SELEX process against the peptide sequence immobilised on magnetic bead as solid support. A 40 nucleotides long random degenerated oligonucleotide library with two flanking regions for primer binding was taken as the initial pool of candidate sequences that offers a diversity of the random sequences

to a degree of 10^{24}. As discussed in the chapter 2, for a relatively low molecular target a short aptamer library is preferable to reduce the size gap between aptamer and target for efficient selection of the aptamer candidate. However, a larger library can offer more probable conformations formed by the aptamer sequneces that increase the changes of binding of the target with high affinity (Ruscito, & DeRosa, 2016). Therefore, a 76 nucleotides (~22-24 KDa) long aptamer library containing a 40 bp long random region was used for SELEX against target peptide SV-14 (1.63 KDa). The peptide SV-14 was selected as target as it contained the immunostimulatory celiac disease epitope present in LMW-GS. Considering the association between of high binding affinity with high molecular weight of target (McKeague & DeRosa, 2012), the target peptide was chosen by including the additional amino acid sequence with the epitope to a length of 14 amino acids. Importantly, the sequence SV-14 can be generated through enzymatic digestion of gluten with a cocktail of enzyme containing pepsin, trypsin, chymotrypsin, elastase and carboxypeptidase (Dørum et al., 2010). This offers the advantage of detecting the peptide fraction by the selected aptamer in enzyme hydrolysed gluten samples if the target peptide is inaccessible (or buried inside) in the intact protein. The grand average of hydropathicity index (GRAVY) of -1.707 of SV-14 indicates that it is hydrophilic peptide, however it is more hydrophobic than the peptide GQ-14. SV-14 was also found to be dissolved in deionised water. The CD study on the peptide SV-14 in aptamer binding buffer reveals that mostly it forms random coil structure.

The SELEX was carried out for 18 rounds for selection of the aptamer against SV-14 with incorporation of two negative SELEX rounds at the beginning and after 6th round. The stringency of the SELEX conditions were increased after 4th round and continued till the 18th round. However, the aptamer pool after enrichment in 16th round of SELEX was retrieved for cloning and sequencing as high stringency in the round 18 led to loss of aptamer candidates to a large extent. A total of 10 potential aptamer sequences were obtained by Sanger sequencing. Based on the *in-silico* studies, only two aptamer sequences with lowest Gibb's free energy change value which implies the highest structural stability in selection buffer among the 10 sequences were selected for further studies.

The characterization of binding between aptamer apt_M09P with flanking regions and peptide target SV-14 in 1x ABB through ITC reveals that affinity between the two biomolecules with a dissociation constant of 17.6 µM and 8.33 mM for a primary and secondary binding sites in aptamer respectively. The specificity of the aptamer apt_J91P was also demonstrated through ITC when allowed to interact with a non-target peptide GQ-14

which didn't form complex. The measured thermodynamic parameters of ITC revealed that the binding is favourable by change in enthalpy ($\Delta H < 0$) and unfavourable by change in entropy ($\Delta S < 0$) at temperature 25°C for the first site of binding. This type of binding characteristics is very common in aptamer and target interaction, which has been seen in case of a respective RNA aptamer domain binding to small molecular target c-di-GMP (Umuhire et al., 2019), a DNA aptamer binding to small molecules L-argininamide and D-argininamide (Lin et al., 2009), a DNA aptamer binding to L-tyrosinamide (Lin et al., 2008), a DNA aptamer binding to the protein target Streptavidin (Kuo et al., 2013), a DNA aptamer binding to cocaine, quinine and primaquine (Slavkovic et al., 2018) etc. among many others. In case of aptamer developed against the 33mer immunogenic peptide of gliadin subunit of gluten, the aptamer developed showed a favourable entropy and unfavourable enthalpy of binding with target. This was suspected due to the comparatively more hydrophobic nature of the target peptide (GRAVY is -1.079) (Amaya-González et al., 2015). The highly favourable enthalpy when compensated by a high unfavourable entropy in aptamer-target binding, the binding mechanism implies an involvement of hydrogen bonding and electrostatic interaction along with conformational change of the aptamer (Lin et al., 2009). The hydrogen bonding and the electrostatic interactions between small molecular target and aptamer account for the negative enthalpy change. The unfavourable negative entropy change is likely arise due to the loss of degree of freedom when more disordered aptamers before binding changes to a well-defined state after binding with the target. Apart from the conformational change of aptamer, other major contributor in the overall negative entropy change is likely due to a decreased solvation entropy. The aptamer selected against small molecular target Cocaine was found to possess two binding sites with one high and another low affinity (Slavkovic et al., 2018), which was also observed in aptamer apt_M09P in our study through ITC when thermograms were fitted with two site sequential binding models.

The CD study to examine the secondary structure of the selected aptamer candidate apt_M09P reveals that it forms duplex B-form DNA structure which likely due to formation of stem-loop fold. The G-quadraplex structure that provides the chemical and thermal stability to the aptamers was not observed in the secondary structure of apt_M09P. The behaviour of unfavourable entropy and favourable enthalpy change during binding are associated with the induced-fit binding model of small molecular targets binding to aptamer which induces a local folding events in aptamer to initiate binding (Bishop et al., 2007; Lin et al., 2008; Lin et al.,

2009; Amano et al., 2016). The local conformational change of the aptamer apt_M09P when binding to SV-14 was confirmed by the CD study.

3.5 Conclusion

In this chapter, we report the successful selection of aptamer candidate apt_M09P against immunostimulatory celiac disease epitopic peptide SQQQPPFSQQQQPV present in the low molecular weight subunit of glutenin. The binding affinity in terms of dissociation constant (K_d) of the aptamer candidate selected was found to be 17.6 µM for primary site of binding and 8.33 mM in the secondary site of binding for the target SQQQPPFSQQQQPV in aptamer binding buffer. The aptamer has been found to form a stem-loop secondary structure. The binding characterization reveals that the binding is enthalpically driven and local conformational change occurs in aptamer during binding. The limit of detection (LOD) evaluated through direct-ELAA was found to be 20.00 µM.

3.6 References

1. Amano, R., Takada, K., Tanaka, Y., Nakamura, Y., Kawai, G., Kozu, T., & Sakamoto, T. (2016). Kinetic and thermodynamic analyses of interaction between a high-affinity RNA aptamer and its target protein. Biochemistry, 55(45), 6221-6229
2. Amaya-González, S., López-López, L., Miranda-Castro, R., de-los-Santos-Álvarez, N., Miranda-Ordieres, A. J., & Lobo-Castañón, M. J. (2015). Affinity of aptamers binding 33-mer gliadin peptide and gluten proteins: Influence of immobilization and labeling tags. Analytica Chimica Acta, 873, 63-70.
3. Bonilla, J. C., Ryan, V., Yazar, G., Kokini, J. L., & Bhunia, A. K. (2018). Conjugation of specifically developed antibodies for high-and low-molecular-weight glutenins with fluorescent quantum dots as a tool for their detection in wheat flour dough. Journal of agricultural and food chemistry, 66(16), 4259-4266.
4. Chang, K. Y., & Yang, J. R. (2013). Analysis and prediction of highly effective antiviral peptides based on random forests. PloS one, 8(8), e70166.
5. Dewar, D. H., Amato, M., Ellis, H. J., Pollock, E. L., Gonzalez-Cinca, N., Wieser, H., & Ciclitira, P. J. (2006). The toxicity of high molecular weight glutenin subunits of wheat to patients with coeliac disease. European journal of gastroenterology & hepatology, 18(5), 483-491.

6. D'Ovidio, R., & Masci, S. (2004). The low-molecular-weight glutenin subunits of wheat gluten. Journal of cereal science, 39(3), 321-339.
7. Gasteiger, E., Hoogland, C., Gattiker, A., Duvaud, S. E., Wilkins, M. R., Appel, R. D., & Bairoch, A. (2005). Protein identification and analysis tools on the ExPASy server (pp. 571-607). Humana press.
8. Kuo, T. C., Lee, P. C., Tsai, C. W., & Chen, W. Y. (2013). Salt bridge exchange binding mechanism between streptavidin and its DNA aptamer–thermodynamics and spectroscopic evidences. Journal of Molecular Recognition, 26(3), 149-159
9. Lexhaller, B., Tompos, C., & Scherf, K. A. (2017). Fundamental study on reactivities of gluten protein types from wheat, rye and barley with five sandwich ELISA test kits. Food Chemistry, 237, 320-330.
10. Lin, P. H., Tong, S. J., Louis, S. R., Chang, Y., & Chen, W. Y. (2009). Thermodynamic basis of chiral recognition in a DNA aptamer. Physical Chemistry Chemical Physics, 11(42), 9744-9750.
11. Lin, P. H., Yen, S. L., Lin, M. S., Chang, Y., Louis, S. R., Higuchi, A., & Chen, W. Y. (2008). Microcalorimetrics studies of the thermodynamics and binding mechanism between L-tyrosinamide and aptamer. The Journal of Physical Chemistry B, 112(21), 6665-6673.
12. Mitea, C., Kooy-Winkelaar, Y., van Veelen, P., de Ru, A., Drijfhout, J. W., Koning, F., & Dekking, L. (2008). Fine specificity of monoclonal antibodies against celiac disease–inducing peptides in the gluteome. The American journal of clinical nutrition, 88(4), 1057-1066.
13. Pearce, T. R., Waybrant, B., & Kokkoli, E. (2014). The role of spacers on the self-assembly of DNA aptamer-amphiphiles into micelles and nanotapes. Chemical Communications, 50(2), 210-212.
14. Prante, M., Schüling, T., Roth, B., Bremer, K., & Walter, J. (2019). Characterization of an Aptamer directed against 25-hydroxyvitamin D for the development of a competitive aptamer-based Assay. Biosensors, 9(4), 134.
15. Scopes, R. K. (1974). Measurement of protein by spectrophotometry at 205 nm. Analytical biochemistry, 59(1), 277-282.
16. Serrano, C. M., Freeman, R., Godbe, J., Lewis, J. A., & Stupp, S. I. (2019). DNA-peptide amphiphile nanofibers enhance aptamer function. ACS applied bio materials, 2(7), 2955-2963.

17. Slavkovic, S., Churcher, Z. R., & Johnson, P. E. (2018). Nanomolar binding affinity of quinine-based antimalarial compounds by the cocaine-binding aptamer. Bioorganic & Medicinal Chemistry, 26(20), 5427-5434.
18. Sreerama, N., & Woody, R. W. (2000). Estimation of protein secondary structure from circular dichroism spectra: comparison of CONTIN, SELCON, and CDSSTR methods with an expanded reference set. Analytical biochemistry, 287(2), 252-260.
19. Umuhire Juru, A., Patwardhan, N. N., & Hargrove, A. E. (2019). Understanding the contributions of conformational changes, thermodynamics, and kinetics of RNA–small molecule interactions. ACS chemical biology, 14(5), 824-838.
20. Wang, Y., Tong, Y., Zhou, J., Yang, D., & Fu, L. (2023). Purification and immunoglobulin E epitopes identification of low molecular weight glutenin: an allergen in Chinese wheat. Food Science and Human Wellness, 12(3), 720-727.
21. Whitmore, L., & Wallace, B. A. (2004). DICHROWEB, an online server for protein secondary structure analyses from circular dichroism spectroscopic data. Nucleic acids research, 32(suppl_2), W668-W673.
22. Woldemariam, K. Y., Yuan, J., Wan, Z., Yu, Q., Cao, Y., Mao, H., ... & Sun, B. (2022). Celiac disease and immunogenic wheat gluten peptides and the association of gliadin peptides with HLA DQ2 and HLA DQ8. Food Reviews International, 38(7), 1553-1576.
23. Zhang, Y., Hu, M., Liu, Q., Sun, L., Chen, X., Lv, L., ... & Li, H. (2018). Deletion of high-molecular-weight glutenin subunits in wheat significantly reduced dough strength and bread-baking quality. BMC plant biology, 18(1), 1-12.

Chapter 4

Development of aptassays for detection of Celiac disease epitopes in wheat gluten

Chapter 4: Development of aptassays for detection of Celiac disease epitopes in wheat gluten

Abstract

***Introduction**: This chapter describes the preliminary investigations carried out to check the applicability of the selected aptamers apt_J91P and apt_M09P in development of bioassays.*

***Method**: The gold nanoparticles of size were synthesised by following a modified Turkevich Method. The aptamers, apt_J91P and apt_M09P were surface absorbed on nanoparticles in the 'gold nanoparticle based aptamer assay' where addition of high salt concentration leads to aggregation of the nanoparticles in absence of the respective peptide targets. The presence of peptide target prevents the aggregation of the nanoparticles. Apt_J91P was utilised in the 'aptamer mediated magnetic bead based extraction assay', where aptamer conjugated to biotin captures the target peptide, isolated by streptavidin conjugated magnetic beads and analysed with MALDI-TOF.*

***Result**: The aptamers apt_J91P and apt_M09P were successful in detecting their respective target peptides GQGQQGYYPTSPQQ and SQQQPPFSQQQQPV in aptamer binding buffer. The aptamers demonstrated their specificity when allowed to interact with unrelated peptides as target.*

***Discussion**: Both assay formats were successful in detecting the respective targets of the aptamers, however, for detection of the target peptides in food matrix, further future investigation are needed to be carried out.*

4.1. Introduction

The aptamers have two broad area of applications, one being used as a probe for detection of analyte to develop bioassays or biosensors while other being used as a therapeutic molecule or as a drug delivery vehicle. The objective of this thesis work is to develop an aptamer based bioassay for detection of the celiac disease epitopes of glutenin in wheat based food products. As recognition molecules, aptamers have been incorporated in various types of bioassays such as Enzyme-Linked Apta-Sorbent Assay (ELASA), nanoparticle based calorimetric assays, fluorescent based assays, Rolling Circle Amplification (RCA) assay etc. and various types of biosensor platforms such as calorimetric, electrochemical, surface plasmon resonance (SPR), fluorescence, chemiluminescence, piezoelectric etc. As discussed in the chapter 1 for detection of gluten, few aptasensors and aptaassays based on methods such as electrochemical (Amaya-González et al., 2015), label-free impedimetric (Malvano et al., 2017), real-time apta-PCR (Pinto et al., 2014) etc. have been developed which offers the limit of detection in the nanomolar or ppm range. The aptamers developed against the 33-mer toxic peptide from gliadin were incorporated into an electrochemical sensor platform and their feasibility in detecting the gluten or gliadin in heat processed and hydrolysed food samples were evaluated. The electrochemical sensors using aptamer against 33-mer toxic gliadin protein were found to be successful detecting gluten in the range below the legislated threshold of gluten in gluten free products set by EU. This method, however, required extraction of glutenin from food samples by treating with an extraction buffer (Amaya-González et al., 2015; López-López et al., 2017).

For examine the feasibility of the aptamer candidates, apt_J91P and apt_M09P selected against the immunostimulatory peptides present in HMW-GS and LMW-GS subunit, we carried out preliminary studies by incorporating the aptamer in two formats of bioassay, which are aptamer based nanoparticle calorimetric assay and magnetic bead based selective extraction of the analyte. Aptamers have been explored recently to use with nanoparticle in order to design simple bioassays of qualitative and semi-quantitative nature. Incorporation of nanoparticles in bioassays or biosensors offers the advantage of calorimetric detection, even recognizable by naked eyes and notably, they are cost effective (Hui et al., 2007). Generally immobilization of aptamer are required on gold nanoparticle surface with thiol-based conjugation chemistry in most of the nanoparticle based aptasensors. However, in case of the method developed by Hui et al., 2007, the aptamer are absorbed on the nanoparticle surface without requirement of any modification of the aptamer and can carry out nanoparticle aggregation test based on binding

of the aptamer with target at high salt concentration. Antibodies developed against the peptide fraction of glutenin subunits were applied in assays where the monoclonal antibodies conjugated to the sepharose beads were incubated with a pepsin/trypsin digest of wheat flour. The bound peptide fraction were eluted and analysed by mass spectroscopy to check the specificity of the antibody for digested wheat fraction (Mitea et al., 2008). Antibody based co-immunoprecipitation of the protein is very common technique. Kim et al., 2014 demonstrated the similar application of co-precipitation of specific protein target from cell lysate using aptamer immobilised on magnetic beads with successful outcome (Kim et al., 2014). Based on these observations in published literature, we examined the feasibility of using apt_J91P for application in selective extraction of GQ-14 through magnetic bead based analyte extraction assay.

4.2. Materials and Methods

4.2.1. Chemicals and Reagents

Dynabeads MyOne carboxylic acid was purchased from Invitrogen Thermo Scientific (USA). Streptavidin magnetic beads and Low molecular weight (LMW) DNA ladder were procured from New England Biolabs (USA). Peptide SV-14 was purchased from Biotechdesk, India. α-Cyano-4-hydroxycinnamic acid (4-HCCA) MALDI-matrix was procured from Sigma Aldrich (India). The biotinylated aptamer sequences were purchased from Integrated DNA Technologies (USA). All other chemicals were analytical grade and cited wherever necessary.

4.2.2. Gold nanoparticle based calorimetric assay

4.2.2.1. Synthesis of gold nanoparticles

Gold nanoparticle were synthesized by a size controlled method, following a modified Turkevich Method used by Dong et al., 2020. 50ml of 0.25 mM HAuCl4 (Sigma-Alrich) is heated with vigorous shaking till boiling. Volume of 34 mM (1 % by weight) Sodium citrate was added to reach the molar ratio (MR) of 3.2 to achieve the size of nanoparticle synthesized between 10-50 nm. The synthesised nanoparticle solution was characterised by UV-vis-NIR spectrophotometer (Shimadzu UV-1900UV visible spectrometer) by scanning absorbance in the range 300-600 nm. The shape and size was also evaluated by FESEM.

4.2.2.2 Calorimetric Assay using apt_J91P

The gold nanoparticle based calorimetric assay was performed by following the method used by Hui et al., 2007 with slight modifications. 200 µl of gold nanoparticles were mixed with 30 µl 5 µM unmodified aptamer apt_J91P in 1x aptamer binding buffer in a 1.5 ml microcentrifuge tube and incubated for 30 min. The hydrodynamic diameter of the nanoparticles after addition of aptamer was checked to confirm surface adsorption of aptamers on it using Dynamic Light Scattering (DLS). 30 µl of 10 µM peptide target GQ-14 in water was added to the gold nanoparticle and aptamer solution in the tube. The solution was allowed to stand for 15 minutes. 100 µl of 0.5 M NaCl solution was added to produce colour change due to aggregation of nanoparticles induced by salt at high concentration. Simultaneously, the experiment was also carried out in other tube, where the nanoparticles absorbed with aptamer apt_J91P were also added with 30 µl of 10 µM SV-14. In other two tubes, nanoparticle without absorption of aptamer and nanoparticles with aptamer absorbed were added with 100 µl of 0.5 M NaCl solution for positive and negative control experiment respectively. The absorption of the solution were scanned between 300-900 nm on a UV–vis–NIR spectrophotometer (Shimadzu UV-1900UV visible spectrometer)

4.2.2.3. Calorimetric Assay using apt_M09P

The calorimetric assay using apt_M09P was performed by following the same method as used in **section 4.2.2.2**. Calorimetric assay was performed to examine the specificity of the aptamer towards target peptide SV-14. Simultaneously, the assay was also carried out by incubating an unrelated peptide PV-12 (PQQPPFQQQQPV) as negative control. In other two tubes, nanoparticle without absorption of aptamer and nanoparticles with aptamer absorbed were added with 100 µl of 0.5 M NaCl solution for positive and negative control experiment respectively.

4.2.3. Magnetic bead based target extraction assay using biotinylated apt_J91P

Apt_J91P was synthesised with attachment of biotin at it's 5′ end (Btn-ATACCAGTCTATTCAATTCTCCTGAGCTATCTGGAAAGAGATAGTATGTGCAATCA). 500 picomoles of biotinylated-aptamer apt_J91P (apt_J91 with flanking primer binding regions) was incubated with 1000 picomoles of GQ-14 peptide target at room temperature in a

total volume of 100 µl made by adding 1x aptamer binding buffer. It was followed by incubation for 1h with gentle tilt rotation. 20 µl of streptavidin was taken and the storing buffer solution was removed. It was added to the 100 µl solution of aptamer-target solution and incubated for 30 minutes. After incubation, the streptavidin magnetic beads were washed with 1x aptamer washing buffer once and subsequently with 1x aptamer binding buffer once. The magnetic beads were then dispersed in 50 µl of sigma water (nuclease free). The target peptides bound to aptamer were eluted by heating it at 95 ℃ for 7 minutes. The eluted target samples were analysed by MALDI-TOF. For negative control experiment, an unrelated peptide SV-14 was incubated with aptamer J91P in the same as followed for GQ-14.

4.3. Results

4.3.1. Gold nanoparticle based calorimetric assay

4.3.1.1. Synthesis of gold nanoparticles

The gold nanoparticles were synthesis using a modified Turkevich Method that controlled the size of the synthesised particles in the range of 10-50 nm. The synthesis of gold nanoparticles were confirmed by colour change from yellowish colour to wine red colour. The maximum absorbance of the gold nanoparticle at wavelength between 520-530 nm confirmed the synthesis of size between 12 and 41 nm (He et al., 2005) as seen in the **figure 4.1**. The FESEM image of gold nanoparticle reveals the spherical shape and average size between 30-50 nm as seen in figure **4.2**.

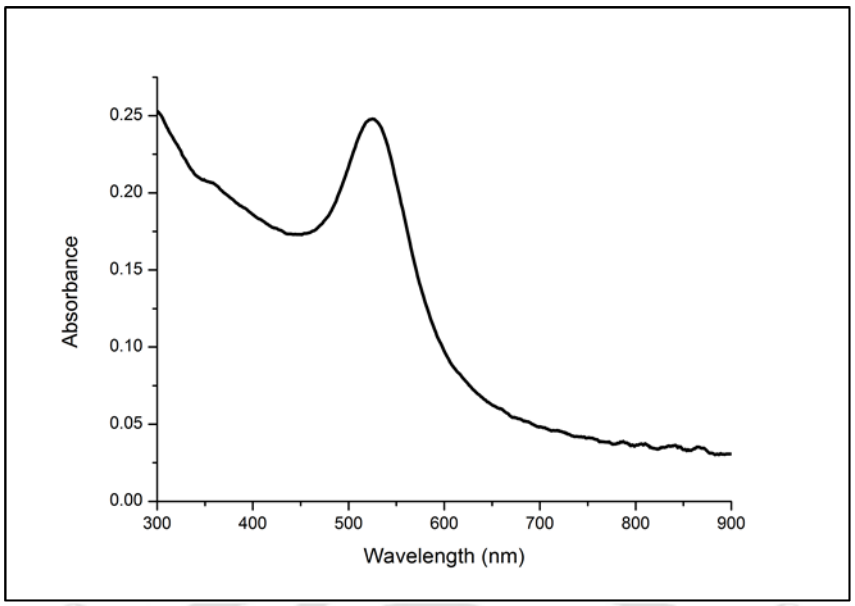

Figure 4.1 Absorbance of synthesised gold nanoparticle at wavelength range 300-900nm

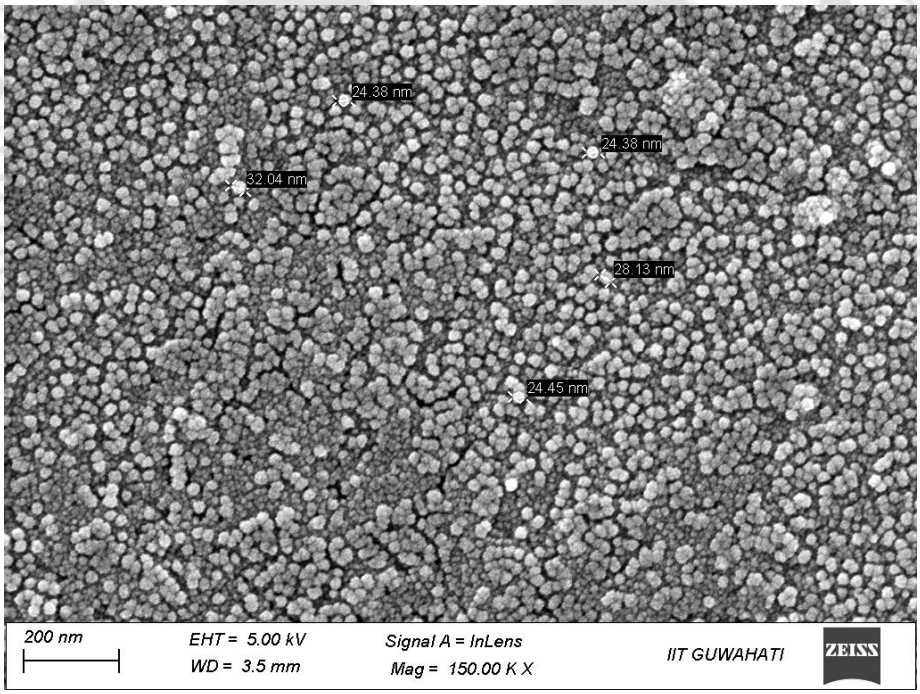

Figure 4.2 FESEM image of synthesized gold nanoparticles at 150.00K X magnification revealing average size between 30-50 nm

4.3.1.2. Calorimetric Assay using apt_J91P

The specificity of the aptamer apt_J91P was evaluated by a simple gold nanoparticle based calorimetric assay using the unmodified aptamer. For this, the synthesised gold nanoparticles were incubated with aptamer apt_J91P for 30 min. After incubation the hydrodynamic diameter of the aptamer incubated gold nanoparticles were measured using DLS and compared with the bare gold nanoparticles. The average hydrodynamic diameter of gold nanopartilce incubated with aptamer was found to be 53.70 nm whereas for bare gold nanoparticles, it was found to be 33.64 nm as shown in **figure 4.3**.

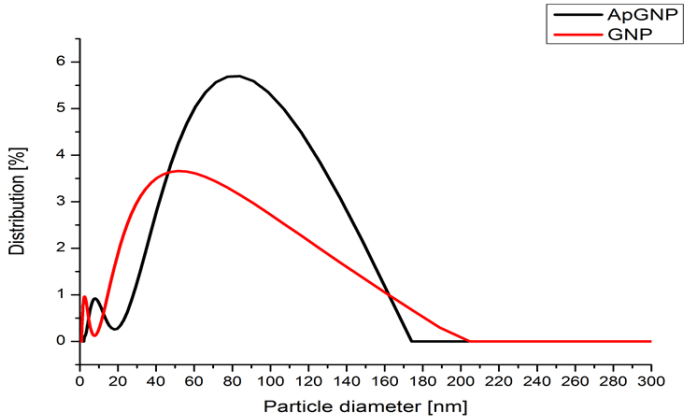

Figure 4.3 The distribution of hydrodynamic diameter of synthesized gold nanoparticles (GNP) before (red) and after (black) adsorption of aptamer (ApGNP) on nanoparticle's surface

The gold nanoparticles are prone to aggregation at high salt concentration. The nanoparticles are negatively capped by citrate that provides repulsive force to balance the van der waals attraction with adjacent nanoparticles which make the particles stable. The repulsive force is screened by addition of high salt concentration leading to formation of aggregates which results in change of colour from wine red to dark blue. Surface adsorption of polyanionic aptamer on the gold nanoparticles prevents the aggregation at high salt concentration by counterbalancing the van der waals attraction with electrostatic repulsion. However, presence of a target molecule which induce conformational change of the aptamer molecule that leads to detachment from nanoparticle surface and binding with the target (Hui et al., 2007). The detachment can be characterised by treating the nanoparticles with high salt concertation which leads to formation of aggregates. **Figure 4.4** shows the aggregation formation in case of

incubation of bare gold nanoparticle (GNP) with salt which shows the breaking of the characteristic peak of nanoparticle at 520-30 nm. The incubation of nanoparticles with absorbed aptamer apt_J91P (J91P-GNP) with target GQ-14 also shows slight shift of maximum absorbed wavelength towards blue colour which indicates the specificity of the aptamer for peptide GQ-14. The control experiment with SV-14 didn't yield any colour change which signifies the specificity of the apt_J91P.

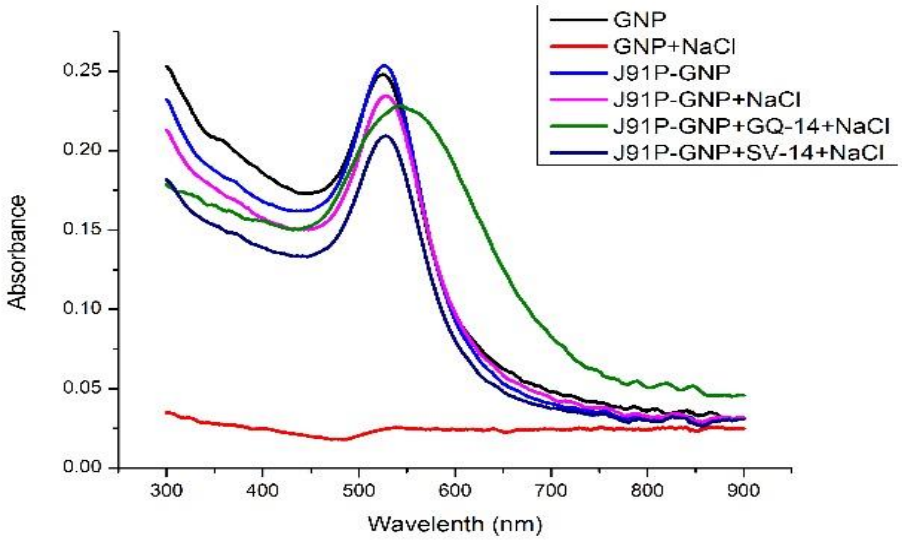

Figure 4.4 UV-VIS spectra of aptamer (J91P) based gold nanoparticle aggregation incubated with target peptide GQ-14 and control peptide SV-14

4.3.1.3. Calorimetric Assay using apt_M09P

The specificity of the aptamer apt_M09P was evaluated by a simple gold nanoparticle based calorimetric assay using the unmodified aptamer. For this, the synthesised gold nanoparticles were incubated with aptamer apt_M09P for 30 min. After incubation the hydrodynamic diameter of the aptamer incubated gold nanoparticles were measured using DLS and compared with the bare gold nanoparticles. The average hydrodynamic diameter of gold nanopartilce incubated with aptamer was found to be 99.91 nm whereas for bare gold nanoparticles, it was found to be 41.44 nm as shown in **figure 4.5**.

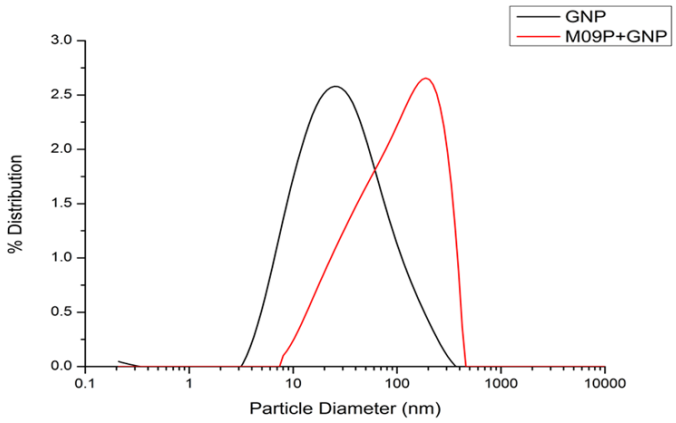

Figure 4.5 The distribution of hydrodynamic diameter of synthesized gold nanoparticles (GNP) before (black) and after (red) adsorption of aptamer on nanoparticle's surface (M09P + GNP)

The calorimetric assay using gold nanoparticles and aptamers shows the aggregate formation in case of incubation of bare gold nanoparticle (GNP) with salt which shows the breaking of the characteristic peak of nanoparticle at 520-30 nm. The incubation of nanoparticles with absorbed aptamer apt_M09P (M09P-GNP) with target SV-14 also shows slight shift of maximum absorbance wavelength towards blue colour as shown in **figure 4.6** which indicates the specificity of the aptamer for peptide SV-14. The control experiment with PV-12 didn't yield any colour change.

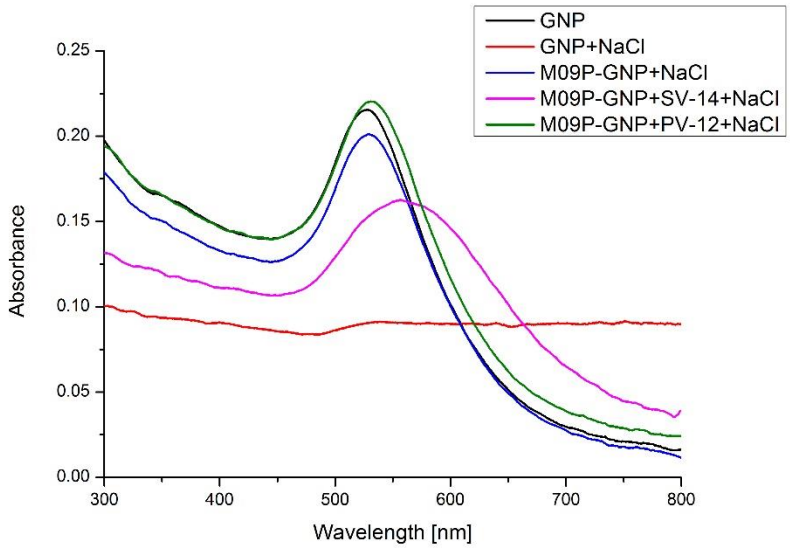

Figure 4.6 UV-VIS spectra of aptamer (M09P) based gold nanoparticle aggregation incubated with target peptide SV-14 and control peptide PV-12

4.3.5. Magnetic bead based target extraction assay using biotinylated apt_J91P

The magnetic bead based assay using biotinylated aptamer apt_J91P was carried out to check the ability of the aptamer to selectively bind to the target. The GQ-14 peptide incubated with biotinylated-aptamer J91P which was later eluted by heating. The heat eluted targets form aptamer-target complex was analysed with MALDI-TOF as mass spectroscopic methods offers much higher sensitivity than the calorimetric tests. The eluted solution extracted after the interaction between GQ-14 and biotinylated-aptamer J91P showed the peak of the peptide GQ-14 at the monoisotopic masses of 1540.838 ($[M+H]^+$) and 1584.59 ($[M+2Na-H]^+$) Da with adducts as shown in the **figure 4.7 A**. This confirms the affinity of the apt_J91P towards the peptide target GQ-14. Peptide SV-14, which is not related to GQ-14 was taken as a negative control by incubating with apt_J91P to test the specificity. The MALDI-TOF analysis of the eluted solution from interaction between apt_J91P and SV-14 did not show the characteristic peak of peptide SV-14 at molecular weight 1626.72 Da (**Figure 4.7 B**). The peaks obtained in this elute is likely due to from biotin attached to aptamer and streptavidin of magnetic beads as heating leads to slight elution of degraded biotin and streptavidin from magnetic beads (Citartan et al., 2016). The same peaks can be seen in another control experiment in **figure 4.7 C** where no target was incubated with biotinylated aptamer. It was only incubated with the streptavidin magnetic beads.

A

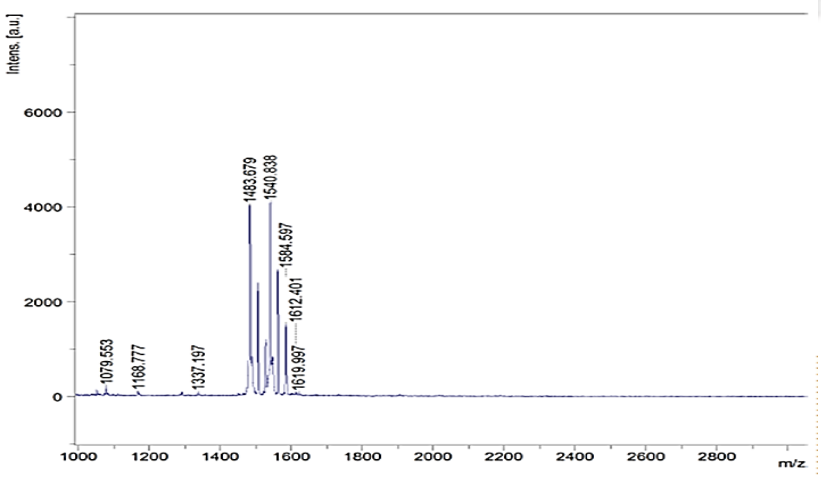

B

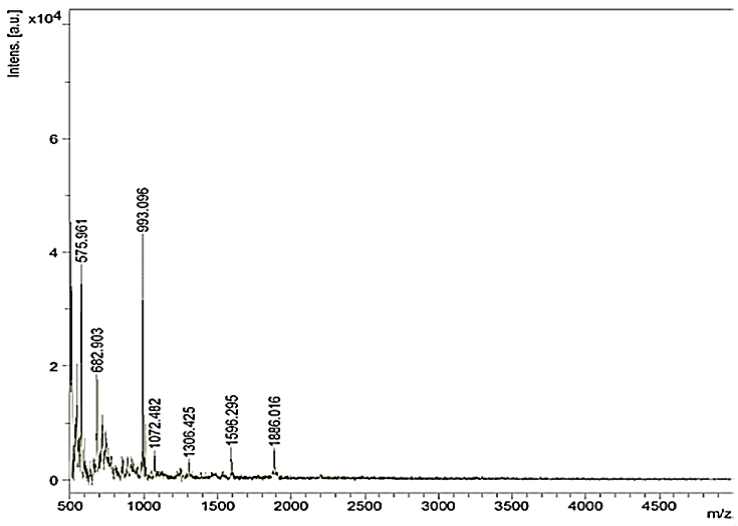

C

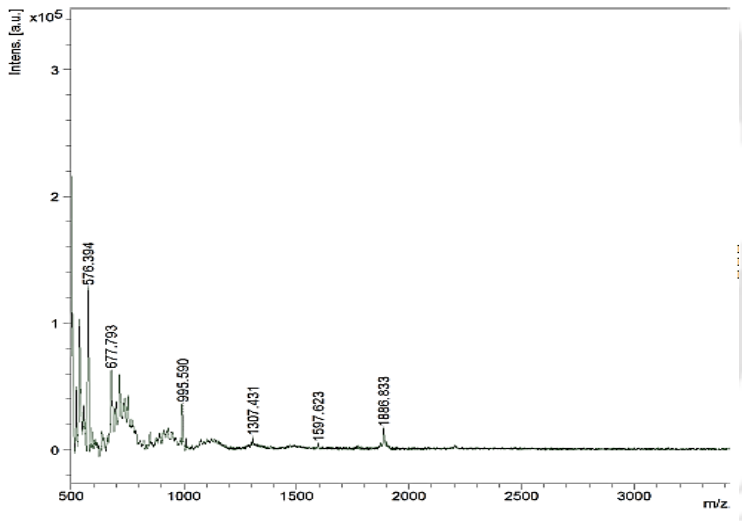

Figure 4.7 MALDI spectrum of elute from **A)** interaction between biotinylated aptamer J91P and GQ-14 showing the monoisotopic mass associated with the peptide GQ-14 **B)** interaction between biotinylated aptamer J91P and SV-14 showing the monoisotopic mass of the contaminates **C)** biotinylated aptamer without incubation with any target (as control experiment)

4.4. Discussion

This chapter addresses the objective of development of an aptamer base bioassay for detection of immunotoxic celiac disease epitopes of glutenin. The aptamers apt_J91P and apt_M09P selected against peptide targets GQGQQGYYPTSPQQ (GQ-14) of HMW glutenin subunit 1Bx13 and DX5 and SQQQPPFSQQQQPV (SV-14) of LMW glutenin were evaluated for their applicability in development of aptamer based bioassays. The preliminary evaluation of the applicability were done by carrying out two formats of aptamer based assay. First, an aptamer mediated gold nanoparticle based calorimetric assays was carried out using the aptamers apt_J91P and apt_M09P. The assay is based on the formation of aggregates by nanoparticles induced by high salt concentration to produce blue colour in presence of the target molecule. The presence of the target can be qualitatively determined through this assay. For this, the aptamer apt_J91P and apt_M09P were absorbed on the surface of the nanoparticles. The absorption of single stranded DNA aptamers on the surface of the gold nanoparticles occurs through electrostatic and noncovalent interactions (Nguyen & Jang, 2021). The aptamers absorbed on the surface of the gold nanoparticles counterbalance the van der waals attraction between nanoparticles with electrostatic repulsion which makes the nanoparticles dispersed in solution and exhibits characteristics wine red colour. Conformational change of aptamer during binding with target leads to dissociation of aptamer from gold nanoparticle surface and at this point the aggregation of the nanoparticles occurs with induction by high salt concentration. Advantage of this method is that it does not require modification of the aptamer with any functional moieties. We examined the salt aggregation of the aptamer absorbed nanoparticles with addition of respective targets GQ-14 and SV-14 which exhibited the shift of colour towards blue indicating positive interactions. Addition of the peptide that are not specific for the aptamers did not show any colour change confirming their specificity. However, further optimization and other experiments are required to detect the target peptide in real food samples. We have also carried out aptamer mediated magnetic bead based extraction of the analyte GQ-14 by using biotinylated aptamer apt_91P. This method of analyte detection uses a mass spectroscopic technique making it more sensitive than calorimetric method. The analyte GQ-14 was incubated with the biotinylated aptamer apt_91P in aptamer binding buffer and the aptamer-target complex was extracted by using a streptavidin immobilised magnetic bead followed by heat elution of the target in nuclease free water. The eluted solution was analysed by MALDI-TOF mass spectroscopy that revealed the successful extraction of the target peptide GQ-14. The peptide SV-14 was also incubated with the biotinylated apt_91P in the magnetic bead based extraction assay, however the characteristic molecular weight of the target SV-14

was not observed in mass spectroscopic peaks confirming the specificity of the aptamer apt_91P for peptide GQ-14. The experiments carried out in order to evaluate the feasibility of the selected aptamer to use in bioassays for detection of target peptide are preliminary in nature. Further studies are required in future to explore the possibilities of the aptamer candidates selected against the immunostimulatory peptides of glutenin for practical application in detection in wheat and wheat based food samples.

4.5. Conclusion

The feasibility of the aptamers apt_J91P and apt_M09P for application in aptamer based bioassay development were evaluated in this chapter. The unmodified aptamers apt_J91P and apt_M09P showed the affinity in detecting the respective target peptides GQGQQGYYPTSPQQ (GQ-14) of HMW glutenin subunit 1Bx13 and DX5 and SQQQPPFSQQQQPV of LMW-GS subunit of wheat(*Triticum aestivum*) gluten in selection buffer through gold nanoparticle based aptamer assay. Aptamer apt_J91P has also been demonstrated the affinity for target GQGQQGYYPTSPQQ in aptamer selection buffer through aptamer mediated magnetic bead based extraction assay. For practical applicability of the aptamer candidates for detection of target peptides in complex food matrices, more elaborate studies required in future.

4.6. References

1. Amaya-González, S., de-Los-Santos-Álvarez, N., Miranda-Ordieres, A. J., & Lobo-Castañón, M. J. (2015). Sensitive gluten determination in gluten-free foods by an electrochemical aptamer-based assay. Analytical and bioanalytical chemistry, 407, 6021-6029.
2. Citartan, M., Ch'ng, E. S., Rozhdestvensky, T. S., & Tang, T. H. (2016). Aptamers as the ‘capturing’agents in aptamer-based capture assays. Microchemical Journal, 128, 187-197.
3. Dong, J., Carpinone, P. L., Pyrgiotakis, G., Demokritou, P., & Moudgil, B. M. (2020). Synthesis of precision gold nanoparticles using Turkevich method. KONA Powder and Particle Journal, 37, 224-232
4. D'Ovidio, R., & Masci, S. (2004). The low-molecular-weight glutenin subunits of wheat gluten. Journal of cereal science, 39(3), 321-339.

5. Franaszek, S., & Salmanowicz, B. (2021). Composition of low-molecular-weight glutenin subunits in common wheat (*Triticum aestivum* L.) and their effects on the rheological properties of dough. Open Life Sciences, 16(1), 641-652.
6. He, Y. Q., Liu, S. P., Kong, L., & Liu, Z. F. (2005). A study on the sizes and concentrations of gold nanoparticles by spectra of absorption, resonance Rayleigh scattering and resonance non-linear scattering. Spectrochimica Acta Part A: Molecular and Biomolecular Spectroscopy, 61(13-14), 2861-2866.
7. Kim, K., Lee, S., Ryu, S., & Han, D. (2014). Efficient isolation and elution of cellular proteins using aptamer-mediated protein precipitation assay. Biochemical and biophysical research communications, 448(1), 114-119.
8. López-López, L., Miranda-Castro, R., de-Los-Santos-Alvarez, N., Miranda-Ordieres, A. J., & Lobo-Castañón, M. J. (2017). Disposable electrochemical aptasensor for gluten determination in food. Sensors and Actuators B: Chemical, 241, 522-527.
9. Nguyen, D. K., & Jang, C. H. (2021). A Simple and Ultrasensitive Colorimetric Biosensor for Anatoxin-a Based on Aptamer and Gold Nanoparticles. Micromachines, 12(12), 1526.
10. Wei, H., Li, B., Li, J., Wang, E., & Dong, S. (2007). Simple and sensitive aptamer-based colorimetric sensing of protein using unmodified gold nanoparticle probes. Chemical Communications, (36), 3735-3737.

Chapter 5

Summary and future prospects

Chapter 5: Summary and future prospects

5.1. Summary

The present study demonstrates the selection of aptamer candidates against two immunostimulatory peptides GQGQQGYYPTSPQQ (GQ-14) of HMW glutenin subunit 1Bx13 and DX5 and SQQQPPFSQQQQPV (SV14) of LMW-GS subunit of wheat (*Triticum aestivum*) gluten. The aptamer apt_91P and apt_M09 were selected against the peptide target GQ-14 and SV-14 respectively. The affinity in terms of dissociation constant (K_d) of both the aptamers against the targets were determined to be in the micromolar (μM) range. The affinity of aptamers are desirable in nanomolar range for successful application in development of biosensor and bioassay. The success of aptamer selection and obtaining high affinity are largely influenced by the molecular structure and physiochemical nature of the target compounds. The analysis of the binding characteristics of the both selected aptamer by ITC and CD reveals that their binding characteristics follows the nature of the aptamers selected against small molecular targets. Compared to the larger targets such as protein molecules which offers a diverse binding pockets including both hydrophobic and hydrophilic environment for aptamers to bind efficiently, the small molecular targets limited by its molecular arrangement and size are challenging for selection of aptamer. Therefore, many published literature reports the affinity of many aptamer selected against smaller molecules exhibit an affinity in low to mid micromolar range. Nevertheless, the present work is believed to be the first of its kind in terms of selecting aptamer candidate against the immunostimulatory peptide sequences of celiac disease present in glutenin subunit.

5.1.1. Selection and characterization of specific aptamers against toxic celiac disease epitopic peptide GQGQQGYYPTSPQQ

In brief, we synthesised peptide sequence GQGQQGYYPTSPQQ of high molecular weight glutenin containing a celiac disease epitope through fmoc solid phase synthesis method. We carried out conventional SELEX for the successful selection of aptamer candidate against the synthesised immunostimulatory peptide. The binding affinity in terms of dissociation constant (K_d) of the selected aptamer viz. apt_J91P was found to be 2.26 μM for primary site of binding and 4.385 mM in the secondary site of binding for the target GQGQQGYYPTSPQQ in aptamer binding buffer. The binding affinity of 81.3 μM (K_d) was determined between the aptamer and target interacting in deionized water. The aptamer has been found to form a stem-loop

secondary structure. The binding characterization by ITC and CD studies reveals that the binding is both enthalpically and entropically driven and local conformational change occurs in the aptamer during binding.

5.1.2. Selection and characterization of specific aptamers against toxic celiac disease epitopic peptide SQQQPPFSQQQQPV

In summary, we carried out the successful selection of aptamer candidate apt_M09 against immunostimulatory celiac disease epitopic peptide SQQQPPFSQQQQPV present in the low molecular weight subunit of glutenin by conventional SLEX method. The binding affinity in terms of dissociation constant (K_d) of the aptamer candidate selected was found to be 17.6 µM for primary site of binding and 8.33 mM in the secondary site of binding for the target SQQQPPFSQQQQPV in aptamer binding buffer. The aptamer has been found to form a stem-loop secondary structure. The binding characterization through ITC and CD studies reveals that the binding is enthalpically driven with an unfavourable entropy and the local conformational change was observed in aptamer during binding.

5.1.3. Development of aptassays for detection of CD epitopes in wheat gluten

Briefly, we checked the feasibility of the aptamers apt_J91P and apt_M09P for application in aptamer based bioassay development. The unmodified aptamers apt_J91P and apt_M09P showed the affinity in detecting the respective target peptides GQGQQGYYPTSPQQ of HMW glutenin subunit 1Bx13 and DX5 and SQQQPPFSQQQQPV of LMW-GS subunit of wheat (*Triticum aestivum*) gluten in selection buffer through gold nanoparticle based aptamer assay. Aptamer apt_J91P has also demonstrated the affinity for target GQGQQGYYPTSPQQ in aptamer selection buffer through aptamer mediated magnetic bead based extraction assay.

5.2. Future prospects of this study

In the present study, two novel aptamers were selected against the two peptide fractions containing epitopes of celiac disease present in glutenin subunit of gluten protein. We investigated the affinity and binding characteristics of these two aptamers. The preliminary studies for their application into bioassays were also carried out. However, these two aptamers

suffers from limitations like low affinity indicated by the dissociation constant (K_d) in micromolar range. The future direction of the work should be towards improving the binding affinity of the both aptamer sequences. The computational techniques like *in-silico* maturation (ISM) can be adopted for further evolution of the nucleotide sequences of the aptamer in order to obtain a high level of affinity initially through *in-silico* docking followed by *in-vitro* experiments. In addition to this, the truncation study on the aptamer sequence length could lead to identification of the optimal sequence of the aptamer which will offer higher affinity than the present. Another strategy for increasing the affinity of the aptamer sequences could be replacement of the natural bases in the sequences with artificial based. For instance, introduction of artificial base (7-(2-thienyl)imidazo[4,5-b]pyridine) has led to increase in the affinity of a aptamer by 1000 folds. Further, for development of the aptamer based assay, detailed optimization of assay parameters is required. Utilization of the high resolution proteomics approaches with combinations of MS-Grade proteolytic enzymes to produce protein digest could aid in the detection of the target peptide by these aptamer candidates in real wheat and food samples.

Curriculum Vitae

Jon Jyoti Kalita was born in 4th February, 1989 in Assam, India. He obtained Bachelor of Engineering (B.E) in Biotechnology from MVJ College of Engineering under Visvesvaraya Technological University, Belagavi, Karnataka with distinction (73.49%) in 2012. He obtained his Masters of Technology (M.Tech) in Food Engineering and Technology from Tezpur University (Central University), Assam with a CGPA of 8.36 in 2015. He qualified the Graduate Aptitude Test in Engineering (GATE) on Biotechnology in 2012 and recieved of AICTE-GATE Scholarship for M.Tech programme. He carried out dissertation on '*Detection of mycobacterium tuberculosis using immunological methods*' and '*Optimization microwave-vacuum drying process in order to attain better texture and survivability of lactic acid bacteria*' as part of his B.E. and M.Tech programms respectively.

The author joined the PhD programm in July, 2015 at Department of Biosciences and Bioengineering, Indian Institute of Technology Guwahati, Guwahati-781039, Assam, India. He received the Institute Fellowship (IIT Guwahati) under the funding by the Ministry of Human Resource Development (MHRD), New Delhi. The focus of his thesis work is development of DNA aptamer against celiac disease epitopes present in the glutenin subunit of gluten protein. He had presented posters in international conferences, BIODIVERSE 2018 held at IIT Guwahti and ICAN-2017 held at Assam Don Bosco University, Guwahati. At the time of compilation of the thesis, he had publish a peer-reviewed article and a book chapter related to thesis work. As a part of collaborative work, he has published two peer-reviewed research articles and three book chapters. During the PhD programm, he performed his teaching assistantship duty as an operator of MALDI-TOF at the Central Instruments Facility (CIF), IIT Guwahati during 2016-2020. He was also a teaching assistant to the online course 'Genome editing and Engineering' taught by Prof. Utpal Bora under National Programme on Technology Enhanced Learning (NPTEL) funded by the Ministry of Education, Govt. of India during July-October, 2022.

Appendix

Food Control 145 (2023) 109406

Contents lists available at ScienceDirect

Food Control

journal homepage: www.elsevier.com/locate/foodcont

Recent developments in application of nucleic acid aptamer in food safety

Jon Jyoti Kalita [a], Pragya Sharma [b], Utpal Bora [a,c,*]

[a] Department of Biosciences and Bioengineering, Indian Institute of Technology Guwahati, Guwahati, 781039, Assam, India
[b] Department of Bioengineering and Technology (GUIST), Gauhati University, Guwahati, 781014, Assam, India
[c] Centre for the Environment, Indian Institute of Technology Guwahati, Guwahati-781039, Assam, India

ARTICLE INFO

Keywords:
Aptamer
Food safety
Aptasensor
Bioassay
Food matrix

ABSTRACT

Food, a basic necessity of life, is often contaminated with harmful agents like pathogenic microorganisms, biotoxins, allergens, antibiotic residues, pesticides, heavy metals etc. Application of efficient, sensitive, reliable and cost-effective analytical technologies to detect the level of contaminants is one of the first steps in ensuring food safety. Oligonucleotide aptamers comprising of short sequences of DNA or RNA are emerging as an alternative to antibodies in development of novel biosensors or bioassays for analysis of various food contaminants. In the pursuit of developing a perfect analytical method, several design strategies involving nanomaterials, biological reagents, microfluidics etc. have resulted in several disruptive innovations. Currently, aptamers are utilised in affinity columns and various sorbent surfaces for selective extraction of analyte from food matrix. Taking advantages of target responsive characteristic and cross-linking ability of aptamers, hydrogel based sensing materials have been developed. In this review, we present an overview on the recent developments in application of aptamers in evaluating food safety and the influence of food matrices on the performance of aptamer based analytical methods.

1. Introduction

Aptamers were discovered in 1990 by two groups working independently, namely i) Craig Tuerk and Larry Gold and ii) Andy Ellington and Jack Szostak. They are now emerging as a new class of nucleic acid based bio-recognition elements opening a new window of opportunities for numerous applications in biomedical research, especially in disease diagnosis and therapeutics. Successively, the detection capability of aptamer has been successfully exploited in environmental contaminant analysis. A considerable amount of research has also been carried out on the prospects of utilising aptamer as a probe for food quality control and safety. Food safety is an issue of prime importance as food materials that sustain human life could also act as a source of recurrent or occasional health hazard. Apart from the intrinsic toxic agents in food, e.g. harmful microorganisms, viruses, prions, toxic peptides, toxic secondary metabolites like cyanogenic glycosides etc., contamination with several other chemicals or toxic agents during various processes of food production and processing, e.g. pesticide and herbicide residues, acrylamide, nitrosamines chloropropanols, monosodium glutamate, mutagenic polycyclic aromatic etc. make it unsafe for consumption (see Table 1).

Food is a diverse mixture of different organic compounds along with trace minerals and chemical compounds which may be present as secondary metabolites. Many of these endogenously produced metabolic compounds are responsible for making raw or unprocessed food unsafe for consumption. For instance, several legume beans contains trypsin inhibitors (Friedman & Gumbmann, 1986) and certain edible fruits or vegetables such as cassava, cherry or bamboo shoot contain cyanogenic glycosides(Long et al., 2020), for which processing or cooking is required to make it safe for consumption. On the contrary, in case of certain food materials, applying a processing method leads to generation of toxic compounds due to biotransformation, e.g. heat treatment of processed meat results in formation of nitrosamines when amines in food interact with nitrogen oxides of food additives or air (Herrmann, Duedahl-Olesen, & Granby, 2015). Likewise carcinogenic compound acrylamide can be generated after heating of carbohydrate-rich food (Wenzl, Lachenmeier, & Gökmen, 2007), while biogenic amines commonly forms in fermented foods (Spano et al., 2010). Specific compounds present in food can be allergic to a group of people with genetic predisposition. There are large number of proteins, e.g. β-conglutin in Lupine, Ara h1 in peanut, gluten in wheat (Khedri, Ramezani, Rafatpanah, & Abnous, 2018) or αS1-casein (Bos d 9) in milk etc. and

* Corresponding author. Department of Biosciences and Bioengineering, Indian Institute of Technology Guwahati, Guwahati, 781039, Assam, India.
E-mail address: ubora@iitg.ac.in (U. Bora).

https://doi.org/10.1016/j.foodcont.2022.109406
Received 9 April 2022; Received in revised form 10 September 2022; Accepted 25 September 2022
Available online 29 September 2022

CHAPTER 11

Food Allergens: Detection and Management

JON JYOTI KALITA,[1] PAPORI BURAGOHAIN,[1]
PONNALA VIMAL MOSAHARI,[2] and UTPAL BORA[1,2]

[1]*Department of Biosciences and Bioengineering, Indian Institute of Technology Guwahati–781039, Assam, India*

[2]*Center for the Environment, Indian Institute of Technology Guwahati–781039, Assam, India, E-mail: ubora@iitg.ernet.in*

ABSTRACT

Food allergy is one of the public health concerns whose prevalence is now increasing globally. Food allergy was initially identified to be prevalent mostly in European countries, however, introduction of newly explored ingredients in food preparation and increased use of processed foods have given rise to it's prevalence in other parts of the world including India. New medical studies in a country like India has revealed the prevalence of food allergies in the Indian population, which can be referred to as just the tip of the iceberg. Food allergies can cause a mild immune response to severe cases of anaphylaxis and death. The presence of allergens in trace amount in food items by cross contamination or raw material adulteration possesses a risk for sensitized individuals. Several analytical methods based on immunological assays, mass-spectroscopy, DNA amplification and hybridization have been developed to detect allergenic peptides and proteins, but each method has its own advantages and disadvantages. Challenges lie in the detection of allergens hidden in the complex food matrix of raw materials and especially in processed foods. New generation analytical method like biosensors based on different transducers like optical, electrochemical, and piezoelectric have been developed to address the need for food process industries. Application of nanomaterial in biosensor enables the development of analytical methods

with more sensitivity, selectivity, portability, and time and cost-effectiveness. Despite the regulation like food allergens labeling, undeclared allergens in food items cause trouble. Food allergen management can be done in food industries by applying standard guidelines based on GMP and HACCP, using risk assessment tactics and communicating the risk with consumers. In this book chapter, we discuss the advancements in various food allergens detection analytical methods and management of it in food manufacturing industries.

11.1 INTRODUCTION

Although we frequently consider allergy as a Western disease, in realism it is recklessly becoming a global ailment with increased prevalence in developed nations. In the last two to three decades food allergies have reportedly affected 5% of adult and 8% of children population of western countries (Sathe et al., 2016; Sicherer and Sampson, 2018). Food allergies are also not uncommon in Asia and Africa, with societies increasingly adopting a Western lifestyle, are noticing expanding rates of allergic syndrome across age groups especially in children. Even in India 1–2% of the total population is affected by food allergies (Gangal and Malik, 2003).

The growing use of processed and readymade food items, food safety issue has become a matter of concern. At the present situation, a cure for food allergy is not available, because the overall understanding of the underlying molecular mechanisms involving the immune reactions is lacking (Sathe et al., 2016b). The only treatment available currently is to avoid the foods causing allergy. In western nations food allergies are a matter of great concern with government agencies creating regulations on allergens and offending foods. Proper food labeling has become very important to maintain consumer safety on a worldwide basis (Prescott et al., 2013).

Allergies are hypersensitivity of the immune system characterized by the production of IgE antibodies against the allergens (antigen that cause allergic reactions) that may enter the human body through different exposure routes: oral, respiratory, skin, gastrointestinal, etc., (Sampson and Burks, 1996). The term "Food allergy," a type of hypersensitivity (type I hypersensitivity/immediate hypersensitivity) is the manifestation occurring due to an immune response towards some food proteins (potential allergens) causing vigorous immunologic reactions involving IgE antibodies in susceptible hosts. Although food allergies mostly involve IgE mediated immune reactions, but other immune mechanisms resulting from T-cell mediated inflammation or

ELSEVIER LICENSE
TERMS AND CONDITIONS

Apr 05, 2023

This Agreement between Mr. Jon Kalita ("You") and Elsevier ("Elsevier") consists of your license details and the terms and conditions provided by Elsevier and Copyright Clearance Center.

License Number	5506361325099
License date	Mar 12, 2023
Licensed Content Publisher	Elsevier
Licensed Content Publication	The Lancet
Licensed Content Title	Coeliac disease
Licensed Content Author	Carlo Catassi,Elena F Verdu,Julio Cesar Bai,Elena Lionetti
Licensed Content Date	25 June–1 July 2022
Licensed Content Volume	399
Licensed Content Issue	10344
Licensed Content Pages	14
Start Page	2413
End Page	2426
Type of Use	reuse in a thesis/dissertation
Portion	figures/tables/illustrations

TH-3201_156106013

Number of figures/tables/illustrations	1
Format	both print and electronic
Are you the author of this Elsevier article?	No
Will you be translating?	No
Title	DEVELOPMENT OF DNA APTAMERS AGAINST SELECTED CELIAC DISEASE EPITOPES IN GLUTENIN
Institution name	Indian Institute of Technology Guwahati
Expected presentation date	May 2023
Order reference number	Jon_thesis_fig
Portions	Figure 1 Pathophysiology of coeliac disease
Requestor Location	Mr. Jon Kalita Department of Biosciences and Bioengineering Indian Institute of Technology Guwahati Kamrup Guwahati, Assam 781039 India Attn: Mr. Jon Kalita
Publisher Tax ID	GB 494 6272 12
Total	0.00 USD

Terms and Conditions

INTRODUCTION

1. The publisher for this copyrighted material is Elsevier. By clicking "accept" in connection with completing this licensing transaction, you agree that the following terms and conditions apply to this transaction (along with the Billing and Payment terms and conditions established by Copyright Clearance Center, Inc. ("CCC"), at the time that you opened your Rightslink account and that are available at any time at http://myaccount.copyright.com).

TH-3201_156106013

GENERAL TERMS

Marketplace

Order Date	06-Mar-2023	Type of Use	Republish in a thesis/dissertation
Order License ID	1330690-1		
ISSN	1545-3278	Publisher	ANNUAL REVIEWS
		Portion	Image/photo/illustration

LICENSED CONTENT

Publication Title	Annual review of immunology	Rightsholder	Annual Reviews, Inc.
		Publication Type	e-Journal
Date	01/01/1983	URL	http://arjournals.annualreviews.org/loi/immunol
Language	English		
Country	United States of America		

REQUEST DETAILS

Portion Type	Image/photo/illustration	Distribution	Worldwide
Number of Images / Photos / Illustrations	1	Translation	Original language of publication
Format (select all that apply)	Print, Electronic	Copies for the Disabled?	No
		Minor Editing Privileges?	Yes
Who Will Republish the Content?	Academic institution	Incidental Promotional Use?	No
Duration of Use	Life of current edition	Currency	USD
Lifetime Unit Quantity	Up to 499		
Rights Requested	Main product		

NEW WORK DETAILS

Title	Developemnt of aptamer against selected glutenin celiac disease epitopes	Institution Name	Indian Institute of Technology Guwahati
		Expected Presentation Date	2023-05-02
Instructor Name	Prof. Utpal Bora		

ADDITIONAL DETAILS

Order Reference Number	jon-1-phdthesis-2	The Requesting Person/Organization to Appear on the License	Jon Jyoti Kalita

REQUESTED CONTENT DETAILS

Title, Description or Numeric Reference of the Portion(s)	Figure 3	Title of the Article/Chapter the Portion Is From	Integration of Genetic and Immunological Insights into a Model of Celiac Disease Pathogenesis
Editor of Portion(s)	NA		

TH-3201_156106013

Volume of Serial or Monograph	NA	Author of Portion(s)	Valerie Abadie, Ludvig M. Sollid, Luis B. Barreiro, and Bana Jabri
Page or Page Range of Portion	493-525	Issue, if Republishing an Article From a Serial	N/A
		Publication Date of Portion	1983-01-01

Marketplace Permissions General Terms and Conditions

The following terms and conditions ("General Terms"), together with any applicable Publisher Terms and Conditions, govern User's use of Works pursuant to the Licenses granted by Copyright Clearance Center, Inc. ("CCC") on behalf of the applicable Rightsholders of such Works through CCC's applicable Marketplace transactional licensing services (each, a "Service").

1) Definitions. For purposes of these General Terms, the following definitions apply:

"License" is the licensed use the User obtains via the Marketplace platform in a particular licensing transaction, as set forth in the Order Confirmation.

"Order Confirmation" is the confirmation CCC provides to the User at the conclusion of each Marketplace transaction. "Order Confirmation Terms" are additional terms set forth on specific Order Confirmations not set forth in the General Terms that can include terms applicable to a particular CCC transactional licensing service and/or any Rightsholder-specific terms.

"Rightsholder(s)" are the holders of copyright rights in the Works for which a User obtains licenses via the Marketplace platform, which are displayed on specific Order Confirmations.

"Terms" means the terms and conditions set forth in these General Terms and any additional Order Confirmation Terms collectively.

"User" or "you" is the person or entity making the use granted under the relevant License. Where the person accepting the Terms on behalf of a User is a freelancer or other third party who the User authorized to accept the General Terms on the User's behalf, such person shall be deemed jointly a User for purposes of such Terms.

"Work(s)" are the copyright protected works described in relevant Order Confirmations.

2) Description of Service. CCC's Marketplace enables Users to obtain Licenses to use one or more Works in accordance with all relevant Terms. CCC grants Licenses as an agent on behalf of the copyright rightsholder identified in the relevant Order Confirmation.

3) Applicability of Terms. The Terms govern User's use of Works in connection with the relevant License. In the event of any conflict between General Terms and Order Confirmation Terms, the latter shall govern. User acknowledges that Rightsholders have complete discretion whether to grant any permission, and whether to place any limitations on any grant, and that CCC has no right to supersede or to modify any such discretionary act by a Rightsholder.

4) Representations; Acceptance. By using the Service, User represents and warrants that User has been duly authorized by the User to accept, and hereby does accept, all Terms.

5) Scope of License; Limitations and Obligations. All Works and all rights therein, including copyright rights, remain the sole and exclusive property of the Rightsholder. The License provides only those rights expressly set forth in the terms and conveys no other rights in any Works

6) General Payment Terms. User may pay at time of checkout by credit card or choose to be invoiced. If the User chooses to be invoiced, the User shall: (i) remit payments in the manner identified on specific invoices, (ii) unless otherwise specifically stated in an Order Confirmation or separate written agreement, Users shall remit payments upon receipt of the relevant invoice from CCC, either by delivery or notification of availability of the invoice via the Marketplace platform, and (iii) if the User does not pay the invoice within 30 days of receipt, the User may incur a service charge of 1.5% per month or the maximum rate allowed by applicable law, whichever is less. While User may exercise the rights in the License immediately upon receiving the Order Confirmation, the License is automatically revoked and is null and void, as if it had never been issued, if CCC does not receive complete payment on a timely basis.

7) General Limits on Use. Unless otherwise provided in the Order Confirmation, any grant of rights to User (i) involves only the rights set forth in the Terms and does not include subsequent or additional uses, (ii) is non-exclusive and non-transferable, and (iii) is subject to any and all limitations and restrictions (such as, but not limited to, limitations on duration of use or circulation) included in the Terms. Upon completion of the licensed use as set forth in the Order Confirmation, User shall either secure a new permission for further use of the Work(s) or immediately cease any new use of the Work(s) and

SPRINGER NATURE LICENSE
TERMS AND CONDITIONS

Apr 05, 2023

This Agreement between Mr. Jon Kalita ("You") and Springer Nature ("Springer Nature") consists of your license details and the terms and conditions provided by Springer Nature and Copyright Clearance Center.

License Number	5502410221561
License date	Mar 05, 2023
Licensed Content Publisher	Springer Nature
Licensed Content Publication	Springer eBook
Licensed Content Title	Extraction, Separation, and Purification of Wheat Gluten Proteins and Related Proteins of Barley, Rye, and Oats
Licensed Content Author	Arthur S. Tatham, Simon M. Gilbert, Roger J. Fido et al
Licensed Content Date	Jan 1, 2000
Type of Use	Thesis/Dissertation
Requestor type	academic/university or research institute
Format	print and electronic
Portion	figures/tables/illustrations
Number of figures/tables/illustrations	1
Will you be translating?	no

TH-3201_156106013

Circulation/distribution	1 - 29
Author of this Springer Nature content	no
Title	DEVELOPMENT OF DNA APTAMERS AGAINST SELECTED CELIAC DISEASE EPITOPES IN GLUTENIN
Institution name	Indian Institute of Technology Guwahati
Expected presentation date	May 2023
Order reference number	jon_thesis_1
Portions	Figure 1
Requestor Location	Mr. Jon Kalita Department of Biosciences and Bioengineering Indian Institute of Technology Guwahati Kamrup Guwahati, Assam 781039 India Attn: Mr. Jon Kalita
Total	0.00 USD
Terms and Conditions	

Springer Nature Customer Service Centre GmbH Terms and Conditions

The following terms and conditions ("Terms and Conditions") together with the terms specified in your [RightsLink] constitute the License ("License") between you as Licensee and Springer Nature Customer Service Centre GmbH as Licensor. By clicking 'accept' and completing the transaction for your use of the material ("Licensed Material"), you confirm your acceptance of and obligation to be bound by these Terms and Conditions.

1. Grant and Scope of License

1. 1. The Licensor grants you a personal, non-exclusive, non-transferable, non-sublicensable, revocable, world-wide License to reproduce, distribute, communicate to the public, make available, broadcast, electronically transmit or create derivative works using the Licensed Material for the purpose(s) specified in your RightsLink Licence Details only. Licenses are granted for the specific use requested in the order and for no other use, subject to these Terms and Conditions. You acknowledge and agree that the rights granted to you under this License do not include the right to